

THE RESPONSE OF BURIED uPVC PIPES  
TO SURFACE LOADING

BY

CHRISTOPHER DAVID FOSS ROGERS, B.Sc.

Thesis submitted to the University of Nottingham  
for the degree of Doctor of Philosophy

May 1985

**TO MY WIFE**

## CONTENTS

	PAGE
Abstract	i
Acknowledgements	ii
Notation	iv
<b>CHAPTER ONE</b>	
<b>INTRODUCTION</b>	<b>1</b>
1.1	The Role of Buried Pipes 1
1.2	The Structural Requirements of a Buried Pipe 2
1.3	The Use of uPVC Pipes for Building Drainage 6
1.4	The Approach Adopted for the Research 8
1.5	Terminology 9
<b>CHAPTER TWO</b>	
<b>LITERATURE REVIEW</b>	<b>11</b>
2.1	A Brief History of Buried Pipe Research 11
2.2	Loads on Buried Pipes 14
2.3	Prediction of Diametral Strain in Buried Flexible Pipes 16
2.3.1	Spangler's Development of the Iowa Formula 18
2.3.2	Barnard's Method 23
2.3.3	Molin's Method 24
2.3.4	German Developments 27
2.3.5	Bossen's Formula 29
2.3.6	The USBR Equation 30
2.3.7	Watkins' Method 33
2.3.8	Closed Form Solutions 35
2.3.9	Finite Element Studies 36

	PAGE
2.3.10 Gumbel's Method	37
2.4 Experimental and Field Investigation of Buried Flexible Pipes	46
2.4.1 Experimental Studies at the TRRL	47
2.4.2 Howard's Investigations	56
2.4.3 Other American Research	63
2.4.4 Dezseryi's Experiments	66
2.4.5 Broere's Experiments	68
2.4.6 Soini's Experiments with Soft Soils	72
2.4.7 European Field Measurements	74
2.5 Concluding Discussion	79
<b>CHAPTER THREE RESEARCH PHILOSOPHY</b>	<b>87</b>
3.1 Introduction	87
3.2 Methods of Investigation	88
3.3 Performance Parameters	92
3.4 Factors Influencing Pipe Deformation	93
3.4.1 Surface Load	93
3.4.2 Ratio of Cover Depth to Pipe Diameter	94
3.4.3 Ratio of Bedding Thickness to Pipe Diameter	95
3.4.4 Ratio of Trench Width to Pipe Diameter	96
3.4.5 Shape of Trench	96
3.4.6 Type of Bedding and Sidefill	96
3.4.7 Method of Laying Bedding and Sidefill	97
3.4.8 Type and Method of Laying Backfill	98
3.4.9 Type and State of Insitu Soil	99
3.4.10 Groundwater Level	100

	PAGE	
3.4.11	Quality of Pipe Material	100
3.4.12	Pipe Class	100
3.4.13	Pipe Abnormalities	101
3.4.14	Longitudinal Bending Effects	101
3.4.15	Temperature	102
3.4.16	Time	102
3.4.17	Settlement of the Pipe and Fill	102
3.5	Boundary Conditions	103
3.6	Experimental Considerations	105
3.7	Philosophy Behind the Test Programme	108
<b>CHAPTER FOUR</b>	<b>EXPERIMENTAL STUDY OF PIPE BEHAVIOUR</b>	<b>110</b>
4.1	Introduction	110
4.2	Equipment	111
4.2.1	The Test Pit	111
4.2.2	Loading Arrangement	114
4.2.3	The Test Box	118
4.3	Instrumentation	119
4.3.1	Measurement of Pipe Deformation	119
4.3.2	Measurement of Pipe Wall Strain	127
4.3.3	Measurement of Soil Strain	128
4.3.4	Measurement of Total Soil Pressure	131
4.3.5	Additional Instrumentation	133
4.3.6	Data Logging Facilities	133
4.4	Experimental Procedure	135
4.4.1	Random Sampling and Initial Measurement	136
4.4.2	Installation Procedure	137
4.4.3	Measurement of Pipe and Soil Response	139

		PAGE
	4.4.4 Exhumation of Pipe and Trench Reinstatement	141
4.5	Pipe Material Classification	143
4.6	Programme of Experimental Work	143
	4.6.1 Unconfined Line Load Tests	143
	4.6.2 Programme of Box Experiments	144
	4.6.3 Programme of Pit Experiments	148
<b>CHAPTER FIVE</b>	<b>RESULTS OF EXPERIMENTAL WORK</b>	<b>151</b>
5.1	Introduction	151
5.2	Buried uPVC Pipe Behaviour	154
	5.2.1 Vertical Diametral Strain	154
	5.2.2 Pipe Wall Strain	167
	5.2.3 Shape of Deformation	178
	5.2.4 Pipe Settlement	181
	5.2.5 Soil Strain	183
	5.2.6 Soil Pressures	186
	5.2.7 Surface Settlement	188
5.3	Pipe Classification Results	189
<b>CHAPTER SIX</b>	<b>SOIL CHARACTERISATION</b>	<b>191</b>
6.1	Introduction	191
6.2	Methods of Soil Characterisation	192
	6.2.1 The Triaxial Test	192
	6.2.2 In Situ Measurements	193
	6.2.2.1 The Proving Ring Penetrometer	194
	6.2.2.2 The Geotester	194
	6.2.2.3 The Pocket Penetrometers	195

	PAGE	
6.2.2.4	The Shear Vane	195
6.2.3	The Compaction Fraction Test	195
6.2.4	Particle Size Distribution	197
6.2.5	Index Tests and B.S. Compaction Test	198
6.3	Experimental Procedure	198
6.3.1	In Situ Soil Characterisation	198
6.3.2	Laboratory Tests	200
6.4	Results	200
6.4.1	Comparison of In Situ Soil Strength Testing Devices	200
6.4.2	Laboratory Methods of Classification	206
6.4.3	Determination of Soil Stiffness from Soil Strength Measurements	210
6.4.4	Correlation with Pipe Behaviour	214
<b>CHAPTER SEVEN</b>	<b>THEORETICAL STUDY</b>	<b>220</b>
7.1	Introduction to Theoretical Techniques	220
7.2	Linear Elastic Layer Analysis	221
7.2.1	BISTRO and its Use	221
7.2.2	Simulation of Load	222
7.3	Linear Elastic Modelling of Buried Pipe Installations	226
7.3.1	PAFEC and its Use	226
7.3.2	Boundary Conditions	227
7.3.3	Simulation of Load	230
7.3.4	Parameter Studies	232
7.3.5	Correlation with Experimental Data	234

<b>CHAPTER EIGHT</b>	<b>CONCLUSIONS AND THE WAY FORWARD</b>	238
8.1	The Behaviour of Buried uPVC Pipes	238
8.2	Soil Characterisation	239
8.3	Recommendations for Future Work	240
<b>REFERENCES</b>		244
<b>APPENDIX A</b>	<b>SUMMARY OF EXPERIMENTAL DATA</b>	252



## ABSTRACT

A comprehensive review of methods of theoretical prediction of, and experimental investigation into, buried flexible pipe behaviour is presented. The factors that influence this behaviour are isolated and methods for their measurement suggested. Two pipe test facilities based on a 4.1m long x 2.1m wide x 1.9m deep sunken pit and a smaller reinforced box, have been developed and these are described together with the philosophy behind their use. The development of appropriate instrumentation techniques for the measurement of pipe and soil response is reported together with the results of preliminary experiments to prove their ability.

A programme of full-scale tests on 160 mm diameter, shallow-buried uPVC pipes in which current building drainage practice was simulated, was conducted in both the pit and box. The programme included investigations of the influence of bedding, sidefill type and sidefill compaction on the response of such pipes to construction traffic loading. The performance of the pipe-soil structure was determined from photographs of the deformed shape of the pipe, and measurements of pipe wall strain, soil strain and total soil pressure. In addition to trends in the vertical diametral strain of the pipe, therefore, those in the shape of deformation, which is shown to vary considerably, and the reaction of the soil were determined. A simple theoretical model of this situation was developed using finite element techniques and its response to load was correlated with that of the pipe in the experiments. This work is reported herein and is set into the context of past and future developments.

The results of a programme of soil characterisation, both in situ on cohesive soil and in the laboratory on granular material, are presented and their implications for the development of a method of site assessment of potential sidefill materials are discussed.



## ACKNOWLEDGEMENTS

I would firstly like to thank the British Plastics Federation who both sponsored and took a close interest in the project.

I wish to thank Professors Rex Coates and Peter Pell who, in their turn, provided the extensive facilities of the Department of Civil Engineering.

In particular, I would like to thank Professor Stephen Brown who supervised the research with the diligent qualities that brought him his D.Sc. and his chair in Civil Engineering during the last three years.

The experimental work was conducted with the able and willing help of Mike Langford, who played the role of a stout-hearted workhorse throughout. Thanks are also due to Nick Thom, who magnanimously tested in his triaxial cells my granular materials instead of his own. The early assistance of Barry Brodrick and Norman Hardy in developing instrumentation is gratefully acknowledged, as is that of all the technicians who helped with the project and suffered the construction of the pit with outward indifference. Bill Robinson undertook the considerable photographic duties involved in the experiments with care and patience. Outside support came from many sources, notably the Butterley Brick Company and the researchers at the Transport and Road Research Laboratory and the Water Research Centre, who donated the unbaked Keuper Marl bricks and advice respectively.

This thesis was produced in a surprisingly short time thanks to the outstanding skill and professionalism of Hilda Ratcliffe and Beverly Watson, who typed the text and tables. Caroline Brayley produced the figures, and Tony Holmes the photographs, with evident talent.

I wish to thank all the members of the Department of Civil Engineering who offered stimulating conversation during the last three years, some of which took the form of advice. In particular, I would like to thank the members of

the Pavement Research Group and the other researchers, past and present, among whom I now have many friends. This inspite of some of them being surveyors.

Finally, I would like to thank my wife, Cathie, for her love, encouragement and support throughout the research. She has patiently helped to develop my style of English and has always taken an interest in the progression of the work, despite the subject matter. I would also like to thank my sons Edward and William, both of whom were born during the project, for their refreshing outlook on life. I have greatly enjoyed returning to University and tackling the problems of research, and all those mentioned above have contributed to this enjoyment.

## NOTATION

Capital Letters

A	constant in equation (2.13) dependent upon bedding conditions and including conversion factors
$B_t$	trench width (m)
C	Buisman's soil coefficient
$C_f$	construction factor (percentage vertical deflection)
D	mean pipe diameter (m)
$D_{80}$	diameter of soil particles (m), the subscript (as a percentage) denotes the proportion of particles in a material that are smaller than this diameter
$D_f$	design factor
$D_o$	outside diameter of pipe (m)
E	Young's Modulus (kPa)
E'	Modulus of Soil Reaction (kPa)
E''	secant modulus obtained from the oedometer test (kPa)
$E_p$	Young's Modulus of pipe material (kPa)
$E_s$	Young's Modulus for soil derived as a tangent modulus (kPa)
$E_s'$	Young's Modulus for soil derived as a secant modulus (kPa)
$E_s^*$	plain strain modulus for soil (kPa)
$E_{s1}$	Young's Modulus for soil surrounding pipe derived as a tangent modulus (kPa)
$E_{s2}$	Young's Modulus for natural soil derived as a tangent modulus (kPa)
$E_2$	elastic modulus of the sidefill used in equation 2.11 (kPa)
$E_{50}$	secant modulus of elasticity at 50% of failure strength (kPa)
G	Shear Modulus (kPa)
$G_s$	secant Shear Modulus (kPa)
I	second moment of area of the pipe cross-section about the diameter ( $\text{mm}^4$ )
$I_f$	inspection factor (percentage vertical deflection)

K	Bulk Modulus (kPa)
$k_a$	Rankine's coefficient of active earth pressure at rest
$k_b$	bedding constant, dependent on $\alpha$ , used in equations 2.1 and 2.3
$K_d$	dead load lateral pressure ratio
$K_o$	Rankine's coefficient of earth pressure at rest
L	length (m)
$M_s$	confined modulus of soil (kPa)
$N_y$	distortional hoop thrust (kPa)
$N_{y1}$	hoop thrust due to distortional pressure component (kPa)
$N_{y2}$	second order distortional hoop thrust due to uniform pressure acting on deformed pipe (kPa)
$N_z$	hoop thrust due to uniform pressure component (kPa)
Q	soil stiffness correction factor
$R_s$	Stiffness Ratio used by Watkins and Soini
S	pipe-soil stiffness factor used in equation 2.8
$S_f$	soil stiffness factor used in equation 2.13 (kPa)
$S_{fp}$	flexural stiffness of the pipe ring (kPa)
$T_f$	time lag factor
Y	flexural stiffness parameter for pipe/soil system

#### Lower Case Letters

c	coefficient in equation 2.6 dependent upon Poisson's Ratio and other factors
$c_u$	undrained shear strength (kPa)
$c_v^*$	deflection coefficient used in equation 2.10
e	voids ratio
$e_s$	Modulus of Passive Resistance of Soil (kN/m)
h	thickness of material, particularly depth of cover (m)
k	coefficient dependent on the shape of deformation used in equation 2.25

$n$	critical buckling mode, also
$n$	installation parameter used in equation 2.12
$p$	pressure at sample surface (kPa)
$P_h$	horizontal pressure on the pipe (kPa)
$P_{hd}$	free-field horizontal pressure (kPa)
$P_{hs}$	horizontal pressure due to uniform surcharge (kPa)
$P_{ht}$	horizontal pressure due to concentrated surcharge (kPa)
$P_q$	vacuum pressure (kPa)
$P_s$	uniform surcharge (kPa)
$P_v$	vertical pressure on the pipe (kPa)
$P_v'$	vertical reaction from bedding (kPa)
$P_{vd}$	free-field vertical pressure (kPa)
$P_{vs}$	vertical pressure due to uniform surcharge (kPa)
$P_{vt}$	vertical pressure due to concentrated surcharge (kPa)
$P_w$	hydrostatic pressure (kPa)
$P_y$	distortional pressure component (kPa)
$P_z$	uniform pressure component (kPa)
$q$	deviator stress (kPa)
$q_c$	pressure on penetrometer cone (kPa)
$r$	mean radius of pipe (m)
$s$	settlement (m)
$s_p$	settlement of the pipe invert (m)
$t$	pipe wall thickness (m)
$w$	water content (%)
$w_c$	vertical load per unit length of pipe (kN/m)

#### Greek Characters

$\alpha$	bedding angle (degrees)
$\alpha_1$	elastic arching factor

$\alpha_2$	ratio of trench width to pipe diameter
$Y$	unit weight of soil ( $\text{kg/m}^3$ )
$Y'$	submerged unit weight of soil ( $\text{kg/m}^3$ )
$Y_h$	shear strain ratio used in equation 2.14
$Y_w$	unit weight of water ( $\text{kg/m}^3$ )
$\Delta_h$	horizontal diametral reduction (m)
$\Delta_v$	vertical diametral reduction (m)
$\delta$	deflection (m)
$\delta_h (= \delta_x)$	horizontal deflection, sometimes used to describe that of the pipe (m)
$\delta_v (= \delta_y)$	vertical deflection, sometimes used to describe that of the pipe (m)
$\delta_y$	distortional, or out-of-round deformation (m)
$\delta_y^*$	distortional deformation caused by loading (m)
$\delta_{y0}$	initial out-of-roundness (m)
$\delta_{y1}$	deformation due to distortional pressure component (m)
$\delta_{y2}$	second order distortional deformation due to uniform pressure acting on deformed pipe (m)
$\delta_{y3}$	long-term distortional deformation (m)
$\delta_z$	deformation due to uniform pressure component (m)
$\epsilon_w$	circumferential strain in the pipe wall
$\epsilon_s$	relative compression of material in direction of stress, also
$\epsilon_s$	shear strain of soil used in Fig. 6.9
$\epsilon_x$	horizontal compression of the soil at the side of the pipe
$\nu$	Poisson's Ratio
$\nu_p$	Poisson's Ratio for the pipe material
$\nu_s$	Poisson's Ratio for soil
$\zeta$	Sidefill stiffness correction factor used in equation 2.11
$\rho$	density ( $\text{kg/m}^3$ )
$\rho_d$	dry density ( $\text{kg/m}^3$ )



$\rho_w$	density of water (kg/m <sup>3</sup> )
$\sigma_h$	horizontal stress (kPa)
$\sigma_v$	vertical stress (kPa)
$\sigma_3$	cell pressure (kPa)

### Abbreviations

BF	Backfill
BF(s)	Surface of backfill
CB	Concrete ballast
CBR	California Bearing Ratio
CF	Compaction Fraction
GL	Granular Layer
LC	Lightly Compacted
NS	In situ, or naturally occurring, soil
NS(s)	In situ soil to the side of the trench
NS(B)	In situ soil below the trench
P	Pipe
PG	Pea gravel
QT	Quarry tailings
RS	Reject sand
SC	Silty clay
SF	Sidefill
UC	Uncompacted
VDS	Vertical diametral strain
WC	Well, or thoroughly, compacted

### Stages of Test

EOI	End of installation
55 ON	55 kN applied
55/30	55 kN static load applied for 30 minutes

E055 <sub>s</sub>	End of 55 kN static load sequence
E055 <sub>c</sub>	End of 55 kN cyclic load sequence
70 ON	70 kN applied
70/30	70 kN static load applied for 30 minutes
E070 <sub>s</sub>	End of 70 kN static load sequence
E070 <sub>c</sub>	End of 70 kN cyclic load sequence
EOT	End of test

## CHAPTER ONE



## 1 INTRODUCTION

### 1.1 The Role of Buried Pipes

Passages through the ground have been required for a variety of reasons since civilisation began and have become necessary for civilisation to continue. Passages for personal access are thought to date from as early as the 22nd century BC when an arched opening was constructed in a trench under the temporarily diverted River Euphrates. The earliest engineer known by name in the ancient world is Eupalinus of Megara who built a 1000m long tunnel for water-supply on the island of Samos in the 6th century BC. This tunnel, regarded as one of the three great engineering feats in the Greek world, was a precursor of the major public health engineering works that are currently so topical. The Romans were renowned for their sophisticated systems of underground passages for the transport of fluids, their engineering skill extending above ground to ducts for the passage of hot air for a form of central heating. In modern times, the scale of underground openings has increased dramatically to permit the passage of large volumes of fluid, people or vehicles. These larger openings and all tunnels, which have been loosely defined as big enough for a man to work in or move along, lie outside the bounds of this project. It is to the smaller openings known as pipes that the project is directed.

The principal use of pipes, which are usually buried out of either convenience or necessity, are transportation, communications, and the supply and removal of fluids. As these functions are essential for modern life pipes have become a necessary part of the "infrastructure", a word now used to describe the physical framework on which modern civilised living is

based. In particular, pipes are commonly used for the supply and distribution of water and gas, and the removal of domestic and industrial waste. Porous pipes have a widespread application in land drainage, and the desirability of keeping cables out of sight has led to the use of pipes as service ducts also. The demand for new pipes, for whatever reason, has been augmented by the need for replacement of existing pipes, especially those of Victorian origin, which are wearing out. For these reasons, buried pipes are a major factor in the current debate on infrastructure renewal.

## 1.2 The Structural Requirements of a Buried Pipe

The basic structural requirement of a buried pipe is the provision of an opening of dimensions and permanence suited to the function it is to perform. In general the physical properties of the pipe that must be maintained over its lifetime are its size, shape, line and level, together with its ability to prevent the ingress or egress of fluids through its wall. The main exception to this is the case of land drainage, in which porous pipes, formed from either porous materials or holed impermeable materials, are used and the maintainance of their porosity is essential.

These structural requirements have been met in many different ways. In ancient times water was allowed to flow under gravity through channels hewn in rock or stone, and these were covered where appropriate. The brick lined sewers of the 19th century are now accepted as remarkable examples of vernacular architecture and superb workmanship. It was in 1842 that John Roe, surveyor of the Holborn and Finsbury district, put his mind to the design of sewer systems at the request of Edwin Chadwick (1800-1890), who was then secretary to the Poor Law Board set up in 1834. Roe had

previously invented the widely adopted egg-shaped sewers, introduced wide curves (not less than 25ft. radius) to remove sedimentation at joints, and reduced the size of drains serving short streets and courts from 4ft. 6in., which allowed man entry, to 15ins. Roe's brief was to work on a series of experiments to ascertain for different discharges and gradients the most economical sizes of pipe, and the best materials for their construction.

Chadwick wrote at that time

As the old formulae, now in use, are founded on imperfect data and experiments, and not only give results so far above what experience shows to be the fact, but which, even if they were correct, would be of most limited application, they are obviously uncertain guides, and it is better to trust to our observations of what actually takes place. This is in fact experimenting on the largest and safest scale.

In reply to later questioning on the value of these experiments, he replied that drainage was a matter of gauging and experiment which, if carefully conducted, would eventually remove all grounds for differences of opinion. His words are still relevant 140 years on and no more eloquent apology for the work presented hereafter could be devised.

Developments since that era have yielded two basic methods of economic fulfillment of the structural and other requirements for buried pipes. The first involves the use of rigid pipes on a rigid bed such that the inherent strength of the pipes is sufficient to withstand applied loads by bending action in the pipe walls. Such pipes are subject to brittle fracture if the applied loads are too great or significant differential settlement occurs. The second method involves the use of flexible pipes which reach equilibrium in the ground under load by deforming. Such pipes rely on the properties of the surrounding materials to provide support and can fail in three ways: by buckling or excessive <sup>compressive</sup> hoop strain in surrounds providing relatively good support, or by excessive deformation. Failure of the pipe in these cases can be difficult to define if complete collapse does not result.

Installation of any pipe, irrespective of its category, can be effected either by trenching and reinstatement, or by insertion using such techniques as thrust-boring or mole-ploughing. Before the various pipe materials are discussed, the loads that pipes have to withstand in common use will be considered. Pipe installation by traditional methods (i.e. trenching) will lead to loads in its plane of cross-section from the placing and compaction of fill materials. Where insertion methods are used, longitudinal tensile or compressive forces will develop. Dead loads are applied by overlying soil, particularly where a pipe passes under an embankment, and structures. Intermittent vehicle loads are often applied to buried pipes, though sometimes only at the construction stage, and these constitute the most important source of external live loads for such structures. Depending upon the use to which the pipe is put, considerable loading can also be applied by internal pressure or vacuum. Other, generally less important, sources of load arise from thermal expansion and contraction, and shrinkage and creep, of the pipe material, and resulting stresses should be added to those induced in the pipe during its manufacture.

Rigid pipes were the traditional solution to the problem of resistance to load and included those made from cast iron, clay, concrete and asbestos cement. The range of widely available flexible pipes, hitherto consisting of ductile iron or thin-walled steel, which was often corrugated in large diameter pipes, has been augmented in recent years by many types of plastic pipes, both reinforced and unreinforced. These include pipes made from unplasticized polyvinylchloride (uPVC), polyethylene (PE), glass reinforced plastic (GRP) and reinforced plastic matrix (RPM), though many pipes with different properties in terms of strength, stiffness, toughness, durability, chemical stability and ease of installation, are available. Another recent development involves the use of flexible joints for rigid



pipes to combine the advantages of both.

The dividing line between rigid and flexible pipe behaviour has become blurred with the advent of these new forms of pipe construction, and various methods of categorising the pipes have been proposed. Marston (1930) defined flexible pipes as those capable of sustaining a diametral strain of 3% without signs of cracking or other structural damage. Such deformation was thought to be necessary before support from the lateral passive pressure of the material beside the pipe was mobilised. A more rational approach uses the ratio of stiffnesses of the soil and the pipe ring, a concept that is well established in the design of tunnel linings. The distinction between rigid and flexible pipes is of little importance, however, if the composite pipe-soil system, rather than two distinct entities, is treated as the structure under consideration. In this way external and inherent system loads are resisted by composite action according to the relative stiffnesses.

From these ideas of relative flexibility, it can be seen that to design a pipeline, an appreciation of both pipe and fill properties and their interaction is necessary. In the case of an inflexible pipe, design is primarily concerned with the structural properties of the pipe ring and the material on which the pipe is laid. Where the pipe has great flexibility, the structural properties of the material both beside and above the pipe also become important, particularly their ability to resist both vertical and horizontal pressures without large deformations. It is at this point that the economics of the provision of structural support to the passage must be considered. The relative costs of providing a rigid pipe and stiff bed or a flexible pipe and suitable pipe surround material have to be weighed together with those of the system in service. This can only be done for specific applications and it is to one particular application that this work is primarily directed.

### 1.3 The Use of uPVC Pipes for Building Drainage

Building drainage accounts for a large proportion of the market in pipes of small diameter. This has been traditionally supplied by clay and concrete pipes, but in relatively recent times, after a brief interest in pitch fibre, flexible pipes of unplasticized polyvinylchloride (uPVC) have become popular and they now command over 30% of the market. The design of rigid pipes for this application is well established. It involves prediction of pressure at the crown of the pipe caused by dead and live loads and provision of a pipe with a safe crushing strength. Design of buried flexible pipes is more complex because of the need to predict soil properties. Various methods of design have been proposed, but none are irrefutably applicable to small diameter uPVC pipes, and all are either too inaccurate or imprecise to be of use. At this point the history of uPVC pipe is necessary for a complete understanding of the current specifications.

The first uPVC pipes were manufactured in Europe before the second world war and were used, albeit it on a small scale, as pressure pipes in the water supply industry (Gehrels, 1972). Deformation of these pipes was found to be relatively small because of their tendency to re-round under internal pressure. The early 1950s saw a rapid growth in this application. At this time the building drainage market in Great Britain was dominated by the clay pipe manufacturers, whose product was traditionally buried in an unreinforced concrete surround. Questioning of the need for such an expensive installation requirement, and of its conservatism in the light of experiments at the Building Research Station in the early 1960s, led to the omission of the matrix from the surround material, resulting in gravel or shingle fills.

When uPVC pipes were first used for non-pressure applications in

Europe in the mid-1950s, there was little understanding of the behaviour of buried flexible pipes. Thin-walled pipes were chosen for the first installations on the assumption that the pipe need only act as a liner to protect the waterway from ingress resulting in collapse, analogy being made to the tracks of moles. Early failures resulted from excessive deformation and collapse of the pipe ring under load. The situation was exacerbated by marketing techniques that described uPVC pipes as virtually indestructable, which led to mishandling of the pipes in transit and lack of care in their installation. Unplasticized PVC pipes were first manufactured in Great Britain in 1957, but were little used until 1962 when the first British Standard was introduced and the first flexible push-fit joint became available.

Gravel surrounds were soon adopted in the recommended installation procedures and a limit on deformation was called for. Earlier work in America had established that structural problems occurred in large diameter, thin-walled, corrugated steel culverts at deformations of approximately 20%. Similar values were obtained from early samples of uPVC pipe tested at the Building Research Establishment, though values of more than 33% deformation have since been reached before reversal of curvature, and by implication incipient failure, occurred. Application of a factor of safety of four, to cover variations in material properties and standards of workmanship on site, resulted in a limit of 5% on diametral strain for buried uPVC pipes.

Current installation recommendations (BSI, 1980) in effect retain these safeguards.\* The recommendations state

It is desirable that vertical deformation should be limited to 5% on completion of the backfilling, which can only be achieved by proper compaction of the backfill.

The Compaction Fraction test is included for the selection of suitable pipe surround material, which should extend from at least 100mm below the pipe

\* It also recommends a minimum cover depth of 0.9m to the finished surface of a road unless special protection is afforded.

to its crown. The limits of the test are such that single sized rounded, or pea, gravel, which alone satisfies the test with ease, is almost invariably specified. This material has the additional advantage of having similar properties whether compacted or not, thereby being safe for unsupervised installation work.

The need to import pea gravel in almost every case where uPVC pipe is laid has led to the surround constituting a large proportion of the total cost of an installation. The relevance of these recommendations, based on research into large diameter corrugated steel pipes, clay pipes and early uPVC pipes, while undoubtedly conservative, is as yet unresolved.

#### 1.4 The Approach Adopted for the Research

The aim of this research project is to question the efficiency of current practice for the installation of buried, non-pressure uPVC pipes as used in building drainage. The problem is essentially structural and the solution will provide the means for a better engineering design. The correct use of the materials forming the structure, in this case the pipe and surrounding fill, with due regard to their function will lead to greater efficiency and hence economy. The results of this work will provide engineers with some more of the information required for the design of uPVC pipes and will provide for the introduction of engineering to a subject that has hitherto relied on proven performance from conservative installation practice.

The investigations reported herein follow the well defined and established methods of product research. Problem definition and its background have largely been covered in the above sections. A thorough review of the literature on the subject was conducted in order to determine

whether sufficient information, in the form of experimental evidence and methods of theoretical prediction, was available for the design of uPVC pipes in building drainage applications. The quality of the published data is assessed and areas in which work is outstanding are detailed. This work is presented in Chapter 2. A review of the methods available for the outstanding research and a discussion of the philosophy behind the approach are presented in Chapter 3. Details of the experimental investigations, the equipment for which had to be developed before the experimental work could begin, are given in Chapters 4 and 5. Associated materials testing is discussed in Chapter 6. A preliminary theoretical study of the problem, which was primarily conducted to determine the feasibility of such work in extrapolating the experimental data, is presented in Chapter 7, and includes the results of attempted correlation between theoretical and experimental performance. Conclusions are drawn from the project in Chapter 8 and suggestions for further work are discussed.

### 1.5 Terminology

In order to avoid confusion in the use of varied terminology, particularly when discussing the work of other establishments, standard terms have been used throughout this thesis. These are defined below and summarised in Fig. 1.1 for reference.

The "crown" of the pipe is the uppermost point on the pipe circumference and the "invert" lowermost, both points lying on the vertical axis. The pipe "springings" are the diametrically opposite points on the pipe circumference that lie on its horizontal axis. The "shoulders" and "haunches" of the pipe are the points that lie equally between these orthogonal axes through the pipe cross-section in the upper and lower

segments respectively.

The "insitu" soil is that which occurs naturally on a site and in which trenches are excavated for the installation of pipes. The "bedding" layer consists of a structural material placed onto the trench bottom and in which the pipes are seated before further fill is introduced. The "sidefill" is the main structural component of the installation and usually extends from the invert to the crown of the pipe. An "arching" layer consists of a structural material of varying thickness placed above the pipe crown in order to relieve the pipe crown load. "Backfill" is the material used to reinstate the trench to the level of the surrounding area and commonly consists of the excavated "insitu" soil.

"Vertical diametral strain", commonly abbreviated to V.D.S. in the text, is defined as the reduction in the vertical diametral measurement divided by the original diameter. Diametral strain across any other axis is similarly defined.

## CHAPTER TWO





## 2 LITERATURE REVIEW

### 2.1 A Brief History of Buried Pipe Research

The first major research into the structural aspects of buried pipes was conducted by Marston at the Iowa State University, Ames, USA, in the early years of this century. The original objective was to find a rational and comprehensive method for the determination of the loads to which a buried pipe would be subjected in practice. The work was later extended by Spangler and Schlick, who became pioneers of structural research into flexible and rigid pipes respectively. The progress at Iowa was described by Spangler (1948) in an exhaustive report. Apart from some research in Switzerland by Voellmy in the late 1930s, little new work on the subject was done until Barnard (1957) proposed a variation of Spangler's design method for flexible pipes.

Apart from the experimental confirmation of the Marston-Spangler theory, there was little full-scale research activity until the early 1960s. Since then, however, investigations of the behaviour of rigid pipes have been commissioned in America by the US Bureau of Reclamation, and in the United Kingdom by the Ministry of Housing and Local Government, the Building Research Station and the Transport and Road Research Laboratory (Clarke, 1968; Bulson, 1985; and others). Product-based research has also been undertaken, notably by the American Concrete Pipe Association and the Clay Pipe Development Association (UK). This work has led to the production of design tables for buried rigid pipes (Young and Smith, 1970) and design recommendations (Young and O'Reilly, 1983).

Flexible pipe design has been diversified because of the wide range of the pipes described as flexible. For culverts placed in well compacted

fill beneath an embankment, it was suggested that the only structural requirement of the pipe wall was to resist the ring compressive stress. This idea formed the basis of the Ring Compression Theory developed by White and Layer (1960) and adopted by the American Iron and Steel Institute for the design of thin-wall metal culverts.

A second approach involves design against buckling failure, which is particularly prevalent in thin-walled flexible pipes buried in well compacted fills at a cover depth of more than one pipe diameter. Equations for the calculation of the critical radial pressure were produced by Cheyney (1963) and Meyerhof (with Baikie, 1963; and with Fisher, 1963). These have been recommended for use in pipe design (Compston et al, 1978), though considerable further work (notably Luscher and Hoeg, 1964 and 1965; Butterfield and Duns, 1966; and Bulson, 1966 and 1969) was available. More recent experimental work by Allgood and Ciani (1968), and Bulson (1972) indicates that the design equations are at variance with the results for deeply buried pipes, and this was confirmed by Cheyney (1976) who presented a theory that more closely fitted the test data.

For cases where the "hydrostatic" pressure effect, or deformation restraint, is less dominant, failure by excessive deformation is the most common mode of failure. This occurs in cases where the ratio of pipe stiffness to soil stiffness is greater than those in which buckling failures are prevalent, effectively those using thicker-walled flexible pipes, such as those made from unreinforced plastic and corrugated steel sheets, or poorer pipe surrounds. Spangler's proposed method of design (1941) formed the basis of much of the subsequent, mainly experimental, work in America, and only relatively recently have new methods of deformation prediction been sought there. Research has been conducted in Scandinavia, the Netherlands and Germany since the mid-1960s both to predict and explain the behaviour of plastic pipes, and different

prediction formulae have resulted from each. Investigations in the United Kingdom have usually involved the Transport and Road Research Laboratory and have included both full-scale and model tests, the latter using a geotechnical centrifuge.

Traditional design methods involve a check of all three criteria. Recent studies have been conducted by Gumbel (1984) towards a unified theoretical approach to flexible pipe design and these provide a useful contribution to the subject. Experimental verification of his design method has been undertaken at the Transport and Road Research Laboratory. The research conducted in different countries has largely reflected the methods of use therein; American research has typically considered embankment conditions whereas the Dutch, and to a lesser degree the Scandinavian, work has concentrated on the effects of sand and weak clay fills. The deflection of buried flexible pipes and its prediction will be discussed in greater detail in subsequent sections. Before this is done, some rationalisation of the considerable literature on the subject is necessary.

The work on prediction of pipe crown load, though principally developed for rigid pipes, will be outlined for completeness. Other research into the behaviour of buried rigid pipes has no relevance and will be omitted. It has been stated that uPVC pipes in normal use are not susceptible to failure by excessive hoop stress or buckling. For either of these conditions to occur, the deformation restraint of the soil (as defined by Luscher and Hoeg, 1965) has to be sufficiently great. For the relatively thick-walled pipes in normal use this is only likely to occur at large cover depths, such as those occurring under high embankments. This has been verified by field observations, particularly those of Gehrels and Elzink(1982), and by the experiments to verify Gumbel's design method (O'Reilly et al, 1982), in which the failure mode for underground uPVC

pipes was found to be excessive deformation. In these tests, buckling was induced in very thin-walled uPVC pipes having a standard dimension ratio (SDR)<sup>\*</sup> of 100, but such pipes are manufactured for above ground use only. For this reason, only design methods involving deflection prediction will be reviewed here. An exposition of all flexible design methods is presented elsewhere (Bulson, 1985; Gumbel, 1984).

Review of full-scale experimental work has been limited to that involving uPVC pipe because of the difference in the behaviour of pipes of other materials. Work on other types of flexible pipe has only been included where general behavioural trends can be inferred, such as when linked to design methods, or where model tests have been performed. Information has also been cited where it has a relevance to the design of equipment and instrumentation for full-scale tests.

## 2.2 Loads on Buried Pipes

The first authoritative research into the loads on buried pipes was conducted at the University of Iowa by Marston and involved extensive analytical and experimental investigations. An early publication (Marston and Anderson, 1913) detailed his theory of loads on pipes in trenches and was supported by experiments on rigid pipes. Research into the loads on rigid pipes continued at Iowa where Marston was soon joined by Spangler and Schlick. A review of this work was published by Marston (1930), who distinguished between pipes buried in trenches and those under embankment conditions, both positive and negative projecting. The work was extended by Schlick to cover loads on pipes in wide ditches. The theories resulting from this work, which provide for the calculation of vertical earth pressure on buried pipes, have been widely accepted and are comprehensively

\* SDR =  $D/t$

reported by Spangler (1960), Clarke (1968) and Bulson (1985). The theory, as applied to trenches, assumes a uniform distribution of the pipe crown pressure over the width of the pipe and is based on the relative vertical movement of the overlying purely frictional backfill, the concept originally used in the analysis of arching over a yielding trapdoor.

Marston's theories were based on full-scale experiments, and Spangler, in his review of the Iowa research (1948), found good agreement when attempting to correlate these results with the predicted loads. Similar experiments were conducted at the University of North Carolina, USA, and these again showed good agreement. Little new work was published on the subject until the 1960s, when Wetzorke and Christensen proposed variations to the value of the ratio between vertical and horizontal pressure used in the design, resulting in a lower pressure on the pipe crown. Marston's theories were used as the basis for the prediction of external loads on buried rigid pipes published by the Building Research Station (Young and Smith, 1970) and developed in a guide published by the Transport and Road Research Laboratory (Young and O'Reilly, 1983).

When considering the earth loads applied to flexible pipes, Spangler (1941) again recommended the use of Marston's theories. In tests under embankment conditions he found that the vertical pressures on rigid pipes were about three times as great as those on flexible pipes. From this he concluded that any method of deformation prediction should consider specified conditions of load and installation. Spangler's use of the earth load theory that he helped to establish accounted for his neglect of the initial component of horizontal stress as he treated vertical load and horizontal pipe displacement as two distinct phenomena. In contrast, the theory of pipe loads developed by Voellmy in Switzerland in the late 1930s assumed that load was applied to the pipe by a wedge of soil bounded by inclined sliding surfaces (Fig. 2.1). This resulted in the inclusion of an

initial horizontal pressure component when describing the pressure distribution around flexible pipes. Subsequent work in Germany and Scandinavia took account of this theory in the production of design methods.

The influence of surface loads on the vertical stress at the pipe crown has traditionally been determined using the elastic theory propounded by Boussinesq and, particularly for shallow buried pipes, these loads are often dominant. Measurements on experimental pipelines laid beneath a major road (Trott and Gaunt, 1976) indicated that construction traffic provided the most severe loading condition, in which heavily laden vehicles passed over pipes on an incomplete road surface. Measurements of vertical stress on the crown of clay pipes showed that the values caused by construction traffic were three times greater than those when the road was in use. In the case of uPVC pipes, it was found that pipe deformation had largely stabilised after the passage of the first few vehicles and that virtually no increase occurred once the pavement was complete. When simulating building drainage, therefore, it is clear that surface loads will in this case also have most influence on pipe behaviour. A summary of the methods suggested by Gumbel and Wilson (1982) for the calculation of loads on buried flexible pipes is presented in Fig. 2.2. Their paper suggests that free-field horizontal and vertical stresses  $p_v$  and  $p_h$  respectively) should be determined and that these should be converted into uniform ( $p_z$ ) and distortional ( $p_y$ ) components for use in the calculation of pipe behaviour.

### 2.3 Prediction of Diametral Strain in Buried Flexible Pipes

A history of the development of diametral strain prediction for buried

flexible pipes is included here to illustrate the philosophy behind the research, both experimental and theoretical, that has subsequently been conducted. A major review of such work was written by Gumbel (1984) as a prelude to his formulation of a unified design method, and this will provide the reader with a more detailed and critical appraisal of the various design methods. In his critique, Gumbel distinguishes between interaction analyses in which the soil support is modelled by discrete linear springs and those in which it is modelled by an elastic continuum. Gumbel argues, quite rightly, that the latter is to be preferred, because it allows the pipe and soil to be analysed as a composite structure, thereby avoiding the need to estimate the statically indeterminate pressure distribution at the pipe-soil interface. While this is the method adopted in the preliminary theoretical investigations reported in Chapter 7, it is the analyses based on discrete linear springs that have generally influenced experimental work and it is to this that attention is focused. The discussion herein explores the implications of such work for the design of full-scale experiments.

The fundamental approach to all simple pipe-soil interaction analyses, as Gumbel acknowledges, involves the assumption of initial and equilibrium pressure distributions around the pipe wall. The difference between the two is accounted for by the compression (or extension) of soil springs in response to outward (or inward) movement of the pipe wall, thereby relating pipe deformation to the applied load and the pipe and soil stiffnesses. As stated earlier, the approach to the distribution of applied loads has an important influence on the initial pressure distribution and consequently the design method as a whole.

### 2.3.1 Spangler's Development of the Iowa Formula

The first comprehensive exposition of the structural design of flexible pipes was issued by Spangler (1941) from the Iowa Engineering Experiment Station. This document cited the behaviour of large diameter corrugated steel culverts under earth loading as experimental verification of the proposed theoretical analysis, which was based upon the experimentally determined distribution of pressures around a flexible pipe shown in Fig. 2.3. The load due to earth fill is uniformly distributed over the width of the pipe, after Marston. This is matched by a vertical bedding reaction, the extent of which is defined by the bedding angle ( $\alpha$ ) and which is dependent upon the width of bedding and the flexibility of the pipe. The horizontal pressure distribution is due to passive soil resistance, which is a function of sidefill density. Experimental work showed that, for any particular soil state, the horizontal pressure at any point on the pipe wall was directly proportional to the horizontal movement of that point, this ratio being defined as the Modulus of Passive Resistance of the soil,  $e_s$  (kPa/m). Assuming the deformed shape of the pipe to be elliptical (this term has been adopted by common usage in the literature, and will be used herein, to describe the shape of relatively unrestricted deformation, though the true shape is described by Lusher and Hoeg, 1964, as oval), a parabolic distribution of horizontal pressure over the central 100° was proposed.

Experimental work was used to validate the thin-ring elastic theory for pipes with more than 3% diametral strain and, using the above pressure distribution, static analysis led to a formula for immediate horizontal diametral reduction  $\Delta_h$

$$\Delta_h = \frac{K_b w_c r^3}{E_p I + 0.061 e_s r^4} \quad (2.1)$$



where  $K_b$  = bedding constant dependent upon the bedding angle  
 $w_c$  = vertical load per unit length of pipe  
 $r$  = mean radius of pipe  
 $E_p I$  = bending stiffness of the pipe ring

Experimental work resulted in the introduction of a deflection lag, or time dependent, factor (typically in the range 1.0 to 1.5) to the numerator of this expression when used to calculate long-term diametral strain. The Modulus of Passive Resistance of soil was found to be difficult to quantify and this led to a study of its characteristics by Watkins and Spangler (1958). Their work resulted in a redefinition of the stiffness parameter as the Modulus of Soil Reaction ( $E'$ ) where

$$E' = e_s r \quad (2.2)$$

By rearranging equation 2.1 and substituting this expression, the well-known expression for horizontal diametral reduction is obtained

$$\Delta_h = \frac{K_b w_c}{E_p I / r^3 + 0.061 E'} \quad (2.3)$$

For general use, Spangler suggested an  $E'$  value of 700 psi (5MPa) for any backfill when placed at 90% of its maximum dry density.

It has been widely stated (Joekes and Elzink, 1985, and others) that the equation is of the general form

$$\text{horizontal diametral reduction} = \frac{\text{vertical load factor}}{\text{pipe stiffness} + \text{soil stiffness}} \quad (2.4)$$

For flexible pipes, the stiffness of the pipe ring is small in comparison with the stiffness of the soil and this resulted in the formulation by Meyerhof of an approximate version of the expression

$$\Delta_h = 2.7 P_h/e_s \quad (2.5)$$

where  $P_h$  = horizontal pressure on pipe =  $2w_c r$ .

By relating  $e_s$ , which is not related to a standard soil property that can be readily measured in the laboratory, to the constant of horizontal soil reaction, which can, approximate solutions were achieved (Bulson, 1985). The importance of soil stiffness in the calculation led to an intensive research effort over the last forty years to quantify  $E'$  for design. This took several different forms, the most empirical being the back analysis of field data from 113 installations covering a wide variety of pipe and fill combinations (Howard, 1977). From this study, he concluded that it was fill compaction that had the greatest influence on the value of  $E'$  and that the deflection lag factor, when applied to equation 2.3, ranged between 1 and 6. Single  $E'$  values were produced for groups of materials and their relative densities and these are reproduced in Table 2.1. Although the variation in  $E'$  was smaller where good quality fills were used, considerable differences were found in  $E'$  values for similar installations. To measure  $E'$  in the laboratory in a situation more closely matching the conditions thought to prevail beside a flexible pipe, the Modpares device, shown in Fig. 2.4, was developed (Watkins and Nielson, 1964). Further attempts to quantify  $E'$  in the laboratory were carried out by Bhandhausavee (1968), and more particularly Nielson (Nielson et al, 1969). Jaaskelainen (1973) produced a comprehensive report on the various methods of obtaining a suitable soil stiffness term in which he points out the compression of the fill material is attributable to both volumetric and shear strain, though no distinction is usually made.  $E'$  is usually estimated from Young's Modulus ( $E$ ) and Poisson's Ratio ( $\nu$ ) rather than bulk and shear moduli. He concludes that  $E'$  must be measured in laboratory tests and

**Table 2.1 Recommended E' Values for use in the Iowa Formula  
(after Howard)**

Soil type for sidefill	E' for degree of compaction of sidefill in MPa			
	None material dumped	Slight < 85 % proctor	Moderate 85-95% proctor	High > 95 % proctor
Fine-grained soils with medium to high plasticity	No data available, consult a competent soils engineer. Otherwise use E' = 0.			
Fine-grained soils with medium to no plasticity and < 25% coarse-grained particles	0.34	1.37	2.74	6.86
Fine-grained soils with medium to no plasticity and > 25% coarse-grained particles	0.69	2.74	6.86	13.71
Coarse-grained soils with < 12% fines	1.37	6.86	13.71	20.57
Crushed rock	6.86	20.57	20.57	20.57
Accuracy in terms of % deflection	± 2	± 2	± 1	± 0.5

Note: Values applicable only for fills less than 15m.  
If bedding falls between two compaction categories,  
select lower E' value or average the two values.

recommends the use of the oedometer, because it is in relatively common use, although results from the cylinder apparatus were more encouraging. Parmalee and Corotis (1974) applied finite element techniques to analyse the problem and found  $E'$  to be a function of pipe stiffness and height of fill in addition to the soil properties. Despite these efforts to quantify  $E'$ , Spangler acknowledges in his later work (such as the discussion of Watkins and Moser, 1971) that  $E'$  is a semi-empirical constant and that values based on judgement and experience should be used in design.

When applying the Iowa formula to uPVC pipes used in building drainage applications, there are several factors to consider. The theory was developed and verified for large diameter corrugated steel culverts usually under earth load in embankment conditions, a situation far removed from the one considered in this project. For small diameter, shallow buried pipes, the most severe loads will result from traffic and the bedding conditions will be difficult to ascertain. It has also been shown (Howard, 1972; Soini, 1982), and will be further demonstrated later, that the assumption of elliptical deformation, on which the pressure distributions are based, is not valid in certain circumstances. This will also affect the determination of vertical diametral reduction, previously gained from the predicted horizontal value by the assumption of elliptical deformation. A further difficulty lies in the evaluation of load using Marston's theories, which, as discussed in section 2.2, are dependent upon the relative flexibility of the pipe ring and the sidefill. The main restriction on the use of the formula lies in the assignation of  $E'$  to the sidefill, which, as Gumbel reiterates, is heavily dependent upon the initial lateral pressure due to fill placement and compaction and the overall distribution of ground stresses caused by surcharge loads, in addition to the other factors mentioned above.

The method and its shortcomings have been discussed in some detail to

illustrate both the background to current research programmes and the danger of preconceived ideas in research of this kind. The somewhat greater success of the Scandinavian and European work is probably due in part to the detachment from the early American ideas and the need for Gumbel's fresh approach from fundamental principles is clear. Other design methods will be discussed in lesser detail to highlight the developments in thought on the subject.

### 2.3.2 Barnard's Method

In connection with research carried out on behalf of the American Water Works Association, Barnard (1957) proposed a different design method which was later adopted by them. He regarded the horizontal pressure exerted by the pipe wall on the sidefill as similar to the pressure of a strip footing having a width equal to the central  $100^\circ$  arc of the pipe. This analogy assumes that the "horizontal settlement" becomes insignificant at a distance of 2-3 pipe diameters from the wall (Fig. 2.5) and is equal to the shortening of a uniformly stressed earth column of length  $L/2 = 1.25D$ . The method involves a similar assumption of equilibrium earth pressure distribution under load to that of Spangler (Fig. 2.3), but has the advantage of accounting for the acting lateral soil pressure, as the initial horizontal pressure, in the design. Vertical crown pressure is equated to the overburden pressure, thereby removing the influence of pipe flexibility from its determination, and the radial pressure is modified by a shape factor, which accounts for local changes of curvature in the deforming pipe wall.

### 2.3.3 Molin's Method

Molin devised a method of pipe deformation prediction based on experimental work at the Chalmers Institute of Technology, Gothenburg, on glass fibre reinforced polyester pipe (Molin, 1967). The experiments themselves are of no consequence here, but the implications for pipe design drawn from the results are extremely important and these are reflected in his later design proposals. For this reason, these findings will be discussed here before the method is outlined.

The vertical load on the pipe due to the dead weight of the earth fill was found to be less than the total overburden pressure at pipe crown level, and a field measurement of approximately 70% of the overburden pressure was thought to be typical. Since the load depends on, among other factors, the ratio between the vertical compression of the pipe and the sidefill, the degree of compaction of the sidefill was thought to influence the load. However, the load was considered unlikely to exceed the weight of the overlying fill in the case of flexible pipes. Pipe deformation in non-cohesive material was found to depend upon the stress in the soil, soil compaction, particle shape, and particle size distribution. While acknowledging that fill material is only elastic to a limited extent, he considered that values of modulus of elasticity and lateral compression coefficient were required for analysis. The use of a secant modulus to describe deformation behaviour and a tangent modulus to describe buckling behaviour was suggested. The cylinder apparatus was used to determine the modulus of elasticity ( $E_s'$ ) of the soil and this produced reasonable results except for very loose fills, in which the  $E_s'$  value was overestimated, probably because of the limited room for particle rearrangement in the apparatus. The oedometer test overestimated the  $E_s'$  value by a greater amount.

For equilibrium of a buried circular ring section with a low ring

stiffness to be reached, he postulated that a roughly even distribution of earth pressure is required. What little inherent stiffness the pipe has will cause the attraction of a slightly higher proportion of vertical load. Since the horizontal pressure on the pipe must be greater than the static earth pressure, a deformation of the pipe is necessary to fulfill this criterion. The magnitude of the deformation is governed entirely by the deformation characteristics of the sidefill. From the literature, it was deduced that elliptical pipe deformation was to be expected, but he discovered that for pipes of very low rigidity, irregular pipe deflections occurred. These were attributed to variations in earth pressure and sidefill characteristics. Where the effect of rocks below the pipe was simulated, high local deformation occurred immediately, after which the deformation curves were roughly parallel to those of undisturbed sections.

For the earth pressure distribution thus described, the pipe cross-section was said to act as a compressed ring with small moments (cf. White and Layer, 1960). For pipes of low wall stiffness, buckling is then the critical factor in pipe design, the buckling load increasing with the degree of compaction of the sidefill. Whereas traditional calculation of ring moments (Spangler, 1941) is independent of pipe stiffness, experimental evidence indicated that ring moments are proportional to both the stiffness and the deflection of the pipe. Excessive moments can be controlled, therefore, by a limit on deflection and by thorough compaction of the sidefill. In cases of low pipe stiffness or large diameter, the stresses induced by sidefill compaction were found to be greater than those in the permanent state after backfilling.

Variation in load on the pipe, such as that due to traffic loads, internal pressure, and varying groundwater level, were found to cause variation in the pipe deformation. Since the pipe only partially recovered on removal of the load, increasing deformation was thought to occur under

repeated load, possibly leading to failure. Where traffic loads are likely to occur, minimum cover depths and standards of sidefill treatment were thought to be necessary.

These wide ranging conclusions represent a major contribution to the understanding of flexible pipe behaviour and formed the basis of his design method, the derivation of which involved the assumption of a uniform equilibrium pressure distribution (Fig. 2.6). Using this, Molin integrated the lateral soil compression caused by horizontal stress in excess of the earth pressure "at rest", determined from elastic theory. This led to an expression for the change in the horizontal diametral measurement given by

$$\Delta_h = c \cdot \frac{p_v}{E_s'} \quad (2.6)$$

where  $p_v$  = total applied vertical pressure

$E_s'$  = secant modulus of the sidefill

$c$  = dimensionless coefficient

The coefficient ( $c$ ) is a function of the Poisson's Ratio of the fill ( $\nu_s$ ) and, therefore, the lateral coefficient of earth pressure at rest ( $K_0$ ).

The results of further experimental work provided the basis of his design method using this equation (Molin, 1971), which is of the form

$$\Delta_v/D = \frac{p_v}{E_s'} \times \frac{0.083}{S + 0.122} \quad (2.7)$$

where  $\Delta_v$  = vertical diametral reduction

$D$  = original mean diameter of pipe

$S$  = stiffness factor

The stiffness factor is defined as



$$s = \frac{E_p I}{E_s r^3} \quad (2.8)$$

These equations can be combined to produce an expression of the standard format, given by equation 2.4, as follows

$$\Delta_v/D = \frac{0.083 p_v}{E_p I/r^3 + 0.122 E_s} \quad (2.9)$$

For calculation of the secant modulus of the fill, Molin recommends the hollow cylinder apparatus. In this form, it can be seen that the expression does not differ fundamentally from the Iowa formula.

#### 2.3.4 German Developments

The first major departure from the pressure distributions suggested by Spangler and Molin was that proposed by Howe et al (1966). They noted that the distribution of earth pressure around the pipe circumference depends upon the "deformability" of the pipe and denounced the labelling of pipes as rigid or flexible, preferring to use a relative scale of rigidity. They recognised that the magnitude of the earth pressure at any point around the pipe circumference is the result of pipe-soil interaction, thereby being statically indeterminate, and that the movement of the pipe springings under load is both outward and downward. Assuming that the invert of a flexible pipe does not settle, the vertical pressure on the underside of the pipe near to the springings will consequently be greater than that near the invert, as shown in Fig. 2.7.

Leonhardt proposed an improvement, considered by Gumbel to be the

first real advance, on the Iowa method of prediction by considering pipe deformation as a function of the excess of vertical pressure over the applied horizontal pressure (Leonhardt, 1972). He also observed that the uniform invert reaction proposed by Spangler was appropriate for a rigid pipe on an elastic bedding, but that for a flexible pipe, the distribution proposed by Howe et al (1966) was more likely to be accurate. Using a slightly modified version of the method propounded by Barnard (1957), he calculated pipe deformation using a combination of the two extremes of invert reaction, the pressure distribution used depending on the relative stiffness of the pipe. The artificial precision of such pressure distributions when compared to practice led to the reversion to a uniform invert pressure distribution in the version adopted by the Abwasser Technische Vereinigung (known as the ATV method).

The earth pressure distributions assumed by Leonhardt in his design method (ATV, 1978) are shown in Fig. 2.8, in which the combination of uniform and distortional pressures are clearly distinguished. His apparently simple formula for the calculation of vertical diametral strain is

$$\Delta_v/D = c_v^* \frac{p_v - p_h}{E_p I/r^3} \quad (2.10)$$

where  $p_v$  and  $p_h$  are the vertical and horizontal components of pressure and  $c_v^*$  is the deflection coefficient. It is in the calculation of this coefficient that the sophistication of this method manifests itself. Substitution of the relevant factors and rearrangement yields an equation of the standard form as follows

$$\Delta_v/D = \frac{0.083 (p_v - p_h)}{E_p I/r^3 + 0.077 \xi E_2} \quad (2.11)$$

where  $\xi$  is a correction factor, applied in cases where the *insitu* soil forming the trench wall is less stiff than the sidefill, and  $E_2$  is the modulus of elasticity of the sidefill. Determination of the load parameters is particularly complicated with both earth and imposed loads being dependent upon such factors as the elastic stiffnesses of the backfill, sidefill, trench bottom and the pipe itself. Recommended values for the parameters required in the calculation are given in the design manual (ATV, 1978). The recommended values for the modulus of elasticity of the sidefill are included in Fig. 2.8.

This level of sophistication for what can only be, at best, an approximate method of deformation prediction, because of the nature of the parameters involved and the assumption of an equilibrium pressure distribution, is questionable. The necessity of assumed values for the numerous parameters would lead to doubt over any specific answer and widely differing values could be obtained for any particular installation type depending upon the degree of conservatism applied. It is thought that consistent use of conservative parameters would render the method useless for practical design (Gehrels, 1982).

### 2.3.5 Bossen's Formula

A wholly theoretical approach was adopted by Bossen in the Netherlands (Bossen, 1967) in the mid 1960s and has been widely used by Dutch engineers, although other theories are now usually preferred. His approach is basically similar in concept to the previous methods and is based on the applied pressure distribution shown in Fig. 2.9. The formula that he

developed may be expressed as

$$\Delta_v/D = \frac{(0.05 + 0.0267n) + p_v}{E_p I/r^3 + 0.067 p_v (C-3.5-1.5n)} \quad (2.12)$$

where  $n$  is an installation parameter and  $C$  is Buisman's soil coefficient, for both of which he suggests values (Fig. 2.9). Calculation of the applied vertical load due to surcharge is based on an equivalent soil load, the total load parameter being influenced by the compaction applied during installation. The soil stiffness term in the equation is similarly dependent upon the applied compaction, but also on the vertical pressure. The demise of this formula is probably a reflection on its accuracy, at least in relation to the more recently developed methods, and has been included principally because of the approach adopted in its formulation.

#### 2.3.6 The USBR Equation

In contrast to the above methods of deformation prediction, a strictly empirical relationship based upon back-calculated parameters from field measurements of buried flexible pipes is reported by Howard (1981B). The data were obtained from studies at the United States Bureau of Reclamation and the resulting equation bears its name. The method was proposed as follows

1. Prediction of vertical rather than horizontal deflection;
2. Prediction of deflection immediately after backfilling (initial deflection), as distinct from the deflection when maximum load is reached;
3. Prediction of long-term deflection based upon initial deflection;
4. Prediction of both average and maximum (peak) deflections;
5. Use of prism load on the pipe rather than the Marston load theory;

6. Incorporation of a design factor to permit actual or safe design parameters to be calculated; and
7. The use of a soil stiffness factor rather than the Modulus of Soil Reaction.

The method is, however, restricted to cases where the depth of cover is 15m or less and where the trench wall support provided by the insitu soil is at least as good as the sidefill. The equation, which essentially follows the standard format of equation 2.4, is given by

$$\Delta_v/D = T_f \frac{A Y h}{E_p I/r^3 + S_f D_f} + C_f + I_f \quad (2.13)$$

where  $T_f$  = time lag factor

$A$  = combination of conversion factors and bedding constant

$Y$  = backfill density

$h$  = depth of cover

$S_f$  = soil stiffness factor

$D_f$  = design factor

$C_f$  = construction factor (percentage V.D.S.)

$I_f$  = inspection factor (percentage V.D.S.)

The initial deflection referred to here is that which occurs between the completion of the sidefilling, when "negative" deformations are often recorded, and the completion of the backfilling. Delay in measurement of the latter, even of a few days, can cause significant increases in the value. Soil load is calculated using wet density unless part of the backfill becomes submerged, in which case the buoyant value is used for that part. Guidance on the choice of the soil stiffness factor, which is analogous to the  $0.061 E'$  used in the Iowa formula, is given in Table 2.2, the values bearing roughly the same relationship to those of  $E'$  in Table

Table 2.2 Parameters for use in the USBR Equation (after Howard)

Sidefill Soil Classification	Degree of Compaction			
	Dumped	Slight < 85% Proctor	Moderate 85-95% Proctor	High > 95% Proctor
Highly compressible fine-grained soils	Soils with medium to high plasticity or significant organic content. No data available.			
Fine-grained soils with medium to no plasticity and <25% coarse-grained particles	$S_f = 0.02^{**}$ $T_f = 1.5^*$ $C_f = 2.0$ $D_f$ for A = 1.0 B = 0.5 C = 0.3	$S_f = 0.08$ $T_f = 2.0^*$ $C_f = 2.0$ $D_f$ for A = 1.0 B = 0.5 C = 0.3	$S_f = 0.16$ $T_f = 2.5^*$ $C_f = 1.5$ $D_f$ for A = 1.0 B = 0.67 C = 0.5	$S_f = 0.69$ $T_f = 2.5^*$ $C_f = 1.5$ $D_f$ for A = 1.0 B = 0.75 C = 0.67
Sandy or gravelly fine-grained soils with medium to no plasticity and >25% coarse-grained particles. Coarse-grained soils with fines: Sands, gravels with >12% fines	$S_f = 0.07$ $T_f = 1.5^*$ $C_f = 2.0$ $D_f$ for A = 1.0 B = 0.5 C = 0.3	$S_f = 0.16$ $T_f = 2.0^*$ $C_f = 2.0$ $D_f$ for A = 1.0 B = 0.5 C = 0.3	$S_f = 0.41$ $T_f = 2.5^*$ $C_f = 1.5$ $D_f$ for A = 1.0 B = 0.67 C = 0.5	$S_f = 1.03$ $T_f = 2.5^*$ $C_f = 1.0$ $D_f$ for A = 1.0 B = 0.75 C = 0.67
Clean coarse-grained soils: Sands, gravels with <12% fines	$S_f = 0.08$ $T_f = 1.5$ $C_f = 2.0$ $D_f$ for A = 1.0 B = 0.67 C = 0.5	$S_f = 0.27$ $T_f = 2.0$ $C_f = 2.0$ $D_f$ for A = 1.0 B = 0.67 C = 0.5	$S_f = 0.82$ $T_f = 2.5$ $C_f = 1.0$ $D_f$ for A = 1.0 B = 0.75 C = 0.67	$S_f = 1.37$ $T_f = 2.5$ $C_f = 0.5$ $D_f$ for A = 1.0 B = 1.0 C = 0.75
Crushed rock	$S_f = 0.41$ $T_f = 2.0$ $C_f = 1.0$	$D_f$ for A = 1.0 B = 0.67 C = 0.5	$S_f = 1.37$ $T_f = 3.0$ $C_f = 0.5$	$D_f$ for A = 1.0 B = 1.0 C = 0.75

Note: \* Double  $T_f$  value if bedding will become saturated

\*\* All  $S_f$  values are in MPa

2.1. It is in the design, time-lag, construction and inspection factors, recommended values for each of which are also given in Table 2.2, that the philosophy of this method differs from that of the Iowa formula. The design factor is introduced to provide, in effect, confidence limits to the design data, a value of 1.0 giving an average value and the two further values representing two levels of safety factor. The time-lag factor is introduced to quantify the increase in deformation with time in relation to the immediate deformation, as distinct from that occurring when maximum load is reached. The construction factor is included to account for the fluctuations in deformation along the length of a pipeline, quoted as  $\pm 2\%$  V.D.S. by Howard (1977) and  $\pm 3\%$  V.D.S. by Gehrels (1972), caused by variation in the insitu soil and the laying technique of the sidefill. The inspection factor is used to reflect the likelihood of adherence by a contractor to the installation specification and is an attempt to quantify the "site practice factor" referred to by Boden (1976).

The equation is again more suited to American conditions, for example no guidance is given on the treatment of surface loads, and is of little direct relevance to building drainage in the United Kingdom. It does, however, illustrate clearly the prevalent thoughts on the subject of flexible pipe design and possibly some desperation at the failure of the Iowa formula to produce accurate predictions. While it is a partial improvement on the Iowa formula, if only in its attempts to isolate the parameters for which values are difficult to assign, it remains subject to the same conceptual error of failing to treat the pipe-soil system as the basic structure.

#### 2.3.7 Watkin's Method

Watkins, while working at the Iowa State University, played a major

role in the refinement and revision of the Iowa formula, (Watkins and Spangler, 1958) and he continued to investigate the subject in great detail thereafter. He eventually dismissed the formula as inadequate (Watkins, 1970) because of the inaccuracy of its predictions of deformations in the field, the values being generally overestimated. His own research at the Utah State University led to the development of a further design method for the prediction of diametral strain of large diameter buried flexible pipes subjected to external soil pressure (Watkins and Smith, 1973). The method is based on empirically determined design charts relating pipe deformation to measurable properties of the pipe and soil. Two dimensionless coefficients are used in the design. A "Ring Deflection Factor" is defined as the ratio of the vertical diametral strain of the pipe to the vertical compression ( $\epsilon_s$ ) of the sidefill. This factor is plotted against the Stiffness Ratio ( $R_s$ ) of the soil stiffness ( $E''$ ) to the flexural stiffness of the pipe ( $E_p I/D^3$ ), as shown in Fig. 2.10. Watkins recommends the use of the oedometer (or confined compression) test for the determination of  $\epsilon_s$  and  $E''$ , the latter being calculated as a secant modulus.

Watkins' experiments indicated that the Ring Stiffness Factor tended to an asymptote at unity, implying that for pipes of very low stiffness, the vertical diametral strain of the pipe does not exceed the compression of the adjacent sidefill. Gumbel (1984) points out that this is incorrect, Watkins being misled by errors in his earlier analysis. The tests reported by Watkins and Smith (1973) are for relatively rigid steel pipes and Gumbel cites later work on far more flexible pipes, with a Stiffness Ratio of up to an order of magnitude greater, which showed that the Ring Stiffness Factor reached approximately twice the value predicted by Watkins. Soini (1982, A) predicts even higher values for flexible pipes in soft soils and this approach is discussed further in section 2.4.6. The method again neglects the horizontal pressure component and this resulted in flaws in the design



of Watkins' much criticised experiments (Spangler, 1971), which are discussed in a later section of this review

### 2.3.8 Closed Form Solutions

The most notable contribution to this type of analysis in the field of buried flexible pipes was by Burns and Richard (1964), who produced an "exact" solution for an elastic circular pipe buried in an isotropic, homogeneous, elastic medium of infinite extent and subject to a uniform vertical pressure. Solutions were provided for cases where the pipe-medium interface was treated as both frictionless and fully bonded, and were applicable only where the cover depth was greater than one pipe diameter. This analysis is the one most used in attempts to adapt closed form solutions to buried pipe design. Its initial application was in the derivation of expressions for parameters used in the Iowa formula, which again shows the preconceived ideas of pipe behaviour resulting from the early American work. In later work it was directly applied to the development of non-dimensional design charts relating deflection and other parameters to the properties of the pipe-soil system.

The derivation of the solution was based on the confined modulus of the soil medium ( $M_g$ ) and its Poisson's Ratio ( $\nu_g$ ), and the resulting deflections are sensitive to both parameters. As Gumbel notes, although the confined modulus is a more rational index of backfill stiffness than  $E'$ , the need to quantify the Poisson's Ratio of the soil introduced a new element of uncertainty. In addition, the analysis contains only one load parameter, surface pressure, and is again subject to the conceptual error of neglecting the applied horizontal pressure component.

### 2.3.9 Finite Element Studies

Various finite element studies of buried pipes have been conducted since the late 1960s and these are discussed in greater detail by Gumbel (1984). These have been conducted mostly in America and are directed towards large diameter pipes under earth load. Gumbel isolates the three main areas of study as individual structure analysis, parametric studies, and the generation of design charts. Such work in this project has taken the form of a preliminary parametric study using linear elastic soil models, principally to assess the feasibility of extension and sophistication of the finite element work, possibly leading to the production of design charts. In this review, a single method will be cited to illustrate the range of soil models currently in use and summarised by Bulson (1985).

The program was developed at the US Naval Civil Engineering Laboratory and is entitled CANDE, an acronym for culvert analysis and design. Elements are used to model the pipe, the pipe-soil interface and the soil, and it is the properties of the latter that are of interest. Three soil models have been used.

(a) A linearly elastic soil model has been used to provide an approximate description of the behaviour of flexible pipes. The model was found to produce reasonable accuracy when used for parametric studies.

(b) An incremental elastic soil model involves the application of the linear model in a series of steps, assuming that the stiffness of the soil increases with greater vertical pressure. This assumption is valid if the soil is in confined compression.

(c) A variable modulus soil model, which relates the secant shear modulus ( $G_s$ ) to the maximum shear modulus ( $G_{max}$ ) and the hyperbolic shear strain ( $Y_h$ ) in the form

$$G_s = \frac{G_{\max}}{1 + Y_h} \quad (2.14)$$

where  $Y_h$  is dependent on the ratio of the shear strain to a reference shear strain.

The expression has been found to produce good agreement with experimental data from large diameter conduits. Further details of this work can be found in Katona et al (1976).

#### 2.3.10 Gumbel's Method

A design method using the composite pipe-soil system as the basic structural unit is introduced by Gumbel and Wilson (1981) and presented in greater detail, with slight modifications, in Gumbel et al (1982). A comprehensive description of its development is given in Gumbel (1984). By considering the soil as part of the structural system, the need to estimate statically indeterminate pressure distributions is eliminated and all pipe-soil interaction forces, which themselves have no direct bearing on the design of the pipe, are included in the elastic analysis. It is then possible to derive a direct relationship between statically determinate system loads and the relevant performance parameters. Ring deflection and pipe buckling are considered as the performance criteria, ring strength being of secondary importance as a design criterion for flexible pipes.

The buried pipe structure used in the analysis is idealised as a linearly elastic system consisting of a long, thin-walled cylinder deeply embedded in a uniform weightless soil medium and subject to two-dimensional loading in the plane of cross-section. Terms are defined for both flexural and compressive stiffness of the pipe ring in terms of the elastic constants ( $E_p$ ,  $\nu_p$ ) of the pipe material and soil stiffness is defined as

the plain strain modulus,  $E_s^*$ , where

$$E_s^* = \frac{E_s}{(1 - \nu_s^2)} \quad (2.15)$$

and  $E_s$  = Young's modulus for the soil

$\nu_s$  = Poisson's ratio for the soil.

Pipe-soil interaction parameters are also defined for compression and flexural stiffness, the flexural stiffness ratio being most important and defined as

$$Y = E_s^*/S_{fp} \quad (2.16)$$

where  $S_{fp} = E_p I/D^3$  = flexural stiffness of pipe ring.

Using this ratio, typical ranges of system behaviour are defined for different pipe materials and these are presented in Fig. 2.11. In this classification, rigid behaviour is said to occur when more than 90% of the distortional load is carried by the pipe ring, flexible behaviour when less than 10% is thus carried.

External loading on the system is represented by uniform vertical and horizontal pressures,  $p_v$  and  $p_h$ , which are defined as the free-field total stresses at the pipe mid-height. The contributions to  $p_v$  and  $p_h$  by backfill weight, surcharge and groundwater pressure are calculated by standard techniques of soil stress analysis, and these are discussed in section 2.2. The dead load lateral pressure ratio,  $K_d$ , relates the free-field horizontal pressure,  $p_{hd}$ , and vertical pressure,  $p_{vd}$ , due to dead load as follows

$$P_{hd} = K_d P_{vd} \quad (2.17)$$

and is a function of the soil properties, method of construction, degree of compaction, pipe stiffness and proximity of the trench walls. The relative importance of these factors has yet to be established, although the state of compaction of the backfill is known to have a significant effect.

Provisional design values for  $K_d$  are recommended for various soil groups (defined in Table 2.3) as follows

Soil Group	Loose Backfill	Compacted Backfill
I	0.2 - 0.4	0.3 - 1.0
II	0.3 - 0.5	0.4 - 1.0
III	0.2 - 0.7	0.5 - 1.0
IV	0.1 - 0.8	0.6 - 1.0

For uncompacted (loose) backfill,  $K_d$  values could range from fully active,  $K_a$ , to a value at rest,  $K_0$ , and for soils from Groups III and IV the lowest probable values have been selected to allow for the possible presence of air voids. For compacted backfill, the lowest probable value corresponds to  $K_0$ . Values of  $K_d$  approaching 1.0 imply more uniform loading conditions, and those approaching zero more distortional conditions. A range of values should be used in design unless the critical performance criterion has been identified, where the following rules apply.

1. If deflection is critical, assume the lowest probable value of  $K_d$ .
2. If buckling is critical, assume the highest probable value of  $K_d$ .

The loads on the system are divided into uniform and distortional components of pressure, as shown in Fig. 2.12 which illustrates their separate and combined effects. The uniform pressure component,  $p_z$ , is defined as

**Table 2.3 Backfill Groups and Corresponding Provisional  $E_s^*$  Values for Design**

Soil Group	Description	Fines Per Cent	Comments
I	GRAVEL	<5	Clean to slightly clayey silty GRAVELS
II	SAND	<5	Clean to slightly clayey silty SANDS
III	GRANULAR WITH FINES	5-35	Clayey/silty or very clayey/silty GRAVELS OR SANDS
IV	COHESIVE (Liquid limit less than 50)	>35	Inorganic CLAYS/SILTS of low to medium plasticity
NOT SUITABLE AS STRUCTURAL FILL - organic soils, high plasticity soils, chalk			

Soil Group	Worst probable / average value of $E_s^*$ , MPa, for assumed backfill density		
	Loose <85% BS max	Medium 85-95% BS max	Dense >95% BS max
I GRAVELS <5% fines	5 15	20 30	30 40
II SANDS <5% fines	2 5	10 20	20 30
III GRANULAR WITH FINES (5-35% fines)	1 3	5 10	10 15
IV COHESIVE >35% fines, LL<50	0 0.2	0.5 2	1 3

Note: BS max is the maximum dry density achieved in 2.5 kg rammer compaction test (Test No.12 to BS 1377).  
Fines are particles passing the 63  $\mu\text{m}$  sieve.

$$p_z = \frac{1}{2} (p_v + p_h) \quad (2.18)$$

and, acting alone, it produces a uniform diametral strain,  $\delta_z$ . The distortional pressure component,  $p_y$ , is defined as

$$p_y = \frac{1}{2} (p_v - p_h) \quad (2.19)$$

and, acting alone, it produces an out-of-round deformation. The uniform pressure distribution is resisted primarily by the compression stiffness of the pipe ring, the elastic arching factor ( $\alpha_1$ ) denoting the proportion, and the distortional pressure is resisted by the flexural stiffness of the pipe. A second order distortional effect is produced by the uniform pressure component acting on the different vertical and horizontal projected areas of the deformed pipe ring, a reverse of the tendency of elliptical pipes to re-round under internal pressure. The combination of these two effects for ring deflection is illustrated in Fig. 2.12. Two load transfer conditions are considered at the pipe-soil interface in the tangential direction, no slippage (full friction) and full slippage, whichever is conservative to be used for design.

Buckling occurs in a pipe wall by local deformation and is usually associated with a relatively circular deformed pipe cross-section. One of the many simplifications made in the analysis is the assumption that the pipe circumference deforms into  $n$  equal sinusoidal waves when it buckles, as shown in Fig. 2.13. The critical buckling mode, that is the integral value of  $n$  which yields the lowest theoretical value of buckling pressure, increases as a function of the flexural stiffness ratio ( $Y$ ). Thus, for

thinner-walled, or more flexible, pipes in stiff soils, a high  $n$  value is likely to occur if the pipe buckles. Conversely, for typical uPVC pipes installed in backfilled trenches, the large deformation mode ( $n$  value of 2) is more likely to occur (see Fig. 2.13) and this may be treated as failure by excessive deformation.

In the calculation of deformation, initial out-of-roundness,  $(\delta_{y0})$ , which is established in the pipe by the time the backfill has reached the level of the pipe crown, is included in the design and the uniform deflection component  $(\delta_z)$ , which is relatively small compared to the distortional component  $(\delta_y)$  is neglected. The equation for short-term distortional, or out-of-round, deformation is then given by

$$\delta_y = \delta_{y0} + \delta_y^* = \delta_{y0} + \delta_{y1} + \delta_{y2} \quad (2.20)$$

The increment of deformation caused by external loading  $(\delta_y^*)$  is composed of the first- and second-order components  $(\delta_{y1}$  and  $\delta_{y2})$  shown in Fig. 2.12.

The first-order component is expressed as

$$\delta_{y1} = \frac{4 p_y}{108 S_{fp} + E_s^*} \quad (2.21)$$

This expression, derived from elastic theory, is similar in form to the Iowa Formula, but has the important difference that the distortional pressure instead of the vertical crown pressure is the numerator. A further term  $(\delta_{y3})$  is added to account for long-term deformation.

A set of design charts for buried flexible pipes has been produced for various proportions of uniform and distortional load, a typical chart being shown in Fig. 2.14. The parallel set of diagonal lines represents the load/deflection response for pipe-soil systems with various values of the



flexural stiffness ratio ( $Y$ ). The influence of the second order distortional effect is demonstrated by the curvature of these lines at large deflections. The buckling limit, the line of which intersects these curves, delineates an area of the chart (below the line) in which the pipe wall remains stable. Within this zone, the factor of safety against buckling for any point on a load/deflection curve (constant  $Y$ ) is determined by the value of  $p_y/S_{fp}$ . It will be noted that the value of deflection,  $\delta_y$ , at which buckling occurs decreases as  $Y$ , and therefore the flexibility of the pipe, increases. The discontinuities in the buckling limit correspond to changes in the critical buckling mode,  $n$ . An alternative representation of static response for a pipe-soil system, which illustrates the different ranges of system behaviour as a function of  $Y$  is given by the loci of constant values for  $p_y/E_s^*$ . For  $Y > 1000$ , the flattening of these curves shows that deformation is virtually independent of flexural pipe stiffness,  $S_{fp}$ , and the system is described as flexible. For  $Y < 10$ , deflection is virtually independent of soil stiffness and the system is described as rigid. In the intermediate range of  $10 \leq Y \leq 1000$ , both pipe and soil contribute significantly to the support of distortional loads. It can be seen that higher buckling modes ( $n > 2$ ) first become critical at the start of the flexible range.

The range of values of the load distribution parameter for which design charts are available is  $0.05 \leq P_y/\alpha_1 P_z \leq 0.8$ . Once the free-field pressures have been calculated and the relevant chart chosen, a complete description of pipe behaviour is available. Performance limits are set, such as minimum allowable deflection ( $\delta_y$ ) and minimum factor of safety against buckling, and this provides a zone from which suitable combinations of pipe and soil properties may be chosen to provide the optimum design. Either sidefill design for a particular type of pipe, or pipe design for a particular soil type, may be selected.

The charts are only as good as the input data, however, and difficulty is found in assigning a value to the soil modulus ( $E_s^*$ ), which is a measure of the bulk response of the backfill around the pipe and cannot be measured directly from laboratory tests on small soil samples. In the field it is affected by trench geometry, the method of placing and compacting backfill, and the insertion and withdrawal of trench support. Prediction of  $E_s^*$  can only be made from back-analysis of deformation data from field or experimental installations, therefore, though it is a genuine soil property and can theoretically be correlated to some independent measure of backfill stiffness. Provisional values of  $E_s^*$  are given in Table 2.3 for four backfill soil groups, the lower value in each case being for shallow cover depths and minimum site supervision, and this is the value recommended for general design use. With a high degree of control and supervision, any soil may be used, but with low levels of control, groups I, II and certain soils from group III are recommended. Gumbel (1984) states, however, that the experimental evidence used to substantiate the provisional  $E_s^*$  values quoted in the table is so limited that no entry is supported by more than one result. This fact, allied with the uncertainty in assignation of a value of the dead load lateral pressure ratio ( $K_d$ ), in which Gumbel places much store and for which a range of values are recommended in design, renders the method somewhat impotent as yet for the calculation of a specific, economic design.

The present shortcomings, which are acknowledged by Gumbel, are thought to be essentially due to the lack of experimental evidence and should not detract from the rational theoretical derivation, which is soundly based on fundamental principles and thorough in its approach. As with all design methods, its acceptance will depend upon its ease of use, which will be improved by further definition of the parameters, and evidence of its competence in accurate prediction. Its applicability to

small diameter uPVC pipes, which often have little care taken in their installation, is likely to be limited, because the uniformity of soil conditions assumed in the method is less likely to occur in a material which is, at most, compacted in one layer. The applicability of the method to the narrow trench condition, in which the properties of the insitu soil are thought to influence the stiffness of the sidefill, is also uncertain, although reference is made to the dependence of  $E_s^*$  on trench geometry. The aspect of trench wall friction has been discounted in discussion of the load calculation. Another factor that is difficult to quantify in design, and has greater importance for pipes of small diameter, is the "bedding in" effect. Gumbel extensively considers existing work in his discussion of methods of quantifying  $E_s^*$  (Gumbel, 1984), in which he describes the justification of Jaaskelainen (1973) in using the oedometer test to model the stiffening response of pipe deformation as mistaken. He attributes this effect to a "bedding in" phenomenon associated with the first 2 or 3% of pipe deformation. No attempt to isolate this factor has been made, however, rather preference is given to assuming overall soil stiffness behaviour from back-analysed field data.

In order to validate this design method, loading tests have been performed on buried plastic pipes at the TRRL and are reported by O'Reilly et al (1982). Four pipes commonly used in practice were investigated: Class 'B' uPVC (SDR = 33.4, tests 3P and 4P), GRP (test 5P), MDPE (test 6P) and RPM (test 7P), together with class 'O' uPVC pipe (SDR = 100, tests 1P, 2P and 8P) that represents a more flexible pipe in which buckling was likely to occur. 300mm diameter pipes were used and were buried in uncompacted sand of roughly constant density with a cover depth of 300mm. The results of these tests, together with those of tests on steel pipes, are shown in Fig. 2.15, in which the load/deflection curves are plotted on the design chart for the case where  $p_y/\alpha_1 p_z = 0.4$ , the middle of the

suggested range of values for uncompacted sand. All the curves, with the exception of that for test 2P, reach the buckling limit, with the pipes that failed by deflection crossing the area denoted by a buckling mode of  $n = 2$  (see Fig. 2.13). Not all curves are parallel with the Y lines of the design method because of the non-linearly elastic behaviour of the soils.

The report concludes that the design method provides a reasonable model of soil-pipe behaviour, but that a large amount of further experimental work is required to allow the method to be developed into an accepted design procedure. The loading tests on plastic pipes indicated that unacceptably high deformation is the likely failure mode in practice, but that very thin-walled uPVC pipes will buckle in the manner predicted by the model.

#### 2.4 Experimental and Field Investigation of Buried Flexible Pipes

Considerable world-wide effort has been expended on experimental research into the behaviour of buried flexible pipes since Spangler conducted his famous series of tests in the 1920s and 1930s. The advent of plastic pipes of various material types led to a significant increase in this research over the past twenty years, much of it product based. As indicated above, there is a wide range of pipes that are classified as flexible and the behaviour of each under similar conditions is often markedly different. For this reason, only those experimental investigations involving uPVC pipes have been included in the ensuing discussion except where a point of general validity is discernable.

Three broad categories of experimental work have been undertaken, consisting of model tests, field investigations and full-scale experiments. The most notable model tests have been performed in a geotechnical

centrifuge, and a programme of tests at the Transport and Road Research Laboratory to validate these is discussed. Field studies have been carried out in America, mostly on large diameter steel pipes to obtain information on soil properties and pipe performance for use in empirical or semi-empirical design formulae, and in Europe. A study of particular interest involved the field measurement of many lengths of uPVC pipe in service and this will be discussed later. Most of the work has involved full-scale experiments, however, and this is of most interest here.

#### 2.4.1 Experimental Studies at the TRRL

Trott and Gaunt have researched the behaviour of buried flexible pipelines at the Transport and Road Research Laboratory (TRRL) since 1970 and, with Stevens, performed laboratory tests on small diameter uPVC pipes with interesting results. Field investigations of a steel pipeline of 1.83m diameter at the point where it passes under a minor road are reported by Trott and Gaunt (1972). Internal deflections, pipe wall strains and soil pressures were measured at two sections under the road. A compacted sand bedding and sidefill was used for installation and a negative vertical deformation of 4mm (0.2%) was recorded at the end of sidefill placement. Subsequent deformations under vertical load were very small (also about 0.2%), as were pipe wall strains, and conclusions were difficult to draw from these results. Soil pressure measurements were lower directly above the pipe crown than to either side and the horizontal pressure at the side of the pipe was in reasonably good agreement with horizontal deflection. Attempts to correlate measured deflections with those predicted by the Iowa Formula were unsuccessful, and this was attributed to the different loading conditions and the high E' value for the compacted sand. However, the use of finite element analysis to predict deflections and stresses in the pipe

and soil produced promising results.

Field experiments on 300mm diameter pipelines of various materials installed beneath the Marlow-Bisham bypass are described by Trott and Gaunt (1974, 1975 and 1976). Pipes made of uPVC, clayware, asbestos cement and steel were laid in 0.75m wide trenches at cover depths of 0.7m below the surface of the subgrade and 1.2m below finished road surface, as shown in Fig. 2.16. The steel pipe was of a non-standard type, having a ring stiffness that was approximately the same as the uPVC pipe, and was chosen in order that direct comparisons of behaviour could be made. In each case the pipes were laid on a 150mm bedding of 10mm single size gravel, with the same material used as sidefill and extending to 150mm above the pipe crown. Excavated clay was used as backfill and was thoroughly compacted in 200mm thick layers. Instrumentation was installed to measure strains in the pipe wall (clay, asbestos cement and steel pipes) and horizontal and vertical deflection (uPVC and steel pipes). Soil pressure was measured above all pipes and at the sides of the uPVC and steel pipes. Readings were taken at three sections along each length of pipe, as shown in Fig. 2.16. Four loading situations were studied;

1. The effect of pipe laying and trench backfilling.
2. Construction traffic loading.
3. Controlled loading tests on the completed pavement surface, using the HB loading rig.
4. When in normal use.

Fig. 2.17 shows the deflections of the uPVC pipe during installation and after 31 months of normal use, when vertical deflections of 1.5, 2.5 and 2.9% were recorded below the acceleration, nearside and offside lanes respectively. Differences in individual deformations were thought to occur because of random movement of construction traffic, variations in compaction during installation, and the variation in the stiffening effect

caused by differing distances to the joints in the pipe. Fig. 2.18 shows the vertical and horizontal pressures recorded adjacent to the uPVC pipe over the same period. The same pattern of behaviour is followed by pipe deformation and vertical pressure during the backfilling period, with a relatively low horizontal pressure (5 kPa) indicating that little passive pressure has developed at this stage.

The passage of loaded scrapers, the principal form of construction traffic, caused a marked increase in both deformations and pressures. Fig. 2.19 shows the permanent and transient diametral reductions caused by the passage of scrapers, from which it can be seen that nearly all the total increase in permanent deflection was caused by the passage of the first 10 axles. Reference to Fig. 2.17 shows that the vertical diametral strains of the pipe at the three measured sections were at this stage roughly stable, subsequent construction traffic and pavement laying operations causing no increase in deflection. The vertical and horizontal pressures continued to increase, however, with the horizontal pressure being greater during part of the construction stage (Fig. 2.18). This redistribution of pressure around the pipe was thought to account for the relatively stable deflected form following the initial application of scraper loads, the pipes approaching a state of 'ring compression' as opposed to the earlier 'ring bending' behaviour. The transient pipe deformations caused by the passage of the HB load over the completed pavement were very small and produced no significant increase in permanent deformation, the corresponding transient vertical and horizontal pressures being about 20 kPa. Transient pressures due to the construction traffic driving on the sub-base over the steel pipe, which were thought to be similar to those over the uPVC pipe, were recorded. Values of up to 160 kPa were measured during the passage of loaded scrapers, with corresponding pressures of 20 kPa for concrete lorries. In each case the maximum permanent vertical diametral strain was

well below 5% of the original diameter.

The deformation data for the steel pipe resembled closely those for the uPVC pipe. The bending strains recorded for the steel pipe were generally closely related to the pipe deformations. The distribution of bending strain for the pipe in the nearside and acceleration lanes at two stages, both immediately after backfilling and 175 days after installation, are shown in Fig. 2.20. It can be seen that the strain distribution of the pipe under the nearside lane after 175 days is markedly asymmetrical, indicating a skew deformation of the pipe. In both cases, the theoretical symmetrical strain distribution which would be produced by a uniform pressure distribution across the crown and invert is shown. These theoretical values of bending strain were derived from the tables of bending moments and diametral strains of a pipe subjected to various load distributions computed by Picken and Vaughan (1973). Comparison of theoretical and experimental results indicated that pipe deflections can be used to estimate approximate bending strains at the pipe crown and invert if a certain load distribution on the pipe is assumed. The report concludes that construction traffic provides the most severe loading case for flexible pipes, which commonly have less cover during construction than after completion.

A programme of full-scale static and dynamic loading tests on buried flexible pipes was instigated at the TRRL in 1975, and the first part of this programme is reported by Gaunt et al (1976). The layout of the test-pit and loading facility at the TRRL is shown in Fig. 2.21. The pit was filled with an imported sandy clay soil which was placed and compacted at its natural water content (16-18%). Pipes were installed in trenches using typical site practice methods. Load was applied by five jacks bearing onto square plates of  $0.09\text{m}^2$  area. The jacks were operated sequentially to simulate a rolling wheel load, or singly or in groups to apply static load.



Four tests were carried out on 300mm diameter class B uPVC pipe to BS 3505 installed in 1.0m wide hand-dug, parallel-walled trenches with 0.75m cover depth. The layout of the four tests is shown in Fig. 2.22. Each installation was subject to load regimes of 5, 10, 20, 40, 60, 80 and 100 kN cyclic loads in which the jacks were operated sequentially, followed by static loads of 40, 60, 80 and 100 kN. Each increment of cyclic loading was continued until no further permanent deformation of the pipe occurred. This state was usually reached after 100–200 cycles of a simulated rolling wheel travelling at creep speed. Static load was applied by the three centre jacks, each increment being maintained for six hours.

The structural performance of the installations was assessed from measurements of pipe deformation, pipe wall strain and total pressure in the fill surrounding the pipe. The layout of instrumentation is shown in Fig. 2.22. Deformation was measured both vertically and horizontally by means of a spider device, in which the strains in sprung steel arms were measured by resistance foil strain gauges (R) and related to movement of the arms. Pipe wall strains were monitored by resistance foil strain gauges glued to the internal (test 1 only) and external faces of the pipe at intervals of 45° around the circumference. A limited number of gauges were also attached in the longitudinal direction. Measurements were taken during each stage of backfilling, cyclic loading and static loading, and during exhumation of the pipes after testing.

Diametral strain of the pipe is usually considered to be the critical structural performance parameter, a maximum value of 5% permanent vertical diametral strain being quoted for design purposes. Fig. 2.23 shows the build-up of vertical diametral strain for each installation. The effect of sidefill compaction is illustrated by the curves for tests 1 and 2, with a maximum permanent deflection of 17% for uncompacted clay after the application of the 80 kN static load compared with just over 1% for thoroughly compacted clay. In both cases where the pipe was installed in

uncompacted gravel, a permanent deformation of approximately 4% was recorded, the compaction of the clay backfill making little difference to the values. In the two cases where the soil was compacted over the pipe (tests 2 and 4) cyclic loading up to 40 kN had no effect on pipe deformation, probably due to the stress history caused by the tamping process.

Graphs of pipe wall strain against vertical deflection indicate that the properties of the soil dominate the creep<sup>\*</sup> behaviour of the pipe-soil system. Fig. 2.24 predicts long-term creep behaviour of the pipe-soil systems by extrapolation of results from measurements taken at various times during the six hour application of the 100 kN static load. The results for the 80 kN load have been used for test 1 as it was not practicable to sustain 100 kN on uncompacted soil. However, the results obtained by such a projection should be treated with extreme caution because of the short base line from which the projection was made; they probably represent an overestimation of the creep, and, therefore, pipe deformation, that would occur in practice. In spite of this, with the exception of the uncompacted clay sidefill, the creep deflections do not exceed 5%. The most satisfactory performance, in this respect, was obtained by the granular pipe surrounds.

For rigid pipes, the traffic loads used in design tables (Young and Smith, 1970, and others) are calculated from the Boussinesq elastic theory. Fig. 2.25 shows the average pressure increases on the uPVC pipes for the various static loads plotted against pressures calculated by the theory and in all cases a good agreement is found. It is suggested, therefore, that the Boussinesq method is suitable for the prediction of traffic loadings on buried flexible pipes. For tests 2, 3 and 4, the effective loads over the pipe due to the 100 kN surface load are 65, 56 and 70 kN/m respectively. Despite these very high loads, no evidence of structural distress was

\* although not acknowledged in the paper, the effect referred to as creep is primarily one of soil consolidation.

detected in the pipes. The measured horizontal deformations indicate that all installations with the exception of that of the uncompacted clay provided a support equivalent to an  $E'$  value of roughly 5 MPa or greater, which was consistent with the currently recommended  $E'$  value for the sidefill (Clarke, 1968).

The report concludes that an equally high standard of pipe performance can be achieved with both gravel and clay sidefills if the clay is compacted properly, the most economic installation being determined by whether it would cost more to import fill material or implement a high standard of workmanship. It was similarly concluded that the variation in the performance of a pipe with the quality of workmanship of its installation is considerable for certain soils.

An extension of this test programme is reported by Trott and Stevens (1979) in which six further installations were studied, the various bedding and backfill materials being detailed in Table 2.4. Sandy clay was used as the bedding and sidefill material in five tests (1, 2, 8, 9 and 10) at four states of compaction. Tests 6 and 7 used waste materials as a possible alternative to conventional granular material. In test 8, the 100 kN static load was applied for 94 hours instead of 6 hours in order to produce a more accurate estimate of long-term creep deformation. The deformation results for sandy clay bedding and sidefill indicated that hand tamping (test 9) reduces the diametral strain, when compared with the uncompacted state (test 1), by about half at the higher loads. An increase in compactive effort above one pass of a vibro-tamper produced a negligible reduction of the final deformation. The vertical diametral strain of the pipe in thoroughly compacted colliery washings (test 6) was similar to that in uncompacted gravel. Uncompacted sand and uncompacted incinerated municipal waste produced similar pipe deformations.

A further research programme was instigated to compare results of

Table 2.4 Details of Fill Materials used in TRRL Tests (after Trott and Stevens)

Test No	Bedding Material	Condition	Moisture Content (%)	Backfill Material	Condition	Remarks	Maximum Deflection (%)
1	Sandy clay	Uncompacted	16.5	Sandy clay	Uncompacted	Pipe laid on trench bottom	19.2
2	Sandy clay	Compacted 3-4 passes	16.5	Sandy clay	Compacted 3-4 passes	Vibro-tamper used for compaction	4.0
3	10mm single size gravel	Uncompacted	2.1	Sandy clay	Uncompacted		4.6
4	10mm single size gravel	Uncompacted	2.1	Sandy clay	Compacted 3-4 passes	Vibro-tamper used for compaction	4.8
5	Fine aggregate sand	Uncompacted	4.1	Sandy clay	Uncompacted		8.5
6	Colliery washings (filter cake)	Compacted 3-4 passes	25.5	Sandy clay	Uncompacted	Vibro-tamper used for compaction	5.1
7	Incinerated municipal refuse	Uncompacted	14.7	Sandy clay	Uncompacted		8.0
8	Sandy clay	Compacted 3-4 passes	16.5	Sandy clay	Uncompacted	Vibro-tamper used for compaction	6.8
9	Sandy clay	Hand tamped	16.5	Sandy clay	Uncompacted		11.0
10	Sandy clay	Compacted 1 pass only	16.5	Sandy clay	Uncompacted	Vibro-tamper used for compaction	7.0

model tests on buried flexible pipes, using the Cambridge geotechnical centrifuge, with a full-scale prototype installation in the Transport and Road Research Laboratory (TRRL) test pit (Trott et al, 1984). A thin-walled, steel pipe was buried in sand and subjected to a line load along its length in both cases. The installation at the TRRL involved a 1.0m diameter pipe, strain gauged around both the internal and external circumference, and buried with 250mm of cover. Fourteen load cases were used, in which the load was applied at one of five positions, before the pipe was loaded to failure. A scale model of this arrangement was used in the centrifuge.

The results showed that the strain distributions, failure loads, and deformed shapes obtained from the two pieces of apparatus were in good agreement. More important was the character of the strain distributions. The strain profile of the pipe caused by compaction of the sidefill in 200mm thick layers took the form of an exaggerated V-shape, with tensile strain on the internal surface at the pipe springings and compression at the crown and invert. Little strain occurred at the shoulders and haunches. This indicated "negative" elliptical deformation, an observation borne out by an increase in the vertical, and reduction in the horizontal, diameter of 1.6% and 1.5% respectively. The external strain profile was the mirror image of the internal profile. Under the centrally positioned strip loading, the internal strain profile showed high tensile strain at the pipe crown, higher compressive strain at the shoulders, small tensile strain at the pipe springings and negligible strain below the horizontal axis. This is consistent with the "heart-shaped" deformation discussed in Chapter 5. The external strain profile again mirrored this behaviour remarkably accurately, indicating little compressive hoop strain in the pipe when under load. The localised nature of these strains, and therefore deformations, reflects the shallow cover depth ( $0.25D$ ) and narrow load

platen ( $0.6D$ ) in relation to the pipe diameter ( $D$ ), and the great flexibility of the pipe. The use of well compacted sand, a good sidefill material, is also partly responsible for such localised behaviour. A poorer material would allow distribution of the effects to the lower part of the pipe and produce deformation of a more elliptical nature. The deformed shape of the pipe on exhumation, after being loaded to failure, was heart-shaped in both cases.

The research carried out at the TRRL is closely related to the situation being considered in this project and has consequently been reviewed in considerable detail here. Certain information, such as the surface deformation in the pit experiments, which could be expected to be considerable in cases where the backfill is uncompacted, is lacking. Despite this, the information presented was of much use in planning the full-scale experiments.

#### 2.4.2 Howard's Investigations

Full-scale installations were tested in a reinforced box at the US Bureau of Reclamation and are reported by Howard (1972A). The reinforced box was approximately 2m cubed with an opening in the end wall in order to gain access to the pipe during testing (Fig. 2.26). Pipes of 450, 600 and 750mm diameter were used, corresponding to effective trench widths (trench width divided by pipe diameter) of 4.67, 3.50 and 2.80 respectively. In total, 14 experiments were performed in which sections of unlined steel pipe were buried in lean clay at 90 or 100% of its Proctor maximum dry density. Three different pipe wall thicknesses were used in the test programme. Despite the fact that these tests were on steel pipes, both the experimental approach and the results are of interest, and these have been outlined in the ensuing paragraphs.

To reduce friction between the soil and the container wall, a coat of petrolatum was applied to the walls and was covered with polythene film. Clay was then placed up to the underside of the pipe in layers, each of which was compacted to the required density. The pipe was placed directly onto the clay surface, stiffened to prevent negative deflections during the laying of the sidefill and braced to prevent the pipe from rising during compaction of material below the horizontal axis. The clay sidefill and backfill were then completed by compaction in layers as before.

Four pressure cells were attached to the outside wall of the pipe at 90° intervals and cells were also placed on the wall of the container at depths below the surface of 1200mm (at the same level as the horizontal axis of the pipe) and 600mm. A circumferential ring of 16 or 20 strain gauges was fixed in the pipe. Deflections were measured both with micrometers and a revolving dial gauge. T shaped aluminium pieces were buried in the soil at predetermined locations in order to monitor soil movement. Telescopic tubes with small plates on the end were placed on the horizontal axis of the pipe to measure horizontal soil movements. A uniform surface pressure was applied to the box, and increased at one hourly intervals.

Of the five pipes installed in clay at 100% Proctor maximum dry density, the two stiffest deformed and the other three failed by elastic buckling at deflections of less than 10%. The results for the stiffest pipes buried in clay at two different densities, showed that the pipes deformed elliptically. Deformation of the pipe buried in clay at 100% Proctor maximum dry density was approximately half that in the less dense clay.

The soil pressure recorded at the crown of the pipe was between 50% and 75% of the applied surcharge, the stiffer pipes attracting the higher pressures. The measured pressures on the bottom of the pipe were erratic,

probably due to the effect of sidefill compaction. The pressures on the top and bottom of the pipe varied linearly with load up to diametral strains of 7-8% when the recorded pressures began to decrease, apparently due to soil arching. The pressure at the side of the pipe was 100-150% of the surcharge pressure in the case of elliptically deformed pipes, and 50-100% for rectangularly deformed pipes. Side pressure values compared reasonably well with the Iowa predictions for elliptically deformed pipes, but were lower for those that deformed rectangularly indicating a departure from the assumed pressure distributions.

Elliptical deformation, characterised by plastic hinges developing at  $90^\circ$  and  $270^\circ$  (the pipe springings), tended to occur in the stiffer pipes, whereas more flexible pipes deformed rectangularly with plastic hinges developing at  $45^\circ$ ,  $135^\circ$ ,  $225^\circ$  and  $315^\circ$ . The ratio of horizontal to vertical diametral strain for elliptical pipe deformation was in the range 0.8 to 0.9 and for rectangular deflection was between 0.6 and 0.8. The deflected form was predicted from strain gauge readings, which showed high compressive strains on the internal surface at the critical points, as shown in Fig. 2.27. For flexible steel pipe, Spangler (1941) states that failure by collapse occurs at vertical deflections of approximately 20%. Failure of the pipe in Howard's experiments was defined as the formation of a plastic hinge at any point in the pipe. This generally occurred between 16% and 20% vertical diametral strain, deformation being generally linear up to 15%. Following the formation of the plastic hinges, the load/deflection curves for elliptically deformed pipe did not change significantly, with final deflections ranging from 20 to 27% under a uniform surface pressure of 700 kPa. None of the elliptically deformed pipes collapsed. In the case of rectangularly deformed pipes, downward buckling and collapse of the pipe crown occurred soon after the formation of the plastic hinges.



The influence of the container on the results was deduced from the readings of the wall-mounted pressure cells. For the 450mm diameter pipe (corresponding to effective trench width of 4.67) all of the pressure cells on the box wall registered the same values of pressure, which is consistent with the assumption that the container has no effect on the results. For the larger pipe diameters, however, the lower gauges registered considerably higher values of pressure. In the case of installations where the clay was placed at 90% of the Proctor maximum dry density, the pressure on the upper cell was about 50% of the vertical surcharge load, whereas with the denser clay the values were about 75%. In general, half of the horizontal soil movement between the pipe and the container wall occurred within 150-225mm of the pipe. From here the movement curves were linear until they converged at the container wall, indicating that in these cases the container did influence the results. Howard recommends that these tests should be correlated with field measurements to determine the exact extent of this influence.

This test programme was extended, using an identical experimental procedure, to include pipes of glassfibre reinforced plastic (GRP), polyethylene (PE) and uPVC pipe (Howard, 1973). Reinforced plastic matrix pipes were the subject of an earlier, unseen, report (Howard, 1972B). The performance of each was compared with those of steel pipes having a similar pipe ring stiffness ( $E_p I/r^3$ ) value. The GRP pipe deformed slightly less than the RPM pipe and between 50 and 100% more than the corresponding steel pipes. Both thermoplastics pipe (uPVC and PE) deformed similarly to steel pipe, however. The PE pipe deformed rectangularly under load (see Fig. 2.27) until a vertical diametral strain (V.D.S.) of 42% was reached, at which point the pipe showed no signs of structural distress. The pipe recovered to 94% of its original diameter 2 months after exhumation. In contrast, crazing (fine, hairline cracks) of the inner surface of two of

the three GRP sections occurred between 10 and 20% V.D.S. Subsequent loading caused the crazing to gradually develop into definite longitudinal cracks where the internal surface of the pipe wall was under tension. The remaining GRP pipe suddenly produced longitudinal cracks at about 40% V.D.S. While these results are of interest, it is in the detailed experimental data, included in an appendix, that the most important information is contained and it is to this that attention is now drawn.

The graph of load against vertical and horizontal diametral strain of the uPVC pipe after 1 minute of its application is presented in Fig. 2.28, on which is included the diametral strain ratios ( $\Delta_h/\Delta_v$ ) at various stages of the test. For this graph, and in all subsequent discussion, data after one minute of each load application are used. In his earlier paper (Howard, 1972A), Howard quotes diametral strain ratios of 0.8 to 0.9 as representing elliptical deformation (a perfect ellipse would give 0.91) and 0.6 to 0.8 for rectangular deformation. The ratios for the uPVC pipe are approximately 0.8 up to a V.D.S. of approximately 20%, thereafter reducing until a value of 0.69 is reached. This implies that a departure from purely elliptical deformation occurs at an early stage of the test and this is shown to be the case by the internal pipe wall strain profiles (Fig. 2.29). Profiles at two levels of surface load (140 and 280 kPa) are given, at each of which the diametral strain ratio was approximately 0.82. In each case the tensile strain at the invert was far greater than that at the crown, and the compressive strain at the springings was matched by that at 22.5° below the horizontal axis. This indicates that the deformation is of an inverted "heart shape", in which most action occurs at and below the pipe springings, although Howard describes the deformation as semi-elliptical. The deformed shape of the pipe in each of the tests was determined from measurements of pipe wall movement at 15° intervals around the internal circumference of the pipe using a dial gauge mounted on a

longitudinal shaft. The shapes of the uPVC pipe at the start of the test and under the 210 kPa load are shown in Fig. 2.30, in which the behaviour suggested by the strain profiles can be discerned. Such variation in deformed shape is discussed in greater detail in Chapter 5 of this thesis.

The measurements of earth pressure on the walls of the box were similar at both the level of the pipe springings and 600mm above it (Fig. 2.31), implying that the walls of the box did not influence the behaviour of the uPVC pipe. The effective trench width in this case was 5.26, making the observation consistent with the findings of Barnard (1957), Dezsényi (1975) and others. Measurement of soil movement beside the uPVC pipe was unsuccessful because of equipment failure, but the pattern of movements was similar in all other tests and the results from an installation involving a 450mm diameter PE pipe have been reproduced in Fig. 2.32. This shows that nearly 50% of the soil compression occurs within 230mm of the pipe wall, which is equal to half of the pipe diameter, although the earlier report (Howard 1972A) indicated that this distance was constant whatever the pipe diameter.

The V.D.S. of the uPVC pipe at the end of the test was 32%, at which point the pipe showed no signs of structural distress.

General observations of flexible pipe behaviour in the tests conducted by the USBR are reported by Howard (1981A). Vertical diametral elongation, or negative deformation, of buried flexible pipes, although resisted by bracing in the tests described above, has been observed during compaction of the sidefill material and values of up to 5% of the vertical diameter have been recorded. Howard considers the measurement of this effect to be essential if the behaviour of the pipe and soil are to be accurately quantified.

Variation in the deformed shape of such pipes is reiterated and rectangular deformation is associated with large ratios of soil to pipe

stiffness. Where pipes have deformed rectangularly, the horizontal diametral strain was found to be much less than the V.D.S., in some cases only 20% of the V.D.S. Greater horizontal than vertical diametral strains have also been measured, but where diametral strain ratios ( $\Delta_h/\Delta_v$ ) of more than 0.95 are obtained it is recommended that the data be checked. Howard considers that elliptical deformations may be expected for dumped and lightly compacted sidefills, but that the deformed shape of pipes in moderate or highly compacted sidefill will depend upon the stiffness of the pipe.

He states that the increase in horizontal diameter of a flexible pipe under load influences the soil at the side of the pipe to a distance of about 2.5 pipe diameters from the pipe wall. This will often mean that the properties of the insitu soil will influence the behaviour of the pipe. If the insitu soil is stiffer than the sidefill, he recommends a minimum trench width for pipe installation, completion and inspection of joints, and adequate compaction of the sidefill, especially under the haunches. Where the insitu soil is of similar strength to the sidefill, the sidefill should extend one pipe diameter on either side of the pipe to allow for natural variations in the properties of the trench wall. Where the insitu soil is less stiff than the compacted sidefill, the sidefill should extend at least two pipe diameters on either side of the pipe. Because of its potentially significant influence on pipe behaviour, the insitu soil should be investigated thoroughly before pipes are laid.

When selecting bedding and sidefill materials, the maximum particle size should be such that abrasion of the pipe during placement, and point loading of the pipe wall, are avoided. A maximum particle size of 20mm is recommended for uPVC pipe, with clean, coarse-grained soil to be used under the pipe haunches in order to provide as much support as possible. The possibility of migration of fines from fine-grained natural soil into

coarse-grained fill material should be borne in mind as this may result in loss of pipe support. The same effect may occur from sidefill to bedding material, with loss of support being even more acute. It is also recommended that fine sands should not be used as sidefill in areas where the water table is high, because saturation of such soil results in a significant loss of strength.

The research carried out by Howard is again more suited to American practice, using large diameter pipes under large earth loads, but the experimental procedure and results were of general use in their description of flexible pipe behaviour and of particular use when planning the full-scale experiments. The extent of the influence of the box walls, which is particularly important for the large diameter pipes tested, is uncertain and, as Howard acknowledges, requires estimating from field investigations. The type of externally applied load used further reduces the absolute relevance of the results to those of this project, but the comparative data presented is valid and was produced with thorough attention to detail. The work consequently represents an important contribution, both directly and indirectly, to the full-scale testing of buried uPVC pipes.

#### 2.4.3 Other American Research

Further investigations of the behaviour of large diameter corrugated steel culverts have been conducted in America, notably by Watkins and Moser, with the aim of predicting pipe deflection, and in particular, assessing the ability of the Iowa Formula to predict deflection. Watkins and Moser (1971) describe tests on 1.5m diameter corrugated steel pipe under simulated embankment conditions in a test facility of similar design to that shown in Fig. 2.33. The most interesting aspect of this work is the criticism of the tests, and in particular the test facility, levelled

in the ensuing discussion. The relatively rigid tank in which the pipe is buried allows a soil surround equal to one pipe diameter and this was considered to inhibit the flexible nature of the pipe to the extent that the results could not be applied directly to practical installations.

Laboratory load tests on uPVC pipe to determine its structural response under embankment conditions are detailed by Moser et al (1973). 1.5m lengths of 0.305m and 0.610m diameter pipe were surrounded by fine sand in the test cell shown in Fig. 2.33, and uniform pressure was applied in increments to the surface. It should be noted that for the larger diameter pipes, the same ratio of test cell width to pipe diameter was used as the much criticised experiments referred to above. The pipes were laid on well-compacted sand and backfilled with sand at two different densities. The density of the sand is related to the AASHTO T-99 standard density, with high density sand at 90-94% of this density and medium density sand at 82-87%. Strain gauges were glued to both the internal and external faces of the pipe wall on the horizontal axis, and on the internal face of the pipe wall at the crown. The results of these tests are summarised in Fig. 2.33, in which the Standard Dimension Ratio (SDR) is defined as the ratio of pipe diameter to wall thickness. It is apparent that the optimum value for the SDR in relation to vertical diametral strain of the pipe is 37-38. The graph of total pipe wall strain in the pipe crown against deflection indicates that a thicker-walled pipe has a higher strain at the same deflection. This does not indicate that a thinner-walled pipe will be strained less in use, however, because it will deform more than a thicker-walled pipe under any given load. Pipe wall strain is composed of two parts, bending and ring compression. Measurement of strain on both faces of a pipe wall will allow the strains to be distinguished. Ring compression strain and, therefore, total strain, will be greater for the same pipe deflection in denser soil, although this difference is relatively

small because bending strains are generally considerably larger than ring compression strains in flexible pipes. These results should be viewed with caution, however, particularly those indicating the somewhat unexpected result for the optimum SDR value, because of the influence of the cell on the results.

Moser (1981) also investigated the validity of the limit of 0.5% strain in the pipe wall suggested by Chambers and Heger (1975) for the design of uPVC pipes. The maximum strain in the pipe wall due to bending is calculated by the following formula, in which the deflected form is assumed to be elliptical,

$$\epsilon_{w \max} = \pm \left[ \frac{t}{D} \right] \left[ \frac{3\Delta_v/D}{1 - 2\Delta_v/D} \right] \quad (2.22)$$

where  $\epsilon_{w \max}$  = maximum strain in the pipe wall, assumed to occur at the crown or invert of the pipe, due to bending or flexure

t = pipe wall thickness

D = pipe diameter

$\Delta_v$  = decrease in vertical diametral measurement.

This equation is valid for vertical deformations up to 10% of the pipe diameter. By rearrangement of this formula, vertical diametral strain can be calculated from pipe wall strain measurements using

$$\Delta_v/D = \frac{\epsilon_{w \max} (D/t)}{3 + 2\epsilon_{w \max} (D/t)} \quad (2.23)$$

Thus the limits of V.D.S. corresponding to a strain limit of 0.005 (0.5%) for pipes with SDR (or D/t) values of 35, 38, 41, 51 and 65 are 5.2, 5.6,

6.0, 7.3 and 8.9% respectively. Research in Holland has shown that pipe deformations far in excess of these values have been reached without damage to the pipe. Research in Germany suggested that the threshold strain at which crazing will occur in the long term is 0.8% and that this should be the limit. There was no evidence, however, that this strain will eventually lead to failure.

Moser carried out constant strain tests, which simulate a more severe condition than occurs in practice, as part of his investigation. Certain pipes failed when attempting to reach the required strain, the minimum strain at which failure occurred being 33%. In only one case did a pipe fail during testing (i.e. under constant strain conditions), and that was after less than 24 hours at a strain of 50%. The tests reported in the paper had been in progress for more than 3 years. Crazing was clearly evident at strains of 10% and above. Small visible cracks appeared in the initial straining process and these appeared to be stable. Cracks at 50% strain were more noticeable and not stable. No additional cracks were noticed once the constant strain value was achieved. There is no indication that any of the samples strained up to 40% will fail in the future. Moser also carried out stress relaxation tests in which sections of pipe were held at constant deflections and the load on the constraining apparatus was measured. He concludes that a 50 year strain limit would correspond to a V.D.S. that is far greater than designers would allow and that strain does not, therefore, provide a design basis for uPVC sewer and drainage pipes.

#### 2.4.4 Dezsenyi's Experiments

A series of box tests was performed at the Hungarian Institute for Building Science on flexible pipes of different materials (uPVC, PE and



GRP) and stiffnesses, principally to assess the various methods of deformation prediction. The pipes were buried in sand at different states of compaction. Both load and pipe deformation measurements were taken. Field measurements of sewer pipes were also made, and several interesting trends were noticed.

Properties desirable in the soil surrounding the pipe are homogeneity and density sufficient that the passive soil reaction may be developed. It also should extend an appropriate distance around the pipe, particularly to the side. The distance to which the soil influences pipe behaviour is  $2.5 D$  either side of the pipe centreline, where  $D$  is the pipe diameter, as shown in Fig. 2.34(a). Trench widths typically vary between  $2D$  and  $4D$ , thus pipe deformation is usually dependent upon the insitu soil in which the trench is dug. A correction factor ( $Q$ ) is applied to the sidefill compression modulus ( $E_s$ ) to account for this behaviour, where

$$E_s = Q E_{s1}. \quad (2.24)$$

Values of  $Q$  may be found from the graph shown in Fig. 2.34(b), for the relevant ratio of  $E_{s1}$  to  $E_{s2}$ , the compression modulus of the insitu soil. This correction is remarkably similar to that quoted by Leonhardt (1982) and used in the ATV (1978) method, and as the text does not make its origin clear, it can be assumed to be taken from the German work.

The results of the experiments and additional field investigations showed that the method adopted by Hoganas (and attributed to Molin) predicted deformation most accurately, while the Iowa Formula and that attributed to Howe-Leonhardt both underestimated deformation.

#### 2.4.5 Broere's Experiments

In his description of tests on uPVC pipes under practical conditions, Broere (1984) states that the literature contains no data to suggest that the methods of deformation calculation expounded therein apply to Dutch conditions, where sand, clay and peat soils predominate. He also notes that there is a scarcity of information on the behaviour of uPVC pipes under internal pressure and no measurements of such pipe performance have been produced. This is probably due to the difficulty in making such measurements. In an attempt to provide this information, Broere conducted eight tests on 500mm diameter Class 41 uPVC pipe, in which the deformation was measured using 36 strain gauges equidistantly spaced around the external circumference of the pipe. Each pipe was laid under distinctly different conditions in the field and the resulting deformations were compared to predictions using Bossen's theory.

After calibration in the laboratory under simulated field conditions, using an internal measuring device to produce a profile of the deformed pipe, the technique was successfully applied to the practical installations. A typical result is shown in Fig. 2.35 in which the pipe has a V.D.S. of 3.5% before pressurisation and this reduces to 1.5% after an internal pressure of 0.35 MPa was applied. The base line of the pipe wall strain profile is displaced by a constant tensile strain because of the internal pressure, as shown in Fig. 2.35(a), the tensile strain being calculated by the boiler<sup>\*</sup> formula. The curve forming the strain profile is plotted about the new base line. The strain on the internal surface of the pipe is found by assuming a mirror image of the external strain profile, as shown in Fig. 2.35(b). Although no mention is made in the text, it would appear that the pipe is assumed to exhibit no ring compression under load, behaviour under load being purely flexural.

The installation conditions for the pipes used in the test programme

\*  $(D-t)/t = 2 (p_{zmax}/p_z)$  where  $p_z$  is the working pressure and  $p_{zmax}$  is the permissible design stress.

are summarised in Table 2.5, in which the "gully" refers to a preformed, part circular channel of slightly greater radius than the pipe and depth of about one third of the pipe diameter. The installations using sand and clay fill materials are of most interest and discussion will be restricted to these. In each case the pipes were buried with a cover depth of 1.25m, in the manner shown in Table 2.5 and were loaded by the excavator traversing the surface of the backfill. Compaction of the sand sidefill was carried out both at the level of the pipe springings and 300mm above the pipe crown. Compaction of the clay involved careful ramming below the haunches and up to the level of the pipe springings, but thereafter no compaction was applied.

The pipe in the well compacted sand installation (Pipe 1) had a vertical diametral strain (V.D.S.) of 0.5% at the end of installation and underwent little change over 6 months without internal pressure. In contrast, the pipe in uncompacted sand (Pipe 2) had a V.D.S. of 3.2% at the end of installation, the pipe again exhibiting no significant change while unpressurised over 6 months. The pipe wall strain profile for this pipe (Fig. 2.36) shows elliptical behaviour in the upper half of the pipe, but a flattening of the invert leading to an "inverted heart" shaped profile, a phenomenon discussed in greater detail in Chapter 5. This behaviour is attributed to a combination of the good support of the relatively stiff trench bottom and the poor support of the loose sand below the pipe haunches. The corresponding pipe laid in the gully (Pipe 3) deformed in a similar manner to pipe 2 in its upper half, but strain concentrations occurred at the haunches where the pipe left the support of the gully. On application of an internal pressure of 0.35 MPa, a uniform tensile strain component was noticed in the strain readings. Pipe 1 showed little change in its largely undeformed profile, whereas the V.D.S. of Pipes 2 and 3 reduced by half to 1.5%, the shape of the deformed profiles remaining

Table 2.5 Details of Broere's Field Investigations

Test Reference	1	2	3	4	5	6	7	8
Location	Dellenweg, Epe		Aquaterp, Lelystad		C. Rodenhuis, Bergambacht			
Trench bottom	Flat bottom		Gully	Flat bottom	Gully	Flat bottom		
State of Fill compacted (C) or loose (L)	C	L	L	C	L	L	L	L
Cover depth (m)	1.25	1.25	1.25	1.25	1.25	1.25	0.75	0.75
Trench width (m)	1.20	0.90	-	1.80	1.80	-	0.90	0.90
Length of time (mths) before pressurisation	6	6	4	6	6	6	6	1
Pressureless: V.D.S. (% calculated) V.D.S. (% measured)	1.41 0.5	3.08 3.0	- -	4.30 2.0	5.28 4.9	- -	- -	3.32 0.9
Under internal pressure V.D.S. (% calculated) V.D.S. (% measured)	0.81 0.5	0.71 1.5	- -	1.78 1.5	2.16 2.0	- -	- -	1.16 0.3

unchanged. The strain profiles exhibited creep under pressure thereafter and rerounding of Pipes 2 and 3 continued with time (Fig. 2.36). The deformations predicted by Bossen's equation were overestimated in each case, and particularly so in Pipe 1 under earth load alone.

The pipe in well compacted clay (Pipe 4) had a V.D.S. of 2.4% at the end of installation with a roughly elliptical deformed shape, though curvature was greater in the upper half of the pipe where no compaction was applied to the sidefill. This V.D.S. continued to increase over 6 months without pressure, at the end of which a value of 3.0% was reached. The pipe in uncompacted clay (Pipe 5) deformed to 4.9% at the end of installation with a slight tendency to the "inverted heart" shape of Pipe 2, although some settlement of the pipe into the trench bottom tended to alleviate the strain concentration at the invert. The V.D.S. was found to reduce over 6 months without pressure. The pipe laid in the gully (Pipe 6) deformed more than Pipe 4, but the deformation reduced with time as for Pipe 5. The unexpected reduction in V.D.S. was attributed to the very wet conditions prevailing over the six month period. Application of internal pressure caused the V.D.S. to halve in Pipe 4 and more than halve in the other two pipes, with all three pipes conforming to an elliptical profile. Rerounding continued to occur under pressure. Bossen's predictions again overestimated the values of deformation, the greatest discrepancy again being with the compacted material around a pipe without internal pressure.

The interesting feature of this work is the use of strain gauges to measure pipe deformation, a practice that was proved to be successful by pipe profile measurements both in the laboratory and in situ. The variation in the deformed shape of the pipe in different sidefills is also of interest, and the need to determine the pipe profile when assessing pipe behaviour is evident. Reference is made to future work to investigate the effects of traffic load and further details of the above tests, the

reporting of which has been brief, may be included in future publications.

#### 2.4.6 Soini's Experiments with Soft Soils

The Technical Research Centre of Finland has carried out theoretical, full-scale experimental and field investigations of thermoplastic pipes. This work is reported by Soini (1982A and B). Acknowledging that savings in pipe material can be made by exploiting the properties of the surrounding soil, he states that the optimum economic installation is one in which the pipe deforms to the level permitted in design. This is a fact that is often overlooked when assessing the performance of an installation. In his approach to design, he reiterates the need to treat the pipe-soil system as the basic structure and this should consist of the pipe, the surrounding fill materials, the insitu soil and, in some cases, the supporting structure (such as wooden piles and planks used in weak Scandinavian soils).

The theoretical study aimed to determine the mean deformation of flexible plastic pipes in three soft sidefill materials: mud, saturated clay and silt, and dry-crust clay/dry silt. The approach adopted by Watkins (Fig. 2.10), involving a graph of Ring Deflection Factor against Stiffness Ratio, was used. The relative vertical compression of the sidefill ( $\epsilon_s$ ) was calculated using mean values of soil compression parameters, and the vertical load on the pipe was taken as the overburden pressure. Theoretical points were calculated for uPVC, and medium and high density PE, pipes in each of the three categories of sidefill type and these are shown on the graph in Fig. 2.37. The agreement between the different pipe and soil types is good. Gumbel (1984), when discussing Watkins' work on the subject, presents such a graph containing empirical data for PE pipes in sand (after Gaube, 1977) and theoretical curves

(after Burns and Richard, 1964). This has been reproduced in Fig. 2.38 and the curves for Watkins and Soini have been added. A considerable difference is apparent between Soini's curve for thermoplastic pipes in soft soils and those from other sources, which are based on flexible pipes in typical fill materials. The discrepancy may be attributable purely to the soil type, although no experimental or field data have been quoted in support of Soini's theory and the fourfold increase in the maximum Ring Deflection Factor must, therefore, await substantiation.

Experimental studies were conducted in a 3.3m long x 2m wide x 4m deep pit, in which thermoplastic pipes were buried in various soils at two levels, as shown in Fig. 2.39. Light compaction was applied to the soil in each case. The load to which the pipes were subject was caused solely by the weight of the overlying fill, probably reflecting the conditions that are prevalent in the Scandinavian countries. In general, the vertical and horizontal diametral strains were found to be of different magnitudes and were described as "obliquely flattened". The pipes buried in dry silt and dry-crust clay had final vertical diametral strains of less than 1% in each case, and these stabilized relatively quickly. In contrast, the pipes buried in saturated clay showed deformations of 0.5 to 1.0% at the end of installation and these increased to between 3 and 4% with a steady increase in deformation. No further account of this work was presented, however, leaving the details somewhat incomplete.

A Pipe-Cruiser was used to measure deformations of pipes in the field. This consists of a device, mounted on runners, that is inserted into the pipe and pulled, from one manhole to the next, along the length of pipe to be measured. It produces a profile of the internal face of the pipe at any point using a telescopic rotating arm which relays co-ordinates to an X-Y plotter. The device has been used with success in pipes of 315mm diameter or more, in particular to investigate the relationship between pipe

deformation and pipe wall strain for field installations. The relationship can be expressed as follows

$$\epsilon_w = k (\Delta_v/D) (t/D) \quad (2.25)$$

where  $\epsilon_w$  = tangential (or circumferential) strain in the pipe wall

$\Delta_v/D$  = V.D.S. of pipe

$t/D$  = ratio of pipe wall thickness to mean pipe diameter

$k$  = coefficient

Where deformation is elliptical the value of  $k$  will be 3.0, and values of pipes in general use have been thought by researchers such as Molin and Jaaskelainen to range from 3.0 to 6.0, because of variations in deformed shape. Results obtained by the Pipe-Cruiser indicate that this variation in shape is considerably greater than supposed, with values of  $k$  ranging from 2.85 to more than 10.

It is clear from these papers that relevant research has been conducted in Finland and other Scandinavian countries, but little of this work has been published.

#### 2.4.7 European Field Measurements

A different, wholly empirical approach to the problem of deflection prediction is the collection and collation of measurements of pipe performance in operational pipelines. The method has the advantage that the pipe performance measurements reflect actual site conditions, thereby removing the need to estimate such factors as the bulk stiffness of the fill, the pressure distribution around the pipe and the influence of site practice. The main disadvantage of the method is the loss of control of



the pipe-soil system being measured, leading to a loss of information on such factors as initial ovality of the pipe, installation procedure, and loading history, especially that from traffic.

Such a series of measurements on uPVC pipes was instigated in Holland in 1967 under the auspices of KOMO, the Dutch authority on quality control of building materials for public works, and is reported in a series of publications by KOMO (1970), Gehrels (1972), Gehrels and Elzink (1979 and 1982), and de Putter and Elzink (1981). A wide variety of pipe size and class, cover depth, fill material and installation procedure were included in the investigation, which was widened to include pipelines in Great Britain, Germany and other European countries. It was acknowledged that the best method of conducting these investigations is to measure pipe deformation during and/or shortly after installation, record the method of installation used and take repeated measurements over the lifetime of the pipe. This was found to be rarely possible, however, and records of pipe installation procedure were often based on assumptions and secondhand evidence. This notwithstanding, it was thought that if sufficient pipelines were measured, the trends in pipe behaviour would become clear and the advantages of the method would be realised.

The device used to measure the dimensions of the pipe in situ consists of a weighted sledge, from which one vertical and two horizontal feelers protrude and contact the pipe wall. Movement of the feelers is recorded electrically and calibrated against known distances before and after testing. The pipe to be measured is cleaned by jetting and the measuring device is pulled through pipe between manholes, thus producing a continuous graph of horizontal and vertical deformation.

Deformation is thought to occur in three stages, which are defined as follows

1. During installation, in which pipe deformation is particularly

influenced by the type of insitu soil, compaction of the fill materials and the soil pressure on the pipe.

2. Due to the influence of traffic loading and associated vibrations, the extent of which is dependent upon the imposed loads and the bedding angle, but also on the further stabilization of the sidefill which will increase its lateral soil resistance.
3. Long-term deflection, which is caused by further stabilization of the pipe and soil and is particularly evident in cohesive soils.

The time-dependent nature of this process is characterised by Gehrels and Elzink (1979) as an "S-shaped" curve of pipe deformation, as shown in Fig.

2.40. Initial deformation occurs during the backfilling process and, on completion, increases slowly due to pipe and soil consolidation. If no further load is applied the deflection curve tends to a certain value and then flattens out with time. If the pipe is subjected to traffic loads, however, the deformation rate increases significantly until equilibrium is reached. Thereafter continued traffic load has no significant influence on pipe deformation. The final deformation value in both cases is thought to be similar. This behaviour has been recorded in other literature, a particularly good example being the field experiments by Trott and Gaunt (1976); the appropriate curve is reproduced in Fig. 2.17.

In the mid 1970s the emphasis switched from previously unrecorded pipes to the collection of replicate data (Gehrels and Elzink, 1979). Results of measurements in Holland, many of which are for pipes buried in wet clay or peat, showed that average long-term vertical diametral strain was between 3% and 10%, with peak measurements of up to 20%. In most of these installations, 'as dug' material was used for the pipe surround, with sand being used where imported material was required. Almost without exception, the surround material was classed unsuitable by the Compaction Fraction test, the method of site assessment recommended in BSI (1973 and

1980), and in no cases have pipes failed by excessive deformation. Thirty-five installations in which granular surrounds were used were studied in the UK. Average V.D.S. measurements for these ranged from 1% to 7.5%, with peak values up to 14%, and in no case did the deformations increase on remeasurement.

A parameter study involving 630 insitu measurements is presented by de Putter and Elzink (1981). Installations are classified in three ways; by sidefill type, pipe class and method of installation. V.D.S. measurements reflecting each of these parameters were plotted against log time in order to produce a general description of behaviour. Three methods of installation are defined to represent both care and degree of compaction and these are shown in Fig. 2.41.

The performance of pipes in sand sidefills classified by this method is summarised in Fig. 2.42. The majority of installations were type 2, or intermediate, and relatively little data was available for pipes with an SDR value of 34 in good or intermediate installations. It should be noted that pipes with an SDR value of 65 were only used in specific, well controlled circumstances, and that in this country uPVC pipes with an SDR value of 41 are used for non-pressure applications. The trends shown by these graphs are as follows:

1. The curves flatten with time, with type 1 installations showing little increase in deflection after backfilling.
2. Installation type strongly affects pipe deflection.
3. Pipe class only has a significance in poor installations.

Further division of the parameters affecting deformation produced other trends:

4. At shallow cover depths, intensive traffic strongly affects the rate of deflection.
5. Where load is due to overburden only, increasing cover depth has only a

slight influence.

Comparison of these measurements with those for pipes buried in pea gravel showed that the average reduction in deformation achieved by using the larger sized material was 0.5% V.D.S. In view of this, the cost of importing pea gravel was considered to be unjustified.

Measurements on pipes surrounded by cohesive material were much fewer in number, although certain trends were again discernable. The pipes surrounded by loam or silty clay had deflections that were 1.2 to 1.5 times as great as those with sand surrounds. Behaviour in clay surrounds, especially in weak alluvial clays, was found to be variable, although average V.D.S. measurements were roughly similar to those of pipes buried in sand. The pipes installed in boulder clay produced similar results to those in sands. In peat areas, better results were obtained with "as dug" surrounds than where sand was imported as sidefill.

Further results of this research are reported by Gehrels and Elzink (1982), and they make some interesting general comments. When considering all measurements taken for uPVC pipes, excluding pipes with an SDR value of 65 which are not normally used, they state that 99% of the measured sections had average deflections of 10% or less, and 97% of the measured sections had maximum deflections of 15% or less. In addition, pipes with vertical diametral strains of more than 20% have been in use for over 15 years without operational problems and failure of uPVC pipe with an SDR value of 51 or less is unknown. The report concludes that a limit on V.D.S. of 8% immediately after installation is sufficiently low to ensure that the pipe will function, with a suitable factor of safety, over its 50 year design life.

This work represents an important contribution to the understanding of the behaviour of buried uPVC pipes by virtue of its practical approach. Much of the field investigation took place on sites in which the excavated

insitu soil, most usually either sand, clay, or less often peat, was used as sidefill, although the extension of the work to other European countries enabled a greater variety of installations to be studied. The limitations of the method have largely been circumvented by the number of measurements made, although only general conclusions have been possible. Nevertheless, the results have enabled some of the previously unknown parameters, such as the "site practice factor" discussed by Boden (1976) and Boden et al (1977), to be estimated and it provides some data for assessing the applicability of the USBR equation (Howard, 1981B) to European conditions.

## 2.5 Concluding Discussion

Much research into the behaviour of buried flexible pipes has been conducted and this is reflected in the amount of published literature on the subject, the content of which is variable in both quality and relevance to this project. In some cases the quality may only reflect the incomplete manner in which it is reported, the advantages of appending detailed results being exemplified by the wealth of information on uPVC pipe behaviour thus presented by Howard (1973). Much of the research has been strongly influenced by the prevailing conditions in the country of origin, in some cases to the extent that extrapolation of the data is tortuous, if not impossible. It is clear that research conducted with preconceived ideas as to its outcome can impair objectivity and reduce its credibility. It is equally obvious when research has been planned with due regard to the fundamental principles of structural mechanics and the author has been aware of this when conducting his research.

Unplasticized PVC pipe is a relatively flexible pipe, that is one with little inherent strength, and in order for it to function structurally when

buried and subjected to vertical loads, it must deform in order that passive lateral support may be derived from the adjacent soil and fill materials. The magnitude of this deformation is dependent upon the properties of both the pipe and the surrounding soil, as well as the magnitude of the applied load, and research has shown these factors to be interrelated, hence the need to treat the pipe-soil system as the basic structure in design. When defining performance criteria for flexible pipes, two parameters are generally considered, ring buckling and excessive ring deformation; a third parameter of excessive hoop strain is of secondary importance. Research has shown that for uPVC pipes of the type used in underground drainage, ring buckling does not occur (O'Reilly et al, 1982, and others) and that excessive hoop strain is no basis for design (Moser, 1981), leaving excessive ring deformation as the principal, or critical, performance criterion. Structural failure by excessive deformation has been shown to occur at diametral strains in excess of 20% (Spangler, 1941; Howard, 1973; Gehrels and Elzink, 1982), but there is a need to limit diametral strain to a lower value than this in order to ensure long term structural stability, unimpaired flow capacity, joint integrity (including that with rigid connections), a cross-section that will accept conventional cleaning equipment and any other locally operative performance criteria (Donohue et al, 1979).

In their appraisal of uPVC sewer pipe deformation, Donohue et al (1979) classify pipe deformation into three categories

1. Initial deformation, or out-of-roundness, caused by pipe manufacture and handling, which produces a constant error in diametral measurements along the length of a pipe. An American Society of Testing Materials (ASTM) Committee investigated this phenomenon and found that values of up to 3% of the diameter could occur, although other sources quote maxima of 2% or less.

2. Deformation caused by installation techniques, which includes local deformation resulting from point loads, uneven bedding, pipe bending or other atypical loading conditions. In their discussion of longitudinal stresses, Janson and Molin (1972) isolate these factors and include differential settlement, which may often be unavoidable. The result of these effects is isolated, or peak, deformation values, which can often be high in relation to the average deformation of a pipe.

3. Diametral strains caused by soil and surface loadings, and it is to these that attention has been drawn in the preceding discussion. Alone of the categories, this is the one that can be rationally analysed and that provides information on the structural behaviour of the pipe-soil system. When analysing deformation data, it is essential to know the relative contributions of these categories if the behaviour of the system is to be understood and its safety assessed. Determination of diametral strain limits for flexible pipes and their subsequent interpretation have been often confused, because of the lack of definition of what factors should be included and whether it is a long- or short-term value. The first limit on vertical diametral strain was proposed by Spangler, who found that large diameter corrugated steel culverts failed by excessive deformation at a diametral strain of about 20% and, by applying a factor of safety of 4, suggested a value of 5% for design. It has been suggested that certain flexible pipes should be braced during installation because "negative" deformation, or vertical diametral elongation, has been shown to exceed 5% of the original diameter during compaction of the fill beside the pipe. There is evidently confusion here, because subsequent action under load would tend to improve, rather than exacerbate, the situation. Donohue et al (1973) treat the limit as a long-term value and, by applying a "deflection lag" factor of 1.5 (Watkins and Spangler, 1958), suggest a 3% limit on short-term vertical diametral strain. In their report, they have already

stated that initial deformation, or out-of-roundness, of up to 3% of the original diameter can occur, thus implying that in those cases no further deformation should be allowed, a situation that is clearly untenable. Before discussing the deformation limit in the context of the standards produced in this country, the work of the Nordic Evaluation Groups on this subject will be cited as an example of the benefits of research.

The Nordic Evaluation Groups were set up to co-ordinate research on buried plastic sewer pipes in Finland, Sweden, Norway and Denmark (Janson and Molin, 1972 and 1981). The first group (NUVG 70) was set up in 1968 with the aim of investigating both the material strength of the pipe and pipe stability in service, with particular regard to the influence of soil mechanics. The recommendations of the group concerning pipe stability were that coarse-grained material, such as sand and pea gravel, should be used for the pipe surround. Because of the lack of long term data, a conservative approach was taken in the choice of allowable pipe material properties. Consequently, the maximum allowable strain in the pipe wall was limited to 0.5%, with a corresponding limit on vertical diametral strain of 5% based upon this strain. An allowance for the normal ovalities of unloaded pipe (initial out-of-roundness), 1% deflection in the case of uPVC, could also be made to increase the allowable deflection slightly, and a single local (maximum) deflection of 7.5% or less was also acceptable. For areas of light loading conditions, uPVC pipe with Standard Dimension Ratio (SDR) value of 50 could be used and for heavy loading, including traffic, an SDR value of 34 was recommended.

The second group (NUVG 80) was set up in 1980 to examine the performance of pipes buried in firm soils over the previous 10 years and to investigate the use of plastic pipes in loose silty and clayey soils. In particular, the group was to question the allowable strain limit introduced in 1970 for plastic pipes, and to develop installation regulations and pipe



stiffness recommendations for non-pressure pipes in loose fine-grained soils. The relaxation of the strain limit would allow an increase in the diametral strain limit, and increase the significance of surrounding soil properties and long-term pipe stability when designing buried plastic pipes.

Results of measurements on pipes in firm soils (sands and gravels) indicated that maximum deformations were due mainly to uneven bedding, were generally below 10% of the original diameter and that average values were generally about 5%. Extrapolation of these results over 50 years indicated that the final diametral strains would not exceed 15%. A study by Janson (1981) indicated that strain in the pipe material caused by diametral strains up to 20% would not give rise to failure over a 50 year period at an average operational temperature of 20°C. A further study by Molin (1981) concerned gravity sewers buried in clay and silt, the pipes being tested in a large tank, in a test field and in use. In addition to pipes buried in sandy soils, uPVC pipes with SDR values of 41, 34 and 26 were tested in both soft and stiff clay with compaction by treading in 100mm layers where appropriate.

Experience of this and other work indicated that larger deflections would be acceptable and a limit on diametral strain of 8% was recommended for uPVC pipe immediately after backfilling, the final value being thought unlikely to exceed 15%. The use of uPVC pipes with an SDR value of 41 in trafficked areas proved to be suitable and such pipes were recommended for use in sandy soils with a good standard of compaction, instead of pipes with an SDR value of 34. All sandy materials were considered acceptable for use, with a limit on the size of stones of 10% of the pipe diameter for pipes greater than 200mm in diameter. The strain limit imposed by NUVG 70 was considered no longer appropriate and could be ignored, thus allowing thicker-walled pipes to be safely used without a concomitant decrease in

the deflection limit. For pipes buried in silty or clayey soil surrounds, the same diametral strain limits as for sandy soils were recommended, although use of such soils was restricted to areas where no more than normal traffic conditions are expected. Recommendations of appropriate SDR values of pipes in specific soil types and at various cover depths were also made. The success of the Nordic Evaluation Groups in rescinding the earlier, necessarily conservative, limits is evident and the resulting guidelines for the installation of uPVC pipes were thoroughly researched and presented.

In this country research into the behaviour of buried pipes has been carried out since the mid 1950s, notably by Clarke and Young, and this resulted in a series of publications on the subject. Early work was concerned more with rigid pipes and the loads thereon, leading to National Building Studies reports from the Building Research Station (Clarke, 1962, 1964 and 1966). A comprehensive summary of this work is presented by Clarke (1968). Emphasis later switched to the Road Research Laboratory (now the Transport and Road Research Laboratory, TRRL) where Page (1966) investigated traffic loads on buried rigid pipes. Young produced further guidelines for the calculation of loads in the form of simplified tables (Young and Smith, 1970) and guidelines for pipe design (Young, 1971). Research into the behaviour of flexible pipes was conducted by Trott, Gaunt and others at the TRRL and some of this has been recounted in detail in section 2.4. Research at the Cranfield Institute of Technology led to a TRRL Supplementary Report on the use of plastics for underground non-pressure pipes (Owston and Young, 1976) and more comprehensive guidelines by Young (1978). Young also summarised current knowledge on the subject of pipe design (Young, 1979).

It has been widely stated that the quality of fill material is the most important influence on flexible pipe behaviour and that suitable

lateral support is afforded by most soils when used as fill if properly treated, the exceptions including peat and weak alluvial clays (Janson and Molin, 1972; Gaunt et al, 1976; and others). The most economic solution to the question of how to provide suitable support depends upon the relative costs of importing good quality material and treatment of the insitu soil. This introduces a further important parameter, a quantification of the standard of workmanship, described by Boden (1976) as the "Site Practice Factor". Allowance must therefore be made for the cost of appropriate site supervision to ensure that the specified treatment of fill has been carried out. Boden states that for small diameter pipelines, the cost of laying the pipe exceeds that of the pipe itself and that economies are most likely to be made from a design that allows a minimum standard of site supervision.

With this in mind, the current installation recommendations (B.S.I., 1980) state "it is desirable that deformation should be limited to 5% at the end of installation" and to achieve this "the pipe should always be surrounded by non-cohesive material" and that "the fill material, particularly the bedding and sidefill, should be properly compacted." For pipes up to 315mm diameter, compaction in one layer is adequate. The Compaction Fraction test is recommended for the assessment of suitable fill materials, which should extend from at least 100mm below the pipe invert to the pipe crown or 100mm above in certain cases. The definition of the short-term diametral strain limit is somewhat vague, but is generally interpreted to apply to the pipe at the end of construction operations, that is after the installation has been subjected to construction traffic loading. To meet this requirement in practice, uncompacted single-sized gravel (pea gravel) is specified, as a 100mm thick bedding layer and sidefill extending to the pipe crown. This material invariably has to be imported and the cost thereof forms a substantial proportion of the costs

of installation. It is to determine the necessity of importing this material to sites where sidefill compaction cannot be specified that this project directs itself.



### 3 RESEARCH PHILOSOPHY

#### 3.1 Introduction

Certain aspects of research into buried flexible pipes, and particularly experimental investigations of uPVC pipe behaviour, have been extensively reviewed in Chapter 2. Of most interest in this project is the behaviour of small diameter (75 to 160mm)<sup>\*</sup> uPVC pipes under conditions that prevail in normal use, although it is hoped that the results of the work will be equally applicable to larger diameter pipes subject to a small further experimental study. In addition, the trends in behaviour elucidated in these investigations will necessarily add to the knowledge on buried flexible pipes, a generic term of which uPVC pipes are a subset. All of the experimental studies reviewed were conducted on pipes of 315mm diameter or greater, and no justification, experimental or otherwise, is evident for the direct application of these results to smaller diameter pipes. Apart from the scaling factor of such parameters as soil particle size and cover depth, differences might also arise because of variation in the distribution of material below the haunches, the thickness of layers for compaction and the arching effects in the backfill.

Of most relevance are the full-scale laboratory experiments carried out at the Transport and Road Research Laboratory on 315mm diameter uPVC pipes under various installation conditions (Trott and Stevens, 1979). The programme included 10 installation types in which the influence of both backfill and sidefill compaction were investigated using the sandy clay insitu soil as sidefill in 5 tests, uncompacted pea gravel in 2 tests and 3 alternative sidefill materials. The necessity of considering a wide range of conditions resulted in a lack of detailed conclusions, and possibly also

\* 160mm diameter pipes were used in the tests

to the lack of detailed information included in the reports of the work. In addition, the need to gain maximum information from limited tests led to the introduction of a load regime that was not representative of site conditions. Thus, while providing good background information, the work does not describe the behaviour of uPVC building drainage pipes in practice.

In view of the absence of published information on this specific problem, the general aims of the project are to develop a facility for the provision of data on small diameter uPVC pipe behaviour, and to produce such data with particular regard to the isolation of the fill material properties that determine the pipe behaviour. Using this information the current installation recommendations can be assessed, and measures leading to economies in the installation of uPVC pipes introduced where appropriate.

### 3.2 Methods of Investigation

There are several approaches that can be adopted when investigating practical situations and each has advantages in different applications. The study of failures is an obvious possibility and will provide a lower bound limit on performance in cases where the reasons for failure can be clearly ascertained. Such an exercise on buried pipes is reported by Brennan and Young (1976), although no relevant failures of non-pressure uPVC pipes are included. Other researchers have stated that there are no known pipe ring failures of uPVC pipe with a Standard Dimension Ratio of 51 or less buried under normal conditions. This, combined with their relatively recent introduction in relation to their design life, would suggest the method to be fruitless. A variation of this field study is the

investigation of uPVC building drainage pipes in use. Measurements of installation performance, accompanied by local excavations to determine fill conditions, would lead to an accurate indication of typical pipe behaviour. Assumptions would have to be made about initial ovality, the method of installation and loading history, and average performance, rather than individual measurements, would have to be used. In addition, practical considerations would limit the amount of information that could be obtained on pipe behaviour, probably to the extent that only deformations could be measured, thereby reducing its effectiveness. Such a field study has been conducted in Holland (Gehrels and Elzink, 1982) and the vast amount of information gathered provides a good indication of the necessarily extensive nature of the method if conclusions are to be clear.

Greater accuracy would be possible if the method was applied to sites where pipes were being newly laid and records of installation procedures and initial diametral measurements could be made. The addition of permanent instrumentation would be possible and this would greatly increase the information that could be obtained from any one installation. True site practice is unlikely to be achieved, however, if foreknowledge of the study is available and there would be a practical limit on the amount of sites that could be treated in this way. A good example of this method of research is reported by Trott and Gaunt (1976).

A further variation would involve full-scale experimentation in a field site. Site practice would be simulated and standardised to produce a high degree of control over installation. Access to the inside of the pipe could be ensured and instrumentation, which would be recoverable at the end of each test, could be installed to monitor both pipe and soil response. Accurate surface loads could be applied by laden wagons and the loading history would be known. A suitable field site would have to be found for these tests, however, with a change of location if the effect of a



different insitu soil is to be monitored. Instrumentation would have to be relatively unsophisticated and processing of data would be necessarily slow due to the lack of laboratory facilities. In addition, the experimental programme may be affected by adverse weather conditions and the cost, both of developing and performing field trials, is likely to be high.

Some of these experimental difficulties could be removed by carrying out full-scale testing in the laboratory. Site practice would be simulated and standardised as above and a greater degree of sophistication of instrumentation would be possible, which could be linked to a computer to facilitate processing. Control over measurements, both inside the pipe and in the soil, would be greater. Although surface load would require simulation, accurate measurement of the load applied to the surface of the backfill could be made. A suitable test facility would have to be developed and, as with a field trial, turnover of test installations would be slow. Development costs would be high, though subsequent running costs would be relatively low. This is the method most often adopted for such work, which is probably a testament to its versatility.

A further laboratory technique that has been employed involves the testing of models. Its application to this project would involve the use of a scaled-down pipe buried in either a real soil or an artificial medium. All aspects of a pipe installation would be simulated and far-reaching assumptions would have to be made on the simulated pipe and soil behaviour, such that full-scale tests would have to be carried out to validate the data. Development of appropriate techniques would be slow, although the degree of control over experimental conditions would be high. The most notable application of model tests to buried pipe research has been the use of a geotechnical centrifuge (Valsangkar and Britto, 1978 and 1979; Trott et al, 1984), a general view on the subject being presented by Roscoe (1968).

The final option involves the use of theoretical techniques for the prediction of buried pipe behaviour. A theoretical model, incorporating assumed pipe and soil properties, would be formed and subjected to theoretical load distributions. Experimental work is necessary to determine the properties of the pipe and soil, and full-scale trials would be necessary to validate the method. A problem of this kind would lend itself to finite element analysis, which is particularly attractive in view of the criticism of other methods reviewed earlier. Development of an appropriate model would be slow, although, once developed, running time would be negligible. Acceptance of the method would be largely dependent upon the experimental work used for its validation, however, rendering the method less suitable as a basis for prediction in the first instance. The use of a wholly theoretical approach is exemplified by Gumbel (1984) and, while being a masterly attempt, its justification lay in its general applicability to flexible pipes and its verification by experimental work is yet to be proved. Although initial results are promising, the time required for validation, as acknowledged by Gumbel, is likely to be great.

A summary of these methods of investigation of pipe behaviour is presented in Fig. 3.1, together with some of the basic considerations for their choice. Two fundamental approaches can be discerned from these alternatives. A finite, and in practice relatively small, set of data can be obtained, either by experimental or field measurement, and can be extrapolated, or generalised, to an infinite set of site conditions by defining the pertinent structural properties of an installation and producing a method of their site measurement. The alternative approach involves the theoretical simulation of the real situation and production of a set of equations or design charts to cover an infinite number of possible site conditions. This method requires experimental determination of structural properties and field validation, together with a method of

measurement of the structural properties of potential materials on site. This project provides a balance between these two approaches, though with the emphasis placed on experimental investigations. Full-scale laboratory experiments were chosen as being the most versatile form of experimentation, in which tight control over the boundary conditions can be applied and acceptability of data without extensive field validation is possible. The reality of experimental simulation can be maximised by careful consideration and application of boundary conditions, and maximum efficiency can be achieved by care in planning the programme of investigations. Extension of the experimental data by theoretical means will also be investigated using finite element techniques, although simple elastic models will be incorporated and this work will take the form of an elaborate feasibility study for possible further extension.

### 3.3 Performance parameters

The critical performance parameter for buried uPVC pipe with a normal Standard Dimension Ratio for underground usage (41 or less in this country) is excessive deformation, as discussed extensively in Section 2.5. The level of deformation at which failure is deemed to have occurred is unimportant in the reporting of results and will be influenced to some degree during experiments by the instrumentation used inside the pipe during the tests. In relating the experimental results to practice, difficulties arise in the interpretation of existing recommended limits, the relation of results to these limits depending upon the realism of the level of applied load and other factors. No consideration will be given to the behaviour of uPVC joints or the relationship between pipe and joint deformation. Joints are tested to 10% diametral strain as a result of

existing standards, and their long-term performance beyond this value is arguable. Joint deformation will only become important if the existing limits on pipe deformation are relaxed and it will, therefore, be the domain of future researchers.

While it is implicit that only the maximum diametral strain of the pipe is important in determining the performance of an installation, measurement of the factors that influence the response of the pipe to load is necessary in order that the pipe behaviour can be explained. Thus, the assessment of pipe performance will be made on the basis of many measurements and their relation to the critical parameter will be sought.

### 3.4 Factors Influencing Pipe Deformation

The factors that are likely to influence pipe deformation are summarised in Fig. 3.2 and will be discussed in greater detail below. The size of the pipe has not been included in this list of parameters but it has been incorporated in those defining trench geometry, on which it has a direct influence. Pipe size also has an indirect influence on the fill and soil parameters, several of the other factors being similarly interrelated. A number of other factors are implicitly included in these parameters or their combinations. These include the pressure distribution around the pipe, which has formed the basis of many design formulae, is statically indeterminate and dependent on several of the parameters listed below. Slippage at the pipe soil interface is likewise included by implication.

#### 3.4.1 Surface Load

It has been established by Trott and Gaunt (1976) that construction

traffic provides the worst potential loading case, as axle loads are often near or above the legal limit for roads and pipes often have less cover than when the finished level is achieved. The loads on the pipe will consequently be due to moving wheels and will be repetitive. The current weight limit for vehicles travelling on roads is 11 tonnes/axle (or 5.5 tonnes/wheel), and this will be spread over the contact area between wheel and ground surface. Wheel loads on building drainage sites are unlikely to be significantly greater than those carried on roads and heavier site loads, such as those from cranes in use, are likely to be kept away from areas in which underground pipes have been buried.

#### 3.4.2 Ratio of Cover Depth to Pipe Diameter

The depth of cover affects both the influence of surface loads and the magnitude of the soil load. By expressing it as a non-dimensional parameter in terms of pipe diameter, a scale factor is introduced which will facilitate the extrapolation of results according to a relationship that is as yet undetermined.

Where no surface load is applied, the load on a buried pipe increases with cover depth. This is illustrated in Fig. 3.3(a), which shows a graph of vertical diametral strain against depth of cover for a 315mm diameter pipe (Gehrels, 1982). The magnitude of the load is governed by such factors as trench wall friction and arching in the backfill. Where a surface load is applied, however, the effect on shallow buried pipes decreases sharply as the cover depth increases. In this case, soil load has little effect on pipe deformation at shallow cover depths. The effect of soil load becomes more dominant with increasing cover depth, the curve closely resembling that for no surface load once a depth of approximately 3m is exceeded. The attenuation of vertical pressure with depth was

investigated as part of the Ministry of Housing and Local Government's brief and the 1967 Report includes a summary of their findings, reproduced in Fig. 3.3(b), which confirms this behaviour. It is clear, therefore, that shallow buried pipes provide the critical case where surface load is applied.

#### 3.4.3 Ratio of Bedding Thickness to Pipe Diameter

Bedding material is laid in the bottom of trenches primarily to provide uniform pipe support and remove the likelihood of differential settlement. This is necessary in soils that are weak and compressible, or which contain large or angular stones that could cause point loads on the pipe wall. The use of bedding material is widespread, however, the advantage of reducing the work involved in hand trimming during excavation being offset against the cost of importing suitable material. Good quality granular material is generally used, as it is largely unaffected by compaction. It has been suggested that, in certain cases, loosening the material of the trench bottom will perform the same function (Gehrels and Elzink, 1982).

A bedding of approved granular material of at least 100mm thickness is recommended (BSI, 1980) in cases where the excavated material does not achieve the standard of compaction resistance required by the Compaction Fraction test.\* In practice, the depth of bedding generally varies from 100mm to 150mm and bears no relationship to the pipe diameter. No data have been published on the influence of bedding on uPVC pipe deformation, however.

\* see page 195

#### 3.4.4 Ratio of Trench Width to Pipe Diameter

Trench widths used in practice are governed by many different factors, notably pipe diameter, insitu soil type, sidefill type and its treatment, trench depth and working room. The recommended minimum trench width is the pipe diameter plus 300mm (BSI, 1980). The effect of increasing the ratio of trench width to pipe diameter is to reduce both the beneficial action of the trench wall in resisting surface load and the influence which the insitu soil has on the performance of the pipe. The point at which the insitu soil has no influence is thought to be where the ratio is approximately 5 (Howard, 1972; Dezsényi, 1975; and Barnard, 1957). Where excavated insitu soil is used as sidefill, a narrower trench will generally afford more support to the pipe, because compaction rarely reinstates a material to its original state.

#### 3.4.5 Shape of Trench

Vertical-walled trenches are generally used for building drainage where possible, variation in shape generally being caused by such adverse soil conditions as unstable trench walls. Sloping trench walls are thought to result in an increase in the load on a pipe due to a reduction in trench wall friction, the effective trench width usually being taken as the width at the crown of the pipe for design.

#### 3.4.6 Type of Bedding and Sidefill

The role of the bedding layer, as discussed briefly in Section 3.4.3, is to provide uniform support to the pipe in order to protect the pipe wall from abrasion or puncture by angular stones or sharp objects, and to reduce the likelihood of differential settlement. The latter phenomenon is most

prevalent and can arise from several sources, such as large stones in the trench bottom, variation in level caused by mechanical diggers and variable underlying insitu soil. The influence of both factors on pipe performance is the creation of isolated peak, or maximum, deformations.

The role of the sidefill is markedly different. The action of a flexible pipe in relieving concentrations of stress above the pipe crown is to deform, thereby developing lateral passive soil resistance on the pipe wall. The magnitude and shape of this deformation are governed predominantly by the properties of the sidefill and in particular its lateral stiffness characteristics. The magnitude of the vertical stress on the pipe crown is dependent upon the relative stiffness of the pipe ring and the soil, hence the vertical stiffness characteristics of the sidefill. The type of material used as sidefill is therefore of particular importance in determining both short-term and long-term pipe performance.

#### 3.4.7 Method of Laying Bedding and Sidefill

The method of laying fill materials reflects both the level of compaction and the care in their positioning, thereby influencing the properties of the materials. The function of the material is important in determining its treatment, and differences exist in laying techniques for bedding and sidefill. When laying bedding, the resulting material should remove the likelihood of differential settlement in the underlying insitu soil and be sufficiently workable or compressible to ensure uniform support. A method used in Holland (Gehrels and Elzink, 1982) involves local loosening of the insitu soil forming the trench bottom so that any hard spots are removed and the settlement of the pipe in relation to the sidefill is increased, thereby encouraging arching in the backfill and reducing the pipe crown pressure. The current British Standard



installation recommendations (B.S.I., 1980) state that the bedding layer should consist of good quality non-cohesive material and should be compacted. The success of either method is dependent upon the characteristics of the material used, the method chosen probably reflecting the philosophy of pipe laying in different countries.

The different function of the sidefill leads to a different approach to its laying. Both the vertical and horizontal stiffness of the sidefill are important in improving pipe performance, thus requiring maximum homogeneity and density of the material. Careful placing of the material will maximise both of these parameters, the critical area being under the haunches of the pipe where access is restricted. The properties of the sidefill will be further enhanced by compaction, by which the vertical stiffness will be directly increased and the horizontal stiffness indirectly, residual lateral stresses also being built in. The benefits of compaction are dependent upon the characteristics of the material being subjected to it; some, such as well graded non-cohesive materials, are very responsive to compaction, whereas others are largely unaffected, compaction only causing the material to "bed in". Certain materials, such as some clays and silts, will only perform well if thoroughly compacted.

In practice the same material is generally used as both sidefill and bedding, whether imported or in situ. In this country pea gravel is invariably used, a material that is largely unresponsive to compaction and which can be easily manipulated to provide uniform support to the pipe invert.

#### 3.4.8 Type and Method of Laying Backfill

The influence of backfill on pipe performance is dependent upon its vertical compressibility and its ability to develop arching over the

flexible pipe. The magnitude of the vertical pressure reaching the pipe crown is partly dependent upon trench wall friction, which develops as the backfill settles in relation to the insitu soil beside it. Spangler (1941) suggested the use of compressible material directly above the pipe in order to induce this effect. The ability of the soil to arch over the pipe crown as it deflects is dependent upon the properties of the backfill and the vertical stiffness of the sidefill.

In practice, the excavated insitu soil is generally used as backfill on building drainage sites. In cases where large or angular stones occur naturally, these should either be removed from the material placed up to 300mm above the pipe crown or other material should be introduced as a protective layer (B.S.I., 1980). The British Standard also recommends compaction of the backfill in 300mm thick layers, although this is rarely carried out in the case of building drainage.

#### 3.4.9 Type and State of Insitu Soil

The main influence that the insitu soil exerts on the behaviour of a flexible pipe consists of the lateral support provided to the sidefill and is dependent upon the ratio of trench width to pipe diameter, as discussed in section 3.4.4. Lateral stiffness of the insitu soil is most important in this respect. Indirect influences include its stability during excavation, thereby governing the shape and width of the trench, and its ability to develop trench wall friction and resist the resulting vertical forces. Where the insitu material is particularly poor protection may be necessary to allow vehicular access, which in turn will influence the vertical load on the pipe.

#### 3.4.10 Groundwater Level

The effect of submerging a buried pipe is threefold:

1. the lateral stiffness of the sidefill will reduce, thereby decreasing its capability to provide lateral support to the pipe,
2. the vertical load due to earth fill will reduce as buoyant, rather than dry, unit weight will apply, and
3. hydrostatic pressure will be applied.

The overall effect is thought to change only the rate at which the maximum deformation is reached, however, the rate of deformation being lower during the early stages when submerged.

#### 3.4.11 Quality of Pipe Material

The material properties of uPVC pipe are thought to be generally consistent between manufacturers and in view of the relative unimportance of pipe ring stiffness compared with that of the soil, its influence on the structural performance of an installation can be considered negligible. Recent information (Lancashire, 1985) suggests that pipes of variable quality are in use, and that this might affect their long-term behaviour, although the critical stage is usually considered to be during construction (Trott and Gaunt, 1976).

#### 3.4.12 Pipe Class

Pipe class effectively determines the pipe wall thickness, or Standard Dimension Ratio (SDR), which affects the inherent strength and flexibility of the pipe. <sup>uPVC</sup> Pipes with an SDR of 41 or less are generally used for underground purposes in this country, although pipes with SDR values of 51 and 65 have been used in Europe.

#### 3.4.13 Pipe Abnormalities

Pipe dimensions can vary both longitudinally and circumferentially. The two potentially most important factors affecting pipe deformation are initial ovality, and its orientation, and variation in wall thickness around the pipe circumference. In practice, manufacturing tolerances ensure that the wall thickness variation is minimal and its influence on pipe performance is negligible. Abrasion of the pipe wall can also lead to local reductions in wall thickness, although the likelihood of this occurring is reduced by recommendations for handling and installation (B.S.I., 1980). While initial ovality is also controlled during manufacture, this phenomenon can also occur due to storage and handling of the pipes and maximum values of 2 and 3% of the original diameter have been quoted. The measurement and orientation of this ovality are important in determining the structural performance of a pipe in practice, as discussed in section 2.5.

Inclusion of this factor when determining the acceptability of the pipe at the end of backfilling is unclear; in the Scandinavian countries an allowance of 1% vertical diametral strain is made in addition to the limit on deformation to allow for this effect (Janson and Molin, 1981).

#### 3.4.14 Longitudinal Bending Effects

Longitudinal bending effects are the result of differential settlements, and occur for a variety of reasons, such as inconsistencies in the trench bottom and where the pipeline crosses a road or ditch. A stress concentration occurs at the critical point and this is relieved by a localised deformation of the pipe, deformation due to surface load thereafter accumulating at the same rate as an undisturbed pipe.

#### 3.4.15 Temperature

The temperature at which the pipes operate will influence the properties of the uPVC forming the pipe wall. In general, only the extremes of temperature are likely to cause any significant difference in behaviour, and these are unlikely to occur in normal practice.

#### 3.4.16 Time

Time is an important consideration both in the short term, in relation to construction traffic loads, and in the long term with regard to creep<sup>\*</sup> behaviour of the pipe and soil. The rate of cyclic loading, that is the time between load applications, and duration of the load both affect the response of the pipe, longer applications of load and shorter recovery periods being considered to cause greater deformation. Repeated application of a particular magnitude of load will cause the deformation to tend to a certain value, the number of applications necessary for this to occur varying with the surrounding soil and quoted variously as 10 (Trott and Gaunt, 1976) and 100-200 (Gaunt et al, 1976). Deformation under continued static load will also tend to a certain value, the curve of deformation against time being approximately exponential. Long-term deformation caused by creep of the pipe-soil structure is similarly dependent upon the properties of the pipe surround, stability generally being achieved faster in non-cohesive than cohesive fills.

#### 3.4.17 Settlement of the Pipe and Fill

Settlement of the various components of an installation are described indirectly by a number of the above factors, but its potential importance in determining the behaviour of a buried uPVC pipe warrants its inclusion

\* creep has been used here to describe all long-term behaviour

here. Various aspects of settlement can be discerned from the above discussion, and it is relative, or differential, settlement that is of most interest. Differential settlement along the length of a pipeline will cause isolated peak deformations, which do not describe true structural behaviour and should be distinguished in analysis. Relative settlement of the surface of the sidefill and the pipe crown determines the vertical pressure applied to the pipe (Marston, 1930) and this can be influenced by the relative stiffnesses of the underlying materials. Settlement of the surface of the backfill in relation to the surrounding insitu soil influences the load applied to the pipe in determining trench wall friction and surface load distribution, and in extreme cases can significantly reduce the depth of cover to the pipe crown.

### 3.5 Boundary Conditions

It is clear from the above exposition that care must be taken in the choice of boundary conditions in order that an accurate simulation of site practice is achieved and that the reasons for variation in behaviour between tests can be discerned. The practical situation of building drainage is of most interest in this project and it is with this in mind that the boundary conditions have been evaluated. In order that the limits of behaviour can be ascertained, the worst likely conditions occurring under normal site practice have been modelled.

The insitu soil chosen for the tests was Keuper Marl, a locally occurring silty clay, which was used to represent a relatively poor site in which a low lateral stiffness could be expected from the trench walls. Shallow buried pipes in trenches of typical width were of most interest and, in consequence, both the cover depth and trench width were taken as

500mm. Vertical walled trenches were used. The pipe diameter was kept constant at 160mm and an SDR of 41 was used throughout. The uPVC pipe used in all experiments was to the appropriate British Standard, each pipe displaying a Kitemark, and was obtained from a local builders' merchant without regard to manufacturer. Other influences, such as groundwater variations, longitudinal bending and temperature, were not included in the investigations.

The magnitudes of surface load were chosen to represent the wheel load of a vehicle at the legal limit for roads in the United Kingdom (5.5 tonnes), and a somewhat greater value (7 tonnes) to represent either an overloaded vehicle or the redistribution of loads occurring in a construction operation, such as a vehicle tipping. These represent axle loads of 11 tonnes and 14 tonnes respectively, and are unlikely to be exceeded on a typical building drainage site. Larger construction traffic loads could be expected on major Civil Engineering contracts, but in such cases precautions in line with the British Standard recommendations are likely to be taken when laying affected pipes. The most severe combination of loads involves the application of static loads followed by cyclic loads (Gaunt et al, 1976). In consequence, the 5.5 tonne (55kN) load was applied statically for 30 minutes before being cycled 150 times at approximately 12 cycles per minute, though with breaks in the sequence in order that readings could be taken. The process was repeated with the 7 tonne load, recovery periods being allowed between each load sequence. At the end of each load sequence, the pipe deformation readings had become approximately stable. This regime was applied to each installation, unless excessive deformation caused the test to be terminated prematurely. A standard load platen was used, the design of which is discussed in greater detail in Chapter 4.

The parameters that were of most interest in the investigations were

the influence of bedding and sidefill on pipe performance, and in particular the type and thickness of the bedding layer, and the type and compacted state of the sidefill. In order to reduce these variables, three bedding thicknesses were investigated (0, 50 and 100mm) and in each case where a bedding layer was used, the material was dumped, levelled and lightly trodden in a manner consistent with the movement of men working in trenches. Once the pipe had been positioned, the sidefill was dumped and levelled, ensuring an even distribution of material around the pipe. Three compacted states of the sidefill were investigated : no compaction, light compaction by systematic treading (2 passes) and thorough compaction by 2 passes of a pneumatic tamper. The method of backfilling used for each installation involved replacement of the excavated silty clay in one layer with thorough compaction at the surface.

By adopting these standard procedures, a tight control over the boundary conditions was achieved and the influence of the varied parameters was clear. The process of isolating and standardising the values of these parameters has been exhaustively described herein, because of the importance attached by the author to details of this kind. A rigorous approach to the reporting of the process was also felt to be necessary in the light of the (apparently) variable data presented in the literature.

### 3.6 Experimental Considerations

The first requirement for the full-scale experimental work was a test facility of suitable size to ensure that the walls and base exerted no influence on the performance of the installation. It is widely assumed that a pit width of ten times the pipe diameter is sufficient to ensure that installation behaviour remains unaffected (Trott et al, 1977), the

\* for details of the sidefill materials used refer to Table 4.3 on page 149



depth to the base being less critical. It was decided, therefore, that a tank of dimensions 3m long x 2m wide x 2m deep would be constructed, which would allow loads to be applied at two points along the length of each installation. For practical reasons, it was decided that this should be constructed below the floor of the laboratory, consequently a pit of dimensions 4.1m long x 2.1m wide x 1.9m deep was formed in order to incorporate an inspection chamber at one end. This meant that the ratio of pit width to pipe diameter used in the tests was about 13, a value that compares favourably with the experimental work at the Transport and Road Research Laboratory, and that installations with cover depths well in excess of 500mm could be investigated.

As a result of the time required for the construction and development of the pit and its associated equipment and instrumentation, a reinforced box was also commissioned in which relatively quick experiments could be performed under well defined, if unrealistic, boundary conditions. This facility enabled the collection of comparative data, under particularly severe conditions of loading, which were of use both in determining the behaviour of uPVC pipe in a wide variety of pipe surrounds and in planning the pit experiments. It was also extensively used for the development of instrumentation techniques. Careful planning of the experimental programmes enabled the data from the box to complement those from the pit.

In order to assess the performance of an installation, the only measurements that are required are the deflections of the crown and invert of the pipe, from which the vertical diametral strain and settlement of the pipe can be determined, and the surface settlement, which may affect the performance of any overlying structure or landscape. These measurements alone would provide little information on the behaviour of the installation and the reasons behind it. In view of the unavoidably long time required to perform the tests and the need to explain the resulting behaviour, it is

essential, therefore, that the maximum amount of information is gained from each installation.

It is clear from the literature that the shape of pipe deformation varies between installations and a method of deducing this is desirable. Two methods have been described in the literature, one involving a photographic technique (Gaunt et al, 1976) and the other strain gauges (Broere, 1984), and both were successfully used in the box. The photographic technique was applied to the pit experiments alone, however, because of the difficulty in mounting strain gauges around the internal circumference and undesirability of altering the characteristics of the pipe-soil interface by external mounting. An independent measurement of vertical diametral reduction was also made, with the additional advantage of providing information on the performance of the pipe during the test. In order to further explain the behaviour of each installation, vertical strains in the backfill and horizontal strains in the sidefill were determined and trench wall pressures were monitored.

A detailed study of the properties of the fill materials and insitu soil was undertaken, using both insitu and laboratory techniques, and tests for consistency of the pipe were also performed. The need to develop a method of soil assessment for use on site resulted in the soil characterization tests assuming a greater significance. The development of the site test ran concurrently with the full-scale experimental work and the results were particularly useful in providing information for use in the theoretical model.

Collection of this information, together with detailed measurements of pipe dimensions and soil surface movements, resulted in a large amount of data describing each test. The relevance of the data was only determined during their subsequent analysis. Much of the information was of use in determining consistency between experiments. The approach was additionally

justified by the need to supply information for the later development of the theoretical model, if found to be feasible by the preliminary theoretical investigations reported herein. Consequently, no apology is made for the apparent lack of an attempt to analyse all these detailed data in the ensuing chapters.

### 3.7 Philosophy Behind the Test Programme

It has been stated above that the project is of an essentially pragmatic nature and one in which realism is aimed at and approximated to in the experimental work. The results of the research are to be applied to site conditions and it is the behaviour of uPVC pipe under these conditions that is of most interest. Nevertheless, the reasons for the observed behaviour have been sought and this was felt to be possible only by the investigation of pipe surround configurations that would be impractical to reproduce on site. The number of experimental installations that could be studied was limited by practical considerations and a careful balance had to be drawn between practically and research orientated experiments. In view of this, it was decided that the pit should be used for installations that simulate potential site practice and that the box should be used primarily to supply data to aid the planning of the pit installations, its secondary role being to produce comparative data on atypical installations.

The first objective was to determine the performance of the standard installation, involving uncompacted pea gravel as full-depth sidefill and 100mm thick bedding, in both the pit and the box. Thereafter, several avenues of investigation were of interest, including the role of the bedding layer, the ability of poor materials to provide suitable support when compacted and the relative performance of uncompacted granular materials of

distinctly different type. It was considered particularly important that the limit of granular sidefill materials that could be used without compaction to produce suitable performance should be estimated, while ensuring that most of the data was practically useful. Where possible, therefore, materials that were readily available throughout the country were chosen as fill with regard to the practical implementation of the results. Experimentation in the box, once the preparatory work for the pit installations was complete, was directed towards the production of data from installations in which good and poor materials were juxtaposed around the pipe, thereby determining the areas in which good support was most effective in reducing pipe deformation.

The experimental work was planned with the intention of being of sufficient variety to describe the behaviour of buried uPVC pipes under a multiplicity of conditions, despite being limited in time by the need to conduct a thorough review of the literature, the subject of which was new to the University of Nottingham, and by the extensive development of equipment and instrumentation. Associated soil testing, both in the laboratory and in situ, is to run concurrently with this experimental work, both to gain a good basic understanding of the soil properties and to produce ideas for the site assessment test for potential fill materials. The combination of these two experimental programmes should provide sufficient information for use in developing a primitive theoretical model of the situation. With these aims in mind the experimental programme was undertaken, but with the additional intention that the programme should be subject to periodic scrutiny and adjustment in order that experience, as gained, was incorporated into the planning. For this reason, much of what has been written above has taken the form of the past tense and no apology is offered for this.



## CHAPTER FOUR



## 4 EXPERIMENTAL STUDY OF PIPE BEHAVIOUR

### 4.1 Introduction

The subject of this project is new to the University of Nottingham and, once other experimental work had been reviewed, careful design of appropriate equipment and instrumentation was necessary in order to conduct the experimental work. Many of the factors considered in the design have been discussed in Chapter 3 and this chapter serves to draw these together in an explanation of the equipment, instrumentation and its use. Brief details have been given elsewhere (Rogers et al, 1985) and this opportunity will be taken to enlarge on these, elucidate the reasons behind the design decisions and describe the development of the various experimental techniques. The methods used for pipe material classification are also described herein; the methods of soil characterisation, in contrast, being considered as a separate entity and presented together with their results in Chapter 6. Finally the programme of experimental work is discussed with regard to the aims of the project.

There were many considerations to be taken into account when planning the experimental work. As with all research of this kind, experimental procedures should be reviewed and updated in the light of experience of use. In this case, however, there was an overriding requirement of consistency of boundary conditions, even with regard to the timing of measurements, and any procedural changes would have to ensure that this was met. The need for efficiency of the test programme was enhanced by the unavoidable delay to its instigation, caused by researching, designing, constructing and testing the means by which it could be carried out. It was essential, therefore, that experimental work should begin as early as



possible and that the first few tests should be used for the dual purpose of testing the equipment and instrumentation, and developing experimental procedures and techniques, in order that the main test programme could be carried out unhindered. In contrast to the limitation on procedural changes, it was desirable that the programme of experimental work should be constantly reviewed and amended, and essential to its efficiency. As discussed in Chapter 3, therefore, the experimental programme and the reasons behind its development are described with hindsight.

## 4.2 Equipment

### 4.2.1 The Test Pit

Of most importance to this largely experimental project was a suitable facility in which the work could be conducted. In addition to the considerations concerning the dimensions of the testing area expounded earlier, factors such as method of load application and ease of operation were also included in its design. It was originally intended that a structure should be built above ground in the laboratory, load being applied to the backfill surface through an independent portal frame. Several alternative structures were evaluated, including a precast concrete box-culvert section, precast concrete retaining wall sections, insitu reinforced concrete walls, propriety types of reinforced concrete formwork, steel tanks and a steel framed timber construction. Reduction of deflection of the container walls to acceptable limits was difficult to achieve economically with any of the proposed structures, however, and the necessity of using a crane to facilitate excavation and reinstatement of the trench, together with the possibility of delays arising therefrom, led to the design and commission of a sunken, reinforced concrete lined pit in

the floor of the laboratory. This had several advantages, the greatest being ease of operation and most realistic simulation of site conditions. The main disadvantage of a longer construction period was counteracted by careful use of other facilities for the development of instrumentation and experimental procedure.

The overall size of the pit, 4.1m long x 2.1m wide x 1.9m deep, was sufficient to provide a 3.0m long testing area and an inspection chamber at one end. The latter was incorporated in order that access could be gained to the inside of the pipe during experiments. Once the laboratory floor had been broken out, excavation for the pit took place in a predominantly granular material. The water table was encountered at a depth of 2.1m below floor level and, to avoid the need for water removal by pumping, the depth of the pit was reduced from 2.0m to 1.9m. The base of the pit is constructed of 150mm thick reinforced concrete on a 50mm weak concrete blinding with 2000 gauge polythene providing a waterproof membrane. The pit walls are also formed of 150mm thick reinforced concrete cast directly against the face of the excavation, a polythene membrane again being added. A water bar spans the construction joint at the base of the walls to ensure that the pit is watertight. A 200mm deep by 150mm wide rebate has been formed along two sides of the pit to accept covering beams when the pit is not in use. The layout and construction of the test pit is shown in Figs. 4.1 to 4.3.

The dividing wall, forming an 850mm wide inspection chamber, is constructed of timber railway sleepers placed on edge and backed by four 152 x 152 x 23mm steel columns. The columns are supported by stub beams bearing against the end wall of the pit, as shown in Fig. 4.2. No significant movement of the pit walls occurred on application of the surface load in the tests using this arrangement.

The pit was lined with heavy duty polythene before the clay insitu

soil was added to prevent loss of water from the clay. Frictional effects at the pit wall were considered to be negligible at this distance under the simulated wheel load used and no particular precautions were taken in this respect. Keuper Marl, a locally occurring silty clay, was chosen as the insitu soil. In addition to its appropriate stiffness characteristics, it had the advantages that its properties were well known and it was readily available. The clay was donated in unbaked brick form by the Butterley Brick Company. There were several advantages of using bricks including ease of handling, reduction of air voids to a minimum thereby increasing homogeneity, and the production of a flat surface to aid compaction. The process of brick manufacture involves grinding and reconstitution of the clay to a certain water content. The clay is then screw fed under a constant pressure through a die. This removes the original stress history of the soil and produces a clay of roughly consistent properties.

The clay bricks were placed as tightly packed as possible in horizontal layers and each layer was thoroughly compacted. The central area received six passes of the triple headed tamper shown in Fig. 4.4, while the edges were compacted with a single headed tamper. In each case the compacting head was 125mm in diameter. The water content of the bricks was 17-19%, a value higher than the optimum (14.5%) to reduce the likelihood of residual interfaces. Each layer was thoroughly scarified after compaction to remove horizontal interfaces, before the next layer was added. The pit was filled to just below floor slab level and was covered with a double layer of polythene to prevent water loss. The process of filling the pit took four weeks to complete and the clay was allowed to stand for a further five months to reach equilibrium before testing could begin.

Five 100mm diameter by 125mm deep cores were taken at every third

layer, from which moisture content and dry density values were calculated. A British Standard Compaction Test (2.5 kg hammer) and tests for liquid and plastic limits were also carried out on samples of the clay. The results, which are presented in Table 4.1 and Fig. 4.5, indicate an air void content of 3 to 5%. In only one case did a core break along an interface during extraction and close inspection of the cores revealed a generally strong bonding between bricks. Fig. 4.6 shows the surface appearance following just one pass of the tamper.

#### 4.2.2 Loading Arrangement

It has been established that the maximum surface load to be applied to each installation was 7 tonnes (70kN) and the method of application was to be simulative of the rear wheel arrangement of a typical construction vehicle. Load was to be applied at two points along the length of each pit installation in succession in order to gain duplicate data and both cyclic and static load was necessary to accurately determine pipe behaviour. With these criteria in mind, though with a design load of 10 tonnes to provide for a further increase in load, the means of loading was designed.

The loading ram is housed in a steel frame which spans the pit and is mounted on rollers. These bear onto parallel longitudinal beams on either side of the pit, the required height to house the ram and load platen being gained by choice of suitable steel beam sizes, as shown in Fig. 4.7. The longitudinal beams are 457 x 191 x 67mm UB sections and these extend beyond the testing area to allow the loading rig to be removed during excavation and pipe installation. The beams are held down to the laboratory floor at 500mm intervals with pairs of 16mm diameter bolts in expanding sockets. The roller arrangement consists of two rollers spaced 500mm apart and held between two 203 x 203 x 86mm UC sections which are 760mm long. The rollers

**Table 4.1 Classification of the Keuper Marl used to fill the Test Pit**

Liquid and Plastic Limits		
Liquid limit		32%
Plastic limit		19%
Plasticity index		13%
% passing 0.425 $\mu\text{m}$ sieve		89%
B.S. Compaction Test		
Maximum dry density		1.82 Mg/m <sup>3</sup>
Optimum moisture content		14.5%
Core Tests		
Layer	Average Moisture Content (%)	Average Dry Density (Mg/m <sup>3</sup> )
3	18.9	1.73
6	18.4	1.73
9	18.1	1.73
12	18.0	1.73
15	17.5	1.87*
19	17.5	1.76

\* Reading inexplicably high

are formed from 100mm diameter, 215mm long steel rods. The central 190mm has been turned down to a depth of 12mm to fit onto the top flange of the longitudinal beams and an axle has been formed through the centre (Fig. 4.7). Two 305 x 127 x 37mm UB sections spaced 630mm apart span the pit and are bolted to the top flanges of the beams forming the roller arrangement. Smaller section steel beams bear onto a 6mm thick steel plate and span between the cross beams. The hydraulic ram is bolted through the plate onto the flange of the small section beams, as shown in the overall view of Fig. 4.8. The ram can be moved laterally to any point along the cross beams, but in this project it was always positioned centrally. Once the loading rig has been located the rolling arrangement is clamped to the underside of the top flange of the longitudinal beam using a 16mm diameter bolt and load spreader (see Fig. 4.7). It is the clamp which transmits vertical load to the longitudinal beam.

The hydraulic load ram used throughout the project was controlled by a Losenhausen control system and had a 20 tonne capacity. This was permanently housed in the loading rig at a height that was dependent upon the means of load distribution used, the height being adjusted by the insertion of small steel sections above the cross beams. It was originally intended that a 320mm diameter load platen, based upon a water filled bag, would be used to apply load directly to the surface of the backfill with an appropriate depth of cover to the pipe. It was apparent, however, that the choice of a poor insitu soil and the backfill specification of excavated silty clay compacted in one layer would render this impractical. It would also be unrepresentative of site practice, because a granular access road would be necessary for the passage of construction vehicles of the type being simulated on such a poor insitu soil. It was decided that a steel platen should be used to transmit the load to the clay surface rather than introducing a granular sub-base, which would introduce a potential variable

to the most important boundary condition.

The design of this load distribution arrangement was based on experiments on the clay in the laboratory, experience of site conditions and theoretical calculations, which are discussed in detail in Chapter 7. When constructing a road, such as a typical housing estate road, on a weak silty clay insitu soil, the recommended thickness of sub-base is more than 300mm (RRL, 1970). It was felt, however, that a 200mm thickness of granular material would be sufficient to allow the passage of most vehicles and that this would be adopted on site in such circumstances. Based on these considerations, a 700mm diameter semi-flexible platen was designed, consisting of a 700mm diameter, 6mm thick mild steel plate in the centre of which a 450mm diameter stiffened platen was located (Fig. 4.9). A load cell is positioned above the platen to provide an independent measurement of load during the tests.

The platen was found to present a convex face to the surface of the backfill under load and produce settlements that were consistent with those expected under site conditions. Using this arrangement, a small area of the platen bears onto the undisturbed insitu soil at each side of the trench, but this mechanism was shown to be adopted by the model materials in the theoretical work and would be expected on site. In practice, the area of contact between the rear wheel arrangement of a vehicle and the surface on which it is riding will depend upon the resistance to deformation that the surface offers. If the surface deforms under load, a greater area of the vehicle wheels will contact the ground until the situation becomes stable, that is the stresses attenuate in a manner that is acceptable to each level of the underlying fill and insitu soil. Surface deformation has to be limited, however, for the access road to perform its function and it was this level of deformation that was considered when assessing the settlement of the platen in the pit

experiments.

#### 4.2.3 The Test Box

The multifarious role of the test box has been described elsewhere, the main considerations for design being speed of construction, sophistication of use and realism of boundary conditions. The former two factors both relate to its efficiency in terms of instrumentation development and planning of the test programme, which constitute its *raison d'etre* and are of paramount importance; the latter relates to the efficiency with which it can fulfill these tasks. It was desirable, therefore, to keep constant as many of the factors affecting pipe behaviour as possible with the result that the box was designed to act as a relatively rigid walled trench. The internal dimensions are 750mm long x 550mm deep with a variable width from 450mm to 750mm in 50mm increments, although a width of 500mm was used throughout the project. The box provides for a thickness of bedding of between 0 and 150mm and a depth of cover of 250mm.

The walls and base of the box, shown in Fig. 4.10, are constructed from 25mm phenolic film faced plywood, the smooth facing of which reduced wall friction. The side walls are backed by three horizontal sections of 100 x 65 x 7mm steel angle welded to vertical sections at each end. The vertical members are bolted through the end wall to a 6mm thick steel plate, which is supported by horizontal sections of 50 x 50 x 6mm steel angle at the top and bottom. The bottom angle sections on all four sides are bolted to the base plywood. A 200mm diameter hole was formed in each end wall to allow access to the pipe and the internal faces of the side walls and the base were milled to accommodate five flush mounted pressure cells and their cable. A layer of clay of appropriate thickness was



compacted into the bottom of the box after which the bedding material (if used) was laid and the pipe installed as in the pit. The depth of cover used in all experiments was 250mm, excavated silty clay being placed in one layer and thoroughly compacted at this level. The backfill in the box installations was, consequently, denser than that of the pit experiments.

Surface load was applied to the box installations using the same hydraulic ram and control equipment as that used for the pit, the reaction being provided by a portal frame bolted to the floor of the laboratory (Fig. 4.11). The load was applied to the clay surface through a 480mm diameter rigid load platen positioned centrally in the box. The same magnitudes and sequence of loading were applied as those to the pit installations. In addition, a dead load was applied to the surface of the clay not covered by the platen and this was of an equivalent magnitude to the weight of the backfill above this level where a 500mm cover depth was used (that is, the weight of a 250mm thick layer of compacted silty clay). In this way, the load subjected to the box installations was far more severe than that used in the pit.

#### 4.3 Instrumentation

##### 4.3.1 Measurement of Pipe Deformation

Pipe deformation is the most important performance parameter and its accurate measurement was essential. Several devices for measurement of vertical diametral reduction have been described in the literature, but all have disadvantages. Measurement by a Linear Variable Differential Transformer (LVDT) has been widely used in buried flexible pipe experiments. The body of the LVDT is fixed either to the pipe wall or to a fixed object inside the pipe and the spring loaded needle rests against the

characteristics of the pipe-soil interface is implicit in the method. Video cameras have been used by certain local authorities to check pipelines, though a method of measurement based on this technique would be expensive to develop.

A further device developed at the TRRL is a ring flash camera.\* The internal deformed profile of a pipe is recorded photographically, together with a datum, and diametral measurements across any axis may be made from the resulting print. This method has many potential advantages over those described above, the main disadvantage being the inability to monitor deformation during a test. In addition, settlement of the pipe can also be determined from the photographs as the boom (which supports the object forming the datum measurement) and the camera are supported independently of the pipe. It was decided, therefore, to develop a ring flash camera for use in both the pit and box experiments. This method would be supplemented by a system of horizontal and vertical linear potentiometers to provide both immediate deformation data and an independent check on the measurements made using the photographic technique.

The photographic technique is based upon a ring flash, which consists of a circular tube about 75mm in diameter and, in conventional use, is located around the lens of a camera in order to provide even illumination for close-up photography. The tube was removed from its casing and mounted on the back of a circular disc of tufnol, a non-conducting material. The disc was carefully machined such that it was exactly 100mm in diameter and was mounted on a 20mm square tufnol boom, as shown in Fig. 4.12. A 96mm diameter perspex disc was mounted on the front of the tufnol disc both to protect the ring flash tube and facilitate location of a shield within the profile of the 100m disc.

The shield is used to form a thin band of light on the pipe wall whilst ensuring sufficient light is thrown down the pipe to silhouette the

\* no publication yet available

wall diametrically opposite. This provides a voltage readout which is proportional to the deflection of the needle from its maximum extension. LVDTs are commonly positioned across both the horizontal and vertical diameters, and have the advantage of providing immediate deflection readings when used in conjunction with a voltmeter and a calibration chart. This method has several disadvantages, however, and these include difficulty in initial location, possible movement during testing and isolated diametral measurement, the latter being particularly serious if maximum diametral reduction does not coincide with an axis of measurement. Another device, which has been used at the TRRL (Gaunt et al, 1976), is a 'spider' instrument consisting of four sprung steel arms radiating from either end of a central body at a shallow angle and in contact with the pipe wall on the horizontal and vertical axes. Changes in strain measurements on the faces of the arms, when deflected, provide an indirect measurement of pipe deformation, once calibrated. The limitations of this method are similar to those of the previous technique. A similar device has been used in Holland on operational drainage pipes (Gehrels and Elzink, 1982) and consists of a weighted sledge with three feelers, one vertical and two horizontal. Deflection of the pipe wall is related to the movement of the arms, positioning and subsequent movement being less of a problem due to the nature of the sledge. A further device used in Holland is a self centring profile recorder, which has a sprung arm (similar to an LVDT) that rotates through  $360^\circ$  and provides a measurement from a central datum to each point around the circumference in terms of voltage, which is fed to a plotter. The disadvantages of this equipment include the possibility of tilting away from the plane of the pipe cross section and the high cost of development and construction. Inference of deflection from external pipe wall strains has been used successfully (Broere, 1984), although many measurements around the circumference are necessary and interference of the

tufnol disc (Fig. 4.13). The electronics of the flash gun are mounted on the rear of the tufnol disc, again within the 100mm profile. Cables lead from this to an external 4v power supply and the camera. For use in the pit, the boom was extended in length by four 500mm long sections of square hollow steel tube. The boom is clamped to a bracket mounted on the dividing wall in the inspection chamber and is located in the pipe at an angle of  $45^\circ$  to the vertical axis to allow measurement of both horizontal and vertical dimensions. The flash is triggered by the shutter release mechanism of the camera, which is similarly mounted in the inspection chamber (Fig. 4.14). A typical photograph taken by the ring flash camera is shown in Fig. 4.15.

Measurements of pipe deformation and settlement were originally made on prints of photographs, taken at successive stages of each test, using a pair of dividers and a scale rule. The size of print was such that the diameter of the illuminated ring was between 105 and 115mm, or between 70 and 75% of full-scale, in each case. The procedure for determining vertical diametral strain involved measurement of the vertical extent of the silhouetted disc and the maximum vertical extent of the illuminated ring projected onto the pipe wall (Fig. 4.16). The diametral measurement of the disc provides a datum measurement, from which the true scale of the photograph can be determined together with the diametral measurement of the pipe. By treating each photograph in this way, the pattern of vertical diametral reduction was determined. Division of each value by the initial external diametral measurement, determined using vernier callipers, resulted in the vertical diametral strain at each point. An independent check of the denominator in this ratio was made by determining the internal diametral measurement from the initial photograph, and measuring the pipe wall thickness at the measured section on exhumation of the pipe. The pipe wall thickness was assumed to remain constant throughout the test.

Measurement across any other axis can be made in a similar manner, pipe settlement being determined from the distance between the lowermost points of the disc and the band of light (invert) at the start and at subsequent stages of the test, the scale factor being determined from the datum as before.

Careful printing of the photographs and design of the shield on the ring flash head, for which several alternatives were tried, led to the consistent production of distinct boundaries to the silhouetted disc and the light ring, from which precise measurement was possible. Despite this, determination of V.D.S. by such a method was slow and laborious, and a more efficient technique was sought. In addition to the measurement of V.D.S. and pipe settlement, it was desirable that the deformed shape, which could be appreciated in a qualitative manner from photographs where significant deformation had occurred, should be quantified.

Of the various options available, all of which involved digitizing the photographs, a technique based upon the reversal of a Hewlett Packard graph plotter (HP7740A) was chosen. This equipment was directly compatible with the Hewlett Packard microcomputer (HB85B) already in use. The photograph to be measured is placed between two sheets of film, the uppermost of which has a means of centring the ring and axes marked at  $22.5^\circ$  intervals radiating from this centrepoint. A sight is fitted to the pen holder and moved across the photograph, which is fixed into position, by the use of a control panel on the front of the plotter (Fig. 4.17). Once correctly positioned, the co-ordinates of the centre of the sight are entered into the memory of the microcomputer and are stored using appropriate software. In this way, average measurements of the datum and vertical and horizontal diameter of the pipe, were obtained together with the co-ordinates of points at  $22.5^\circ$  intervals around the circumference. Suitable software was written to store and retrieve these data, from which manual calculations of

the shape of deformation were made. The graph plotter was obtained at a late stage of the project and the software to use these data to produce drawings of this deformed shape and correlations with pipe wall strain readings has yet to be written. Nevertheless, the usefulness of the system in determining precise measurements of the pipe circumference from photographs has been proved and its extensive use in future work is envisaged.

The accuracy of the method, and means of its improvement, formed the subject of a separate investigation. Three sources of potential error were isolated, these resulting from the alignment of the equipment, production of the image, and measurement from the image. Misalignment of the ring flash head, which is analogous to tilting of the linear potentiometers, can occur during its initial location. The ring flash head is positioned in the plane of cross-section by horizontal and vertical movement of the mounting arrangement in the inspection chamber, after which the arrangement is securely clamped in the vertical direction, horizontal movement being restricted by friction of its bearings. The ring flash head is fixed perpendicularly to the line of the boom, which is approximately parallel to the longitudinal axis of the pipe. Tilting away from the plane of cross-section can occur, therefore, if the boom sags when cantilevering 1.5 or 2.5m to reach the measuring points, or if the boom is at an angle to the longitudinal axis of the pipe. In either case, the diametral measurements made from the resulting photographs will be unaffected, because the ring of light projected by the flash tube is parallel to the plane of the silhouetted disc on which it is mounted and, therefore, the datum measurement. A similar error can occur if the axis of the camera is not parallel to the longitudinal axis of the pipe, a 1% error in measured diameter corresponding to a misalignment of 8%. This is accounted for by the same means, although such misalignment is minimised by the use of a

levelling bubble fixed to the hot shoe of the camera and is unlikely to be significant because of the large focal length in relation to the pipe diameter.

Distortion of the image during its production can arise from several sources and this would lead to its non-linearity across the print; uniform distortion across the image is accounted for by datum measurement as above. Optical distortion can occur if the object is photographed in different parts of the field of view. Good quality photographic equipment, all made by Minolta, was used to reduce this effect and each sequence of photographs was taken in the same central position in the field of view, thereby minimising this error. Film distortion, whether in the camera or during developing and printing, is reduced by using good quality film and by care in its handling. Print paper distortion is likewise minimised in this manner. The error from this source was found to be insignificant from the consistency of photographs produced. This was attributed in part to the fact that the camera remained stationary throughout the test by the use of an air release to trigger the camera shutter and a motor wind.

Error in measurement could arise from print distortion during reading, the physical limits of the equipment and its use. Print distortion is countered by the operator. The use of dividers and a scale rule to measure prints was found to be surprisingly precise, determination of the diameter being achieved to 0.1% in repeated measurements. The mechanical limits of the graph plotter were 0.025mm, judgement by eye being more significant than this, therefore. Extensive trials using the plotter indicated that the average error in measurement of the pipe diameter was 0.052%.

When first developed by the TRRL in a form that could be used to measure pipes in service, it was found that measurement to the nearest 1% could be easily achieved and that far greater accuracy was possible with sufficient care. Many of the sources of error cited during discussions

with the researcher who developed the method have been removed or minimised and, using the method described above, it was felt that an accuracy of 0.1% or better was possible. Correlation of the measurements with those from the system of linear potentiometers was found to be good, the resolution of the potentiometer (to 0.001%) being far more precise than this. In view of this, and that the measurements form a well defined pattern of deformation from which any single measurement can be extrapolated, diametral strains to 0.1% are quoted with confidence and to 0.01% (as in Rogers et al, 1985) with reasonable certainty where the data result primarily from the linear potentiometer readings. In this thesis vertical diametral strain has been quoted to 0.1% as no loss of behavioural description will result.

A system of one vertical and two horizontal linear potentiometers was used to provide additional pipe deformation data, as described above. The information from the vertical potentiometer was of most importance and was recorded at each stage of the test. The two horizontal potentiometers were used primarily to locate the vertical potentiometer centrally in the pipe and to check its orientation in the plane of cross-section as the pipe deformed. A permanent record of tilting was provided by the photographs. Two devices were used to ensure that the potentiometer did not tilt away from the plane of cross-section. That used in the box experiments involved a frame with a long longitudinal leg on which the devices were orthogonally mounted (Fig. 4.18). The frame was of adjustable height and could be easily positioned in the pipe used in the box. No such access could be gained in the pit experiments, the potentiometers instead being mounted on a heavy, self righting sledge (Fig. 4.19). This was located by repeated longitudinal movement until the readings on the horizontal potentiometers were approximately the same. Thereafter no significant horizontal movement was experienced during the test. The readings from the potentiometers were found to be both precise and generally accurate, any tendency to artificial



preciseness being removed from the readings quoted herein, as discussed above.

#### 4.3.2 Measurement of Pipe Wall Strain

Pipe wall strain has been used to determine both the magnitude of pipe deformation (Broere, 1984) and the shape of deformation (Howard, 1973; and others). Although not a critical performance criterion (Moser, 1981) its measurement is desirable for the determination of pipe behaviour, because of its extreme sensitivity to changes in the shape of deformation. As a result, it is the only method by which small changes in deformed shape can be determined with confidence. Pipe wall strain has been successfully measured by both internally and externally mounted strain gauges. External strain gauging was discounted, however, because of the potential interference of the characteristics of the pipe-soil interface by the gauges and wiring or, where used, by their means of protection. The difficulty of strain gauging the internal pipe circumference at a distance of more than 1 metre from each end, together with the uncertainty of producing an accurate result, meant that pipe wall strain was only determined in the box experiments.

Eight equally spaced strain gauges were mounted around the central cross-section of the pipe in the circumferential, or hoop, direction. Single active foil gauges with a 6mm gauge length were used and were glued directly to the pipe wall using M-bond adhesive. Repeated line loading of the pipe across each axis produced a linear response from all gauges, indicating that a good bond was achieved. A strain gauge balancing box was constructed in order to zero the readings before each test. The strain gauges have a linear response up to 3% tensile strain and 2% compressive strain, which was unlikely to be exceeded in normal use.

Resolution of pipe wall strain to 0.3 microstrain ( $3.0 \times 10^{-5}$  strain) was theoretically possible using an analogue to digital converter, although measurements to the nearest 100 microstrain (0.01% strain) were sufficiently precise to determine the shape of deformation. The only significant sources of potential error, therefore, were in the misalignment of the gauges from the plane of cross-section and in their position around the pipe circumference. The results of the line load tests, which are further discussed in section 5.2, showed that remarkably similar strains were recorded in both diametrically and symmetrically opposite gauges, thereby discounting these sources of error.

#### 4.3.3 Measurement of Soil Strain

Compression of the soil and fill in the areas around the pipe is of interest in determining the reasons for the response of the pipe to load under different conditions. It forms an integral part of load (Marston, 1930) and deformation (Watkins and Smith, 1973; Soini, 1982) theories and is treated as the critical parameter when assessing the suitability of potential fill materials by the Compaction Fraction Test (B.S.I., 1980). Soil movement was measured at regular intervals between the pipe and container wall by Howard (1973) by the use of telescopic tubes and soil strain (compression) was deduced. Such a method was not possible in the pit and possibly undesirable in terms of soil disturbance. Inductive strain coils have been used at Nottingham for many years in both soil mechanics and pavement engineering applications (Brown and Brodrick, 1981) for the measurement of strain in soil and pavement materials and were ideally suited to this problem. Pairs of coils, which are wound in the form of flat discs, are positioned in the soil or fill material in either co-axial or co-planar alignment, at a spacing of up to 4 coil diameters. An

a.c. signal is fed to one coil and a voltage is induced in the other, the magnitude of which is a function of the distance between the coils. By means of an inductance bridge, this effect can be translated to an output which is sensitive to small changes in spacing. A soil strain gauge unit, marketed by Bison Instruments (and shown in Fig. 4.23a), is used to balance the phase and amplitude of the reading. Once a balance is achieved, the amplitude dial reading is directly related to the soil spacing and can be determined from calibration curves.

Strain coils with diameters of 25mm and 50mm are available and both have been used in this project. The coils are thought to perform most reliably in homogeneous, fine grained soils with a coil to particle diameter ratio of 50 or greater, because of the likelihood of differential movement away from the plane of measurement. In consequence, 50mm diameter coils were used where possible to reduce this effect. Five pairs of co-axially aligned coils were positioned in the fill materials surrounding the pipe, as shown in Fig. 4.20. Horizontal compression of the sidefill was considered most important, coils being positioned on the horizontal axis of the pipe between the pipe and trench walls (Fig. 4.21). Most compression is known to occur adjacent to the pipe wall (Howard, 1973), but with interference <sup>with</sup> the characteristics of the soil at this point would, by implication, significantly affect the behaviour of the pipe and the coils were positioned centrally in the sidefill, as shown. Vertical compression of the sidefill was also of interest, but could not be determined at the measured section because of signal interference of the horizontal coils. Pairs of coils were placed vertically in the backfill above both the pipe and the sidefill, therefore, in order to infer the mechanism of stress relief above the pipe crown, hence indirectly the vertical compression of the sidefill. In cases where the vertical compression of the sidefill was small in comparison with the deflection of the pipe crown, greater

compression would occur between the coils above the backfill than above the pipe at the same level. Conversely, if the pipe is relatively stiff, compression will be greatest over the pipe. The position of the lowermost coils was determined from similar considerations of interference to the behaviour of the pipe. The strain coils were positioned at the same relative points at the measured cross-sections in both the pit and the box.

Use of strain coils in the materials used as fill in this project was likely to result in significant positional errors. The coils in the sidefill were commonly placed in uncompacted granular materials. Where compaction was applied, it was to the surface of the sidefill and perpendicular to the axis of alignment. In practice no significant movement of these coils occurred during installation, however. Under load, the sidefill was compressed in two directions and by different amounts. Little strain was measured in the sidefill, however, and, although no significant misalignment of the coils was generally found on exhumation, no detailed conclusions could be drawn from the results. The coils in the backfill were placed in loose clay which was thoroughly compacted in one layer, the compaction being at different relative heights above the coils in the pit and the box. This caused a considerable change in the readings. It was uncertain whether this was attributable solely to compression of the soil between the coils or (more likely) to a combination of misalignment and compression. Further apparent compression occurred under load, the final spacing of the coils being ascertained on exhumation. While significant errors in the readings were likely, only those under load were of interest and overall compression was generally sufficient to determine behaviour. The trends in compression conformed to a clearly defined, logical pattern and could be considered to be sufficiently accurate for the purposes required, therefore. For this reason, no detailed calibrations were carried out to quantify the influence of misalignment by lateral

movement or tilting, although sufficient information has been recorded for more detailed analyses of these data in the future if required.

#### 4.3.4 Measurement of Total Soil Pressure

Total soil pressures have been widely measured in buried pipe research and particularly in rigid pipe applications. Spangler (1941) found that the vertical pressure due to earth load on flexible pipes under embankment conditions was approximately one-third of that on rigid pipes and equal to roughly half of the weight of the soil prism above it. Howard's tests on flexible pipes yielded similar results (Howard, 1972A), although arching affected the readings at diametral strains of more than 7%. Pressures on the side of the pipe were found to reflect the shape of deformation, those at the invert being erratic. Howard also measured pressures on the container wall, both on the horizontal axis of the pipe and at a level above the crown of the pipe, in order to determine the influence of the walls on pipe behaviour.

Measurement of pressure on the vertical and horizontal axes of the pipe, while being desirable in determining the pressure distribution around the circumference, would lead to considerable interference of the characteristics of the pipe-soil interface, particularly in pipes of 160mm diameter, and was discounted. The measurement of horizontal pressures on the trench wall (or box wall) was considered feasible, however, and would help to determine the influence of the insitu soil on pipe behaviour. Pressure cells were, therefore, flush mounted in both walls of the trench and the box in the plane of the measured section, one pair on the horizontal axis of the pipe and one pair 175mm above the axis (see Figs. 4.20 and 4.21). The vertical pressure in the base of the trench directly below the pipe invert was also determined, although this was not directly

comparable in all tests because of the variation in the depth of bedding. A suitable pressure cell has been developed at Nottingham and used extensively in pavement applications (Brown and Brodrick, 1981). The design is based on a 64mm diameter, 11mm thick titanium disc with a 30mm diameter strain gauged diaphragm (Fig. 4.22). A further strain gauge balancing box and a power supply were used to operate the pressure cells and, once balanced, the output was found to be linearly proportional to applied pressure. All the cells used in the pit were calibrated in a bench calibrator\*, those in the box being calibrated in situ. Where gravel was used as sidefill and bedding, which was liable to produce false pressure readings because of point loads on the diaphragm, the pressure cells were covered by bags containing fine sand. Somewhat erratic readings resulted and a thin layer of clay of approximately 15mm thickness was used to cover the diaphragm in subsequent tests.

The main source of error likely to arise from these measurements was in the difference between calibration and practical conditions. This was partially removed in the case of the box, where calibration was carried out in situ, but the even pressure distribution over the diaphragm could not be guaranteed in the experiments. In practice, the measurements of pressure were found to be erratic and conclusions could not be drawn from the results.

Measurements of pressure were also made at three points below the load platen in the later pit experiments, the pressure cells being located in the insitu soil near to the edge of the platen, directly below the centre of the platen and midway between these two points. Bench calibration was again used for these cells.

\* Brown and Brodrick (1981)

#### 4.3.5 Additional Instrumentation

Settlement of the load platen was measured at each stage of the pit and box experiments using an independently mounted linear potentiometer, hence the settlement of the backfill surface was deduced. In the pit experiments, the flexibility of the platen and the necessity of offsetting the linear potentiometer resulted in an underestimation of central settlement. A further potential source of error in either test facility was tilting of the platen, thereby rendering the single reading unrepresentative. In practice the recorded settlements were shown to be generally accurate by correlation with measured surface profiles before and after each test, and sufficiently accurate for comparison between tests. Such measurements were useful for the assessment of overall vertical movement in order that soil strains and pipe crown deflection could be put into perspective, comparison of boundary conditions between tests and assessment of theoretical models.

The lateral movement of the box walls was measured by independently mounted dial gauges placed on the horizontal axis of the pipe at either side of the box. Readings to 0.01mm were easily made, box wall movement being consistent between tests, and were useful in quantifying total horizontal movement from the box data.

#### 4.3.6 Data Logging Facilities

The system of data logging used in the experiments was based on a microcomputer and an analogue to digital (A-D) signal converter. This facility could monitor up to 16 channels of analogue input, which was fed from the appropriate balancing units, the data being subsequently stored on tape cassette. The A-D converter (PCI 1280) was made by C.I.L. and has a factory preset gain range for each channel. The device was set to monitor

14 channels of strain gauge devices (strain gauges, pressure cells and load cells) with voltage outputs of less than 0.1V and 2 instruments with outputs in the  $\pm 10V$  range (linear potentiometers). The device has  $\pm 15$  bit resolution (a resolution of  $\pm 0.3 \times 10^6 V$  on the 0.1V range) and takes  $5.5 \times 10^{-5}$  seconds to scan one channel, which was sufficiently fast to ensure synchronisation of readings. The A-D converter has a 4K random access memory available to facilitate repeated scanning of channels during operations where the change in readings occurs rapidly. A Hewlett Packard 85B microcomputer was used to operate the A-D converter and to store and retrieve the data. In each case, the average of 16 scans of each channel was taken by the A-D converter before passing the data to the microcomputer for conversion to standard units and absolute values for storage. Fig. 4.23 shows the data logging equipment together with the soil strain gauge unit and the instrumentation balancing units.

For the box experiments, the readings recorded in this way were those from 8 pipe wall strain gauges, 5 total pressure cells, the load cell, the linear potentiometer across the vertical axis of the pipe and the linear potentiometer measuring surface settlement. For the pit experiments, where no pipe wall strain gauges are used, all 10 trench wall pressure cell readings are monitored together with those from the 3 surface pressure cells used in the later experiments. Soil strain coil readings were taken manually, balancing of the phase and amplitude of the signals being done automatically by the soil strain gauge unit. Dial gauge readings to determine box wall movement were similarly recorded manually at appropriate stages during the box experiments. Other readings of interest, such as the minimum vertical diametral measurement under cyclic load, were also recorded manually together with general descriptive comments on the behaviour of the installation, where appropriate.

A large amount of information describing the performance of each



installation was thus measured and recorded. Where data were stored on cassette tape, subsequent analysis was facilitated by the microcomputer using suitable software. The process of digitizing the deformed profiles of the pipe also involves storage of data on cassette tape and this will similarly allow correlation with other performance parameters using software. In cases where manual recording of data was necessary, unsophisticated procedures of analysis were adopted in which only important data were treated. The potential of software as a means of analysis, correlation and presentation of data has not yet been fully realised and further software development is one of the first objectives of continued work on the project.

#### 4.4 Experimental Procedure

Having isolated the factors that influence installation performance and determined the boundary conditions under which the influence of desired parameters can be quantified, it was important that a well defined experimental procedure should be adopted and adhered to throughout the test programme. Typical site practice was simulated where possible and departures from this, such as the installation of instrumentation, were conducted in a manner that was least disruptive to the overall simulation of building drainage construction. The procedures described hereafter were largely developed during preliminary experiments, therefore, and modifications were only made where no change to the boundary conditions resulted. The procedure for soil characterisation is discussed in Chapter 6 and is only mentioned in this section where it has an influence on the sequence of the experimental work.

#### 4.4.1 Random Sampling and Initial Measurement

In order to ensure that installations were fully representative of site practice, the pipe used in the pit experiments was obtained from a local builder's merchant and was installed without regard to initial ovality or wall thickness variations. On receipt of the pipe, it was inspected to ensure that it displayed a kitemark, which indicates that it had been made to the current British Standard, and for damage. One pipe was rejected because of excessive colour change and scarring of the surface. Two lengths of pipe were used in the box installations, two strain gauges on the first becoming inoperative after excessive straining, and each was orientated about the largest diameter during installation in order to avoid excessive positive initial ovality occurring. Variation in the properties of the pipe between manufacturers were thought to be minimal and these procedures were considered to be justified.

Despite installing each pipe without regard to initial ovality and pipe wall thickness, it was essential that these values were known in order to explain discrepancies in subsequent behaviour. Once cut to length, therefore, axes at 45° intervals were marked along the length of the pipe and numbered in sequence, the initial line being chosen at random. External diametral measurements were taken across the marked axes at the loading points and across the vertical axis at 250mm intervals along the length of the pipe. Levels were also taken along the length of the pipes used in the early tests, but the variation was found to be negligible and visual inspection of longitudinal sagging was substituted. Pipe wall thickness was measured on exhumation of the pipe as this did not change significantly during an experiment.

#### 4.4.2 Installation Procedure

The method of installation was the most important experimental procedure and the one in which variation was likely to have the greatest influence on the results. While simulating the methods of installation used on site as closely as possible, it was evident that a roughly even distribution of material around the pipe was necessary in order to assess the behaviour of each installation properly; poor site practice, as distinct from poor installation quality, was excluded from the experiments, therefore. Practical constraints determined that the trench was hand, rather than machine, dug and that materials were dumped in the trench by hand rather than from an excavator bucket. In all other respects, normal site practice was strictly adhered to when defining installation procedure. The method of installation described herein relates to the pit experiments but is equally relevant to the box installations, with the obvious exception of trench preparation.

Trench excavation and trimming was carried out such that a 500mm wide, vertical walled trench was achieved with a tolerance of  $\pm 5\text{mm}$ . The depth of the trench varied between 660mm and 760mm depending upon the depth of bedding used and was subject to a similar tolerance. In all cases, therefore, the trench bottom was hand trimmed and level. Where bedding material was used, it was dumped into the trench, levelled from the surface and unsystematically trodden to represent the treatment it would receive during levelling, pipe jointing and subsequent levelling of the sidefill. No conscious effort was made to compact the material in this way. The pipe was then positioned in the centre of the trench, seated in the bedding material and protected around the opening in the end wall. In the case of the pit wall, a 200mm square, 125mm thick laminated block was constructed from sheets of expanded neoprene sponge and a 160mm diameter hole was formed in the centre. Minor adjustments were made to accommodate the

position of the pipe by insertion of similarly constructed sponge blocks around the 250mm square opening. Foam rubber strips were used to protect the pipe in the box. In this way fill material loss around the openings was prevented, but deformation of the pipe was unrestricted, by the flexible inserts.

The sidefill was added to the trench from ground level in all cases and a uniform distribution of material around the pipe was ensured, particular care being taken to achieve this beneath the haunches of the pipe. Once the level of the material had reached the pipe springings, strain coils were placed beside the pipe in the manner described earlier, the operation again being conducted from the surface (Fig. 4.24). Particular care was taken to ensure that the coils were correctly aligned. In cases where silty clay was used as sidefill, the clay was pressed firmly around the coils to prevent differential movement during its subsequent compaction. Further fill material was loosely placed around the coils and side filling was completed to produce a level surface, as before. Three levels of compaction were defined for the sidefill material, and these are described as follows

1. No compaction, backfilling continuing once a level sidefill surface had been produced.
2. Light compaction by systematic treading. The sidefill was trodden systematically on alternate sides such that no lateral movement of the pipe occurred and each part of the sidefill received two passes.
3. Thorough compaction, in which a single headed pneumatic tamper, 125mm in diameter, was applied to each part of the sidefill in the same pattern as the lightly compacted case.

Once sidefilling was complete, excavated silty clay was loosely thrown into the trench. The strain coils were positioned in the backfill at appropriate points, clay being locally firmed around them to prevent

movement as before. The loose clay was placed to just above ground level and thoroughly compacted by the single headed pneumatic tamper to produce an approximately flat finished surface. The area immediately below the positions of the load platen were trimmed by hand to ensure a uniform surface. Where surface pressure cells were used, these were then installed with approximately 10mm of cover below the surface of the clay. The surface profile of the pit was measured to the underside of the loading rig and recorded, the areas of most interest being around the two loading positions. The load platen and load cell were then centred over the far loading point, and the load ram was located and clamped into position, as shown in Fig. 4.9. Characterisation of the soil occurred throughout the installation process and this is discussed in Chapter 6.

#### 4.4.3 Measurement of Pipe and Soil Response

The load regime defined in section 3.6 was applied to each installation, the timing of the regime being important in determining the response of the installation to it. Of direct relevance to the timing of the load applications was the sequence of pipe and soil response readings and this had to be kept consistent throughout the test programme. Sufficient readings were taken to accurately define the pattern of response to the static and cyclic loads, and the subsequent recovery periods. Measurement of soil strain being considered less important than the other parameters in this respect. A zero reading of all the measured parameters was taken immediately prior to loading, the sequence of readings taken during the 55kN load sequence being summarised as follows:

1. On application of the 55kN static load, readings were taken immediately and at 5, 10, 20 and 30 minutes thereafter. Soil strain was measured at immediately and after 10 and 30 minutes.

2. On removal of the load, readings of all parameters were taken immediately, after 5 and 15 minutes, and at intervals of 15 minutes thereafter if appropriate. The recovery period was generally between 15 and 30 minutes long.
  3. A complete set of readings was taken immediately prior to the cyclic load sequence.
  4. Cyclic load was applied at approximately 12 cycles per minute, though with a break of 3 to 4 minutes each time a complete set of readings was taken and 1 minute where strain coil measurements were not taken. A complete set of readings was taken after 1, 10, 30, 50, 100 and 150 cycles, partial sets being taken after 5, 20, 40, 70, 90 and 125 cycles. In addition the maximum vertical diametral reduction under load was recorded manually at each of the intervals listed above. When averaged over the full length of time to apply the load sequence, the rate of loading was approximately 4 cycles per minute, which was sufficiently fast to fulfill the requirements of relatively rapid cycling stated above.
  5. On completion of the cyclic load sequence, a complete set of recovery readings was taken at 5, 15, 30 and 120 minutes.
- The same sequence of readings was adopted during the 70kN load regime, though with a final recovery reading taken after 17 hours.

The readings were found to define the pattern of pipe-soil response well, readings generally being stable at the end of each static and cyclic load sequence. Synchronisation of data logging scans with photographs was facilitated by a 10m long air release mechanism to activate the camera shutter. Soil strain readings, which take approximately 3 minutes to complete, were less sensitive to timing and no significant errors were discovered due to their delay. Departures to the time scale of the readings sequence only occurred during equipment or instrumentation malfunction, in which case recovery readings were taken during the period

of delay, but such an occurrence was rare.

#### 4.4.4 Exhumation of Pipe and Trench Reinstatement

On completion of the test, the load platen was removed and the surface profile of the clay was remeasured around each load position. The most important feature of excavation was the determination of the final soil characteristics, the process for which is described elsewhere. The backfill was excavated until the upper strain coils were reached. The position of each coil was determined relative to the original datum and the tilt of the coils was assessed. This process was repeated for the lower coils, and the final separation and alignment of the coils in the backfill were deduced. Excavation continued until the pipe and its surround material had been removed, the final position of the horizontally aligned coils being determined as above. An inspection of the trench was then carried out and any areas that had dried out or become uncontaminated by granular material penetration were removed. The insitu soil in the area of the load platens was also removed. New clay at the average water content of about 17.5% was used to reinstate the trench and was thoroughly compacted into position. Where necessary clay was placed in layers and re-excavated to produce the required trench profile and at the surface around the loading points shuttering was erected and securely braced into position to retain the clay during compaction, hand trimming being necessary once more to complete the reinstatement.

When roughly half of the test programme had been completed and immediately prior to the main investigations of the influence of sidefill type, a major reinstatement of the insitu soil was undertaken. Clay was removed from the surface, trench walls and trench base to a depth of approximately 200mm until clay of roughly original properties was reached.

The pit was then filled to ground level with silty clay in the same manner as when the pit was originally filled. The clay was allowed to stand for a few days, before a new trench was dug and the tests continued. All excavated material was carefully assessed for water content and contamination before being either discarded or stored in air-tight polythene bags for re-use. A plentiful supply of clay was available for use in these experiments, thereby facilitating good control over the condition of the insitu soil.

When not in immediate use, the insitu soil was carefully covered with polythene and sealed against water loss. Where a trench had been excavated, the polythene was held against the walls and base to reduce the flow of air, the surface being covered with at least two layers of polythene sheet at all times. Particular precautions were taken to ensure a good seal around the opening in the trench wall. The reinstated trench was covered in this way and allowed to stand for as long as possible before a new installation was constructed in order to allow the clay to approach equilibrium.

On exhumation, the pipe was remeasured across its vertical axis at 250mm intervals along its length and at 45° intervals around the circumference of the measured sections, as before. The pipe was then cut at the measured sections and pipe wall thickness determined at the same 45° intervals around the circumference. The variation of pipe wall thickness along the length of the pipe was estimated by measuring the wall thickness at either end of the pipe also. In this way the permanent deformation of the pipe and soil was found and the measurements of pipe wall thickness were used to determine the original internal diametral measurements (i.e. before installation) as an independent check on the external measurements.



#### 4.5 Pipe Material Classification

The quality of the pipe material was assessed in order to ensure that the pipe did not constitute a variable in the experiments. Strain controlled compression tests were conducted at Nottingham on rings of each pipe tested to determine their pipe ring stiffness. This has been widely assumed to be the most important characteristic of the structural performance of the pipe and is that included in most design formulae since Spangler (1941) first published his design method.

A 150mm length was cut from the offcut section of each pipe used in the pit installations and axes were marked at 45° intervals around the circumference. The sum of the pipe wall thicknesses across each axis was determined and the weakest axis found. Each length of pipe was then placed between two 150mm square flat plates in an hydraulic testing machine with its weakest axis vertical. A constant strain rate of 12.5mm per minute was applied to the pipe, the load resistance of the pipe being monitored by an integral load cell. The pipe was deformed to 80% vertical diametral strain, measurements of load and deflection of the plates being taken at regular intervals. In this way a measure of the ring stiffness of each section is gained and any significant discrepancy in the values found.

#### 4.6 Programme of Experimental Work

##### 4.6.1 Unconfined Line Load Tests

A series of unconfined line load tests was performed on the 850mm long strain gauged pipe used in the box installations. These were conducted for several reasons, which included the determination of pipe ring stiffness, determination of the relationship between pipe wall strain and pipe

deformation, assessment of instrumentation techniques and the bonding of the strain gauges to the uPVC pipe wall in particular, and confirmation of the shape of the pipe wall strain profile associated with elliptical pipe deformation. Line load was applied incrementally through two diametrically opposed 300mm long x 40mm wide x 30mm thick expanded neoprene sponge strips mounted on similar size wooden blocks. These platens ensured that a uniform pressure was applied over their full area as the sponge conformed to the shape of the pipe during loading. The pipe was loaded until a diametral strain of 5% was registered at which point the load was removed in order that the pipe did not deform plastically (this was thought to occur at approximately 8% deformation). Vertical deformation of the pipe was measured both by a linear potentiometer, to produce a continuous deformation reading during the test, and the ring flash camera.

The pipe was positioned such that a diametrically opposite pair of strain gauges was centred on the load platens. Load was applied in 0.1kN increments until a V.D.S. of roughly 5% was reached and readings of strain gauge outputs and diametral measurements were taken. This process was repeated across each strain gauged axis of the pipe and twice in the case of one pair of strain gauges in order to determine the consistency of the results.

#### 4.6.2 Programme of Box Experiments

Two preliminary series of tests were performed in the box to investigate patterns of loading, to gain a basic understanding of pipe response in a variety of installation types and to develop instrumentation and installation techniques. The first involved complete surrounds (that is bedding, sidefill and backfill) of uncompacted pea gravel and lightly compacted silty clay. These were loaded in 5kN increments to 20kN, 40kN

Table 4.2 Details of Experimental Installations in the Box

Reference	Bedding Type	Bedding Thickness (mm)	Sidefill Type	Sidefill Compaction	Comments
1	Pea gravel	100	Pea gravel	none	standard practice
2	Pea gravel	50	Pea gravel	none	
3	none	0	Pea gravel	none	
4	Pea gravel	50	Pea gravel to springings, silty clay above	none	support to mid-height of pipe only
5	none	0	Pea gravel to springings, silty clay above	none thorough	split sidefill
6	none	0	Silty clay to springings, pea gravel above	thorough	split sidefill
7	none	0	Silty clay to crown, pea gravel 50mm above	thorough	arching layer over 9
8A and 8B	none	0	Silty clay to springings, pea gravel to 50mm above pipe crown	thorough	arching layer over 6; 8A had low water content, 8B high
9	none	0	Silty clay	thorough	
10	none	0	Silty clay	thorough	
11	none	0	Silty clay	light	
12	Pea gravel	100	Silty clay	thorough	
13	none	0	Concrete ballast	light	
14	none	0	Concrete ballast	none	
15	none	0	Reject sand	light	
16	none	0	Reject sand	none	compacted in 2 layers

(at which the pipe in clay deformed excessively and this test was terminated), 60kN, 80kN and 100kN, the 100kN load being cycled in this manner 10 times. Three progressively stronger load platens were used for the gravel experiment. The second series involved typical installations using full-depth uncompacted pea gravel sidefills in conjunction with 100mm, 50mm and 0mm thick pea gravel bedding layers. The load regime used in these tests consisted of seven cyclic load sequences, in which 100 cycles of load were applied and the load was increased in increments of 10kN for each sequence, followed by seven static load applications of one hour duration with one hour recovery between them, the load increasing in magnitude as before.

Once these were complete and the appropriate experimental techniques had been standardised, the main programme of box installations was performed. Details of the installations investigated in the box are presented in Table 4.2 in the approximate order of performance. The first installation investigated was that simulating standard practice, against which all others could be assessed. This was followed by similar installations in which the bedding layer was reduced to a thickness of 50mm and removed. An installation with a full-depth, thoroughly compacted silty clay sidefill placed in one layer was also investigated and these formed the basis of the early experiments in the pit. The first three represented the use of commonly specified imported material and the influence of the bedding layer on its performance, and the fourth the use of well treated insitu soil.

A series of tests was then instigated to discover the influence on pipe performance of materials of different properties juxtaposed around the pipe. The first involved good support up to the mid-height of the pipe and poor support above this, silty clay being loosely placed to the surface of the box and compacted in one layer. Two installations involving split

sidefills of uncompacted pea gravel (UCPG) and well compacted silty clay (WCSC) without bedding were tested to further locate the critical areas with regard to pipe support. In order that a direct comparison of results could be made, an installation involving a WCSC sidefill compacted in two layers beside the pipe was used. The effect of arching in the backfill as a means of relieving pipe crown load was determined in two installations in which 50mm thick layers of UCPG were placed above the pipe crown, one using a full-depth WCSC sidefill and the other a split sidefill (UCPG over WCSC). The influence of a good quality bedding on a full-depth WCSC sidefill was investigated by placing a 100mm thick UCPG bedding below the pipe and the influence of compaction on a full-depth silty clay sidefill was determined. In this way a wide variety of different support conditions were studied while using only two materials as surround.

Four further installations were then used to investigate the influence of new materials. A full-depth concrete ballast sidefill was used both with and without light compaction and without a bedding layer. The installations performed well enough to be repeated in the pit. A reject sand, consisting of roughly equal proportions of fine sand and silt, was then tested in a similar manner with signally poor results. Despite the exceptionally severe boundary conditions in the box, it was thought likely that the performance of the pipe in reject sand would lie without the current performance limit and the only advantage of using this material in the pit without compaction would be to help define the limit on acceptable materials. It was decided, therefore, that materials with grading curves that lie between those of concrete ballast and reject sand would be used in the pit without compaction. At this point the box tests were discontinued in favour of the pit experiments.

#### 4.6.3 Programme of Pit Experiments

The first installation to be tested in the pit was that simulating current site practice and this again set a standard of performance against which other tests could be measured. Details of this installation, together with those of all pit installation types, are given in Table 4.3. The standard installation was followed by a series of experiments that encompassed the range of options generally available on a site with a silty clay insitu soil. The first involved the use of UCPG as sidefill with the pipe laid onto a hand trimmed trench bottom. This was primarily done to confirm the results of bedding influence determined by the box experiments. An installation in which the excavated silty clay was used as sidefill and compacted in one layer was conducted to represent good treatment of the insitu soil in cases where imported material was not used. The results of this installation were also used to determine whether the findings of previous experimental work (Gaunt et al, 1976), that a thoroughly compacted sandy clay performs comparably with an uncompacted gravel, were valid for a poorer clay subjected to the maximum likely level of compaction that could be expected under normal site conditions. This installation was repeated in order to ascertain the repeatability of the pit installations with a sidefill that was extremely susceptible to changes in water content, density (thus compaction) and general installation procedure.

On completion of these tests, attention was focussed on the behaviour of other potential imported materials. There were two situations of particular interest, one being the use of material in the poorest condition (without compaction or bedding) and the other being use under a realistic specification (with a minimum bedding, but without compaction). The need for efficiency in the test programme and replicate data have been emphasized elsewhere, together with the desirability of defining the reasons behind the reported behaviour. With these considerations in mind,

Table 4.3 Details of Experimental Installations in the Pit

Reference	Bedding Type	Bedding Thickness (mm)	Sidefill Type	Sidefill Compaction	Comments
1A	Pea gravel	100	Pea gravel	none	standard practice
2	none	0	Pea gravel	none	
3A	none	0	Silty clay	thorough	insitu soil as sidefill
3B	none	0	Silty clay	thorough	insitu soil as sidefill
4	none	0	Concrete ballast	light	
5	none	0	Concrete ballast	none	clay refurbishment followed test No. 5
6A	Pea gravel	50	Pea gravel	none	
6B	Pea gravel	50	Pea gravel	none	
7A	Concrete ballast	50	Concrete ballast	none	
7B	Concrete ballast	50	Concrete ballast	none	
8A	Building sand	50	Building sand	none	
8B	Building sand	50	Building sand	none	
1B	Pea gravel	100	Pea gravel	none	standard practice
9A	Quarry tailings	50	Quarry tailings	none	
9B	Quarry tailings	50	Quarry tailings	none	
10	Reject sand	50	Reject sand	none	marginal material

it was decided that two full-depth concrete ballast installations, both with and without light compaction, would be used without bedding. At this point the trench was refurbished before a series of more practical installations were investigated using distinctly different, widely available granular materials as uncompacted sidefill and 50mm thick bedding. The materials chosen for this investigation were pea gravel, concrete ballast, building sand and washed quarry tailings, and each installation was repeated in order that four sets of data were obtained for each material. In this way, accurate average data were obtained which were of use in both absolute and comparative terms for direct application to the field and for assessing the theoretical model. Interspersed with these tests was a repeat of that representing current installation practice in order to determine the change in boundary conditions (if any) over the project. Some change in the properties of the insitu silty clay were likely between the first installation, when it was newly laid, and those that followed. The final installation to be studied was one in which reject sand was used in the same configuration as the comparative granular installations. This was performed for a number of reasons, but primarily to define the limit on materials that could be used without compaction and to assess the various potential methods of determining the suitability of soils on site for use as structural fill.





## CHAPTER FIVE



## 5 RESULTS OF EXPERIMENTAL WORK

### 5.1 Introduction

It has been established that pipe deformation, measured in terms of vertical diametral strain (V.D.S.), is the critical performance parameter and it is that on which a limit has been set in installation recommendations (B.S.I., 1980). By performing experiments with constant boundary conditions and variable fill materials, and by measuring V.D.S. in each case, the basic objective of the project was achieved. In order to determine the factors that influence the V.D.S., or performance, of a pipe, measurements of further parameters were made and correlations with both pipe performance and soil properties were attempted.

The following presentation of results has the objective of illustrating both the trends apparent in the pipe performance measurements and the practical implications arising therefrom. Other parameters are introduced in order to further explain these trends and to isolate the fill materials that induce desirable behaviour. Various measurements provided an assessment of consistency between the tests, and this is referred to at appropriate points throughout the chapter. The results of the pipe characterisation tests are then presented. The experimental results are extended in Chapter 6, in which soil characterisation tests are discussed together with the results therefrom, which are correlated with pipe performance. Theoretical studies are described in Chapter 7 and correlation of theoretical with experimental data is outlined. A summary of all important measurements made in the pit and box installations is included in Appendix A for reference. The results of the preliminary tests, which are not directly comparable with the main test programme, are

summarised hereafter in the introduction with the aim of elucidating points of general relevance.

Vertical diametral strain is defined herein as the change in the vertical diametral measurement divided by the original external diameter, their means of determination being described in section 4.3.1. It should be noted here that the values quoted differ slightly in certain cases from those quoted in an earlier exposition of the work (Rogers et al, 1985). This is because patterns of deformation became better defined as more photographs were measured, thereby illustrating false results.

The preliminary tests in which pipe was buried solely in uncompacted pea gravel and lightly compacted silty clay produced some interesting results. The load deformation curves for these tests are summarised in Fig. 5.1 and illustrate clearly the influence of the fill materials on pipe behaviour. Three load platens were used during the pea gravel experiment, platens 1 and 2 being of roughly equal stiffness and considerably less stiff, and strong, than platen 3. The load-deformation graph for this experiment (Fig. 5.1,a) exhibits two distinct virgin pipe compression curves, related to platen stiffness. The general pattern, which is well defined by the 0-60kN curve, involves an initial pipe deformation under low loads followed by a relatively steep gradient until the original maximum load is reached, after which the gradient reduces to that of the virgin pipe compression curve, which is analagous to the virgin consolidation line for soils. On removal of load, an initially steep, but progressively flatter, recovery, or swell back, line was found (these have been omitted from Fig. 5.1 for clarity). The final elastic recovery on the removal of the load was particularly large and the initially flat part of the reloading curve suggests that the residual pressure on the pipe wall was minimal as the wall retracted from the sidefill. This observation is further discussed in connection with the correlation of pipe deformation

with soil test data in Chapter 6. The corresponding curve for clay exhibits a very well defined virgin pipe compression line, elastic recovery of the pipe on removal of load that is proportionately far less than that in gravel, and an initially steep reloading curve. The latter observation implies that no loss of pipe-soil contact occurs at the pipe springings. The cyclic load curves for the pea gravel experiment (Fig. 5.1,b) exhibit progressively smaller permanent strain increments, progressive exaggeration of the deformation under low loads and progressively steeper gradients. These data show clearly the dominant influence of the soil on uPVC pipe performance, the load deformation curves for the pipe being consistent with those expected from the soil alone. In addition, pea gravel is shown to be far more competent at restricting deformation of a pipe buried therein than lightly compacted silty clay.

The results of the second series of preliminary tests are summarised in Fig. 5.2 and these too conformed to a well defined pattern when installation effects were removed. The build-up of vertical diametral strain of the pipe under the cyclic and static load sequences was approximately the same in the installations involving bedding, although the magnitude of V.D.S. under the static loads when applied for one hour was markedly greater where only 50mm was used, this difference becoming far less significant on removal of each load due to large associated elastic recoveries. The application of the 70kN static load was extended to 65 hours for the intermediate (50mm bedding) installation and while causing no apparent increase in the magnitude of deformation under load, the permanent deformation found on removal of the load was significantly increased. It was also discovered that where a long recovery period of 24 hours or more was introduced between the cyclic load sequences, elastic recovery was far greater and was not wholly removed on the immediate application of the next cyclic load, rather a downward kink in the overall pattern occurred. This

implies that accelerated cyclic loading is significantly worse than that applied at a more normal rate, in the case of a building drainage site over months or years; extended static loads likewise provide an ultimately more severe case. The response of the installation in which bedding was not used was progressively greater under the cyclic load sequences, both transient and permanent deformations under static load also developing at a noticeably greater rate than where bedding was installed.

## 5.2 Buried uPVC Pipe Behaviour

### 5.2.1 Vertical Diametral Strain

The boundary conditions imposed on the box installations, while remaining constant between tests, were exceptionally severe in practical terms and were likely to exaggerate any prevalent differences in soil properties, such as water content and density. By keeping such discrepancies of soil character to a minimum through good experimental technique and by measuring the properties of the soil used in each test to explain anomalies in pipe behaviour, data from the box was used to provide a good comparison of installation performance. The boundary conditions imposed on the pit experiments were chosen to match those pertaining to field conditions and, by keeping them constant between tests, good quality data, both comparative and absolute, were obtained. The arbitrary load regime applied to both installations was chosen to cover likely practical load cases and, while comparisons of overall behaviour are important, it is necessary to isolate behaviour under static and after cyclic load for practical extension of results. Similarly, the magnitudes of load were chosen to cover the likely maxima of 11t and 14t axle loads, whereas interpretation of results should be based on experience of loads under

actual site conditions. Such considerations are particularly important when the results are judged against the current recommended limit on pipe vertical diametral strain of 5% at the end of installation.

Pipe deformation data are compared in two ways, by defining the datum measurement as either that at the end of installation, producing data caused by the applied loads alone, or that when positioning the pipe. The installation process was found to produce somewhat variable pipe deformation in experiments of similar type and average values of V.D.S. for comparisons were taken at this stage where possible. Deformation of similar installations under load tended to be more consistent and average values of these data were found to be generally precise. In order to facilitate the comparison of V.D.S. measurements between tests, corresponding values have been represented graphically at salient points during the test. The stages at which V.D.S. was plotted were chosen to illustrate the effects of installation, static load and associated creep behaviour, and cyclic load, thereby summarising the behaviour of the pipe throughout the experiments.

Current standard installation practice involves the use of uncompacted pea gravel (UCPG) both as a 100mm bedding layer and as sidefill. Jointing of uPVC pipes is performed in the trench, thereby ensuring that the bedding layer receives light, unsystematic compaction by treading. Once surrounded by gravel, the pipe is covered by backfill, which typically consists of the excavated insitu soil being placed and compacted in one layer at the surface. Such an installation was the first to be investigated in order that standard data, against which those of other installations could be judged, were obtained. The installation was subsequently repeated later in the test programme, once refurbishment of the clay had been carried out, in order to investigate the influence of stress history of the insitu silty clay on performance of the pipe. The insitu soil in the first installation



had hitherto experienced compression caused by extrusion in the brickworks, thorough compaction when placed and self weight, whereas most of that of the duplicate test had also been subjected to repeated loads of 55kN and 70kN. The average V.D.S. measurements caused by the load regime alone were slightly higher in the first test (2.8%) than the second (2.2%), but the deformations under load, and their subsequent recovery, were considerably greater in the former case. The overall average V.D.S. caused by load alone was 2.5% and, when installation effects were included 2.7%. This latter value is well below the arbitrary 5% limit set on V.D.S. at the end of installation.

The results of a series of tests to investigate the influence of bedding on the performance of a pipe with an UCPG surround are shown in Fig. 5.3, in which average values of V.D.S. were used. V.D.S. at the end of installation (EOI) was small in each case and conformed to no discernible pattern. The curve for the installation in which a 50mm bedding layer was used demonstrated the best pipe performance thereafter, with relatively little increase in V.D.S. on application of the 55kN load (55 ON) and small creep movements as the static load was applied for 30 minutes (55/30). This area of the graph is bounded by vertical lines to indicate that the reading was taken while the load was acting. On removal of the load and subsequent recovery, marking the end of the 55kN static load sequence (E055s), the V.D.S. of the pipe reduced, indicating a significant proportion of elastic recovery. Application of 150 cycles of the 55kN load and further recovery, marking the end of the 55kN cyclic load sequence (E055c), caused the V.D.S. to double and thereby increase to a value above the maximum reached under static load. More importantly, the permanent V.D.S. caused by the cyclic load was considerably greater than that caused by the static load. This pattern was repeated during the 70kN load sequence, with slightly more creep behaviour and a similar increase in

V.D.S., in absolute terms, under the cyclic load. The average final V.D.S. measurement was 2.3% and that caused by the load regime alone was 1.9%, both of which compare favourably with those of the standard installation.

The curve for the installation in which a 100mm thick bedding layer was used exhibits high V.D.S. increments on application of the static loads, considerable creep movements and a large proportion of elastic recovery. This led to greater permanent V.D.S. from the static loads, which in the case of the lower load exceeded that caused by the cyclic load. These observations were caused in part by the behaviour of the first installation, as discussed above, but remained to a lesser degree when the anomalous influences of the first test were removed. Where no bedding layer was used, large increments of V.D.S. on application of the static load were accompanied by relative large creep movements and considerable elastic recovery. The recovery was matched by the cyclic load increments causing the permanent cyclic load deformations to be greater than those after the static load. The final average values of V.D.S. were 4.4% at the end of the test and 4.1% when installation effects were removed.

It was apparent from these data that the influence of reducing the depth of the bedding layer from 100mm to 50mm was to improve the performance of the installation, albeit slightly. Where no bedding layer was used in a trench cut in poor material, pipe deformation was considerably greater, although the final V.D.S. measurement represented good performance in absolute terms. The somewhat unexpected benefits of halving the thickness of the standard bedding layer were confirmed by the results of corresponding experiments in the box (Fig. 5.4). The final deformations of the pipe in the box caused by the load regimes alone for the installations using 100mm bedding (4.9%), 50mm bedding (4.8%) and no bedding (5.5%) layers ranked the materials in a similar order to the pit data, with corresponding values of 2.5%, 1.9% and 4.1% respectively.

A further investigation of the influence of bedding involved the use of uncompacted concrete ballast (UCCB) sidefills, the results of which are shown in Fig. 5.5. Where no bedding layer was used, the effect of installation was greater with a difference in V.D.S. of 0.6%, the curves being separated by an offset of roughly this magnitude thereafter. The average V.D.S. measurements at the end of the tests were 3.0% where no bedding layer was used and 2.4% with a 50mm thick bedding layer, the average values under load only being the same at 2.2%. The only significant influence of the bedding layer in this case was the reduction of the effects of installation, but, as V.D.S. caused by installation was generally variable, further evidence of the effect would be necessary to confirm this finding.

It would appear from the results of installations in which good quality sidefill materials were used, that the difference in performance of a pipe with a 50mm thick bedding layer is no worse, and possibly slightly better, than with a 100mm thick bedding layer. Where no bedding layer was used, the pipe in pea gravel developed higher V.D.S. throughout the test, whereas in concreting ballast the only difference occurred during installation. In practical cases where hand trimming of the trench was not possible, a 50mm thick bedding layer would be required to level the bottom of the trench and there is no evidence to suggest that this should be increased to a thickness of 100mm.

The average results of an installation in which a lightly compacted concrete ballast (LCCB) sidefill was used without a bedding layer are also included in Fig. 5.5. The influence of compaction of the sidefill on the performance of the pipe was an apparent reduction of V.D.S. during installation followed by a markedly reduced response to the 55kN load regime. Thereafter the increments of V.D.S. were approximately similar, though with significantly greater creep effects where compaction was

applied. Final average V.D.S. measurements with (1.9%) and without (3.0%) compaction showed that considerable benefit was gained by systematic treading of the sidefill, though the values caused by the load regimes only (1.5% and 2.2% respectively) were closer.

Corresponding installations were loaded in the box, in which the pattern of deformation under the load regimes in the pit was closely matched. Similar installation deformations were followed by progressively greater deformations throughout the 55kN load sequence where compaction was not applied, the difference thereafter being smaller. The final V.D.S. measurements were 5.4% with light compaction and 6.5% without.

The effect of compaction on the performance of pipes surrounded by full-depth silty clay sidefills was demonstrated in three box installations, in which both light and thorough compaction were applied to the clay in a single layer, and thorough compaction was applied to clay placed in two layers beside the pipe. Where light compaction was used, excessive deformation occurred under the initial static load and the test was terminated after a load of 50kN had been applied. Where well compacted silty clay (WCSC) was placed in one layer the test was terminated after the 70kN static load sequence, at which point the V.D.S. of the pipe was 14.0%. When compacted in two layers, however, the full load regime was applied to the installation, under which a negative V.D.S. of 1.8% was removed and a final V.D.S. of 8.1% was obtained. This represents a considerable achievement for an installation with a sidefill of poor material under the exceptionally severe boundary conditions applied in the box, and the result reinforces the belief that most materials would provide suitable lateral support to a buried flexible pipe if compacted sufficiently well. Where WCSC was placed in one layer beside the pipe in the pit the final V.D.S. was 5.3%, which implies that compaction in two layers would have reduced V.D.S. to well below 5%. Negative V.D.S. was common at the end of

installation in cases where compaction was applied to the sidefill, and was particularly high where split sidefills were used.

It was clear from these results that compaction of the sidefill, even that effected by systematic treading, was of considerable use in reducing the V.D.S. of a pipe buried therein. It was evident that different soils respond to compaction by differing amounts, a fact that is recognised in the Compaction Fraction Test. In a clay sidefill, where the voids between lumps had to be removed, thorough compaction in thin layers was necessary before suitable lateral restraint was mobilised. Where concrete ballast, a well graded material, was used light compaction made a significant difference to an otherwise good material, a result confirmed by experience in highway engineering. Pea gravel, however, was thought to be largely unaffected by compaction because a favourable soil structure would be taken up when laid, compaction probably only affecting the "bedding in" effect at the interface with the surrounding soil.

The main purpose of the experiments was the investigation of the influence of sidefill type on the performance of uPVC pipes buried therein, and this has been effected in several ways. Three materials were used as sidefill in pit installations where no bedding layer was used and a summary of the results therefrom is presented in Fig. 5.6. Deformation of the pipe buried in UCPG conformed to a well defined pattern, with a small, positive V.D.S. at the end of the installation process, relatively large V.D.S. increments caused by the application of the static loads and creep effects, and a considerable elastic recovery on removal of the loads that is matched almost exactly by the permanent strain caused by the cyclic loads. The permanent cyclic diametral strains were greater than those caused by the static load of both magnitudes. The ultimate average V.D.S. was 4.4%. The pattern of V.D.S. measurements of the pipe buried in the UCCB sidefill was quite different from that for the gravel. A large average installation

deformation was accompanied by little response, either initial or creep, to the static loads and significant elastic recovery. A large response to cyclic loads caused permanent V.D.S. increments that exceeded both the previous maxima and the permanent increments caused by the static loads. The average V.D.S. measurement at the end of the test was lower (3.0%) than that for the gravel sidefill. The curve for the pipe in WCSC shows a negative V.D.S. at the end of installation, a response to static loads that is increased greatly by large creep movements and an elastic recovery that is removed by the cyclic load sequences. The permanent diametral strains caused by the static load sequences were relatively more significant to the overall V.D.S., matching the cyclically induced value at the lower load and exceeding it at the higher. The average final V.D.S. was 5.3%.

These results show that, while the overall behaviour is greatly influenced by the type of sidefill material, the response of these soils, hence the pipes buried therein, is considerably different under the differing load regimes. Such observations are reiterated by the results of installations in which five uncompacted granular materials were used as sidefill and bedding, a summary of which is shown in Fig. 5.7. The average curves for UCPG and UCCB are of similar type and magnitude throughout, with the cyclic loads having far more effect on the pipe-soil structure than the static loads. The average curve for washed quarry tailings exhibits greater strains at each stage with a progressively increasing difference between it and the two mentioned above, and in particular a greater susceptibility to creep. The average curve for the pipes buried in building sand shows higher strains still, with proportionally greater strain under static load, much of which was subsequently recovered. The average curve for reject sand (an equal mix of fine sand and silt), which was used in one installation only, exhibits strains of roughly twice those of the pipe in building sand. The progression of increased installation

deformation is continued, after which large strains occurred on application of the static load and, particularly, due to creep effects. Significant elastic recovery occurred on removal of the load, the permanent strain caused by the cyclic loads failing to reach the previous maxima under static load and being far smaller than the permanent static load strain in the case of the 55kN load sequence. In general, it appears that creep effects are greater in materials having a better grading, or a flatter grading curve. The differences in pipe performance were less obvious for the granular materials where a bedding layer was used, which may indicate that better pipe support was provided in such installations, and this indicated that the fill material influences were more dominant in cases without bedding.

A further study of the influence of sidefill properties on the performance of a pipe laid without bedding was conducted in the box. A summary of the results is presented in Fig. 5.8, from which a comparison of the performance of three uncompacted granular materials with that of silty clay thoroughly compacted in two layers can be made. In contrast to the results of corresponding experiments in the pit (Fig. 5.6), the behaviour of the pipes buried in UCPG and UCCB was remarkably similar throughout the tests. The reason for this may lie in the inability of the pea gravel to "bed in" laterally in the box when loaded, whereas in the pit the gravel was found to penetrate the clay trench walls thereby allowing horizontal movement. Concrete ballast, being a well graded material, showed no tendency to "bed in" when used in the pit. Where a WCSC sidefill was used, a large negative V.D.S. at the end of installation was followed by large positive deformation on application of the 55kN load and, because of creep, only a small part of this was recovered on removal of the load. Thereafter the installation behaved in a similar manner to the others, though with somewhat greater deformations and in particular that caused by creep

effects. The pattern of the curve for uncompacted reject sand (UCRS) under the 55kN load sequence exhibited characteristics of both the clay and granular sidefills. A small V.D.S. at the end of installation was followed by a large increase on application of the static load, but was accompanied by proportionally similar creep behaviour to that of the granular materials. Elastic recovery on removal of the load was matched exactly by the permanent strain caused by the cyclic load.

Several behavioural trends were apparent from the series of experiments to investigate the influence of sidefill type on pipe performance. A pipe buried in an uncompacted sidefill that produced ultimately good performance tended to have a small positive V.D.S. at the end of installation, relatively small deformations caused by static load application and creep effects, and a large proportion of elastic recovery on removal of the load. Cyclic load tended to produce greater permanent deformations than the static load. Where compaction of the sidefill was carried out, a negative V.D.S. commonly occurred at the end of the installation process. Where a cohesive material, which invariably required compaction, was used as sidefill a large V.D.S. tended to occur on application of the static load and this was increased considerably by creep movements. A relatively small proportion of this deformation recovered on removal of the static load, cyclic load causing a relatively small permanent increase in V.D.S. in comparison with the static load. A pipe buried in a relatively poor granular material, such as a silty sand, tended to deform greatly on application of the static load but did not exhibit significant creep behaviour under its continued application. Intermediate granular materials tended to fall between the paradigms of the extremes.

In the light of these observations, further data from the pit test in which an UCPG sidefill was used without a bedding layer (Fig. 5.6), was examined to explain the deviation from the pattern set by the UCCB sidefill



and confirmed elsewhere. It was found that the water content of the trench bottom was higher than that used in subsequent experiments and this factor may have contributed to the anomaly. The reason for the difference in behaviour was more likely to be connected with the fact that the pea gravel installation was the second to be performed in the pit and, as for the first standard installation to be investigated, the insitu clay would have been more susceptible to applied load than in subsequent installations.

In an attempt to isolate the areas of the sidefill that were of most importance in resisting pipe deformation, several combinations of WCSC and UCPG were used as pipe surround in experiments in the box. In the first instance, four such combinations were investigated in installations without bedding, the configurations and results being summarised in Fig. 5.9. It was important when analysing these data to consider the influence of indirect compaction on the otherwise uncompacted pea gravel. The result of compaction in such cases was not a significant change in the properties of the gravel, rather an increase in the overall stiffness of an installation by inducing "bedding in" effects. Where full-depth UCPG was used as sidefill indirect compaction arose from compaction of the clay backfill 250mm above the gravel surface, as was the case where UCPG overlay WCSC in equal proportions. Where the latter was inverted, however, thorough compaction of the clay 75mm above the gravel surface caused considerable indirect compaction of the gravel and an extremely stiff pipe surround could have been expected. In each case the water content of the clay used as sidefill and backfill was kept roughly constant between tests.

With reference to Fig. 5.9, the curve for UCPG conforms to the previously well defined pattern of small installation deformation and greater permanent V.D.S. caused by the cyclic, rather than static, loads. The final V.D.S. was 5.9%, or 5.5% ignoring installation effects. The installation with a WCSC sidefill in two layers had a negative V.D.S. of

1.8% after installation with a larger permanent V.D.S. caused by the 55kN static load than when it was cycled, and large creep effects. Under the 70kN load sequence, behaviour was similar to that of the gravel, though with greater creep deformations. The final V.D.S. measurements were 8.1% at the end of the test and 9.9% under the load regime alone. The curves for the split sidefills of UCPG and WCSC both follow the paradigm of the previous installation, with high negative V.D.S. at the end of installation and greater permanent V.D.S. under the 55kN static, rather than the 55kN cyclic, load and under the 70kN cyclic, rather than the 70kN static, load. Both curves exhibit similar creep deformations that were less than those of the full-depth WCSC, but greater than the full-depth UCPG, sidefill. Where UCPG overlay WCSC a higher negative V.D.S. was caused by the installation process (2.4%) than vice versa (1.2%) and this difference manifested itself approximately throughout the test. The final V.D.S. measurements were 4.2% (UCPG over WCSC) and 4.8% (vice versa), both of which were lower than that for the full-depth UCPG sidefill. On removal of the effects of installation the values of V.D.S. were 6.6% (UCPG over WCSC) and 6.0% (vice versa), a reversal of the apparent performance.

These results show that considerable benefits accrue from the inducement of negative V.D.S. during construction, which were apparently greater where compaction was applied at the level of the pipe springings. The order of ranking of sidefills in terms of least susceptibility to load was full-depth UCPG (5.5%), WCSC over UCPG (6.0%), UCPG over WCSC (6.6%) and full-depth WCSC (9.9%). Where installation effects are included, however, the order becomes UCPG over WCSC (4.2%), WCSC over UCPG (4.8%), full-depth UCPG (5.9%) and full-depth WCSC (8.1%). The highest negative V.D.S. occurred where UCPG overlay WCSC. The static loads in this latter test produced similar responses to those where a full-depth UCPG sidefill was used, whereas with clay overlying gravel the static load deformations,

and subsequent elastic recovery, were greater. This indicated that, where a generally competent sidefill is used, deformation will tend to occur in the upper half of the pipe and where the less competent clay was placed at this point the deformation was greater. The ability of the pea gravel to arch above the shoulders of the pipe may also influence the behaviour of the pipe to some degree. In conclusion, therefore, UCPG was better at providing lateral support to the pipe during the load regime, but where mixed sidefills were used, the induced negative V.D.S. during installation caused lower final V.D.S. measurements. The critical point of the installation in resisting applied loads, where generally competent sidefills were used, was that between the crown and the springings.

A further study was performed in which two installations with a 50mm thick UCPG bedding layer, in conjunction with an UCPG sidefill extending to the springings and crown respectively, were tested. Silty clay was placed above the gravel in each case and compacted at the surface of the box. In this way the former installation had particularly poor support at the critical point. The results of these experiments are shown in Fig. 5.10, which shows that the static loads had far greater influence on the pipe in the half-depth sidefill, creep deformations also being greater. This behaviour was accompanied by greater elastic recovery on removal of the loads, but similar behaviour in both installations under the cyclic loads. After the 55kN static load was applied the pipe in the half-depth sidefill had far more permanent V.D.S. than the full-depth sidefill, whereas after the 70kN static load the permanent strain increments were equally small. It was clear from these results that the soil between the crown and springings has a large influence on the behaviour of a buried uPVC pipe under static load and, where a poor material was used, a large V.D.S. was accompanied by significant elastic recovery. A large permanent strain under the initial static load was followed by a typical pattern of

permanent strains thereafter.

A further investigation in the box involved the use of a full-depth WCSC sidefill both with and without a 50mm thick UCPG arching layer directly above the pipe crown. Where no arching layer was present, the V.D.S. of the pipe at the end of the 70kN static load sequence was 14.0%, the test being discontinued at this point. Where the arching layer was included, the V.D.S. of the pipe at the end of the test was 4.1% which represented a remarkable improvement in performance. This latter result was accompanied by relatively low surface settlement data, but the consistency of the water contents of the respective backfills and sidefills, and of their installation techniques, would suggest that these data were low because of the replacement of the least dense part of the backfill by the arching layer. Where the layer was used creep movements were relatively large, as was the permanent V.D.S. under the 55kN static load, whereafter the installation performed like that with a good quality granular sidefill. The implication of these results was that a thin arching layer of single sized rounded material, and of a significant diameter in relation to that of the pipe, served to transmit part of the applied load to the sidefill, thereby relieving the stress on the pipe crown.

### 5.2.2 Pipe Wall Strain

Circumferential strain was measured at 45° intervals around the internal surface of the pipe used in the unconfined line load tests and the test box installations. These data have been presented in either linear or circular plots of the strain profile, depending upon whether the magnitude or distribution of strain was most important. Both absolute and incremental values of strain have been used in the illustration of pipe

behaviour. Where comparisons have been made between installations, the data have been extrapolated to those that would occur at 5% vertical diametral strain, assuming a linear relationship, and an average strain was taken for linear plots, assuming symmetry about the vertical axis. The sign convention adopted throughout this thesis is that tensile strains are positive, and compressive strains negative, and pipe wall strain is assumed to be that on the internal face of the pipe unless stated otherwise.

The distribution of pipe wall strain around the circumference of a pipe will provide a description of its deformed shape if the change in pipe wall strain is solely caused by the local change in curvature of the pipe wall, or the movement of the point relative to the adjacent points on the pipe circumference. Data will be quoted later in this section to support the case for inferring the deformed shape of the pipe from pipe wall strain profiles. When a circular pipe is subjected to a line load across its vertical axis, but is otherwise unloaded, it is widely stated that the pipe will deform elliptically with an extension in the horizontal and reduction in the vertical, diametral measurement. The pipe wall strain profile in such a case will be elliptical also, with tensile strains on the internal surface at the crown and invert, compressive strains at the springings and small compressive strains at the shoulders and haunches. When surrounded by a relatively loose soil and a load is applied to the soil in the same direction, the pipe will again deform approximately elliptically, but the pipe wall strain profile will tend to a V-shape (Fig. 5.11,a). This is caused by the lateral restraint of the soil, or passive pressure developed therein, which induces a greater compressive strain in the pipe springings (Howard, 1973). Where a buried pipe is bedded in a good quality, stiff soil up to its horizontal axis and a vertical load is applied to the soil surface, the pipe will tend to deform to a "heart" shape, in which the pipe crown flattens and the shoulders become relatively more curved with a

roughly even change in curvature below this (Fig. 5.11,b). Such a deformation is accompanied by high tensile wall strain at the pipe crown, high compressive strains at the shoulders and progressively lower compressive strains below this level culminating in low tensile strains at the invert. Diametrically opposite behaviour can occur in cases where the soil around the haunches is poor and that above it is of good quality (Fig. 5.11,c). In cases where exceptionally good lateral restraint is provided at the pipe springings deformation will tend to be "square" shaped, in which the pipe and invert flatten and the shoulders and haunches take up a smaller radius of curvature, the springings remaining largely unstrained. Such a case is shown in Fig. 5.11(d), together with its associated internal pipe wall strain profile. This behaviour, which has been noted by Howard (1973) during experiments with thin walled steel pipe, typically occurs only in cases where thorough compaction is applied to the sidefill at the level of the pipe springings, thereby creating a locally stiff medium. Most of the behaviour observed during the experiments could be explained in terms of these patterns or their derivatives.

The relationship between pipe wall strain and vertical diametral strain in the unconfined line load tests (Fig. 5.12) was linear for each gauge over the range tested, strains in diametrically opposite gauges being almost identical. This indicated that deformation across the vertical axis of the pipe was directly proportional to pipe wall strain in the gauges on that axis, and could be determined therefrom. It also implied that the movement of the pipe wall on the axes of the other gauges could be deduced in a similar manner. The graph also indicated that the bonding of the strain gauges to the pipe wall was good. Pipe wall strain profiles for the pipe at integer percentages of V.D.S. during the unconfined line load test were plotted on a circular axis (Fig. 5.13), in which their elliptical

nature can be clearly seen from the isolated measurements. When the same data were averaged and plotted on a linear axis (Fig. 5.14), a clearer description of the relative magnitudes of pipe wall strain was obtained and the elliptical nature of the profiles were again apparent. It may be concluded, therefore, that the deformed shape of the pipe in these experiments was an ellipse. Similar results were obtained when the pipe was rotated through increments of  $45^\circ$  and the test repeated. This behaviour was quite predictable and the tests were carried out largely to prove the instrumentation techniques.

The influence of the sidefill material on pipe wall strain distribution was demonstrated by the tests in which full depth sidefills of uncompacted pea gravel, well compacted silty clay, lightly compacted concreting ballast and lightly compacted reject sand were used without a bedding layer. Permanent strains at the end of each test, once installation effects had been removed, were extrapolated to those that would occur at a V.D.S., again caused by the loads alone, of 5% for the comparison and these have been plotted on a linear axis (Fig. 5.15). The end points of the tests using silty clay and reject sand sidefills were after the 70kN static load and the 55kN cyclic load sequences had been applied respectively. The curve for the WCSC was, consequently, the only one that was likely to exhibit greater distortional effects from the static load, the nature of the profiles suggesting that this was not the case. All four curves conformed to the same approximate pattern, with high tensile strain in the pipe crown, and equal and opposite strains at the springings (compressive) and invert. Low compressive strains occurred at the shoulders and haunches. The curve for pea gravel exhibited the highest pipe crown and shoulder strains, and the lowest strain at the haunches, the invert strains being approximately equal in each case. The curve for concreting ballast was similar in the upper half of the pipe, though the

strains were of lower magnitude, and had the lowest compressive strains at the springings and highest at the haunches. The curve for clay approximated to a V shape, with that for reject sand being similar, but flatter in the compression zone. It was important when analysing these extrapolated pipe wall strain profiles to consider the ease with which 5% V.D.S. was reached, those pipes in sidefills providing good lateral support possibly developing significant compressive hoop strains.

It may be deduced from these graphs that the pipe in UCPG suffered most movement in the upper part of the pipe, caused by a flattening of the crown and a reduction in radius at the shoulders, the lower strains below the horizontal axis being consistent with elliptical deformation. Pea gravel had been expected to provide good support all round the pipe circumference. The same trend was apparent in the UCCB installation, with higher compressive strains at the haunch indicating movement in that area of the sidefill least affected by compaction. This result was explained by the generally good support provided by this material, especially that at the springings, enforcing the pipe to seek out the weak points in the surrounding soil in order to deform and relieve the pressure concentrations above it. Such behaviour was not necessary in the silty clay installation, where the generally poor support led to large deformations of the pipe and allowed the springings to move with relative ease. This indicated that elliptical deformation, the deformation mode taken up by the pipe where sufficient support was not provided to distort this pattern and that associated with a V shaped strain profile in underground pipes (Howard, 1973), took place. Any departure from a perfect V shaped curve was due to the thorough compaction applied to the sidefill in this installation. The difference between the curve for reject sand and that for silty clay indicated that the sand provided somewhat greater support at the springings, causing greater movement at the shoulders and haunches. The



overall shape reflected the generally poor support offered by this material.

When plotting the profiles of the extrapolated strain increments for the pipe after the 55kN static load had been applied for 30 minutes (Fig. 5.16), considerable difference in behaviour between the installations was found. Very high strains in the crown and shoulders of the pipe surrounded by pea gravel were accompanied by moderate strains at the springings and low strains below this. This was indicative of considerable action to relieve pressure in the top section of the pipe and consistently good support around the pipe. Similar, though less exaggerated, behaviour was apparent in the concreting ballast installation, with greater movement at the haunches and invert again reflecting the lower influence of compaction at these points. The strain profile for the silty clay installation is of a near perfect V form indicating purely elliptical behaviour under load. The more competent reject sand produced lower strains at the invert, and more movement at the shoulders and haunches, than the silty clay, but still conformed to approximately elliptical behaviour. The slightly greater strains below the horizontal axis of the pipe than those above again reflected the reduced influence of compaction towards the invert.

The relationship between the two sets of curves (Figs. 5.15 and 5.16) was important in terms of distortion of the preferred elliptical deformation. It is clear that when surrounded by a poor material the pipe deformed in an elliptical manner under load, and application of further loads, whether static or cyclic, did not change this pattern. When surrounded by a material which provided good support, however, the deformation under load was considerably different from an ellipse and totally dependent on the character of the surrounding soil. Application of the remaining load sequences caused the distortions from an ellipse to become so much less evident that the curves for distinctly different

materials took the same form.

The character of deformation during each phase of the loading sequence requires examination and this will be discussed later in this section. The relationship between pipe wall strain profile and the deformed shape taken up by the pipe is also important and an investigation of this relationship will also be described. Before leaving the topic of soil surround influence on pipe wall strain, however, the results of a series of tests in which both good and poor materials were juxtaposed around the pipe will be presented.

Extrapolated data for four tests in which both UCPG and WCSC were used to surround the pipe are shown in Figs. 5.17 and 5.18, at the end of the test and after 30 minutes of the 55kN static load respectively. The installations used for this comparison were those with a full depth UCPG sidefill, split sidefills consisting of WCSC over UCPG and vice versa, and a full-depth WCSC sidefill overlain by a 50mm thick UCPG arching layer. In the case where WCSC overlay UCPG, there would have been significant indirect compaction of the pea gravel discussed earlier. The result of this would have been penetration of the gravel into surrounding clay surfaces, or "bedding in", and development of a tightly packed structure. All four installations provided good support to the pipe.

As before, the greatest difference in pipe wall strain profiles occurred under static load (Fig. 5.18) and this dictated the forms at the end of the test. The profile under load for full depth UCPG, as described above, exhibited most action in the crown and shoulders and little movement around the haunches and invert. The curve for WCSC over UCPG showed similar behaviour at the crown and shoulders, negligible strain at the springings and low strain at the haunches and invert. In this case the relief of pressure concentrations above the pipe was largely effected in the WCSC, the remaining movements occurring in the haunches and invert with

the support at the springings being remarkably good. Where a split sidefill of UCPG overlying WCSC was used, lower crown and shoulder strains were accompanied by high compressive strains at the haunches and invert, producing a roughly uniform compressive strain between shoulders and haunches. The installation in which the UCPG arching layer was used produced the lowest crown and shoulder strains and highest strains at the haunches and invert.

In view of the competence of each combination at supporting the pipe, it was clear that deformation occurred at the weakest point around the circumference and that this coincided with the location of the WCSC when present. The arching layer evidently performed its function well by diverting the area of most action to the lower section of the pipe, the same behaviour occurring to a lesser degree where UCPG overlay WCSC in the sidefill. Where competent material was used as full-depth sidefill, good restraint in the lower regions forced the pipe to deform in a "heart" shaped manner. In the case of WCSC overlying UCPG, the deformation tended to a "square" shape, though with most movement occurring in the upper section of the pipe which was supported by WCSC.

The curves at the end of the tests retained the characteristics of those when under load while reverting to a more uniform pattern consistent with elliptical deformation (Fig. 5.17). Retention of strains developed under load was greatest in areas associated with WCSC surrounds, which indicated a lower degree of elastic recovery and was consistent with the soil properties. A detailed study of recovery on removal of the static load confirmed this observation.

In order to gain a better understanding of the behaviour under static and cyclic loads, detailed analysis of two tests, using competent sidefills of both pea gravel and silty clay, will be presented. The strain profiles at various stages of a test in which a full depth UCPG sidefill was used

(Fig. 5.19) showed that installation effects were small. The profile under the 55kN static load exhibited large crown and shoulder strains which increased marginally as the load was held for 30 minutes. On removal of the load, the strain at the pipe crown decreased by about 30%, and elsewhere by 60-70%, due to elastic recovery of the pipe. Application of the cyclic load caused large increases in strain at the crown, springings and invert, but had a negligible influence on behaviour at the shoulders and haunches. Application of the 70kN static load caused large strain increments which were similar in type to those of the lower static load and exhibited little creep behaviour. On removal of this load nearly all of the additional strain was lost. The higher cyclic load produced the same results as the lower one.

Corresponding strain profiles for a test in which a full-depth WCSC sidefill was used in conjunction with a 50mm thick overlying arching layer (Fig. 5.20) showed considerable negative deformation at the end of installation, with compression in the crown and invert and tension in the springings. The profile for the 55kN static load indicated a small increase in tensile strain at the crown, moderate increase in compressive strain at the springings and haunches, and a large increase in tensile strain at the invert. A small but significant creep effect was found under load. On removal of the load, roughly 30% of the strain in the pipe crown, and 45-55% elsewhere, was lost due to elastic recovery. Application of the cyclic load again produced most effect at the crown, springings and invert, and no effect at the shoulders. A smaller, though still significant, compressive strain increment occurred at the haunches. The general pattern was repeated during the higher load sequence with about 50% of the pipe crown strain, and 70-85% elsewhere, lost on removal of the static load.

It was clear from these two installations that, when buried in a good material, the pipe exhibited distortional behaviour under load, with little

creep movement and considerable elastic recovery. Application of cyclic loads produced almost perfect elliptical behaviour, thus reducing the distortional influence on the final strain profile. When buried in a poor material, distortional behaviour again occurred under static load if the overall support for the pipe was good (ie, when an arching layer was used, without which elliptical deformation would have occurred), but significant creep movements occurred and elastic recovery was considerably lower. Cyclic load on such an installation produced roughly elliptical behaviour, but tended to exploit areas of weakness, slightly emphasising the distortional effects.

These observations were confirmed by the data from other box installations. It would appear from this analysis that the compressibility, or stiffness, of the surrounding soil plays an important part in resisting deformation, by enforcing distortional behaviour, reducing creep effects and recovering elastically on removal of load.

It has been stated in the literature (Broere, 1984, and others) that the deformed shape of a flexible pipe can be obtained when the circumferential pipe wall strain distribution is known. This was shown to be true for uPVC pipes in the case of the unconfined line load test, where elliptical strain profiles and a linear relationship between pipe wall and vertical diametral strain were found. When confined in a good sidefill, the shape of the strain profile differed significantly from an ellipse and a component of hoop compression would have been expected. In order to investigate these phenomena and to assess the validity of deducing the deformed shape from strain profiles, graphs of pipe wall against vertical diametral strain have been drawn for installations with both good and poor sidefills.

Such a graph for an installation with a full-depth UCPG sidefill (Fig. 5.21) illustrates the case where distortional profiles were produced. At

each point around the circumference except the invert, the pipe wall strain measurements under the static load show higher compressive, or lower tensile, strain than the corresponding values after the cyclic load had been applied, indicating that a compressive component of hoop strain was induced under load. The gauges on the horizontal and vertical axes exhibited a discernable linear relationship through the origin despite this effect, that on the pipe crown being most affected. The cyclic load sequences produced a slightly curved relationship for the pipe crown strain. Strain in the gauges on the springings was remarkably similar. The relationships for the gauges at the shoulders and haunches were of similar type, with large compressive components under static load and a slightly curved, though approximately horizontal line under cyclic load. This reflected distortional behaviour under load followed by elliptical behaviour, in which little change in strain was experienced at these points, when the load was cycled.

A graph of pipe wall strain against vertical diametral strain for the installation using a lightly compacted reject sand (Fig. 5.22) produced signally similar results. In this test only the 55kN load sequence was applied because of large deformations. Compressive hoop strain under load was evident at all points except the invert, and linear relationships between pipe wall strain and vertical diametral strain were produced at gauges on the horizontal and vertical axes. The curves under cyclic load were approximately linear for all gauges. Behaviour at the shoulders and haunches was similar to that of the good installation.

In so far as the behaviour of pipes buried in various materials could be explained by such graphs, it was concluded that the shape of deformation could be deduced from the strain profiles. When analysing such data, it was remembered that the correlation sought ought to have been that between pipe wall strain and change in curvature of the wall, or relative movement

of the point towards the centre of the pipe. The good correlation of pipe wall strain on both vertical and horizontal axes with the change in the vertical diametral measurement was encouraging, therefore, and the behaviour at the shoulders and haunches was explicable.

In conclusion, an unconfined pipe produced an elliptical pipe wall strain profile when loaded, the strains being proportional to vertical diametral strain at each point around the circumference. This was consistent with the expected elliptical deformation of the pipe. When buried, elliptical deformation was accompanied by V shaped pipe wall strain profile and such behaviour was only found with poor sidefills such as silty clay and reject sand. Distortional behaviour, consistent with the character of the sidefill, occurred under static load in pipes that were given good support, behaviour being essentially elliptical under cyclic loads. Elastic recovery of static load deformation was greatest in soils of highest elasticity and in cases where pipe support was best. The arching behaviour of granular soils was important. The deformed shape of a pipe was deduced from the pipe wall strain profiles, the relationship of the latter being consistent with vertical diametral strain measurements.

### 5.2.3 Shape of Deformation

The deformed shape of the pipe at various stages throughout each test was recorded photographically using the ring flash camera. The photographs provided a good qualitative description of the shape of the pipe in cases where significant deformations occurred, but small distortional deformations were difficult to perceive from any single photograph. Roughly elliptical pipe deformation was found in sidefills providing poor lateral support and typical photographs at the start and finish of a test using such a material are shown in Fig. 5.2.3. Where a full depth UCPG

sidefill, which provided good lateral support to the pipe, was used a "heart shaped" deformation resulted (Fig. 5.24). This was characterised by flattening of the pipe crown and a reduction in radius of curvature of the shoulders, behaviour that could be perceived only in pipes with a relatively large V.D.S. (such as those produced in the preliminary tests, 6.3% in the case of Fig. 5.24). Where an arching layer of pea gravel overlay a full depth WCSC sidefill, an inversion of the "heart shaped" profile resulted (Fig. 5.25). Provision of exceptionally good support at the pipe springings led to a "square shaped" pipe profile, such as with a split sidefill (WCSC over UCPG) under the 55kN static load when applied for 30 minutes (Fig. 5.26).

In order to quantify the deformed shapes, a graph plotter was obtained towards the end of the project which, by reversal of its function, could be used to digitize information from the photographs in terms of co-ordinates relative to a datum (the centre of the ring flash disc). Manipulation of the co-ordinates of points at regular intervals around the circumference of the pipe at two stages of a test enabled the movement of the circumference at each point to be determined. The software to perform these adjustments and calculations has yet to be written, but manual calculation was performed in one case to verify the method. In this case, photographs at the start and finish of an experiment using an UCPG sidefill with a 100mm thick bed were taken and points at 22.5° intervals around the pipe circumference were digitized together with points defining the datum. A plot of the movement of each point relative to the datum, which approximates to the centre of the pipe, with settlement effects removed is shown in Fig. 5.27. The profile drawn from the actual measurements indicates clearly a "heart shaped" deformation profile in which most distortion occurs above the level of the springings. This profile is slightly offset sideways, indicating a small horizontal movement of the



pipe (unlikely) or the boom (quite possible, though a corresponding vertical movement would not be) during the test. The movement of the pipe wall at  $22.5^\circ$  to the right of vertical appears to be unusually high, and this was found to result from an error in digitizing. The movement of the pipe wall at  $22.5^\circ$  below the pipe springings was also uncharacteristically high resulting from the difficulty in measurement where the boom obscured the profile. Removing these anomalies, the average deformed profile was remarkably similar to that predicted by the pipe wall strain profiles.

The method of inferring the deformed shape of a flexible pipe from its pipe wall strain profile has been discussed at length in section 5.4.2 and requires little elaboration. The pipe wall strain profile for the corresponding box installation to that measured above is shown in Fig.

5.28. It is important to note that the strain in the internal face of the pipe is proportional to the radius of curvature of the pipe at that point and, therefore, to the movement of the point relative to the adjacent section of the pipe wall, not to an arbitrary datum. Compressive strain at the shoulders shown in the pipe profile for this installation does not mean an absolute movement of the wall at this point away from the centre of the pipe, but an outward movement relative to the pipe crown. Once this is appreciated, the agreement between the deformed shape and that predicted by the internal pipe wall strain profile is shown to be signally good.

Photographs for a corresponding test are shown in Fig. 5.24.

A set of pipe wall strain profiles for a pipe buried in a full depth WCSC sidefill with an overlying 50mm thick layer of pea gravel are shown in Fig. 5.29, from which the inverted "heart shaped" profile can be deduced in a similar way. The photographs corresponding to this installation are shown in Fig. 5.25, which again demonstrate the ability of the pipe wall strain profiles to predict the deformed profile of the pipe.

#### 5.2.4 Pipe Settlement

Settlement of the pipe was found to depend upon several factors and, in general, values of about 3mm or less were recorded at the end of the test. Pipe settlements of this magnitude will not influence the function of the pipe when in use and are, therefore, of academic interest alone.

The two main influences on pipe settlement were the stress acting on the pipe, as distinct from the load applied to the surface of the backfill, and the properties of the soil below it. The former is difficult to quantify in the case of flexible pipes because of their action under load, whereas rigid pipes do not deform significantly under load and the stress acting on the pipe crown can be accurately measured. It has been shown that an arching layer installed above the pipe crown reduced pipe deformation by redistributing vertical stress and this phenomenon could be expected to apply to settlement also. Comparison of data from installations of similar type and without arching layers will largely remove the influence of pipe crown stress, however. The most important influence, as expected, was found to be the properties of the underlying materials and, in particular, the bedding type (if any), bedding thickness and the state of the insitu silty clay forming the trench bottom. In the following discussion, only data from the test pit are referred to and these have been averaged where possible.

The first installation, and to a lesser degree the two following it, exhibited unusually high pipe settlement because of the ready compressibility of the relatively wet, newly laid insitu soil forming the base of the trench. Average settlements in these cases were 10.9mm (full depth UCPG sidefill with 100mm thick UCPG bed), 6.2mm (full depth UCPG sidefill without bedding) and 4.9mm (full depth WCSC sidefill). Thereafter good comparative, consistent data were produced. Where full depth, uncompacted sidefills were used with a 50mm bedding layer a distinct trend

was perceived in the average results for pea gravel (2.5mm), concreting ballast (2.9mm), quarry tailings (3.0mm) and building sand (3.1mm), notwithstanding the significant variation in the individual settlements. The settlements closely followed the pattern set by the Compaction Fraction values for the materials (0.05, 0.24, 0.31 and 0.37 respectively) and produced a roughly linear relationship when plotted. Where a repeat of the first installation (UCPG with 100mm of bedding) was investigated, an average settlement of 2.7mm was obtained, a value slightly greater than where a 50mm bed was used and accounted for by the ability of the extra gravel to reorientate. Where WCSC overlay a similar 100mm UCPG bedding, the settlement reduced to 1.9mm, which reflected the bedding in and induced reorganisation of the particles caused by the compaction of the clay sidefill above. Where no bedding layer was used, significant variation was found in the data and this was thought to reflect the state of the trench bottom. The two installations immediately preceding the refurbishment of the insitu soil, which involved full depth LCCB (1.9mm) and UCCB (0mm) sidefills, had smaller settlements than that for the duplicate installation using WCSC (3.3mm), in which typical insitu clay conditions existed.

Pipe settlement was dependent upon the thickness and type of the bedding material, therefore, with clear trends in behaviour in comparable installations. Variation in the state of the insitu soil, either in its compacted state or water content, was shown to greatly influence the settlement of the pipe. The implied effect of these results on pipe deformation can be summarised in two ways. Where consistent data for installations with bedding layers was concerned, the compression of the bedding material in allowing settlement would be similar to that of the sidefill in allowing lateral movement of the pipe. The ranking of the results, which was roughly the same for both pipe settlement and V.D.S., demonstrated this. Where the state of the insitu soil had a dominant

influence on settlement data, a similar, though greatly reduced, effect would be likely on the lateral support provided to the pipe assuming the trench walls to have the same properties. In practice, the state of the trench walls was found to be roughly constant after the initial installations, a fact borne out by the consistency of the pipe data, and only an indirect effect on V.D.S. could be expected by the penetration of certain granular soils into the base.

#### 5.2.5 Soil Strain

Measurements of soil strain were made using pairs of strain coils located vertically in the backfill, above both the pipe and the sidefill, and horizontally in the sidefill at the level of the pipe springings. Those in the backfill were placed co-axially at such depths that, when the backfill was compacted, the lower coils were about 50mm above the level of the pipe crown and the spacing was approximately 80mm. Coils of 50mm diameter were used (25mm coils were also available) to reduce the likelihood of misalignment and tilting of the coils during installation and loading. Differential movements were inevitable in the loosely placed clay backfill, however, and the measured values of strain coil spacing were often found to be inaccurate when compared with physical measurements on exhumation of the installation. Backfill soil strains between the coils were typically between 5% and 15%. This compares with overall backfill strains of approximately 10-20%, confirming that more compression occurs near the surface than in the main body of the backfill.

Pairs of 50mm diameter coils were also used in the sidefill and were placed with a spacing of approximately 85mm centrally in the 170mm gap between pipe and trench wall. Differential movement of these coils was dependent upon the sidefill type, and its applied compaction where

appropriate, and was found to be less prevalent than in the backfill. The measured sidefill strains were an order of magnitude lower than those of the backfill and, although differential movements would have had a significant influence on the values, the smaller overall movements provided less opportunity for the coils to misalign or tilt. The coils are known to perform better in relatively homogeneous fine grained soils in which correct orientation can be better maintained, and data from pea gravel and concreting ballast sidefills were consequently treated with caution. In each case the coils registered horizontal movements that were well below half the value of the horizontal outward movement of the pipe springings, indicating that the majority of sidefill compression occurred either close to the pipe wall or the trench wall. Howard (1973) found that the majority of soil movement occurred close to the pipe wall in his tests, which is consistent with these findings.

Variation of any single measurement, especially in the backfill, from the average was common, but consideration of the average values for good and poor sidefills produced clear and interesting trends. Where sidefills of pea gravel and concreting ballast were used, in which ultimate V.D.S. of the pipe was typically about 2-3%, the average vertical soil strain in the backfill above the sidefill was approximately 50% greater than that at the same level above the pipe crown. This implied that vertical compression of the sidefill was relatively small providing a stiff base to the overlying backfill being compressed against it. The downward movement of the pipe crown relative to the surface of the sidefill was reflected in the relatively low strain in the central portion of the backfill above it. The sidefill was apparently stiffer in the vertical direction than the pipe, therefore (cf. the relationship between Ring Deflection Factor and Stiffness Ratio used by Watkins and others, and shown in Figs. 2.10 and 2.38). In contrast the installations using well compacted silty clay and

uncompacted building sand sidefills, from which relatively large V.D.S. measurements of 4-6% resulted, exhibited central backfill soil strains that were approximately 25% greater than those at the same level above the sidefill. This indicated that the pipe was apparently stiffer in the vertical direction than the sidefill, causing the sidefill to compress more than the combined action of the V.D.S. and settlement of the pipe. The average compression of the soil between the strain coils above the stiffer sidefills was more than twice as high as that above the clay and sand sidefills, thus illustrating the relative vertical stiffnesses of the sidefills. The average compression of the soil between the coils above the pipe crown was roughly the same for both types of sidefill.

Trends in the horizontal compression of the sidefill were similarly apparent when average values were used, but often obscured when individual values were considered. Where comparable installations using pea gravel and concreting ballast sidefills were used, similar small average soil compressions were found. Average compression of the building sand sidefill between the coils was approximately four times greater than those above, though, at slightly over 1mm, it was small in comparison with the horizontal movement of the pipe wall. The measured compression of the clay was variable, probably due to differential movements of the coils during its compaction, with the average being somewhat greater than that of the gravel and ballast. It was more likely that local compression would occur close to the pipe wall with this material, however.

Despite individual variations in soil strain measurements the data produced interesting trends that were of use in determining the reasons for pipe behaviour. Where a sidefill has a high vertical stiffness, the pipe crown settles relative to the surface of the sidefill and "arching" in the backfill above will be induced. Where the sidefill has a low vertical stiffness, the pipe will tend to attract a greater proportion of vertical

load.

#### 5.2.6 Soil Pressures

Trench wall pressures were measured at five points around each cross-section at which load was applied in the pit and at the corresponding points in the box. Pressure cells were placed in opposite walls on the line of the springings and above the pipe crown, the fifth cell being placed in the insitu soil below the pipe. For use in the box, the cells were let into the box walls such that the diaphragm was flush with the plywood face and calibration was performed in situ. In the pit, the cells were placed in the insitu clay about 10mm behind the trench wall. Calibration of the cells used in the pit was performed in an oil filled bag in which a uniform all round pressure was applied, despite being distinctly different from the experimental condition.

The output from the pressure cells was often erratic, inexplicable jumps in the readings often causing the datum pressure level to be in doubt. This condition manifested itself in the early experiments and became more prevalent in later experiments. In order to accommodate their use in pea gravel installations, the cells were encapsulated in sand bags at the appropriate points. In later experiments the bags were dispensed with, but with no apparent improvement in the pressure cell readings. Where approximately consistent readings were obtained throughout a test, the magnitude of the pressures between tests was found to vary without reason. It is clear from these findings that further detailed investigation of trench wall pressures is necessary, in which accurate boundary conditions for calibration of the cells (probably using a triaxial cell) would be adopted. In view of the secondary role of these measurements in the present project, such work was not justified.

Pressures were measured at three points below the load platen in the later experiments to ascertain the distribution of surface pressure. One cell was placed directly below the centre of the load platen, one in the insitu clay near to the edge of the platen and the third in between. In each case the cells were covered with a 10mm thick layer of silty clay pressed firmly against the diaphragm.

A summary of surface pressures for an experiment in which all three cells produced apparently good readings is shown in Fig. 5.30. The curves indicate that the cells at the centre and the edge of the platen both produced consistent readings under the continuously applied static load, that at the edge registering approximately twice the pressure of that in the centre. The intermediate cell produced variable readings, however, including one excessively high value during the 70kN static load application (which has been removed from the figure). In general the pressures recorded by the cell in the insitu soil were consistently good, the values of pressure under the 70kN load ranging between 130kPa and 200kPa (the value of load divided by the area of the platen was 182kPa). The readings from the cells placed in the backfill were generally variable, however, with both positive and negative pressures being recorded. The curves shown in Fig. 5.30 for these locations should be treated with caution, therefore. The reason for this discrepancy in behaviour is probably associated with the homogeneity of the clay in which the pressure cells buried.

Assuming the consistent pressure readings in the insitu soil to be accurate and roughly uniform over the contact area between the platen and the insitu soil, the proportions of load applied to the insitu soil and the backfill surface were in the ranges 12-20% and 80-88% respectively. These values are reasonable and consistent with the load spreading expected of the platen. This topic is discussed in terms of theoretical predictions in



Chapter 7. Further calibration work is necessary to prove these values, however.

#### 5.2.7 Surface Settlement

Settlement of the load platen was monitored throughout each test and the surface profile of the clay was measured both after installation and prior to excavation. It was found that the overall movements represented closely the behaviour at each comparative stage of the test and it is the average final settlements that are used to describe behaviour herein. Surface settlement was governed mainly by the properties of the insitu soil and the backfill and, to a lesser degree, by the vertical compression of the pipe and sidefill. It could be expected, therefore, that the surface settlement of the first installation (149mm), and to a lesser degree the two subsequent installations (98mm and 106mm), would be greatest and that those immediately preceding the refurbishment of the Keuper Marl insitu soil (63mm and 52mm) would be lowest. This was shown to be the case. Careful control of the clay used for backfilling the trench and local replacement of the insitu clay around the load platens largely removed the other potential differences.

Where full-depth, uncompacted sidefills were used with 50mm thick bedding layers, the average settlements were 65mm (pea gravel), 93mm (concreting ballast), 83mm (building sand) and 99mm (quarry tailings). The relatively low average value for the pea gravel installations suggests that the V.D.S. measured in these tests might be underestimated, but comparison of pipe settlement data and other measurements indicates that this is not the case. Comparison of the results of the first installation, in which a full depth UCPG sidefill was used with a 100mm thick bedding layer, with that of the duplicate installation showed that although surface settlement

was considerably different (149mm and 87mm respectively) the V.D.S. of the pipe in each case (2.8% and 2.2% under load alone) did not vary by a large amount. This difference was significant, however, illustrating the value of auxilliary measurements in helping to explain abnormal behaviour. The average surface settlements for full-depth UCCB sidefills with (93mm) and without (52mm) a 50mm thick bedding layer indicated that the V.D.S. of the latter may have been artificially low, thereby concealing the benefit gained by introducing a bedding layer. When data from the box installations were examined it was considered unlikely that the error in this case was great, but further work would be needed to prove this. Where full-depth WCSC installations were compared, the first, which was conducted while the clay was still new, had a higher average surface settlement (106mm) than that of its duplicate (65mm). The average V.D.S. measurements (6.2% and 4.7% respectively) were also significantly different, but installations using such materials as sidefill were known to be extremely sensitive to other factors, such as the water content and compacted state of the sidefill. Despite diligent attempts to keep these factors constant between the tests, it is likely that the discrepancy was mainly attributable to them.

Surface settlement measurements were found to be useful in determining consistency, and explaining abnormalities, between experiments. While its influence on any particular installation was variable, it provided a good indication of the state of the clay forming the insitu soil and the backfill.

### 5.3 Pipe Classification Results

Strain controlled load tests were conducted at Nottingham on 150mm

lengths cut from each pipe installed in the pit. The load carried by each pipe when orientated about its weakest axis, that is the axis across which the sum of the pipe wall thicknesses was lowest, placed between flat plates and subjected to a slow constant strain rate has been plotted against deflection to determine whether significant behavioural differences could result from this source (Fig. 5.31). No distinction is made between the 16 curves because of their remarkable similarity up to 80% V.D.S. Two lengths of pipe were used in the box installations, each cut from the same pipe, and these were not considered to vary in properties during the test programme. It was concluded that the pipe did not constitute a variable factor between tests when analysing the results.

## CHAPTER SIX



## 6 SOIL CHARACTERISATION

### 6.1 Introduction

Characterisation of the insitu soil and fill materials was carried out with two distinct objectives in mind. The first involved determination of the structural properties of the various materials in order to both explain the observed behaviour of the pipes buried therein and tune the theoretical model. A single test could be used to achieve this, such as the triaxial test in which samples of the materials could be subjected to accurately simulated insitu loadings. The second aim was the development of a relatively unsophisticated test that could be performed on site to assess potential fill materials by measurement of a relevant structural property. To fulfill this requirement, several different methods of soil characterisation were necessary in order that their results could be correlated with a measure of pipe performance. It was particularly important that marginal materials could be properly assessed by the chosen method(s) and the characterisation of fine grained soils was included in the study. The results of this work have, therefore, been presented in different ways to distinguish between the various avenues of investigation.

The structural characteristics of each material used in the experimental work were determined using the triaxial test. Single samples of the granular materials were tested at a typical water content and density, whereas many cores of the Keuper Marl insitu soil were tested to cover a wide range of water contents and densities. A number of commercially available insitu soil strength testing devices were also used to characterise the Keuper Marl and the results were correlated with those from corresponding triaxial test cores. In this way the ability of each

device to accurately measure soil strength was determined. It has been widely stated in the literature that soil stiffness is the most important soil parameter in determining the behaviour of a buried flexible pipe. A correlation of soil strength with soil stiffness has been attempted to assess the value of the insitu devices, therefore. Granular materials could not be classified by such means and two other methods were used, the Compaction Fraction test and particle size distribution. The results of all three general methods of soil characterisation were then correlated with pipe performance.

## 6.2 Methods of Soil Characterisation

### 6.2.1 The Triaxial Test

The triaxial test was used to characterise each material used in the investigations, the methods used for cohesive and non-cohesive soils being different. In the case of Keuper Marl, 19mm diameter x 38mm long samples were taken from the bedding and sidefill of all early pit and box installations by driving sample tubes into the clay surface. This led to an increase in the density of the clay by an amount dependent upon its original density and water content. For tests on pea gravel and concreting ballast, 152mm diameter x 305mm long samples were prepared by placing the materials without compaction into a mould. The water contents of the two materials were the same as those at delivery and use in the tests. A pressure was applied to the sample by an internal vacuum, followed by an external fluid pressure while the sample was being set up, and this provided a degree of initial compaction. The same method of sample preparation was used for the other granular materials, although smaller samples of 76mm diameter x 152mm length were constructed. None of the

methods of preparation produced samples with the same stress history as that experienced by the sidefill during installation, but in each case the resulting material approximated closely to that obtaining in the sidefill.

Triaxial test procedure has been comprehensively described elsewhere (Bishop and Henkel, 1962, and others) and will not be repeated herein. Quick undrained tests were performed on the Keuper Marl samples under a constant cell pressure of 100kPa and the stress strain behaviour of the material was determined. The larger samples of granular materials were subjected to cyclic cell pressure between 30 and 150kPa for 50 cycles before being loaded until near failure under a constant 50kPa cell pressure. The maximum deviator stress was then cycled 1000 times. On sample measurement of axial and radial strain was possible with the larger samples. The water content and density of all samples was determined on completion of the tests.

#### 6.2.2 In Situ Measurements

Four insitu strength testing devices were used to characterise the clay. One relatively expensive cone penetrometer was chosen for use with the three cheap pocket devices, thereby providing an immediate means of assessment of the unsophisticated devices in the immediate area of their testing, rather than from a core taken in the general area. Each of the instruments performed best in homogeneous cohesive material and their use was generally only successful in the Keuper Marl. A fifth insitu device, the Shear Vane, was used in relatively weak clay to provide a further measurement of strength for comparative purposes. Much of the early data collected were correlated with those from the triaxial test, usually from one or two core samples taken at the same level of the installation.



#### 6.2.2.1 The Proving Ring Penetrometer

The most sophisticated insitu device tested was the Proving Ring Cone Penetrometer, which cost £400 and might be too expensive for use as a general site test for marginal soils. It consists of a 30° cone screwed into the end of a graduated rod, which is in turn attached to a proving ring with an internal dial gauge. A handle is attached to the upper surface of the proving ring, as shown in Fig. 6.1. The dial gauge is set to zero and the cone is pushed at a constant rate into a flat surface of the soil until just immersed. The driving force is removed and the dial reading is recorded before the instrument is reset. The resistance to penetration is determined from the dial reading using a calibration chart. The results from the Proving Ring Penetrometer are, therefore, operator dependent, but consistent data can be easily obtained with careful use.

#### 6.2.2.2 The Geotester

The Geotester is a form of pocket penetrometer that costs £40 and claims to produce basic soil strength parameters. It consists of a short rod attached to the spring of a dial gauge and onto the other end of which can be screwed one of five interchangeable heads of various size of type (Fig. 6.1). A 6mm plain head is used to provide similar data to those of the pocket penetrometers detailed below. One of the remaining four heads can be chosen, depending upon soil type and stiffness, to give the cohesion or angle of friction of the soil. The head is pushed at a steady rate into a flat surface of the soil until just immersed, as before. The relevant parameter is read from calibration charts using the dial gauge reading.

#### 6.2.2.3 The Pocket Penetrometers

The two pocket penetrometers, which measure complementary ranges of unconfined compressive strength of 0-500kPa and 300-1500kPa, were of similar construction to the Geotester (Fig. 6.1) and cost £17 each. The resistance to penetration of a 6mm diameter flat-ended rod when pushed at a steady rate into the soil is shown on the dial gauge in terms of unconfined compressive strength. Their use is restricted to fine grained soil and the manufacturers recommend that an average of several readings should be taken.

#### 6.2.2.4 The Shear Vane

The Shear Vane, which is restricted to use in cohesive soils, consists of a rod with four fins mounted at 90° (the vane) at one end, the other being attached to a torsional spring. Two sizes of vane were used to measure a range of cohesion, therefore undrained shear strength ( $C_u$ ) assuming complete saturation, of 0-124kPa. As a consequence it is of use only in relatively weak clay. The vane is pushed into the clay to an appropriate depth and a steadily increasing torque is applied through the spring until the clay fails. The maximum torque is indicated in terms of cohesion on a dial gauge. This instrument was known to produce accurate data from previous work and it provided an independent check on the results from the insitu devices where it could be used.

#### 6.2.3 The Compaction Fraction Test

The Compaction Fraction test is recommended for the assessment of potential pipe surround material in the current British Standard installation recommendations for uPVC pipes (B.S.I., 1980). The equipment

required for the test consists of a 250mm long offcut of 160mm diameter uPVC pipe, a 40mm diameter metal rammer weighing 1kg, a rule and, in certain cases, sieves with 19mm and 38mm nominal mesh sizes. The equipment is, therefore, unsophisticated and inexpensive to provide.

The test consists of three parts. The first involves a visual examination of the material in which that composed of angular particles is rejected. The second involves assessment of particle size, a material being rejected if it contains any particles of more than 38mm diameter or more than 5% by mass of particles over 19mm in size. The third part of the test assesses the ease with which a material can be compacted. The cylinder is placed on a firm, flat surface and the candidate material, which should be at roughly the same water content as that to be used in the trench, is loosely poured into it until exactly full. Excess material is removed, the cylinder is emptied and the contents replaced in four layers, all being completely compacted using the rammer. The distance from the top of the cylinder to the surface of the compacted material divided by the original height (250mm) is the "Compaction Fraction" value for the material. A material with a Compaction Fraction value of 0.2 or less is suitable for general use, a material with a value between 0.2 and 0.3 may be used under special conditions, and a value of more than 0.3 classifies the material as unsuitable.

The Compaction Fraction Test was performed on all of the materials used as sidefill in the experiments. When assessing the silty clay by this method, relatively small lumps were used out of necessity, but care was taken to ensure that the material did not differ significantly from that used as sidefill in the experiments. Nevertheless, the Compaction Fraction value for the silty clay should be treated with caution and is only included in the following sections for completeness.

#### 6.2.4 Particle Size Distribution

The particle size distribution of most of the experimental sidefill materials was determined by dry sieving through a succession of sieves, the exceptions being silty clay and reject sand which required wet sieving. The sieves were stacked in increasing order of standard mesh size with the largest uppermost and dry material of known total mass was placed in the top sieve. The sieves were covered, securely clamped and mechanically vibrated until all particle movement had ceased. The mass of material retained on each sieve was calculated, hence the percentage passing each was determined and the particle size distribution curves were drawn to a logarithmic scale. The choice of sieve sizes used can affect the shape of the curves and care was taken to ensure an appropriate distribution of British Standard sieves for each material. Particle degradation was not found to be a problem with the materials used.

The wet sieving method involves washing the material in the 63  $\mu\text{m}$  sieve under running water to remove all particles of silt size or smaller, thereafter the distribution of the larger particle sizes being determined as before. The distribution of particle sizes between fine sand and coarse gravel was of most interest, as materials with a significant proportion of silt or clay particles tended to require compaction in order to perform suitably. Were this method to be adopted on site, a range of British Standard sieves and a method of weight determination would be the only requirements, the procedure being simple. Determination of the silt and clay particle sizes involves sophisticated sedimentation techniques and is necessarily restricted to the laboratory. It was known from previous studies that the clay content of Keuper Marl is approximately 18%, that of the reject sand being negligible. The structure of the lower portion of the grading curves for these two materials can be estimated, therefore.

#### 6.2.5 Index Tests and B.S. Compaction Test

The Keuper Marl used both to fill the pit and to reinstate the trench during the experiments derived from one of two main batches delivered to the University at an interval of 15 months. Samples from both batches were subjected to the index tests, using the cone penetrometer method of liquid limit determination, and the British Standard Compaction Test by the 2.5kg rammer "Proctor" method. Both tests are detailed in BS1377 (B.S.I., 1975).

### 6.3 Experimental Procedure

#### 6.3.1 In Situ Soil Characterisation

In situ soil characterisation was restricted to the Keuper Marl, attempts to measure the properties of fine granular materials being generally unsuccessful. The devices were used to test the trench bottom, the surface of the sidefill (where appropriate), the surface of the backfill and the surface of the insitu soil below the edge of the load platen, during both installation and exhumation of every pipe. Each level at which measurements were made in the pit was divided into five areas, two beneath the loading points and three elsewhere, from which average data from each device were taken. Two insitu clay areas were isolated at the surface in addition to the five within the trench. Each corresponding level in the box installations was divided into two areas, one below the loading platen. In each area 3 Proving Ring Penetrometer readings, 6 Geotester readings, 12 Pocket Penetrometer readings and, where possible, 6 Shear Vane readings were taken. These were grouped such that for every Proving Ring Penetrometer reading, 2 Geotester and 4 Pocket Penetrometer readings were taken in the immediate vicinity such that a direct comparison of these data could be made. In this way a maximum of 34 average sets of

data were obtained from each pit installation, and 12 from each box installation, each average reading consisting of 3 comparable sets of data.

Water contents were taken, again during both installation and exhumation of the pipe, from each of the areas and levels of the silty clay delineated above, an average for each level generally being found sufficiently accurate to describe the behaviour of the readings. Water contents were similarly determined for all granular sidefills except pea gravel, water content having no significant influence on the behaviour of the latter unless submerged. The water content of the trench walls and base was also determined. Core samples for use in the triaxial test were taken at three appropriate points during exhumation of the early installations and their location was related to the insitu tests for later correlation of data. It should be noted that the correlation of the clay characterisation measurements was based on data from the first batch of clay to remove the influence of any potential difference in properties between batches.

A 400mm square, 400mm deep reinforced box was constructed from phenolic film faced plywood in order that materials without the usual range of water contents and densities could be tested by the insitu devices. A 150mm layer of silty clay was thoroughly compacted in the base and the candidate material was placed above and treated in such a way that a further 150mm thick layer was produced. Care was taken to ensure that the treatment of the material immediately adjacent to the walls of the box was representative of the whole, although the instruments were used in, and cores taken from, the central area alone. This box was not extensively used, the majority of data being obtained from experimental installations.

### 6.3.2 Laboratory Tests

Triaxial testing of the Keuper Marl samples was carried out in three batches because of limited access to the equipment. This necessitated storage of cores for up to three months and in a few cases the material was found to lose water, albeit slightly. The results from these cores, which were isolated using the insitu water content measurements taken in the immediate area of the samples, were not used for direct comparison with the insitu devices. Triaxial testing of representative samples of the granular materials was carried out towards the end of the test programme, the water content of the material being the same as that of the material when used as sidefill in the pit installations.

The particle size distribution curves, or grading curves, for each material were determined from representative samples on delivery. The Compaction Fraction Test was performed on four samples of each sidefill material at the water content at which it was laid in the experimental installation and an average value was found. Further Compaction Fraction Tests were performed on dry samples of the granular materials in order to ascertain the influence of water content on the results.

## 6.4 Results

### 6.4.1 Comparison of In Situ Soil Strength Testing Devices

Before the results from the insitu devices are presented and their correlation with those from other sources is discussed, it is important that the interrelation between the measured parameters is described. The assumption of complete saturation of the Keuper Marl, therefore purely cohesive behaviour, is made when analysing all of the data, the value of Cohesion being equal to the undrained shear strength as a consequence. All

of the tests, both laboratory and insitu, were considered to be carried out under quick, undrained conditions. The two Pocket Penetrometers measure the unconfined compressive strength of the soil, which is equal to twice the undrained shear strength ( $C_u$ ) from the above assumptions. The values of penetration resistance recorded by the Geotester are converted to values of Cohesion, therefore  $C_u$ , using calibration charts. The Shear Vane measures the value of Cohesion and  $C_u$  is read directly from the dial gauge after failure of the clay around the vane. Values of force applied through the ring of the Proving Ring Penetrometer are found from the dial gauge readings using calibration charts and are converted into values of applied pressure ( $q_c$ ) by dividing by the base area of the cone.

In the analysis of the triaxial test data, values of both strength and stiffness have been calculated together with values of voids ratio ( $e$ ) and water content ( $w$ ) for the clay specimens. The value of  $C_u$  is assumed to equal the value of cohesion, or half of the deviator stress at failure, as above. Soil stiffness ( $E_{50}$ ), which will be referred to in later sections of this chapter, is defined as the secant modulus at half of the deviator stress at failure. Values of voids ratio, which are indicative of the compacted state of the soils, have been calculated from values of dry density ( $\rho_d$ ) and water density ( $\rho_w$ ) using:

$$\rho_d = \rho_w \frac{G_s}{(1 + e)} \quad (6.1)$$

where  $G_s$  is the specific gravity of soil solids and taken as 2.65, a value measured in previous work at Nottingham.

A paper by Black (1979), who cites the work of Sanglerat (1972), discusses the relationship between California Bearing Ratio (CBR) and  $C_u$  measured by a cone penetrometer. By combining two empirical, but well



proved, relationships, he states that:

$$q_c/C_u = 30 \quad (6.2)$$

for overconsolidated soils. This value is shown to be at the upper end of the published penetrometer data and therefore verified. Considering values for remoulded soils in the literature, he concludes that the corresponding relationship is:

$$q_c/C_u = 10 \quad (6.3)$$

A method of comparison of the results from the Proving Ring Penetrometer with measurements of undrained shear strength is thereby achieved.

Comparative data from the four penetrometer devices are represented graphically in Figs. 6.2 to 6.4. The first (Fig. 6.2), shows values of  $q_c$  for the Proving Ring Penetrometer plotted against  $C_u$  measured by the Pocket Penetrometers. Distinction has been made between the relatively undisturbed soil data for the bedding, which in each case is the trench bottom, and the extensively remoulded soil data of the upper layers. The graph indicates that nearly all the points of the former lie above the best fit line of the latter. The gradient for the undisturbed material was 7.8, whereas that for the disturbed soil was 6.0. The graph of  $C_u$  (Geotester) against  $C_u$  (Pocket Penetrometers), shown in Fig. 6.3, indicates a roughly linear relationship through the origin with a gradient of 1.14, though with significant scatter. The maximum value of  $C_u$  measured by the Geotester was 206 kPa and, consequently, many tests on the bedding layers registered resistances that were off the scale. The plot of  $C_u$  (Geotester) against  $q_c$  (Proving Ring Penetrometer) (Fig. 6.4), is similar to Fig. 6.3 with a gradient of 0.18, the reciprocal of which is 5.60.

These graphs indicated that the readings obtained by each of the devices were mutually linearly proportional and that if the average of sufficient readings was taken, the cheaper devices could be used to provide accurate data when calibrated appropriately. The ratios of  $q_c/C_u$  for the Pocket Penetrometers (6.0) and Geotester (5.6) were low in comparison with the value chosen by Black (1979) for remoulded soils (10.0) and those quoted by him from the literature (7.6–10.0). The value for the commonly undisturbed soil (7.8), despite being greater than the corresponding disturbed value, was also low in comparison. Assuming that the relationship quoted by Black was correct and that the value of  $q_c$  measured by the Proving Ring Penetrometer was accurate, the reason for the overestimation of  $C_u$  by the inexpensive devices was sought.

A study of the data obtained from the Shear Vane and the triaxial test (Table 6.1), though limited in the former case by a maximum  $C_u$  measurement of 124 kPa, provided the explanation. The values measured by Pocket Penetrometers were typically about 1.5 times greater than those of the vane and triaxial tests. When this factor was included, a modified value of  $q_c/C_u$  of about 9 was obtained, which showed good agreement with the quoted values. For the Geotester, this adjustment was multiplied by the gradient of Fig. 6.3, i.e.,

$$\text{modified } q_c/C_u = (1.5 \times 1.14) \times 5.6 = 9.6 \quad (6.4)$$

which again indicated good agreement.

The results of this investigation showed that the strength measurements made by the Shear Vane and triaxial test were similar and provided accurate absolute data against which those from the insitu tests could be judged. When comparing data from the insitu test devices significant scatter of results was observed, even when average values were

**Table 6.1 Comparison of  $C_u$  Values Measured by the Pocket Penetrometers, Shear Vane and Triaxial Test**

Sample No.	Average value of $C_u$ (kPa)			Ratio*
	Pocket Penetrometer	Shear Vane	Triaxial Test	
1	150		96	1.6
2	92		74	1.2
3	228		155	1.5
4	223		142	1.6
5	203	109		1.9
6	219		189	1.2
7	163	107		1.5
8	194	109		1.8
9	173		120	1.4
10	157		120	1.3
11	157	106		1.5
12	153	100		1.5

\* the ratio quoted is that between the value of  $C_u$  measured by the Pocket Penetrometers divided by the corresponding shear vane or triaxial test, as appropriate

plotted. Scatter is common when dealing with soil data, however, and the overall pattern of measurements was such that a single line could be perceived with confidence. When considering that most of the measurements were made on clay that had been recently excavated and relaid in various states of compaction, the agreement between readings over an area of about  $0.25\text{m}^2$  was good.

In order to further characterise the silty clay and to determine the reasons for the scatter of results, the influence of water content ( $w$ ) and voids ratio ( $e$ ) on soil strength was investigated. The triaxial test data were used to determine the relationships between  $C_u$  and  $w$ , and  $C_u$  and  $e$ , which are shown in Figs. 6.5 and 6.6 respectively. Both plots show the expected decrease in strength with increasing water content or voids ratio.

Graphs of  $q_c$  vs  $w$  for the Proving Ring Penetrometer (Fig. 6.7) and  $C_u$  vs  $w$  for the Pocket Penetrometers and Geotester (Fig. 6.8), in which average values were used, were similar to the corresponding plot for the triaxial tests (Fig. 6.5) and included the same degree of scatter. Consequently, it was concluded that the various insitu test devices responded to the strength variation of the Keuper Marl caused by changes in both water content and state of compaction.

Data from the four penetrometers were linearly proportional, but the values of strength measured by the Pocket Penetrometers and the Geotester were approximately 1.5 to 1.8 times too great. The discrepancy between the measured values might result, in part, from the semi-spheres of influence of the devices with smaller samples registering higher strengths, a phenomenon thought to occur in London clay. The cheaper models could be used with confidence, therefore, provided that the average of sufficient readings was taken and that calibration with a more sophisticated device, or laboratory data, could be made. Were either of the cheaper devices to be adopted as part of a site assessment test for marginal soils after

treatment, a comprehensive system of tests, under closely controlled conditions, on a wide range of cohesive soils would be required for calibration purposes. A range of values for suitable soils would accompany such recommendations. The adoption of a cone penetrometer would remove the need for such widespread calibration to determine absolute values, an "operator independent" device based upon a falling weight system being most desirable.

These comparisons have been made using soil strength measurements, whereas a measure of soil stiffness is necessary for the ranking of sidefill materials. A method of relating strength and stiffness would be required before the devices could be used with confidence.

#### 6.4.2 Laboratory Methods of Classification

The triaxial tests performed on samples of Keuper Marl to obtain data for comparison with the insitu test devices also yielded information on stiffness for use in both theoretical work and material classification. The stress/strain behaviour of Keuper Marl was found to be heavily dependent upon water content and void ratio, selection of a single general value being impossible. An average value of stiffness for Keuper Marl at a specific water content, or voids ratio, could be found from an appropriate graph summarising data from many such tests, and this is further discussed in section 6.4.3. The typical range of measured stiffness values was about 3 - 25 MPa.

Analysis of the results of triaxial tests on granular materials involved the calculation of bulk (K) and shear (G) moduli from the appropriate loading and unloading curves produced during the tests. Values of Young's Modulus (E) were then determined using

$$E = \frac{9 \text{ KG}}{3K + G} \quad (6.5)$$

These values would not be significantly affected by small changes in the typical water contents used, and the similarity between the prevailing conditions during sample preparation was likely to lead to good comparative data. The number of load cycles for which the stiffnesses were calculated was dependent upon the comparison required (see Fig. 6.9). Pipe performance data at the end of each test was compared to the triaxial test stiffnesses at 50 cycles of load, representing the point at which significant changes were mostly complete. Pipe performance on initial application of load was related to triaxial test stiffnesses during the second cycle of load, the first being difficult to model with a single value.

Bulk and Shear Moduli were calculated as secant values between the extremes of deviator stress for each material (Fig. 6.9). The loading curves for the fiftieth cycle were generally linear and modulus definition (i.e. tangent or secant) was consequently unimportant. Those for the second cycle tended to be markedly curved and the secant Moduli that were derived from them were strictly average values. Young's Modulus was calculated during the fiftieth load cycle for pea gravel (286 MPa), concreting ballast (272 MPa), building sand (100 MPa) and washed quarry tailings (110 MPa). During the second cycle of load, the values of Young's Modulus for pea gravel (222 MPa), concreting ballast (158 MPa), building sand (59 MPa) and washed quarry tailings (84 MPa) were significantly lower. No data were obtained for the reject sand because the samples reduced in length by more than 10% on application of the initial internal pressure, rendering the instrumentation on the sample unusable. Compaction of the sand during sample preparation would have produced an incomparable result

and was not done.

Each material used as sidefill in the test installations was classified by particle size distribution. The grading curves for each (Fig. 6.10) define clearly the grading and particle sizes, together with a broad classification of material type. No account was taken of other physical properties such as particle angularity or surface texture. The use of a logarithmic scale for particle size enabled a vast range of sizes to be accommodated, but only the granular components equivalent to a fine sand or larger were of interest. The Keuper Marl had a clay content of 18% and a silt content of 56% and, as these components dictated its behaviour, it was classified as a silty clay. Reject sand, the by-product of a sand and gravel recovery operation, consisted of 52% sand and 48% silt (assuming a negligible clay content), most of the sand being fine grained. Its classification was strictly a silty sand, reject sand being a general term for sub-standard sand, whatever its inadequacy.

The remaining materials were of a wholly granular nature, their properties depending upon the relative position and gradient of the particle size distribution curve. Pea gravel was found to be an essentially single sized gravel, the majority of particles being between 5mm and 10mm in diameter. Building sand was similarly found to have essentially single sized particles, its classification being a medium sand. In contrast to these two materials, concreting ballast was shown to be a well graded material with a flatter gradient, hence its other name of all-in-aggregate. Washed quarry tailings also conformed to this pattern, the particle sizes ranged between fine sand and fine gravel.

Such classification was of use in defining the expected behaviour of a material. A large single sized material was known to arch over a greater distance than a similar small material, and a well graded material was known to produce a stiffer medium, when compacted, than that with a poor

grading. The method was an obvious candidate for the ranking of granular materials because of this attribute, but was likely to be of little use in classifying cohesive soils because other effects, such as particle attraction, become dominant.

The Compaction Fraction test, which is the currently recommended method of material classification, was conducted on each of the sidefill materials. The materials were tested in the state in which they were delivered and the granular materials were also tested when dry. Where Keuper Marl was used, the clay was broken down into small lumps before the pipe was loosely filled. The average Compaction Fraction values were as follows

Table 6.2 Compaction Fraction Test Results

Material	CF (natural)	CF (dry)
Pea gravel	0.05	0.05
Concreting ballast	0.24	0.10
Washed quarry tailings	0.31	0.15
Building sand	0.37	0.17
Reject sand	0.42	0.25
Silty clay	0.53	-



In general, the average of four tests is quoted for each material, in each state, with good repeatability. While the results from the dry granular materials did not reflect the characteristics of the materials used as sidefill in the installations, they demonstrated the necessity of testing at the proper water content if significant errors were to be avoided.

The triaxial test provided the most information about a soil and, despite the difficulty in obtaining a truly representative sample, was found to be the most accurate form of classification. It is strictly a laboratory test, expensive to perform and, therefore, wholly unsuitable for building drainage applications. Determination of the particle size distribution of granular materials, however, is a simple process using unsophisticated equipment and the results provide a qualitative description of material behaviour. Use of this method for determination of silt and clay contents necessitates further equipment and controlled conditions, rendering it unsuitable for such fine grained soils. The Compaction Fraction test requires least equipment and is also quick and simple. Experience has shown it to be little used, however, and doubt has been cast on its ability to classify soils. The determination of the ability of the three methods to provide a quantitative description of material behaviour in terms of pipe response is discussed in detail in section 6.4.4.

#### 6.4.3 Determination of Soil Stiffness from Strength Measurements

Soil stiffness could be directly determined only from the stress/strain curves produced by the triaxial test. In the case of Keuper Marl, a large number of quick undrained tests were performed on samples of varying water content ( $w$ ) and voids ratio ( $e$ ), from which values of both undrained shear strength ( $C_u$ ) and secant modulus ( $E_{50}$ ) were calculated. The aim was to investigate the influence of water content and state of

compaction on the stiffness of a cohesive material, and to determine the relationship between  $C_u$  and  $E_{50}$ . This had the effect of assessing the ability of the insitu test devices to measure the stiffness of a soil indirectly.

When defining a single value of stiffness for a soil which exhibited non-linear elasticity, various options were available. The stress/strain relationship for Keuper Marl took the form of a curve with a progressively decreasing gradient, until failure was reached and the gradient became zero. Failure was found to occur either by sample shear or barrelling. For the purpose of this work the sample was deemed to have failed in the latter case when 20% axial strain was reached. The stiffness of the material was represented by the gradient of the curve, and this varied considerably depending upon its definition. Where Keuper Marl was used as sidefill, large soil strains were experienced close to the pipe wall and a value of stiffness that reflects the whole of the early section of the curve was required. A secant modulus at 50% of the failure stress ( $E_{50}$ ) was chosen for this purpose.

Triaxial tests were performed on samples from installations in which both batches of clay were used. The influence of water content on soil stiffness is shown in Fig. 6.11, in which distinction has been made between results from the old and new batches of clay (1 and 2 respectively). It is clear that water content had a considerable influence on the stiffness of Keuper Marl. A curve could be drawn with some confidence through the data for the first batch of clay but the points for the second batch were fewer in number and exhibited significant scatter. The second batch was stiffer than the first. A graph showing the influence of voids ratio on soil stiffness (Fig. 6.12) shows similar tendencies but with rather less scatter for Batch 1. The clay forming the different batches came from the same pit, but at different times. This probably led to a slight change in its

composition, which accounted for its change in stiffness characteristics.

In order to investigate this further, the index tests and a British Standard Compaction test were carried out on samples from the second batch of clay and the results were compared with those from the first batch (Table 4.1 and Fig. 4.5). The results of these tests are summarised in Table 6.3, together with those for the first batch of clay.

**Table 6.3** Results of Index Tests and B.S. Compaction Tests on Keuper Marl

Source of Keuper Marl	Batch 1	Batch 2
Index Tests		
Liquid Limit (%)	32	36
Plastic Limit (%)	19	18
Plasticity Index (%)	13	18
B.S. Compaction Test		
Optimum Water Content (%)	14.5	15.5
Maximum dry density (kg/m <sup>3</sup> )	1.82	1.79

It is clear that the properties of the clay vary between batches and the relatively large difference in optimum water content, notwithstanding the changes in Plasticity Index and maximum dry density, accounts for the discrepancy in stiffness shown in Fig. 6.11. Further analysis of the soil strength measurements shown in Figs. 6.5 and 6.6 revealed that the points for both batches of clay were evenly distributed about the respective curves. The soil strength characteristics of the clay were constant between batches, therefore.

The relationship between undrained shear strength and stiffness for Keuper Marl (Fig. 6.13) again reflects the difference in behaviour between the two batches of clay. Where data from both batches of clay are considered, stiffness is shown to be roughly proportional to strength, up to a value of  $C_u$  of about 250 kPa, the relationship being;

$$E_{50} \approx 40 C_u. \quad (6.6)$$

With both  $E_{50}$  and  $C_u$  in kPa. When considering only those data from the first batch of clay, however, a curve was found to more closely represent the distribution of points over the full range of  $C_u$  values. The phenomenon of increased stiffness of the second batch of clay without change in strength manifests itself again on this graph.

It was apparent that the strength of the Keuper Marl was related to its stiffness, though the scatter produced by the newer clay was almost sufficient to obscure the connection. The results produced in this series of tests led to the conclusion that soil strength measurements gave an indication of the likely soil stiffness, but that even a slight change in material properties would significantly affect the relationship. The error may be partly due to the assumption of complete saturation made in calculating the value of soil strength. Fully saturated soil may be

expected to give a better result, because the immediate application of load would be carried by the inherent water rather, than by the soil structure, on compression of the air in the voids and the soil may be treated as fully cohesive. Further work is necessary on this subject, particularly with regard to the behaviour of cohesive soils with different proportions of clay, silt and sand. In particular, the use of larger samples, on which measurements can be made directly, would be necessary to remove some of the inaccuracies of the present tests. The use of different cell pressures would lead to greater accuracy in determining  $C_u$ , and better methods of sample preparation would reduce scatter and the sensitivity of the results to water content and voids ratio.

#### 6.4.4 Correlation with Pipe Behaviour

It has been shown that the behaviour of a buried uPVC pipe is dependent upon the properties of the soil used to surround it. In installations where similar conditions exist, a direct comparison of this soil influence could be made and the results of such tests are presented in chapter 5. Judgement of the soil characterisation tests is wholly based upon the ability of the tests to predict the relative performance of the materials in resisting pipe deformation, and can be made by attempting to correlate the soil properties measured by the test with pipe performance. Before such work is carried out, a careful consideration of the values to be compared is necessary.

Vertical diametral strain is the critical performance criterion for buried uPVC pipes and is the parameter to be minimised when choosing a sidefill material. It was, therefore, used as the measure of installation performance for the comparison. In view of the practical requirement of a bedding layer for most site conditions, only those pit installations in

which a 50mm bedding layer was provided have been considered. Average data from two stages of each test were used. These were, immediately after the application of the 55kN static load and on completion of the loading sequence. In this way, both immediate and long term behaviour may be assessed. Three soil classification tests were used on each of the sidefill materials. The Compaction Fraction test was performed on each material in the state that it was delivered and laid, and on the material when dry. The former results are relevant to this investigation only. Each material has been classified according to particle size distribution and a method of calculating a parameter for comparison will be discussed. In the case of silty clay and reject sand, only those particles that were of sand size were classified by this method. The triaxial test was similarly used to characterise each of the materials, the value of soil stiffness being of most interest.

The Compaction Fraction test provides an indication of the compressibility of uncompactd soil by comparing the volumes of uncompactd and fully compactd material. Comparison of data can only be made with confidence if the material is subjected to the same stress history, which is the case where uncompactd sidefills have been used in the test pit. Graphs of the V.D.S. of the pipe against the Compaction Fraction (C.F.) value of the sidefill for the two stages of each comparative test are shown in Fig. 6.14. While only five points are shown on each curve, all values of V.D.S. and C.F. used are averages of four readings with the exception of the V.D.S. in reject sand (2 readings). Curves can be readily fitted to the data and these conform to a logical pattern, indicating that the Compaction Fraction test does provide an appropriate measure of soil compressibility and that this parameter has a direct influence on pipe deformation. Further data would be required before any definite conclusions could be drawn, but these results are encouraging.

The particle size distribution curves shown in Fig. 6.10 provide a good qualitative comparison of the materials and their likely behaviour, as discussed in section 6.4.2. Consequently, it is an obvious contender for a site test, the necessary equipment and its use both being simple. The deformation results from the pit tests can be explained by the inter-relationship of the curves. Pea gravel and building sand have grading curves of similar shape, but offset by more than an order of magnitude. The larger material will have a greater ability to arch and less opportunity to reorientate beside the pipe under load (thereby being unresponsive to compaction), and this is reflected in the deformations of the pipes buried therein. Concreting ballast has a flatter curve, with significant proportions of medium gravel and medium sand. Such a material will experience considerable stiffening when compacted, part of which is mobilised during installation by indirect compaction caused by placing and compacting the clay above. The resulting material is likely to behave in a similar manner to the pea gravel, the results proving it to be slightly poorer at resisting deformation. The washed quarry tailings grading curve is similar in shape, in its lower half, to that of concreting ballast, but an order of magnitude lower. Pipe support provided by washed quarry tailings will be less than that of concreting ballast, but greater than building sand, because of the relative position of the grading curves. This was reflected in the test results. Reject sand is likely to be considerably poorer than building sand, but, as with Keuper Marl, other effects become dominant at lower particle sizes and such unknown factors as clay content will determine behaviour. Materials can be ranked qualitatively by this method, assuming installation conditions are known, and their general behaviour deduced.

In an attempt to quantify the relationship, factors have been sought to describe the curves in terms of gradient and relative position. A

common method of defining a material is by its Uniformity Coefficient, which relates the diameters below which 60% and 10% of particles lie ( $D_{60}$  and  $D_{10}$  respectively) as a ratio. Such a factor, which represents the gradient of the curve, when multiplied by a point on the curve to represent position (for example  $D_{60}$ ) may define the curve appropriately. While this has the advantage of using an existing measure of soil grading, the results showed that the factor failed to rank the materials in the right order of performance. The reason for this lies in the method of slope determination, which should properly relate the difference between  $D_{60}$  and  $D_{10}$  to that in the percentage passing. A study of the curves showed that the slope of each was best described by that part lying between 80% and 20% passing, corresponding to diameters of  $D_{80}$  and  $D_{20}$  respectively. Each curve could be characterised in terms of grading, therefore, by the following formula:

$$\text{gradient} = \frac{0.8 - 0.2}{D_{80} - D_{20}} \quad (6.7)$$

If the same range is used for each curve, then the gradient is characterised by  $(D_{80} - D_{20})$  alone. Absolute particle size can be characterised by a single representative point on the curve, the diameter at which 50% of particles are smaller being chosen to account for any curvature of the lines between the high and low diameters. The product of the two would define each curve fully, a logarithmic scale being necessary to plot the data sensibly. The relationship may be expressed as

$$\text{pipe performance} = f(\ln (D_{50} (D_{80} - D_{20}))) \quad (6.8)$$

In order to test this theory, a graph of V.D.S. of the pipe against this



factor (Fig. 6.15) was produced, on which points representing average pipe performance at both the end of the test and after the application of the 55kN static load were plotted. The Grading Curve Factor for reject sand was determined by extrapolating the grading curve to obtain  $D_{20}$ , the value of which has a relatively small influence on the Factor in this case. The materials have been ranked in the correct order of performance by the Grading Curve Factor and a curve may be drawn through the points, though with the same reservations concerning lack of data as those for the Compaction Fraction test results. A curve of the type shown was the expected result, the Grading Curve Factor apparently being an inverse function of the Compaction Fraction, though producing a flatter gradient in the area representing marginal materials when plotted against V.D.S. As before, further data is necessary to define the curve properly before any definite conclusions could be drawn, but the results are extremely encouraging both in themselves and in their similarity to the Compaction Fraction values.

The stress/strain relationships produced by the triaxial test provide an accurate method of calculating the stiffness, in terms of Young's Modulus, of a granular material. By ensuring that each sample has a similar stress history, and of a roughly equivalent type to that experienced by the sidefill during installation, both comparative and absolute data can be obtained. It has been widely stated in the literature that soil stiffness is the most important soil property, and much of the work conducted in America has been towards defining such values for soils. The triaxial test, while being too sophisticated to be of practical use, is capable of doing this and the resulting values of soil stiffness should correlate well with pipe performance.

A graph of average V.D.S. of the pipe against the Young's Modulus of the sidefill at two stages of the tests (Fig. 6.16) illustrates the

relationship for five materials. Average data from samples of WCSC have been plotted for reference, although the points will lie well below the line describing the results from the uncompacted granular materials. The results again rank the granular materials in the correct order and appear to conform to the expected trend, but require considerable further verification.

Of the three methods discussed above, the triaxial test has no practical application, its advantage rather being in providing a direct, and generally accurate, measurement of material stiffness in terms of Young's Modulus. It appears likely, however, that the stiffness of the sidefill is the dominant influence on pipe performance, and the factor to be measured, either directly or indirectly, by the adopted test. The Compaction Fraction test is currently specified for the determination of soil suitability and has been shown to be useful in predicting pipe performance. The present limit on the Compaction Fraction value has been shown by the experimental work to be too low, however, and the test is largely unused in practice, despite its simplicity in terms of both method and equipment. In addition, it has the disadvantage that it is very sensitive to small changes in Compaction Fraction at the level at which the limit should be set and is also sensitive to changes in water content, an unconservative value being produced if the material is drier than normal. The particle size distribution method is likewise simple, is not affected by the water content of the candidate materials, and the factor used in the analysis is less sensitive to small changes at the point at which the limit would be set. For these reasons, the method based on the determination of particle size distribution may prove to be the most appropriate for the assessment of fill materials on site. Further work is required to fully investigate the influence of grading and absolute size, in addition to such factors as particle angularity, surface texture of particle and particle degradation.



## CHAPTER SEVEN



## 7. THEORETICAL STUDY

### 7.1 Introduction to Theoretical Techniques

There are several methods of theoretically predicting the behaviour of a geotechnical material, in terms of stress, strain and displacement, at a depth below a loaded surface. These vary in sophistication according to the assumptions made about the properties of the material and the character of the applied load. The degree of sophistication that is required for any calculation is dependent upon the type of problem and whether comparable or absolute data are required. A number of techniques have been used, both in planning the experimental work and in simulating the experimental condition.

Boussinesq (1885) evolved equations for the determination of the six stress components acting at a point in an elastic, homogeneous, isotropic, semi-infinite medium caused by the action of a vertical point load at the surface. The application was extended to a point below a foundation by Fadum (1941) and Newmark (1942). Tables for determining the complete pattern of stress, strain and deflection beneath a uniform circular load were developed by Ahlvin and Ulery (1962), based upon similar assumptions. Burmister (1945) extended the Boussinesq theories to layered systems.

The advent of computers has led to the adoption of the more sophisticated techniques and these have been used in this project in two ways. The effect of introducing a granular layer above the insitu soil was studied using BISTRO, (Peutz et al, 1968) a program for evaluating the response of linear elastic layered systems to surface loading. An approximate parameter study to determine the function of each part of an installation on pipe performance was conducted using the PAFEC finite

element system, assuming linear elastic behaviour for all elements.

Such theoretical techniques are extremely useful in extending data from specific experimental work to general applications as long as their limitations are well understood. The assumption of linear elasticity means that only the immediate response of a single load can be determined with certainty, whereas creep effects and the long term behaviour under repeated loading are commonly required for practical purposes. More sophisticated soil models would be required before account of such behaviour, and predictions of actual pipe performance, can be made. Development of a predictive model using finite element analysis would require extensive full-scale testing to corroborate the theoretical data. A preliminary attempt at correlating theoretical and experimental data has, however, been made.

## 7.2 Linear Elastic Layer Analysis

### 7.2.1 BISTRO and its Use

BISTRO, the name of which is an acronym for Bitumen Structures in Roads, is a computer program for the calculation of stresses, strains and displacements in a multilayer system when subjected to surface loads. The computations are based on application of classical theory of elasticity to layered systems, as set out originally by Burmister (1945). Each layer is assumed to be a homogeneous, linearly elastic material of uniform thickness and infinite horizontal extent. The structure is underlain by a semi-infinite medium. Load is applied as a uniformly distributed, vertical stress acting on a circular area, or combination of circular areas, such that the surface is free from shear stress. A structure, consisting of any number of layers, is defined by the thickness, Young's Modulus and Poisson's Ratio of each layer. The magnitude and extent of the applied

load(s) are required, together with the co-ordinates of the points at which the stresses, strains and deflections are to be calculated. The program calculates the values of the requested parameters and prints them out in tabular form.

This type of analysis is of very limited use in determining the absolute values of soil stresses and deformations for buried pipes. However, it is of considerable use in determining the comparative values of such parameters at a depth below a layered road structure.

#### 7.2.2 Simulation of Load

The application of BISTRO to the case of building drainage was restricted to the simulation of construction traffic loading when applied through a granular layer. The desirability of using a single, reproducible loading arrangement in each test pit installation led to the introduction of a 700mm diameter, semi-flexible, mild steel platen, as detailed in section 4.2.1. The practical situation that this represented was the stress distribution at the surface of the trench backfill caused by the rear wheel arrangement of a heavy truck riding on a typical granular layer in a site road.

Despite the recommendation of a 300mm thick sub-base in Figure 6 of Road Note 29 (RRL, 1978) for a subgrade of the quality of Keuper Marl and the minimum traffic volume, it was felt that a thickness of 200mm would more closely represent practice and would produce a conservative case. Using this value in conjunction with standard analytical techniques (Terzaghi, 1943; Ahlvin and Ulery, 1962), and experience of site traffic, the present platen was designed. The role of BISTRO was, therefore, to justify this design.

Verification could be undertaken in two ways. A certain thickness of



granular layer could be adopted and its properties altered to determine how weak the equivalent layer could be. Alternatively, a typically strong granular material could be used and the thickness varied until an equivalent stress distribution was obtained. Both methods were used, but before this could be done, the load applied to the surface of such a layer had to be simulated.

The wheel of a loaded vehicle presents an elliptical contact surface to a smooth pavement on which it is riding (Kennedy et al, 1978). This has been investigated in the case of a heavy goods vehicle using a standard 40kN load on a dual wheel arrangement and a contact pressure of 550kPa. A good approximation was found to be provided by two circular contact surfaces of 226mm diameter, the centres of which were separated by 376mm (Brown and Brunton, 1984). In highway engineering this is commonly simplified to a single circular loaded area of 320mm diameter, which provides the same total contact area and pressure for equivalent loads. The critical point in the structure under analysis is located centrally below the applied load, so the single loaded area was thought to be conservative for shallow buried pipes.

In order to justify the use of a singular circular load, both single and dual wheel loads were applied to five simulated granular layers of typical Young's Modulus and variable thickness (Table 7.1), and the stress and deflection values at relevant points were compared (see Fig. 7.1). The basic structure used in all BISTRO analyses is shown in Fig. 7.1(a). The granular material overlay a silty clay of the same depth and properties as that in the test-pit facility, the reinforced concrete pit base and the soil below. The points at which comparisons of stress and deflection were made are shown in Fig. 7.1(b), the points bounding the granular layer being of interest in defining the deflected shape of the soil surface and the lower points indicating the equivalent stresses on a pipe installation,

Table 7.1 Summary of Linear Elastic Layer Analysis Data

No. of Run	1	2	3	4	5	6	7	8	9	10	11	12	13	14	15	16	17	18	19	20
Load Type	Ex	D	D	D	D	D	S	S	S	S	S	S	S	S	S	S	S	S	S	S
Layer Thickness (mm)		300	200	150	100	0	300	200	150	100	88	75	50	25	0	200	200	200	200	200
Young's Modulus (MPa)		150	150	150	150	150	150	150	150	150	150	150	150	150	150	50	12	6	3	1
Point A $\sigma_v$ (kPa)	182	70	112	148	190	0	95	179	266	432	492	572	760	886	870	297	459	517	557	591
Point A $\delta_v$ (mm)	8.0	3.6	5.1	6.1	7.5	7.8	4.9	6.0	7.7	10.5	11.5	12.6	15.2	17.6	18.6	8.1	10.6	11.5	12.1	12.6
Point B $\sigma_v$ (kPa)	182	57	75	130	193	872	48	66	75	72	66	55	23	3	0	72	62	56	51	47
Point B $\delta_v$ (mm)	6.0	3.1	4.2	5.1	6.2	9.7	3.1	4.0	4.6	5.0	5.0	5.0	4.8	4.5	4.5	4.5	4.8	4.8	4.8	4.9
Point C $\sigma_v$ (kPa)	84	28	41	51	63	94	30	45	56	72	77	82	93	103	119	56	68	73	77	80
Point C $\delta_v$ (mm)	3.7	1.9	2.4	2.7	3.1	4.0	2.0	2.5	2.9	3.3	3.5	3.6	3.8	4.1	4.5	2.9	3.2	3.3	3.4	3.5
Point D $\sigma_v$ (kPa)	70	27	38	46	57	84	28	40	49	60	63	67	73	79	88	48	57	60	63	65
Point D $\delta_v$ (mm)	3.4	1.8	2.3	2.6	2.9	3.7	1.9	2.4	2.7	3.0	3.1	3.2	3.4	3.6	3.8	2.7	2.9	3.0	3.1	3.2

NOTE:

1. Refer to Fig. 7.1 for location of points at which vertical stress ( $\sigma_v$ ) and deflection ( $\delta_v$ ) were measured
2. Types of load application refer to the experimental platen (Ex), dual wheel loads (D) and single equivalent wheel load (S)

which is shown by a dotted line. Four points of particular interest (A, B, C and D) have been used to summarise the results of the investigations in Table 7.1.

The results show that the single circular load produced a deeper, narrower deflection bowl than that of the dual wheel. The stresses at the level of the crown of the pipe, both centrally under the load and at an offset of 200mm, were greater with the single wheel. As this was the area of most significance to buried pipe installations, the single circular load was considered to produce the conservative case for analysis.

In order to compare data from a wheel load spread through a granular layer with that produced in the experimental work, the load platen of the latter must also be simulated. Were the platen perfectly rigid, a pressure distribution that was greater under the edge than the centre would be expected. If the platen were made progressively more flexible, the pressure below the edge would reduce until a uniform pressure was generated, after which the pressure below the centre would become greater. The theoretical behaviour of the platen used in the test pit experiments, described in section 4.2.1, lies between those of a 700mm diameter and a 450mm diameter rigid platen, assuming the lower plate to be infinitely stiff and flexible respectively. Experience indicated that the platen was sufficiently flexible to remove the effect of increased edge pressures, and, in consequence, a uniform pressure on an area of 700mm diameter was used as the conservative case in comparison with granular structures.

In order to justify the experimental platen, therefore, this load arrangement was applied to the surface of the clay directly in further computations, and the results were compared with those from structures in which various granular layers were used. The first series of structures involved a typically stiff granular layer of thickness varying between 300mm and 0mm. The results of these are shown in Table 7.1 and Fig. 7.2,

the latter showing the influence of layer thickness on vertical stress at points C and D. The thickness which produced a stress at pipe crown level directly below the centre of the platen (point C) equivalent to that produced by the experimental platen was 75mm. At the same level and at an offset of 200mm (point D), the thickness that produced an equivalent stress was 62mm. Both values were considerably lower than the 200mm originally assumed for design and the experimental platen was shown to be conservative.

The second series of structures concerned a 200mm thick granular layer of varying stiffness. The influence of layer stiffness on vertical stress is summarised in Table 7.1, in which deflections are also presented, and Fig. 7.3. An equivalent stress at either point at the pipe crown level was not reached because of a limitation in the program, the stresses caused by all typically stiff structures being considerably less than those using the experimental platen.

### 7.3 Linear Elastic Modelling of Buried Pipe Installations

#### 7.3.1 PAFEC and its Use

PAFEC, the name of which is an acronym for Program for Automatic Finite Element Calculations, was developed at the University of Nottingham primarily for structural applications. It is used to calculate the stresses, strains and displacements in a structure composed of pre-defined elements of prescribed properties. The program has various degrees of sophistication, its application being restricted in this project to a study of the behaviour of linearly elastic, homogeneous materials under applied loads and restraints. Other major assumptions made are that the situation being modelled is symmetrical about the vertical axis and of plane strain,

whereas in practice the latter is not the case. Careful consideration of the loading conditions is required, therefore, in order that accurate approximations to the true case can be made.

The accuracy of any results from a theoretical study using such a program is largely dependent upon the composition of the datafile. A mesh is set up by defining elements of various shapes, and juxtapositions, relative to a set of predetermined nodal points. Both the shape and size of the elements are chosen in sympathy with the expected behaviour of the material at that point, smaller elements being used in areas of most interest. Each element is assigned a set of relevant properties, in this case those that define stiffness, orthogonal behaviour and density. Boundary conditions are applied to the structure in terms of restraints, prescribed displacements and loads. The reaction of the model to these conditions is described both numerically and graphically.

The value of such work lies in the speed with which the effect of property changes can be determined, once the mesh has been set up. The major limitation is that considerable idealisation of the practical situation is necessary and absolute values of system behaviour cannot, therefore, be achieved. Good comparative values may be gained, however, and in this way the influence of changing the properties of certain parts of an installation may be determined. It is only by correlation of theoretical data with those from experiments that the model could be used for predictive purposes, a subject that lies beyond the bounds of this project.

### 7.3.2 Boundary Conditions

There were three aims of the theoretical modelling using PAFEC. The first was to verify that the loading conditions used in the experimental

work were conservative. The second was to determine the influence of the properties of various parts of the installation on the performance of the pipe. Lastly, a correlation of theoretical with experimental data was attempted in order to estimate the value of future work on developing a predictive method of installation design using finite element techniques.

The situation being modelled was that occurring in the test pit used for the experimental work. Symmetry about the vertical axis of the pipe led to the formation of a mesh representing half of the cross-section of the inside of the pit (Fig. 7.4). It was assumed that the reinforced concrete walls and base of the pit were rigid and that nodes lying on the line of these faces were restrained in the perpendicular direction. Further, it was assumed that shear forces along the faces would be small and would be overcome by frictional effects. The nodes were therefore fully restrained along these lines. Nodes lying on the line of symmetry were restrained in the horizontal direction and against rotation, but were free to move vertically.

Simulation of load was achieved in two ways, representing load applied through both the experimental platen and a granular layer. The experimental platen was manufactured from mild steel, and had properties that could be accurately modelled. Difficulty arose in transferring the effects of a circular platen to plane strain conditions. In particular an element thickness, or longitudinal dimension, had to be ascribed to the model, attenuation of stresses with depth only being possible in one direction. It was decided that a 700mm wide, 10mm thick plate would be used below a 450mm wide reinforced strip, and that this would act on a 500mm thick section of the installation. The areas of the platens were the same and any decrease in pipe crown load, caused by a greater area of the platen acting directly onto the natural soil in the model, was offset by the inability of the load to spread longitudinally.

In cases where a granular layer was used, the load being modelled was that of a lorry wheel arrangement acting on a circular area of 320mm diameter. This provided greater difficulty in the determination of an appropriate longitudinal dimension for the elements. It was decided that the element thickness should remain the same in order that the behaviour of the pipe and soil surround would be compatible. The load was applied to the surface of the granular layer through a very stiff, light strip of width 320mm, in order to ensure an even pressure distribution. This meant that the load in the model was applied over a larger area, 320mm x 500mm, than the approximation for the wheel arrangement of 320mm diameter. In cases where a granular layer of about 200mm thickness or less was used, therefore, the stress at the surface of the backfill was less than that of the practical case. At the level of the pipe crown, however, the attenuation of this stress would be greater in practice and the model was consequently conservative.

The magnitude of the applied load was taken as 70kN, the higher load used in the experiments, with half of this value being applied to the mesh. The assumption of linear elasticity allows conversion of the resulting data to those for any other magnitude of load by multiplication by the ratio of the new to existing values.

In all cases, the load due to self weight of the materials was also applied to the system, the value of this load being determined from the density of the materials forming the elements. In practice, the influence of this factor on pipe performance was found to be negligible and only approximate values were required for the model.

The mesh was divided into distinct areas of potential influence for the assignation of material properties (Fig. 7.5). The materials forming the loading platens were kept constant, as was that for the uPVC forming the pipe wall. The backfill was divided into two parts to account for the

compaction applied to the surface layer. The area directly below the pipe was split to allow for the addition of a bedding layer of 50mm or 100mm, the properties of which could be the same as the sidefill. The insitu soil was also split into two parts in order to reflect the pertinent directional property of the clay in the test pit, which received thorough compaction in the vertical direction and was consequently found to have greater vertical stiffness. A series of distinctly different stiffness values, in terms of Young's Modulus, was chosen to cover all likely practical cases, while reducing the number of alternatives to a minimum.

The performance of the various theoretical structures was measured in terms of deflections, both of the pipe wall and the surface of the backfill, as these were measured in the experimental work and were the criteria used to determine performance in practice.

### 7.3.3 Simulation of Load

Realistic methods of load application, whether simulating the experimental or site condition, are discussed in section 7.3.2 and require no elaboration. The values of the soil properties for both insitu and fill materials were chosen to produce deflections, both at the surface and of the pipe, that were similar to those measured in the experimental work. These values were of secondary importance in this investigation as they remained constant throughout. The properties that were varied, and which formed the basis of the study, were the thickness, stiffness and Poisson's Ratio of the simulated site road. In this way, the thickness of a typically stiff, and the stiffness of a typically thick, granular layer that produced equivalent deflections to those with the experimental platen were determined.

In the first instance, a granular layer with a Young's Modulus of 150



MPa was used and the thickness was varied between 0 and 300mm. The effect on vertical deformation of the pipe, defined as the difference between the deflections of the pipe crown and invert, is shown in Fig. 7.6. On this graph is also marked the deformation of the equivalent installation using the experimental platen. The thickness of the granular layer that produced the same vertical deformation of the pipe was 70mm, a value that was well below the 200mm thick layer assumed and a likely practical minimum for a site road on a wet clay. The influence of layer thickness on settlement of the backfill surface, both directly below the centre of the load and at an offset of 300mm, is shown in Fig. 7.7. The thickness that produced an equivalent surface settlement was 90mm in the case of the central position, there being no equivalent at an offset of 300mm. This reflected the shape of the surface deflection bowl, which was deeper, though less extensive, than that of the experimental platen.

A second investigation was carried out in which a 200mm thick granular layer of varying stiffness was used. The effect of this variation on the deformation of the pipe is summarised in Fig. 7.8, from which it was shown that a granular material with a Young's Modulus of 13 MPa produced an equivalent performance. The influence of layer stiffness on backfill settlement is shown in Fig. 7.9, which indicated similar behaviour to the case of the layer thickness variation and an equivalent granular layer stiffness of 29 MPa for the central position. Both stiffnesses were far lower than those of imported materials for use as site roads or sub-base and the conservative case has again been proved.

The influence of the value of Poisson's Ratio of the granular layer on pipe deformation and settlement is shown in Figs. 7.10 and 7.11 respectively, from which it proved to be negligible.

#### 7.3.4 Parameter Studies

The influence of soil properties on pipe performance, measured in terms of pipe deformation, was determined in a series of parameter studies using the PAFEC mesh described above. The basic structure considered was that in which a 50mm bedding layer, with the same properties as the sidefill, was used and the load was applied through the experimental platen. The areas under consideration, which are defined in Fig. 7.5, were the backfill, sidefill, and insitu soil, the latter being split into two parts. Stiffnesses at the upper end of the likely range were found to produce realistic behaviour in earlier work and were used as standard for each part of the installation, in order that each set of elements could be made progressively weaker. These standard values of Young's Modulus and Poisson's Ratio are defined in Fig. 7.12. By keeping all boundary conditions and other element stiffnesses constant, while reducing the stiffness of one part of the installation, the influence of the soil in this area was gauged. In addition, an investigation of the influence of sidefill stiffness on pipe performance, when no bedding layer was present, was carried out by adjustment of the basic structure. A further study, involving the variation of the self weight of the overlying material, was also conducted, but this variable proved to have a negligible influence on pipe behaviour when compared with that of surface load.

The influence of sidefill stiffness on both pipe deformation and pipe settlement is summarised in Figs. 7.13 and 7.14. There was a small but significant increase in vertical deformation of the pipe as the Young's Modulus reduced from 100MPa to 20MPa. Below this, however, the deformation rose sharply. The same pattern was shown by both horizontal deformation and settlement of the pipe, the settlement trend reflecting the compressibility of the bedding layer. When plotted on a logarithmic scale (Fig. 7.14), it was clear that the shape of the deformed pipe also varied

with sidefill stiffness, the curves converging at lower stiffnesses; the ratio of horizontal to vertical deformation increased from 0.54 to 0.98 as Young's Modulus decreased from 100 MPa to 1 MPa. The deflection data in the computer output showed that, with the stiffer sidefill, more than 70% of the movement occurred in the top half of the pipe, whereas the value reduced to approximately 50% as the stiffness reduced. This implied that the pipe took up a "heart-shaped" profile in stiffer sidefills, with the crown tending to flatten, the shoulders being forced outwards and the lower half of the pipe being relatively unaffected. The shape reverted to an ellipse as the sidefill became less stiff.

The influence of natural soil stiffness was determined in two ways (Fig. 7.15). In the first instance the stiffness of the insitu soil to the side of the trench was lowered. The effects of this were both to reduce the ratio of backfill to trench wall stiffness, causing a greater load to be transmitted to the pipe, and to reduce the lateral support of the trench wall to the fill beside the pipe. The graph shows the increased deformation at lower stiffnesses, and pipe settlement increasing to a lesser degree. The second case involved variation of stiffness for the whole of the insitu soil. The difference between these two cases demonstrated the ability of the pipe to settle under load, thereby shedding part of the load to the columns of soil beside the pipe, when low insitu soil stiffnesses were used. This is shown in the graph with values of horizontal and vertical deformation being lower below about 12MPa, and settlement being far greater.

The effect of reducing backfill stiffness (Fig. 7.16) was to significantly reduce both pipe deformation and settlement, indicating that a greater proportion of load was being carried by the natural soil, both directly and because of trench wall friction effects.

The influence of sidefill stiffness on pipe deformation, where no

bedding layer was used (Fig. 7.17), was to flatten the curve at stiffnesses greater than 12MPa and steepen the curve at very low stiffnesses, both in relation to Fig. 7.13. The magnitude of the deformation was higher than when a bedding layer was used at high and very low stiffnesses. The pipe settlement curve showed a slight fall at low stiffnesses, where the backfill has poor support, caused by load shedding to the trench wall. This effect was overshadowed by that of the ready compression of the bedding layer when used (Fig. 7.13). When these data were plotted on a logarithmic scale (Fig. 7.18), it was found that the deformation curves crossed at a sidefill stiffness of 3 MPa, indicating an exaggerated elliptical deformation. The plot of the deformed shape (Fig. 7.19), which was to a greatly exaggerated scale, demonstrated this behaviour.

The value of this study lay in the determination of trends in installation behaviour rather than in absolute performance data. In some cases, the work has corroborated evidence from the experimental investigations, such as in the shape of pipe deformation, and theories of past research studies, such as the beneficial action of weakening the backfill. There is considerable scope for further work in this respect.

#### 7.3.5 Correlation with Experimental Data

In the comparison of theoretical data with data from the experimental work, only those relating to the initial application of load were used to avoid the influences of loading history. The assumption of linear elasticity made in the theoretical work, though an obvious approximation, did allow data from the 70kN load case to be used for evaluating the 55kN load case, used in experiments, by proportioning. Two cases were considered in the correlation: those installations with stiff sidefills, having a Young's Modulus of 20 MPa to 50 MPa, and those with poor sidefills

with a value of 3 MPa. Average values of surface settlement and vertical pipe deformation were taken from the experimental work, both for good and poor sidefills, and these were used as the basis for the comparison. Theoretical installations that produced matching vertical deformations were isolated and ranked according to surface settlement, those producing typical values being most appropriate. The ultimate test was the ability of an installation varying only in sidefill stiffness to match the average experimental values.

The results of these investigations are given in Table 7.2. The considerable quantity of data collected in the earlier computations had shown that certain combinations of backfill and insitu soil stiffness produced reasonable results. It was decided that the upper and lower bounds of backfill stiffness would be used and appropriate insitu soil stiffnesses would be found. The Young's Moduli used for the majority of the backfill (area 1 in Fig. 7.5) were 1 MPa and 3 MPa, with concomitant Moduli for the surface of the backfill of 3 MPa and 6 MPa respectively.

For the upper level of backfill stiffness, a match was found using an insitu soil stiffness of 10 MPa. In this case, deformations in pipes surrounded by stiffer sidefills straddled the average experimental value and those in pipes surrounded by poor sidefills were slightly greater than the average. At the lower level of backfill stiffness, a match was made using an insitu soil stiffness of 6 MPa with the pattern of deformation values being the same as that above. Surface settlement data indicated that the installations with the lower stiffnesses more closely represented the experimental case. In conclusion, the value of Young's Modulus for the insitu soil was in the range 6-10 MPa, a value consistent with the level of backfill stiffness chosen and with the values of  $E_{50}$  found from the triaxial testing of Keuper Marl reported in section 6.3.3.

The correlation of theoretical with experimental data has produced



encouraging results, being consistent both with buried pipe performance and the laboratory test data for the insitu soil materials. In its present form, the finite element program could be expected to provide valuable data on the influence of boundary conditions on pipe performance when subjected to a static surface load. Sophistication of the soil model to include plastic behaviour would probably be necessary before such a program could be used as a predictive tool. The data presented above suggest that this problem could be tackled with confidence.

## **CHAPTER EIGHT**





## 8 CONCLUSIONS AND THE WAY FORWARD

### 8.1 The Behaviour of Buried uPVC Pipes

A thorough review of the literature was conducted and the need for an experimental investigation of buried uPVC pipe behaviour under simulated building drainage conditions was established. A major pipe test facility has been developed together with appropriate instrumentation and, with additional tests in a smaller reinforced box, the behaviour of 160mm diameter uPVC pipes was investigated in full-scale experiments. Comcomitant soil characterisation and preliminary theoretical work were undertaken.

The results of these experiments showed that reduction of the thickness of pea gravel bedding for the standard installation from 100mm to 50mm produced a slight improvement in pipe performance. Removal of the bedding layer altogether produced a significantly worse result, though performance remained good in absolute terms. Removal of a 50mm thick bedding layer from an uncompacted concreting ballast installation caused no change in performance under load, but greater deformation during installation.

Sidefill compaction had a significant influence on pipe performance, the degree of significance being determined by the properties of the soil. Thorough compaction of a silty clay sidefill with no bedding produced a reasonably good pipe performance, whereas excessive deformation occurred during the initial application of load where light compaction was used. Thorough compaction of the clay sidefill in two layers produced a comparable result to that of an uncompacted, good quality granular material. Light compaction of a concreting ballast sidefill resulted in a

smaller pipe deformation than that without compaction.

Various uncompacted granular materials provided good support to the pipe when used for sidefill and for the 50mm thick bedding layer. These included pea gravel, concreting ballast, washed quarry tailings and building sand. A silty sand was shown to be a marginal sidefill material, producing deformations that exceeded, albeit slightly, the present arbitrary limit if laid without compaction.

A good understanding of the behaviour of buried uPVC pipes was obtained from measurements of pipe wall strain, which indicated variations in the deformed shape of the pipe. In particular, stiff sidefill materials induced most deformation above the pipe springings, whereas the introduction of a 50mm thick pea gravel arching layer tended to induce most deformation in the lower half of the pipe. Vertical compression of the sidefill was shown to influence the behaviour of the pipe, with less compressible types producing a better pipe performance. Compaction of the sidefill beside the pipe produced a negative deformation at the end of installation and this was beneficial in limiting the ultimate positive deformation caused by applied load.

A preliminary theoretical analysis of pipe response to initial loading using linear elastic theory has been developed, and successfully correlated with experimental data.

## 8.2 Soil Characterisation

Extensive soil characterisation tests have proved the ability of inexpensive penetrometers, once calibrated, to accurately measure the shear strength of silty clay. The shear strength of Keuper Marl was shown to be approximately indicative of its Young's Modulus, but the water content and

state of compaction of the clay had a considerable influence on its structural properties. The variation in strength, and therefore stiffness, of such a clay would lead to difficulties in proving the suitability of cohesive soils for use as sidefill without extensive further work. Triaxial test results indicated that sidefill material stiffness, in this case Young's Modulus derived as a secant value, governed the behaviour of a buried flexible pipe. The Compaction Fraction test and the use of a factor derived from the grading curves both proved effective means of assessing the suitability of granular materials for pipe installation. The performance limits of the Compaction Fraction test were, however, shown to be set too low. The method based upon the grading curves of potential fill materials may prove to be the more appropriate in defining the suitability of materials that are close to the limit.

### 8.3 Recommendations for Future Work

The recently completed three year project had a well-defined practical application from which the research philosophy was derived. This involved the simulation of typical building drainage site conditions, application of the most severe likely loadings and measurement of pipe performance in full-scale tests. Several combinations of bedding and sidefill, covering a wide range of material types and compaction, were investigated and their performance compared. While providing good, practically useful data in itself, the project has also acted, in effect, as an elaborate feasibility study, in which the problems in development of a design method were clearly defined. The research reported in this thesis indicates that a suitable aim for further work would be to develop a simple design method for buried, non-pressure uPVC pipes, together with on-site material assessment.

Inherent in this would be an examination of the roles of full-scale experiments, soil characterisation tests and theoretical work to ensure that each is complementary.

Initial priorities for such research, necessitating an extension of the current work, would be to define clearly the practical limits on the use of uncompacted fill materials and to investigate the effects of boundary conditions such as trench width and cover depth. In parallel with this would be the further development of the proposed on-site methods of fill assessment, including an investigation of the influence of such factors as particle angularity and surface texture, and the development of the theoretical model of pipe behaviour based on more realistic soil models than those used so far. Thereafter, a unified approach to each section of the research would be necessary in order to produce, develop and prove a design method. Some special full-scale tests would be performed in which boundary conditions that are consistent with those applied in the theoretical model (e.g. plane strain) would be adopted. Soil characterisation would take a different role in which a detailed study of materials in the laboratory would be conducted in order to provide the necessary soil properties for use in the theoretical model. Accurate testing of materials, probably in the triaxial cell, would be necessary. Material samples would require careful preparation such that they closely modelled conditions in the sidefill and loading would be designed to match the stress paths of the materials in situ. Development of the theoretical model would continue in parallel and be gradually updated as data from pipe and soil tests became available. Some field measurements of buried pipes with known installation and loading histories would be highly desirable to reinforce with practical results the laboratory-based ones.

Once developed, the model could be used to produce a set of simplified design charts or tables for use in the design of a specific pipeline. Of

more interest would be a set of standard guidelines for the installation of pipes and the specification of suitable pipe surround materials in cases where they need to be imported. This would be backed up by a method of on-site soil assessment of insitu materials for use as fill, thereby achieving the most efficient method of installation for any particular site.

Once sufficient accurate soil characterisation data were obtained, the pipe performance results could be used to assess the various design methods detailed in Chapter 2 for various soil states. The extensive experimental results obtained during this project have been collated and stored to provide for such a re-analysis. Some field measurements of uPVC pipes that have been in service for several years, together with those on building drainage sites under construction mentioned above, would be valuable in assessing the severity of the boundary conditions imposed in the experimental work.

The factors that affect pipe deformation, which have been isolated and discussed in Chapter 3 of this thesis, all merit investigation. Of particular use would be the extension of the results from small to larger diameter uPVC pipes, which could be achieved by theoretical means backed up by a limited experimental programme. The applicability of the results to flexible pipes made from other materials could be investigated, with relative ease using the facilities developed at Nottingham, and the reasons for any difference in behaviour ascertained. Such work would facilitate useful re-analysis of the data from the somewhat insular experiments that have been discussed in the literature.

Although the possibilities for future investigations are numerous the author considers that a sensible approach would be to select a programme that utilises the major pipe testing facility, the development of which accounted for a considerable proportion of this three year project. The

analogy of the research reported herein as an elaborate feasibility study for a larger project reflects the diversity of opportunities, both practical and academic, that exist. The direct practical application of the results of extended work in this field is likely to lead to economic benefits and, consequently, better engineering design.

## REFERENCES



## REFERENCES

- Ahlvin, R.G. and Ulery, H.H., (1962), 'Tabulated values for determining the complete pattern of strains, stresses and deflections beneath a uniform circular load on a homogeneous half space', HRB Bulletin 342, Washington D.C.
- Allgood, J.R. and Ciani, J.B., (1968), 'The influence of soil modulus on the behaviour of cylinders in sand', HRR No. 249, Washington D.C.
- ATV, (1978), 'Guidelines for the structural calculation of drain pipes and conduits', Abwassertechnische Vereinigung, Arbeitsblatt A127, June.
- Barnard, R.E., (1957), 'Design and deflection control of buried steel pipe supporting earth loads and live loads', Proc. ASTM, Vol.57 : 1223.
- Bhandhauvee, C., (1968), 'Modulus of Soil Reaction as determined from Hveem Stabilometer test (R-value)', New Mexico State University, Las Cruces.
- Bishop, A.W., and Henkel, D.J., (1962), 'The measurement of soil properties in the triaxial test', Edward Arnold, London.
- Black, W.P.M., (1979), 'The strength of clay subgrades: its measurement by a penetrometer', TRRL Laboratory Report 901, Crowthorne, Berks.
- Boden, J.B., (1976), 'The realities of site practice', Ground Engineering, Vol.9, No.1.
- Boden, J.B., Farrar, D.M., and Young, O.C., (1977), 'Standards of site practice: implications for innovation in the design and construction of buried pipelines', TRRL Supplementary Report 345, Crowthorne, Berks.
- Bossen, M.J., (1967), 'Het gedrag van flexibele buizen onder van de belasting door grondruk', Report to KIWA, Rijswijk.
- Boussinesq, J., (1885), 'Application des potentiels a l'etude de l'equilibre et du mouvement des solides elastiques', Paris, Gauthier - Villard.
- Brennan, G., and Young, O.C., (1976), 'Some case histories of recent failures of buried pipelines', Underground Services, Vol.4, Part 1.
- British Standards Institute, (1973), 'Plastics pipework (thermoplastics materials)', BS CP312.
- British Standards Institute, (1973), 'Specification for unplasticized PVC underground drain pipe and fittings', BS 4660:1973.
- British Standards Institute, (1975), 'Method of tests for soils for civil engineering purposes', BS 1377:1975.
- British Standards Institute, (1980), 'Installation of uPVC pipework for gravity drains and sewers', BS 5955 Part 6:1980.

- Broere, J.J., (1984), 'The behaviour of PVC water pipe under practical conditions', *H<sub>2</sub>O*, Vol. 17, No. 9, September.
- Brown, S.F., and Brodrick, B.V., (1981), 'Instrumentation for monitoring the response of pavements to wheel loading', *Symp. on Sensors in Highway and Civil Engineering*, I.C.E., London, 5 February.
- Brown, S.F., and Brunton, J.M., (1984), 'An introduction to the design of bituminous pavements (2nd Edition)', Dept. of Civil Engineering, University of Nottingham.
- Bulson, P.S., (1966), 'The stability of buried tubes under static and dynamic overpressure. Part one: circular tubes in compacted sand', *Military Vehicles and Engineering Establishment Rep. 47.5/7*, Christchurch, Hants.
- Bulson, P.S., (1969), 'The stability of buried tubes under static and dynamic overpressure. Part two: circular tubes in clay', *Military Vehicles and Engineering Establishment Rep. 47.5/14*, Christchurch, Hants.
- Bulson, P.S., (1972), 'Thin-walled tubular structures under soil cover and surface pressure', *Military Vehicles and Engineering Establishment Rep. 7515/18*, Christchurch, Hants.
- Bulson, P.S., (1985), 'Buried structures, static and dynamic strength', Chapman and Hall, London and New York.
- Burmister, D.M., (1945), 'The general theory of stresses and displacements in layered systems', *J. Appl. Phys.*, Vol. 16, No. 2, pp.89-96.
- Burns, J.Q., and Richard, R.M., (1964), 'Attenuation of stresses for buried cylinders', *Proc. of Int. Conf. on Underground Plastic Pipe*, New Orleans, L.A., 30 March-1 April.
- Butterfield, R., and Duns, C.S., (1966), 'An analysis of the buckling of buried cylindrical tubes under surface pressure', *Report CE/7/66*, Univ. of Southampton.
- Chambers, R.E., and Heger, F.J., (1975), 'Buried plastic pipe for drainage of transportation facilities', *Simpson, Gumpertz and Heger Inc.*, Cambridge, Massachusetts, U.S.A..
- Cheney, J.A., (1963), 'Bending and buckling of thin-walled open section rings', *Journal of Eng. Mech. Div., Proc. ASCE*, Vol. 89, EM9, October.
- Cheney, J.A., (1976), 'Buckling of thin-walled cylindrical shells in soil', *TRRL Supplementary Report 204*, Crowthorne, Berks.
- \*
- Clarke, N.W.B., (1962), 'Simplified tables of loads on underground pipelines', *National Building Studies, Special Report No.32*, HMSO.
- Clarke, N.W.B., (1964), 'Pipe laying principles', *National Building Studies, Special Report No.35*, HMSO.
- Clarke, N.W.B., (1966), 'Loading charts for the design of buried rigid pipelines', *National Building Studies, Special Report No.37*, HMSO.
- \* Christensen, N.H. (1967), "Rigid pipes in symmetrical and unsymmetrical trenches", *Danish Geotechnical Institute, Bull. No. 24*.

- Clarke, N.W.B., (1968), 'Buried pipelines', Maclaren and Sons, London.
- Compston, D.G., Cray, P., Schofield, A.N., and Shann, C.D., (1978), 'Design and construction of buried thin-walled pipes', CIRIA Report 78, London.
- de Putter, W.J., and Elzink, W.J., (1981), 'Deflection studies and design aspects on PVC sewer pipes', Proc. of Int. Conf. on Underground Plastic Pipe, New Orleans, L.A., 31 March-1 April.
- Dezsenyi, I., (1975), 'Plastic sewers - calculating deformation', Building Research and Practice, Leyden Pub. Co. Ltd., 5-7 Carnaby St., London, 10 September, pp.278-88.
- Donohue, J., and Associates, (1979), 'PVC sewer pipe deflection', prepared for the Plastics Pipe Institute, a division of the Society of the Plastics Industry Incp, 355 Lexington Avenue, New York.
- Fadum, R.E., (1941), 'Influence values for vertical stresses in a semi-infinite solid due to surface loads', School of Engineering, Harvard University.
- Gaube, E., (1977), 'Calculation of drainage pipes of HDPE and uPVC', Kunststoffe, Vol. 67, No. 6.
- Gaunt, J., Trott, J.J., and Stevens, J.B., (1976), 'Static and dynamic load tests on shallow-buried flexible pipes', Ground Engineering, Vol.9, No.3, April.
- Gehrels, J.F., (1972), 'Experience with plastic sewers and drainage pipes: case study 5', Proc. of 2nd Int. Plastics Pipes Symp., The University of Southampton, 12-14 September.
- Gehrels, J.F., and Elzink, W.J., (1979), 'Experience of long-term behaviour of uPVC gravity sewers', Proc. of 4th Int. Plastics Pipes Conf., The University of Sussex, Brighton, September.
- Gehrels, J.F., (1982), Matters arising from conversation.
- Gehrels, J.F., and Elzink, W.J., (1982), 'More than 15 years of distortion measurement results with uPVC pipes', Proc. of Europipe '82 Conference, Basle, 18-20 January.
- Gumbel, J.E., and Wilson, J., (1981), 'Interactive design of buried flexible pipes - a fresh approach from basic principles', Ground Engineering, Vol.14, May.
- Gumbel, J.E., O'Reilly, M.P., Lake, L.M., and Trott, J.J., (1982), 'Loading tests on buried plastics pipes to validate a new design method', Proc. of 5th Int. Plastics Pipes Conf., The University of York, September.
- Gumbel, J.E., (1984), 'The design of buried flexible pipes', Ph.D. Thesis, The University of Surrey.
- Howard, A.K., (1972 A), 'Laboratory load tests on buried flexible pipe', Journal of American Water Works Assoc., Vol. 64, October.

- Howard, A.K., (1972 B), 'Laboratory load tests on buried flexible pipe. Progress report No. 4 RPM pipe', USBR Report No. REC-ERC-72-38, United States Bureau of Reclamation, Colorado, USA.
- Howard, A.K., (1973), 'Laboratory load tests on buried flexible pipe. Progress report No. 5: GRP, PE and PVC', USBR Report No. REC-ERC-73-16, United States Bureau of Reclamation, Colorado, USA.
- Howard, A.K., (1977), 'Modulus of Soil Reaction (E') values for buried flexible pipes', Journal Geotech. Division, Proc. ASCE, Vol.103, January.
- Howard, A.K., (1981 A), 'Diametral elongation of buried flexible pipe', Proc. of Int. Conf. on Underground plastic pipe, New Orleans, L.A., 30 March-1 April.
- Howard, A.K., (1981 B), 'The USBR Equation for predicting flexible pipe deflection', Proc. of Int. Conf. on Underground Plastic Pipe, New Orleans, L.A., 30 March-1 April.
- Howe, H., Nothen, P.H., and Unger, P., (1966), 'Buried uPVC pipe', Rohre, Rohreitungsbau, Rohreitungstransport, No. 4, August.
- Jaaskelainen, H., (1973), 'Modulus of Passive Resistance for the protective material of flexible pipes', Building Technical and Community Development Publication 6, Technical Research Centre of Finland, Otaneimi.
- Janson, L-E., and Molin, J., (1972), 'Case study 4: practical experience with buried sewer pipes', Proc. of 2nd Int. Plastics Pipes Symp., The University of Southampton, 12-14 September.
- Janson, L-E., (1981), 'Plastic gravity sewer pipes subjected to constant strain by distortion', Proc. of Int. Conf. on Underground Plastic Pipe, New Orleans, L.A., 30 March-1 April.
- Janson, L-E., and Molin, J., (1981), 'Design and installation of underground plastic sewer pipes', Proc. of Int. Conf. on Underground Plastic Pipe, New Orleans, L.A., 30 March-1 April.
- Joekes, D., and Elzink, W.J., (1985), 'Deflection of uPVC sewer pipes, and a new method for measuring and specifying stiffness for plastics pipes', Proc. of 6th Int. Plastics Pipes Conf., The University of York, March.
- Katona, M.G., et al (1976), 'CANDE - a modern approach for the structural analysis and design of flexible culverts', US Naval Civil Engineering Lab., Port Heuneme, California, USA.
- Kennedy, C.K., Fevre, P., and Clarke, C.S., (1978), 'Pavement deflection: equipment for measurement in the United Kingdom', TRRL Laboratory Report 834, Crowthorne, Berks.
- KOMO (1970), 'Experiences with sewage pipes of uPVC having outside diameters of 250mm and more', KOMO Foundation, The Netherlands.

- Lancashire, S., (1985), 'In-service durability of uPVC water main', Proc. of 6th Int. Plastics Pipes Conf., The University of York, March.
- Leonhardt, G., (1972), 'The influence of the Modulus of Soil Reaction on the load-bearing capacity and deformation of flexible pipes', Strasse Brucke Tunnel, Vol. 24, No. 3.
- Leonhardt, G., (1982), 'Soil loads on pipes with different degrees of stiffness', Proc. of Europipe '82 Conference, Basle, Switzerland, 18-20 January.
- Luscher, U., and Hoeg, K., (1964), 'The beneficial action of the surrounding soil on the load carrying capacity of buried tubes', Symp. on Soil Structure Interaction, University of Arizona.
- Luscher, U., and Hoeg, K., (1965), 'The action of soil around buried tubes', Proc. of 6th Int. Conf. on Soil Mechanics and Foundation Engineering, Montreal.
- Marston, A., and Anderson, O., (1913), 'The theory of loads on pipes in ditches and tests on cement and clay drain tile and sewer pipes', Bulletin 31, Engineering Experimental Station, Iowa State College, U.S.A..
- Marston, A., (1930), 'The theory of external loads on closed conduits', Bulletin 96, Engineering Experiment Station, Iowa State College, U.S.A.
- Meyerhof, G.G., and Baikie, L.D., (1963), 'Strength of steel culvert sheets bearing against compacted sand backfill', HRR No. 30, Washington D.C.
- Meyerhof, G.G., and Fisher, C.L., (1963), 'Composite design of underground steel structures', Engineering Journal, Eng. Inst. of Canada, Vol. 46, No. 9.
- Ministry of Housing and Local Government Working Party (1967), on the design and construction of underground sewers, Second Report, HMSO.
- Molin, J., (1967), 'Buried flexible pipes - a study of radial deformations, stresses and load bearing capacity', Chalmers Institute of Technology (Dept. of Soil Mechanics and Foundation Engineering), Gothenburg, Sweden.
- Molin, J., (1971), 'Design principles for buried pipes', English summary, VAV P16, Stockholm.
- Molin, J., (1981), 'Flexible pipes buried in clay', Proc. of Int. Conf. on Underground Plastic Pipe, New Orleans, L.A., 30 March-1 April.
- Moser, A.P., Watkins, R.K., and Bishop, R.R., (1973), 'The structural response of buried PVC pipe', Modern Plastics, November.
- Moser, A.P., (1981), 'Strain as a design base for PVC pipes?', Proc. of Int. Conf. on Underground Plastic Pipe, New Orleans, L.A., 30 March-1 April.

- Newmark, N.M., (1942), 'Influence charts for computation of stresses in elastic foundations', Bulletin of Illinois Eng. Exp. Sta. No. 338.
- Nielson, F.D., Bhandhauvee, C., and Yeb, K., (1969), 'Determination of the Modulus of Soil Reaction from standard soil tests', HRR No. 284, Washington D.C.
- O'Reilly, M.P., Crabb, G.I., and Trott, J.J., (1982), 'Loading tests on buried plastic pipes to validate a new design method', Proc. of 5th Int. Plastics Pipes Conf., The University of York, 10-12 September.
- Owston, C.N., and Young, O.C., (1976), 'The use of plastics for non-pressure pipes underground', TRRL Supplementary Report 240, Crowthorne, Berks,.
- Page, J., (1966), 'Impact tests on pipes buried under roads', Ministry of Transport, RRL Laboratory Report 35, Crowthorne, Berks.
- Parmalee, R.A., and Corotis, R.B., (1974), 'Analytical and experimental evaluation of Modulus of Soil Reaction', Transportation Research Record 518, TRB, Washington D.C.
- Peutz, M.G.F., van Kempen, H.P.M., and Jones, A., (1968), 'Layered systems under normal surface loads', Highway Research Record, Washington.
- Picken, N.W., and Vaughan, G.N., (1973), 'Bending moments and deflections in a pipe under various load distributions', British Ceramic Research Association.
- Poulos, H.G., and Davies, E.H., (1974), 'Elastic solutions for soil and rock mechanics', John Wiley, New York.
- Road Research Laboratory, (1970), 'A guide to the structural design of pavements for new roads', Road Note 29, Third Edition.
- Rogers, C.D.F., Brown, S.F., and Boyle, G., (1985), 'The influence of bedding and sidefill on the response of uPVC pipes to surface loading', Proc. of 6th Int. Plastics Pipes Conf., The University of York, March.
- Roscoe, K.H., (1968), 'Soils and model tests', Journal of Strain Analysis, Vol. 3, No. 1.
- Sanglerat, G., (1972), 'The penetrometer and soil exploration', Elsevier Publishing Co., Amsterdam, London and New York.
- Soini, R., (1982 A), 'Interaction between flexible thermoplastic pipes and soft soils', Proc. of Europipe '82 Conf., Basle, 18-20 January.
- Soini, R., (1982 B), 'Flexible thermoplastic pipes buried in soft soil', Proc. of 5th Int. Plastics Pipes Conf., The University of York, 10-12 September.
- Spangler, M.G., (1941), 'The structural design of flexible pipe culverts', Bulletin 153, Engineering Experiment Station, Iowa State College, U.S.A.

- Spangler, M.G., (1948), 'Underground conduits - an appraisal of modern research', Trans. of ASCE.
- Spangler, M.G., (1960), 'Soil Engineering', International Textbook Co., Scranton, Penn.
- \*
- Terzaghi, K., (1943), 'Theoretical soil mechanics', Wiley, New York.
- Trott, J.J., and Gaunt, J., (1972), 'Experimental work on a large steel pipeline at Kirtlington', TRRL Laboratory Report 472, Crowthorne, Berks.
- Trott, J.J., and Gaunt, J., (1974), 'A study of an experimental uPVC pipeline laid beneath a major road during and after construction', Proc. of 3rd Int. Plastics Pipes Symp., The University of Southampton, 10-12 September.
- Trott, J.J., and Gaunt, J., (1975), 'Results of some recent experiments on underground pipes', Symp. on Research and Development in Sewerage and Drainage Design, Inst. of Public Health Engineers, London, 14 May.
- Trott, J.J., and Gaunt, J., (1976), 'Experimental pipelines under a major road - performance during and after construction', TRRL Laboratory Report 692, Crowthorne, Berks.
- Trott, J.J., Picken, N.W., and Clifford, J., (1977), 'The role of full-scale test pits in buried pipeline research', W.R.C. Conference on Opportunities for Innovation in Sewerage, University of Reading, 21-15 March.
- Trott, J.J., and Stevens, J.B., (1979), 'Loading tests on uPVC pipes installed in cohesive and non-cohesive bedding materials', Proc. of 4th Int. Plastics Pipes Conf., The University of Sussex, Brighton, March.
- Trott, J.J., Taylor, R.N., and Symons, I.F., (1984), 'Tests to validate centrifuge modelling of flexible pipes', Ground Engineering, Vol. 17, September.
- Valsangkar, A.J., and Britto, A.M., (1977), 'The validity of the Ring Compression Theory in the design of buried flexible pipelines', TRRL Supplementary Report 440, Crowthorne, Berks.
- Valsangkar, A.J., and Britto, A.M., (1979), 'Centrifuge tests of flexible circular pipes subjected to surface loading', TRRL Supplementary Report 530, Crowthorne, Berks.
- Watkins, R.K., and Spangler, M.G., (1958), 'Some characteristics of the Modulus of Passive Resistance of Soil - a study in similitude', Proc. HRB, Vol.37, Washington D.C.
- Watkins, R.K., and Nielson, F.D., (1964), 'Development and use of the Modpares Device', Journal of the Pipeline Div., proc. ASCE, January.
- Watkins, R.K., (1970), 'Deposition in the action of Sanford Construction Company versus Kaiser Aluminium and Chemical Sales', Inc. U.S. District Court, Eastern District of Kentucky, 21 February.
- \* Spangler, M.G., (1971), "Response of corrugated steel pipe to external soil pressure - discussion", HRR No. 373, Washington D.C., U.S.A.

- Watkins, R.K., and Moser, A.P., (1971), 'Response of corrugated steel pipe to external soil pressure', HRR No.373, Washington D.C., U.S.A. Includes discussion by Spangler, M.G., and Parmelee, R.A.
- Watkins, R.K., and Smith, A.B., (1973), 'Deflection of buried pipes', Journal of American Water Works Association, Vol. 65, September.
- \* White, H.L., and Layer, J.P., (1960), 'The corrugated metal conduit as a compression ring', Proc. HRB, Vol. 39, Washington D.C.
- Young, O.C., and Smith, J.H., (1970), 'Simplified tables of external loads on buried pipelines', HMSO, London.
- Young, O.C., (1971), 'Drainage Pipelines - 2', Digest 131, Building Research Station, Garston, Watford.
- Young, O.C., (1978), 'The structural design and laying of small underground drains of flexible materials', TRRL Supplementary Report 375, Crowthorne, Berks.
- Young, O.C., (1979), 'Developments in sewerage. Chapter 2: Structural design of pipelines', 1979.
- Young, O.C., and O'Reilly, M.P., (1983), 'A guide to design loadings for buried rigid pipes', HMSO, London.
- \* Wetzorke, M. (1960), "Über die Bruchsicherheit von Rohrleitungen in parallel wandigen Gräben", Veröffentlich. Inst. Siedlungs Wasserwirtsch., Tech. Hochschule, Hannover, 5.



## APPENDIX A



**APPENDIX A**

A summary of important vertical diametral strain measurements of the pipes used in the box and pit experiments is presented in Table A1 and A2 respectively. Details of the sidefill and bedding used for each test have been included. The preliminary experiments, the results of which have been discussed in Chapter 5, have not been included here.

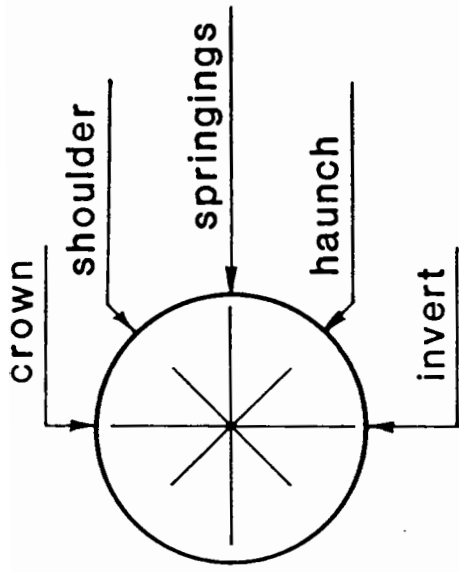
Table A.1 Summary of Data from the Box Experiments

Ref.	PIPE SUPPORT MATERIAL					Original vertical diameter (mm)	VERTICAL DIAMETRAL STRAIN (%)						Comments
	Bedding Type	Bedding Thickness (mm)	Sidefill Type	Sidefill Compaction	Sidefill $\mu$ (%)		Installation	55 kN for 30 minutes	End of 55 kN sequence	End of test	Under Load Alone		
1	Pea gravel	100	Pea gravel	none	-	160.2	0.3	2.8	3.6	5.2	4.9	current practice	
2	Pea gravel	50	Pea gravel	none	-	160.4	-0.1	2.7	3.4	4.6	4.8		
3	none	0	Pea gravel	none	-	159.7	0.4	3.6	4.0	5.9	5.5		
4	Pea gravel	50	Pea gravel to springings, silty clay above	none	16.9	160.7	0.2	6.6	6.1	7.0	6.7		
5	none	0	Pea gravel to springings, silty clay above	none thorough	14.5	159.5	-1.2	3.1	3.1	4.8	6.0		
6	none	0	Silty clay to springings, pea gravel above	thorough none	14.7	161.0	-2.4	1.4	2.0	4.2	6.6		
7	none	0	Silty clay to crown, pea gravel 50mm above	thorough none	14.4	160.6	-1.1	1.1	1.4	4.1	5.2		
8A	none	0	Silty clay to springings, pea gravel to 50mm above crown	thorough none	13.7	160.7	-2.6	-1.4	-1.2	-1.0	1.6		
8B	none	0	Silty clay to springings, pea gravel to 50mm above crown	thorough none	16.5	160.5	-2.1	3.4	4.2	7.2	9.3		
9	none	0	Silty clay	thorough	15.3	162.2	0	7.7	13.3	14.0	excessive deformation after 70 kN static load		
10	none	0	Silty clay to springings, silty clay to crown	thorough thorough	14.4	160.6	-1.8	4.4	5.1	8.1			9.9
11	none	0	Silty clay	light	16.4	163.0	0.6				excessive deformation under 55 kN load		
12	Pea gravel	100	Silty clay	thorough	16.0	160.4	-0.1	13.8					excessive deformation during 55 kN cyclic load
13	none	0	Concrete ballast	light	1.74	160.8	0.1	2.7	3.5	5.4	5.2		
14	none	0	Concrete ballast	none	2.36	160.6	0.2	3.4	4.4	6.5	6.3		
15	none	0	Reject sand	light	20.6	160.5	1.0	9.9	10.8		excessive deformation under 70 kN load as above		
16	none	0	Reject sand	none	15.7	160.2	0.17	9.6	9.6				

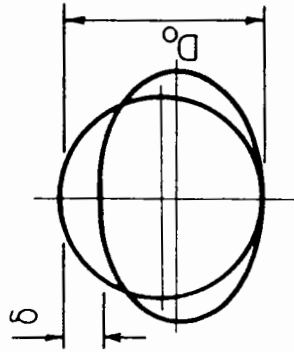
Table A.2 Summary of Data from the Pit Experiments

Ref.	PIPE SUPPORT MATERIAL				Original vertical diameter (mm)	VERTICAL DIAMETRAL STRAIN (%)					Comments	
	Type	Bedding Thickness (mm)	Sidewall Compaction	Sidewall w (%)		Installation	End of Sequence	End of test	Under load alone	Average		
1A	Pea gravel	100	none	-	159.7 159.6	1.2* 1.3*	2.7 2.3	3.9 4.1	2.8 2.8	2.8	current practice	
2	Pea gravel	0	none	-	160.2 160.0	0.7 -0.1	3.1 1.4	5.3 3.5	4.6 3.6	4.1		
3A	Silty clay	0	thorough	15.41	160.5	-1.1 -0.7	2.3	5.4 5.2	6.5 5.9	5.5		
3B	Silty clay	0	thorough	14.96	159.6 159.6	0.1 1.0	1.3 2.2	4.3 6.1	4.3 5.2			
4	Concrete ballast	0	light	3.32	160.2 159.9	0.2 0.6	0.7 1.1	1.6 2.3	1.3 1.7	1.5		
5	Concrete ballast	0	none	3.96	160.4 160.1	0.9 0.8	1.9 1.9	3.1 2.1	2.2 2.1	2.2		
6A	Pea gravel	50	none	-	160.3 160.1	0.4 0.4	1.3 1.5	2.2 2.7	1.8 2.2	1.9		modified load regime at one point
6B	Pea gravel	50	none	-	160.5	0.4	1.2	2.0	1.6			
7A	Concrete ballast	50	none	1.81	160.3 160.2	0.2 0.2	1.2 1.7	2.2 2.9	2.0 2.7	2.2		
7B	Concrete ballast	50	none	2.20	160.5 160.6	0.3 0.1	1.2 1.2	2.2 2.3	1.9 2.1			
8A	Building sand	50	none	5.43	160.2 160.3	0.6 0.9	2.0 2.4	3.5 4.3	2.8 3.4	3.4		
8B	Building sand	50	none	5.42	160.8 160.7	1.3 0.5	3.4 2.1	5.5 3.7	4.2 3.2			
1B	Pea gravel	100	none	-	160.6 160.6	0.1 0.2	0.8 1.0	2.7 2.1	2.6 1.9	2.2	current practice	
9A	Quarry tailings	50	none	2.24	160.5 160.6	0.8 0.4	2.3 1.8	3.7 3.4	2.8 2.9	2.6		
9B	Quarry tailings	50	none	-	160.5	0	1.3	2.2	2.2			
10	Reject sand	50	none	20.49	160.6 160.7	1.0 1.0	5.2 4.7	7.8 6.9	6.8 5.9	6.4		

Note: \* Installation readings for Test 1A were unusually large due to preloading and typical installation values for Test 1B have been used for calculation of absolute strains in the text.



(a) Pipe terminology

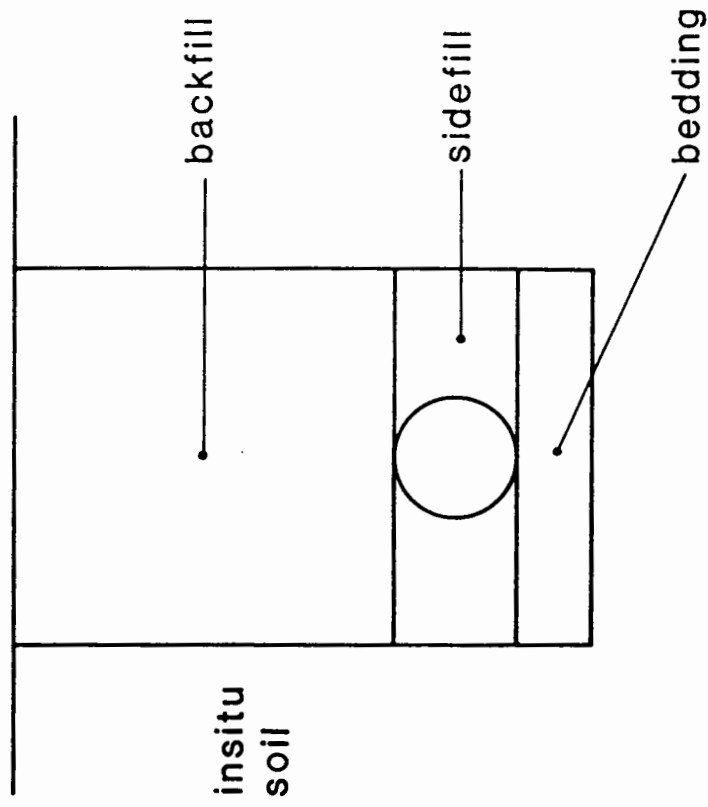


$$\text{V.D.S.} = \delta / D_o$$

$\delta$  = change in internal diameter (mm)

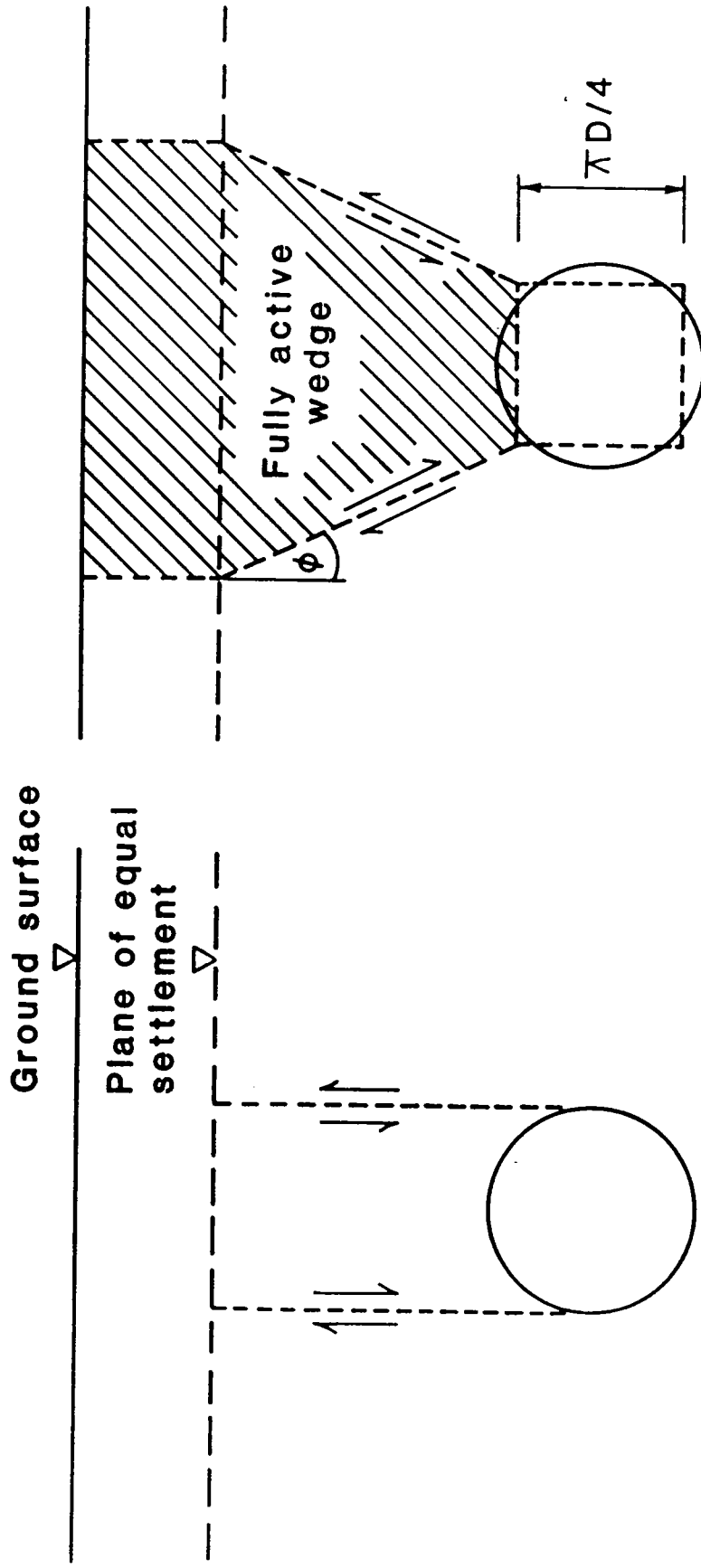
$D_o$  = original external diameter (mm)

(b) Definition of vertical diametral strain



(c) Installation terminology


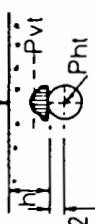
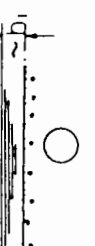
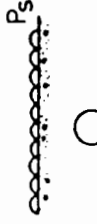


Fig. 1.1 Terminology and Definitions



(a) after Marston

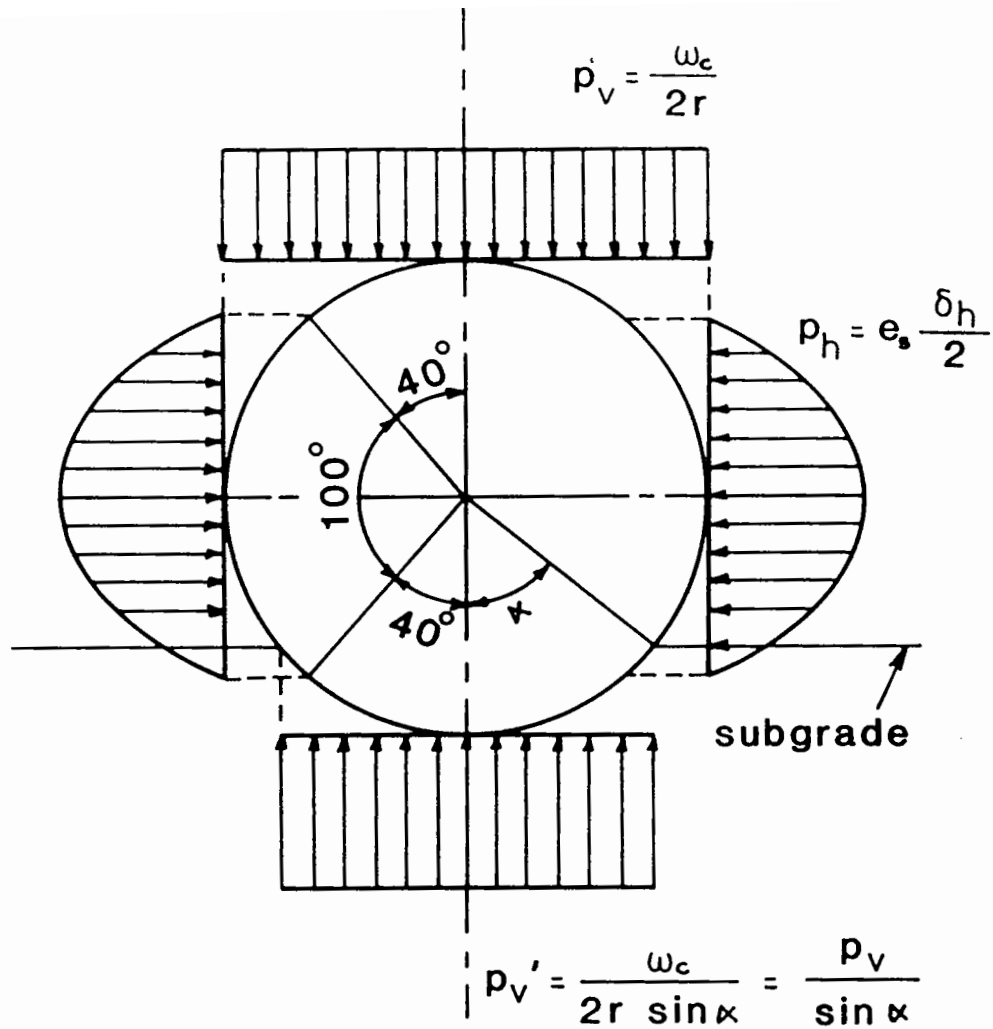
(b) Voellmy (after Bulsen)

Fig. 2.1 Basis of Marston and Voellmy Theories of Earth Load

 <p><u>Backfill load</u></p> <p><math>Y</math> = mean unit weight of soil  For <math>h/D &gt; 2.5</math>  <math>P_{vd} = Y(h + D/2)</math>  <math>P_{hd} = K_d P_{vd}</math></p> <p>For <math>1 \leq h/D \leq 2.5</math>, allowance is made for the weight of soil displaced by the pipe:  <math>P_{vd} = Y(h + D/4)</math>  <math>P_{hd} = K_d Y(h + D/2)</math></p>	 <p><u>Concentrated surcharge</u></p> <p>Use standard elastic stress distributions (Poulos and Davies 1974) to determine vertical and horizontal pressures due to surcharge.</p> <p>For <math>h/D &gt; 2.5</math>:  <math>P_{vt}</math>, <math>P_{ht}</math> evaluated at pipe axis.</p> <p>For <math>1 \leq h/D \leq 2.5</math>:  <math>P_{vt}</math> calculated as mean vertical pressure on plane of width <math>D</math> at pipe crown.  <math>P_{ht}</math> evaluated at pipe axis</p>	 <p><u>Underwater installation</u></p> <p><math>\gamma_w</math> = unit weight of water  <math>Y'</math> = submerged unit weight of soil (<math>= Y - \gamma_w</math>)  Soil effective stress components</p> <p><math>P'_{vd} = Y'(h + D/2)</math>  <math>P'_{hd} = K_d P'_{vd}</math></p> <p>Hydrostatic pressure contributing directly to <math>P_z</math>:</p> <p><math>P_w = \gamma_w(h_1 + h + D/2)</math></p>
 <p><u>Uniformly distributed surcharge</u></p> <p>For surcharge pressure <math>P_s</math></p> <p><math>R_s = P_s</math>  <math>P_{hs} = K_d P_{vs}</math></p>	 <p><u>Traffic wheel loads</u></p> <p>Calculated as combinations of concentrated surcharges.  Values of <math>P_{vt}</math> due to standard UK traffic have been tabulated elsewhere.</p>	 <p><u>Internal vacuum</u></p> <p>Treat vacuum pressure <math>P_q</math> (reduction in pressure below atmosphere) as external fluid pressure contributing directly to <math>P_z</math></p>

**Fig. 2.2 Calculation of Loads on a Buried Pipe (after Gumbel)**



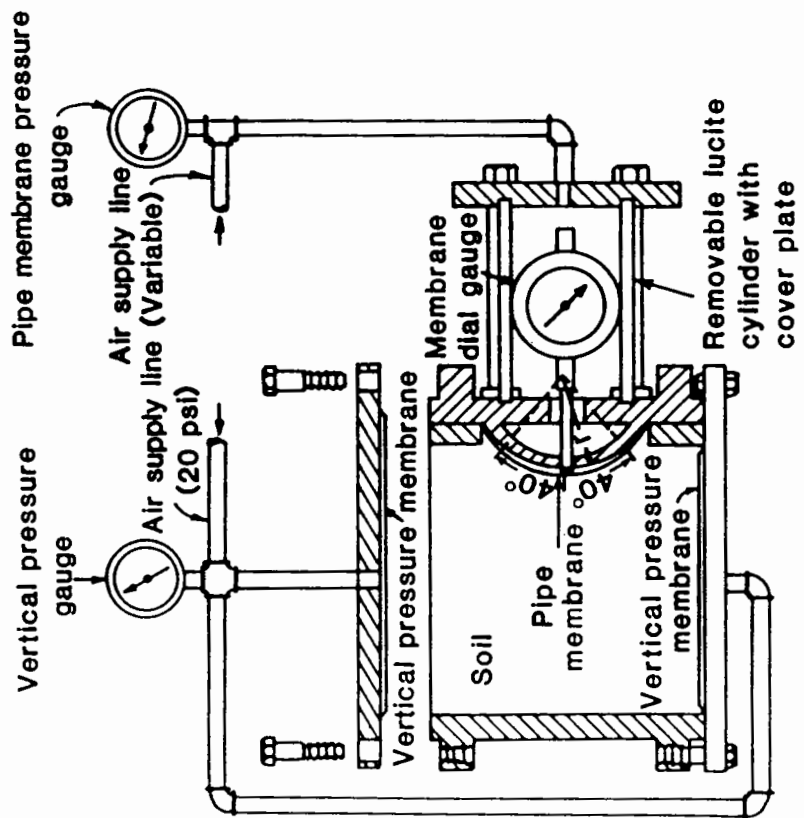


A parabolic distribution of horizontal earth pressure is assumed

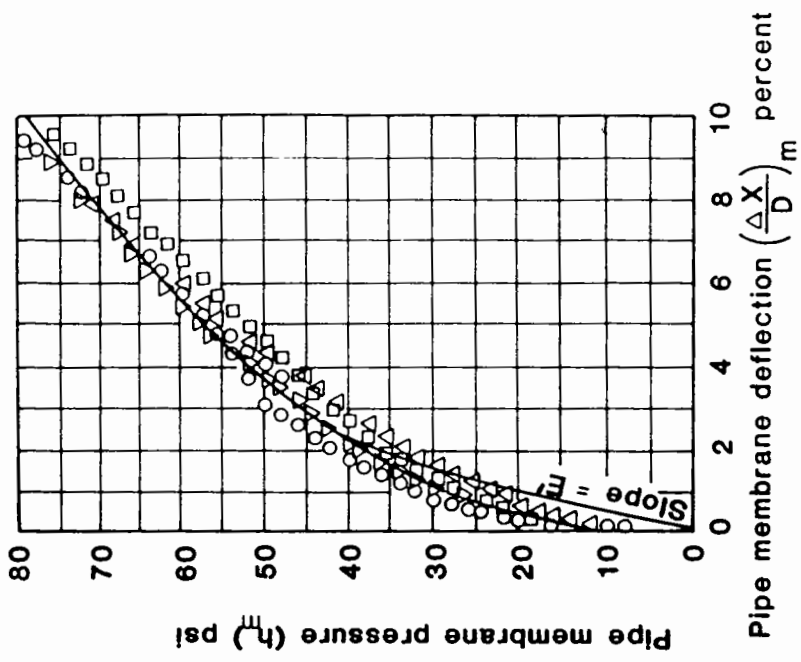
$e_s$  = modulus of passive resistance of soil

$\alpha$  = bedding angle

Fig. 2.3 The Distribution of Pressures Around a Flexible Pipe under Earth Loads (after Spangler)

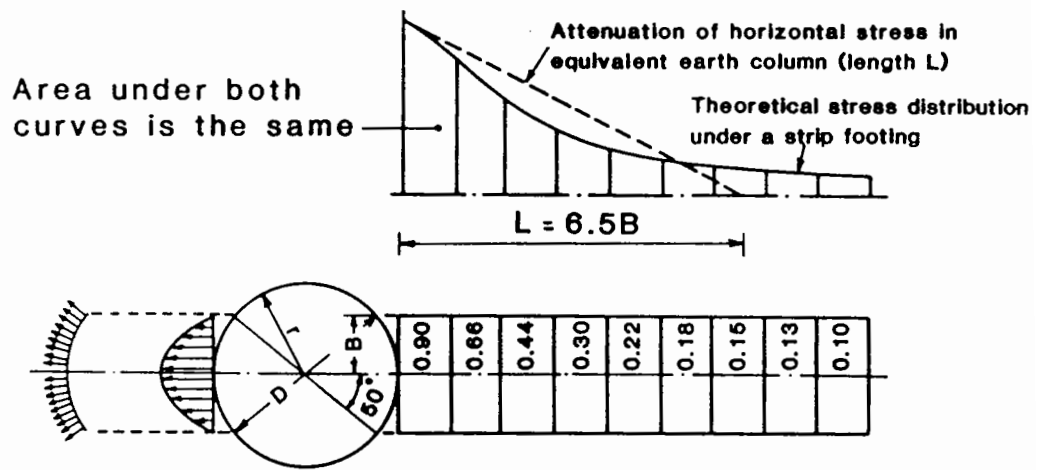


(a) Diagram of the apparatus



(b) Typical response of a backfill soil

Fig. 2.4 The "Modpares" Device (after Watkins and Neilson)



$$B = r \sin 50^\circ = 0.766 r = 0.383 D$$

$$L = 6.5 B = 2.49 D$$

Fig. 2.5 Barnard's Equivalent Earth Column

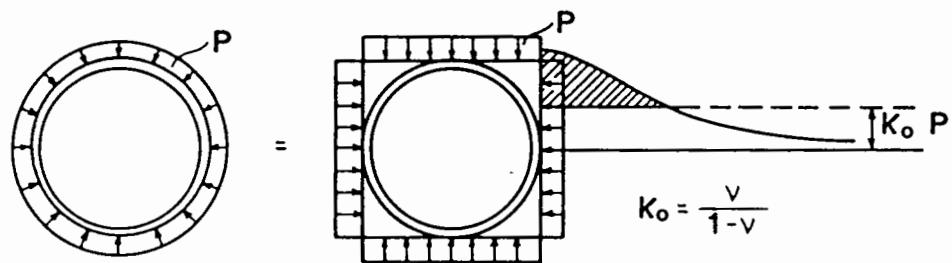


Fig. 2.6 Molin's Integration of Lateral Pressure

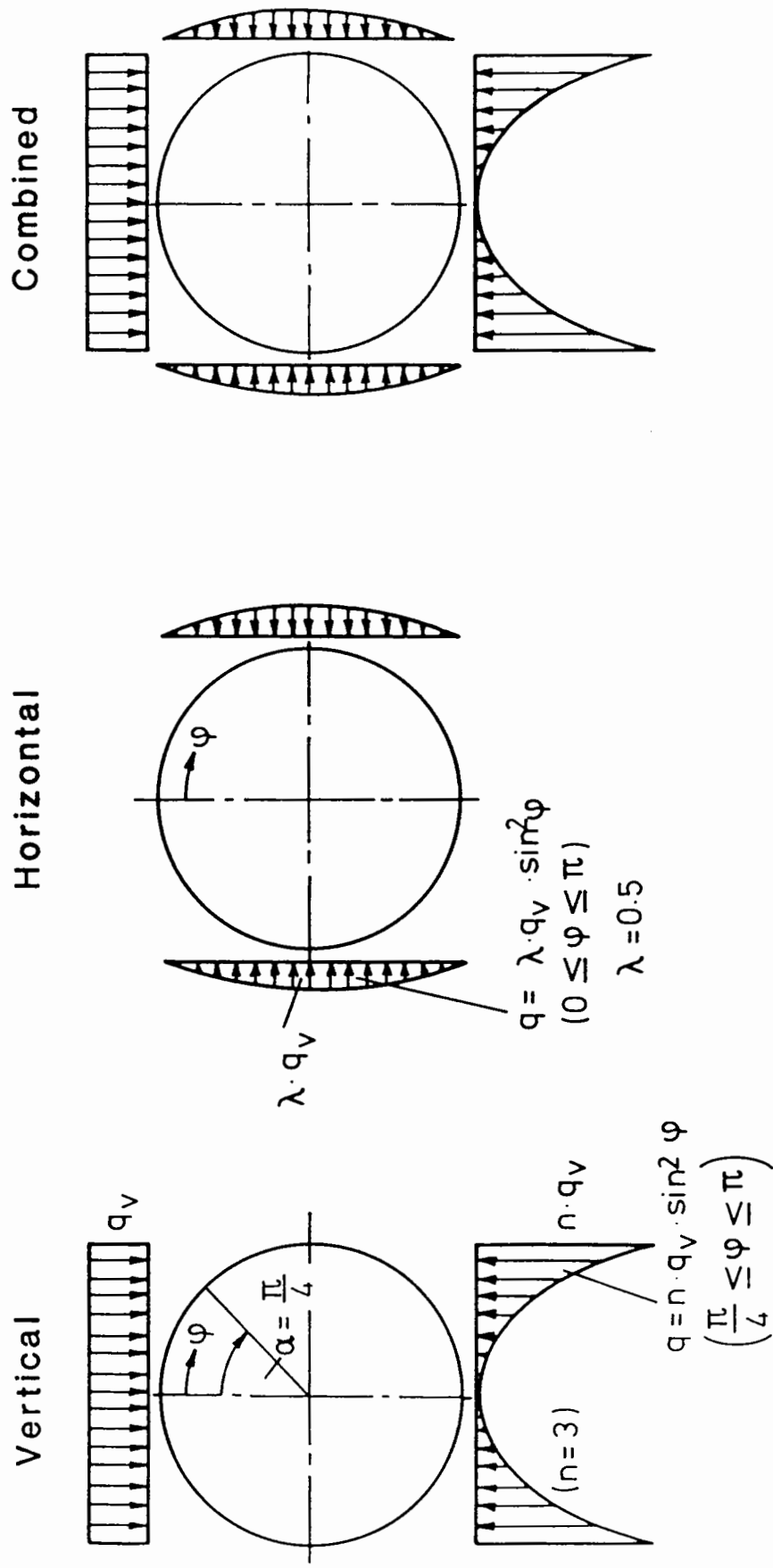
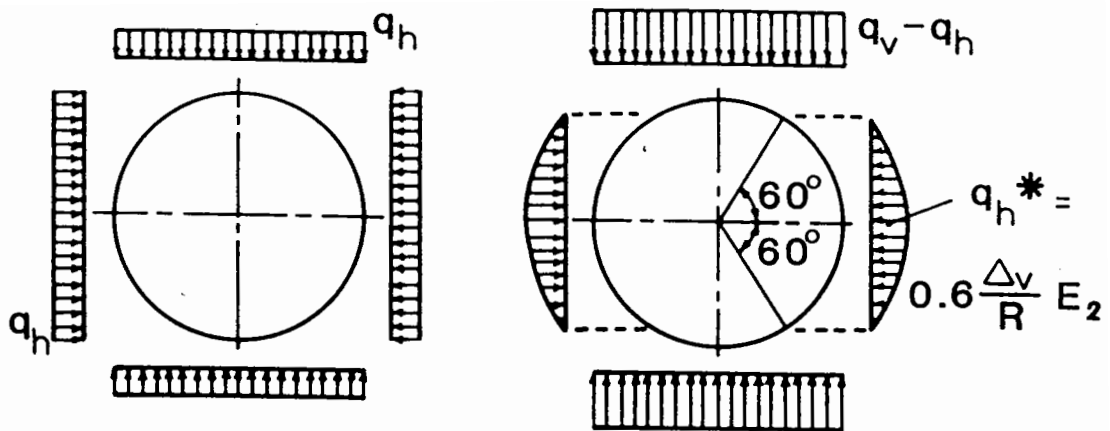
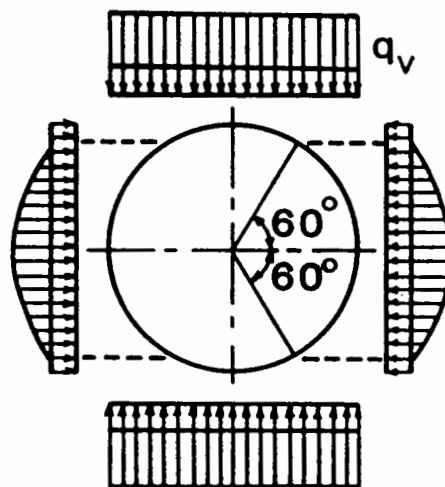


Fig. 2.7 Equilibrium Pressure Distribution (after Howe et al)



(a) Uniform and distortional pressures

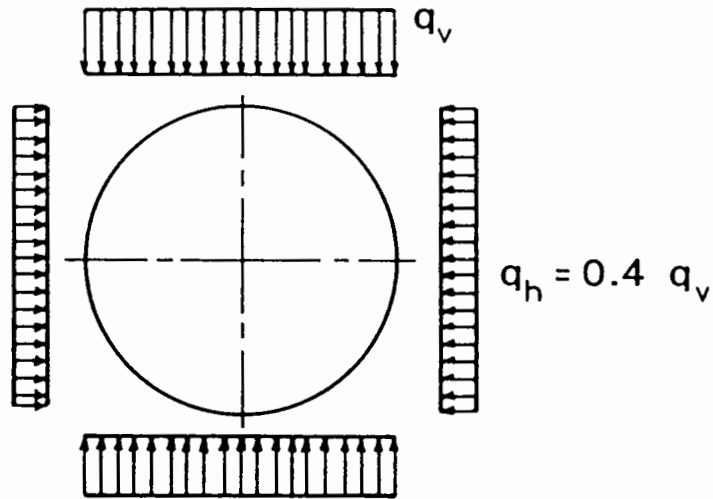


(b) Combined equilibrium pressure distribution

Fill material	Well compacted fill	Tamped fill	Dumped fill
Sand	6.0	3.0	1.2
Sandy clay	3.0	2.0	0.8
Soft clay	2.0	1.3	0.6

(c) Recommend sidefill stiffness ( $E_2$ ) values (MPa)

Fig. 2.8 Basis of Leonhardt's Approach



(a) Equilibrium pressure distribution

$$\frac{\Delta_v}{D} = \frac{(0.05 + 0.0267 n) + P_v}{E_p I / r^3 + 0.067 P_v (C - 3.5 - n)}$$

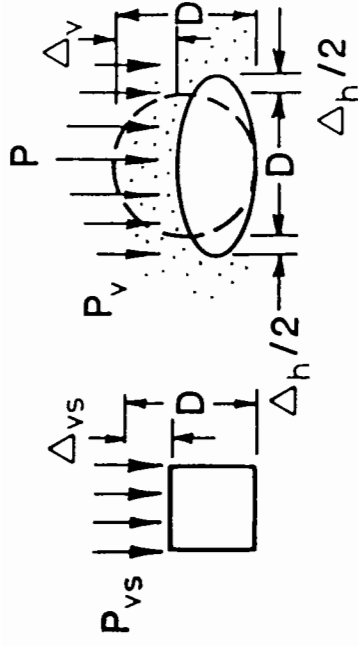
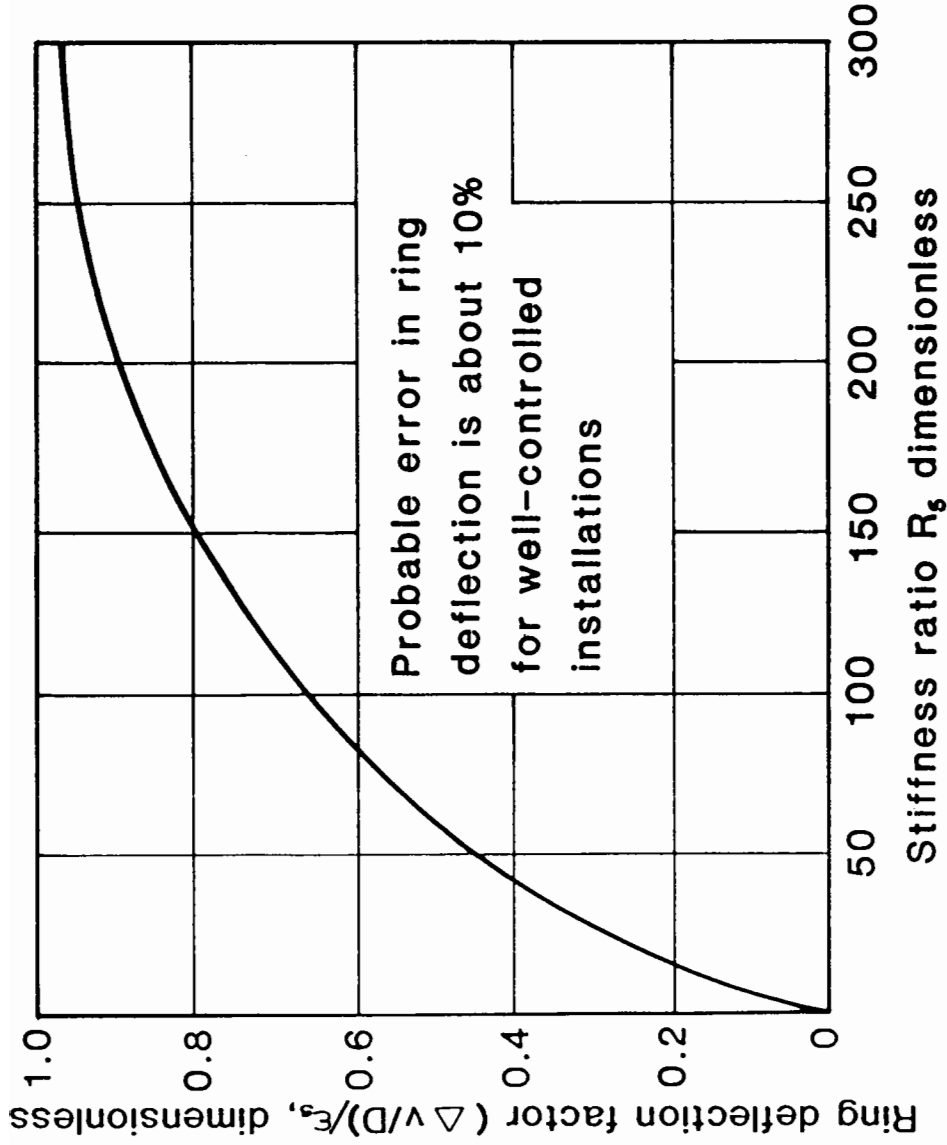
(b) Design formula

Buisman's coefficient (c) : Installation parameter (n) :

sand	> 100	very good compaction	1.0
sandy clay	40-80	good compaction	1.5
clay	25-40	normal compaction	2.0
saturated clay	10-20	poor compaction	4.0

(c) Recommended parameters for design

Fig. 2.9 Basis of Bossen's Predictions



soil alone      pipe and soil

$P_{vs}$  = free-field vertical pressure

$R_s$  =  $M_s D^3 / E_p I$

$\epsilon_s$  =  $\Delta_{vs} / D$

$M_s$  =  $P_{vs} / \epsilon_s$

$E_p I / D^3$  = ring stiffness

Fig. 2.10 Empirical Curve Proposed for Design by Watkins

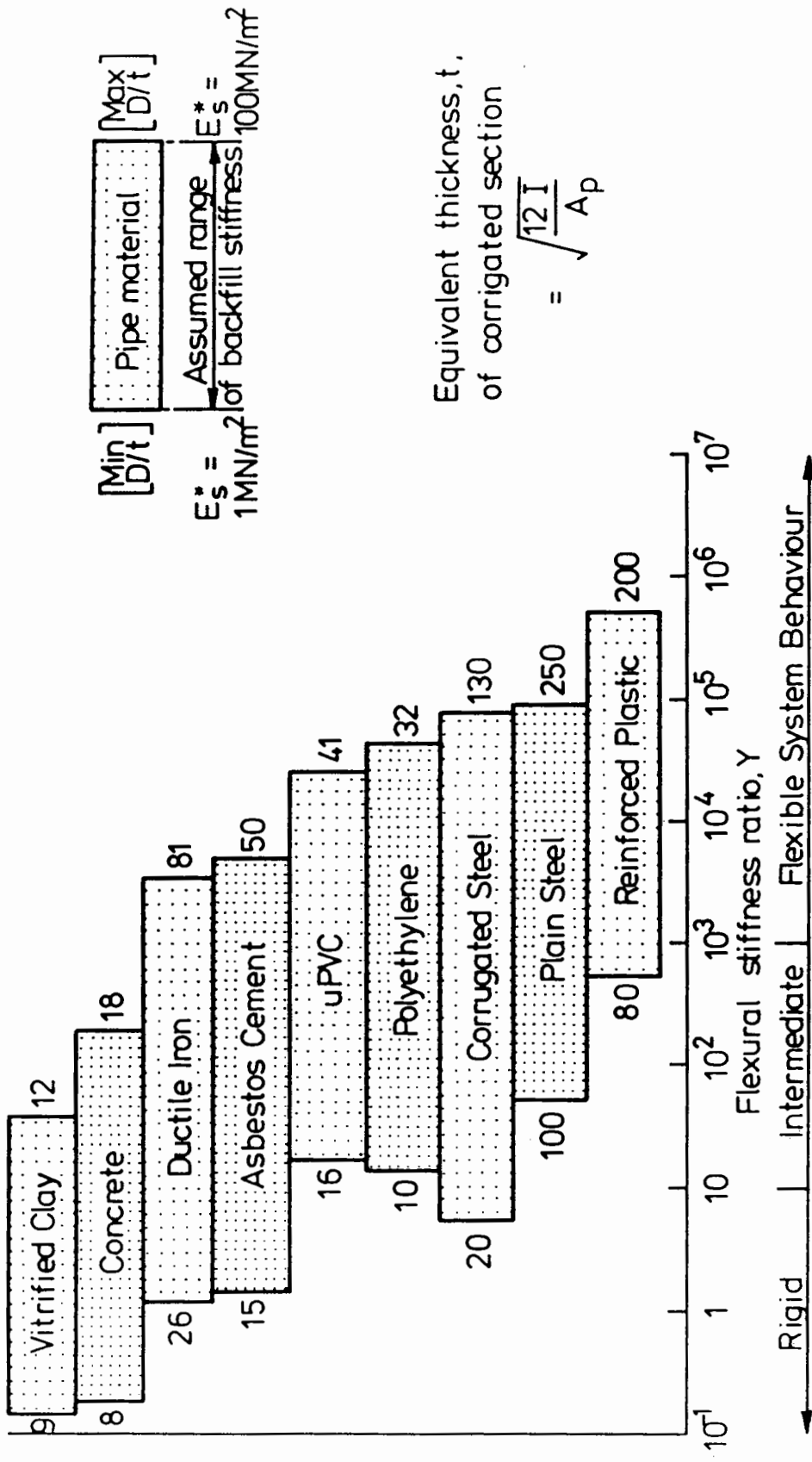


Fig. 2.11 Typical Ranges of System Behaviour for Different Pipe Materials (after Gumbel et al)



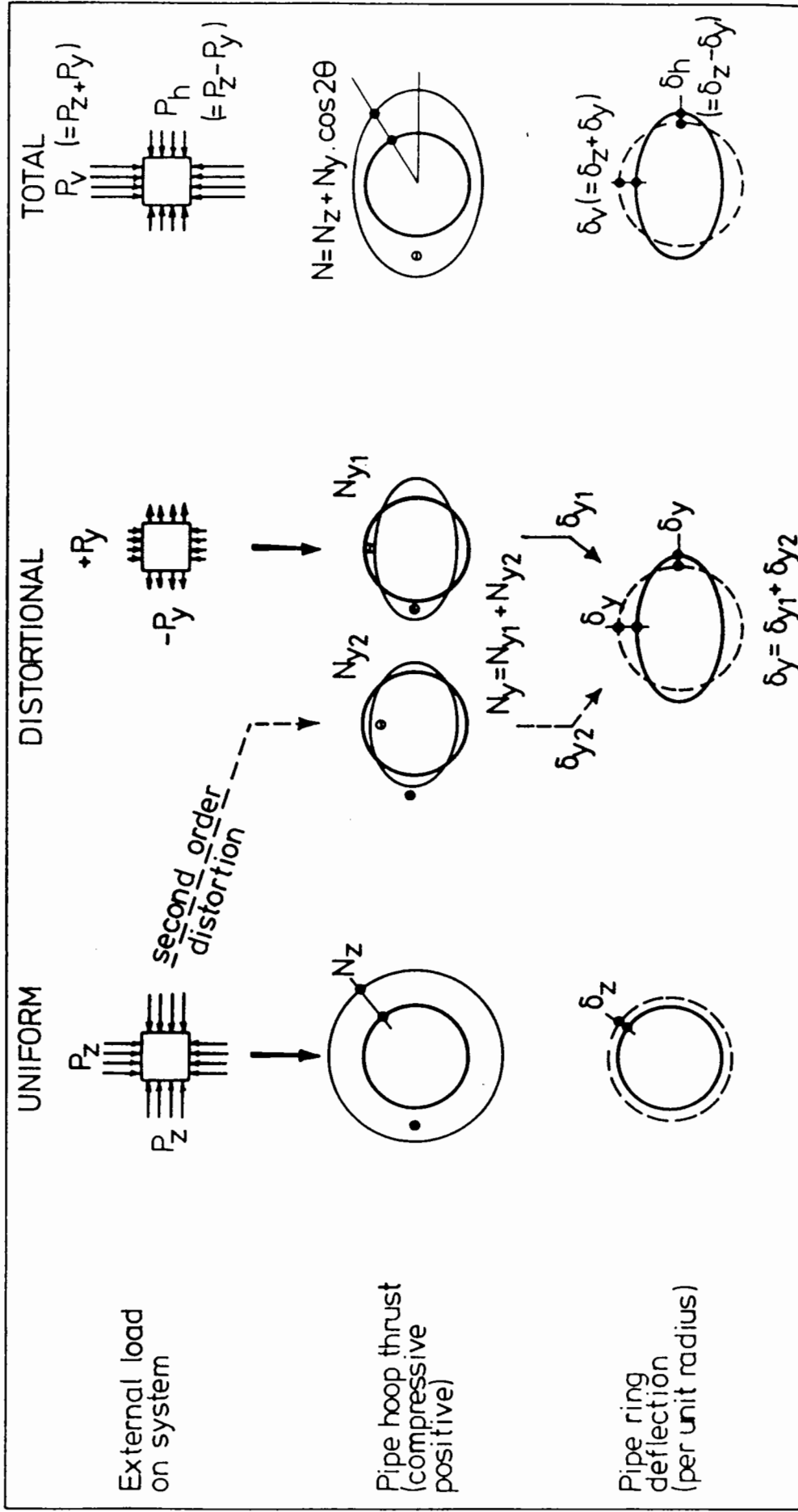
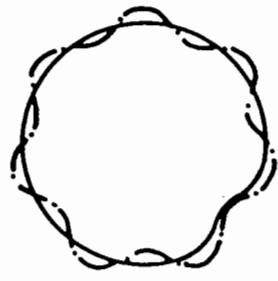


Fig. 2.12 Uniform and Distortional Load Components and Related Effects (after Gumbel et al.)

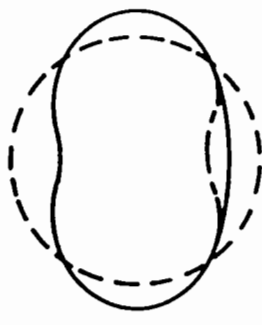
<p> <math>\cdots</math> Theoretical buckling mode  <math>\text{---}</math> Typical buckled shape in practice         </p>
---

$Y \approx 45,000, n = 7$



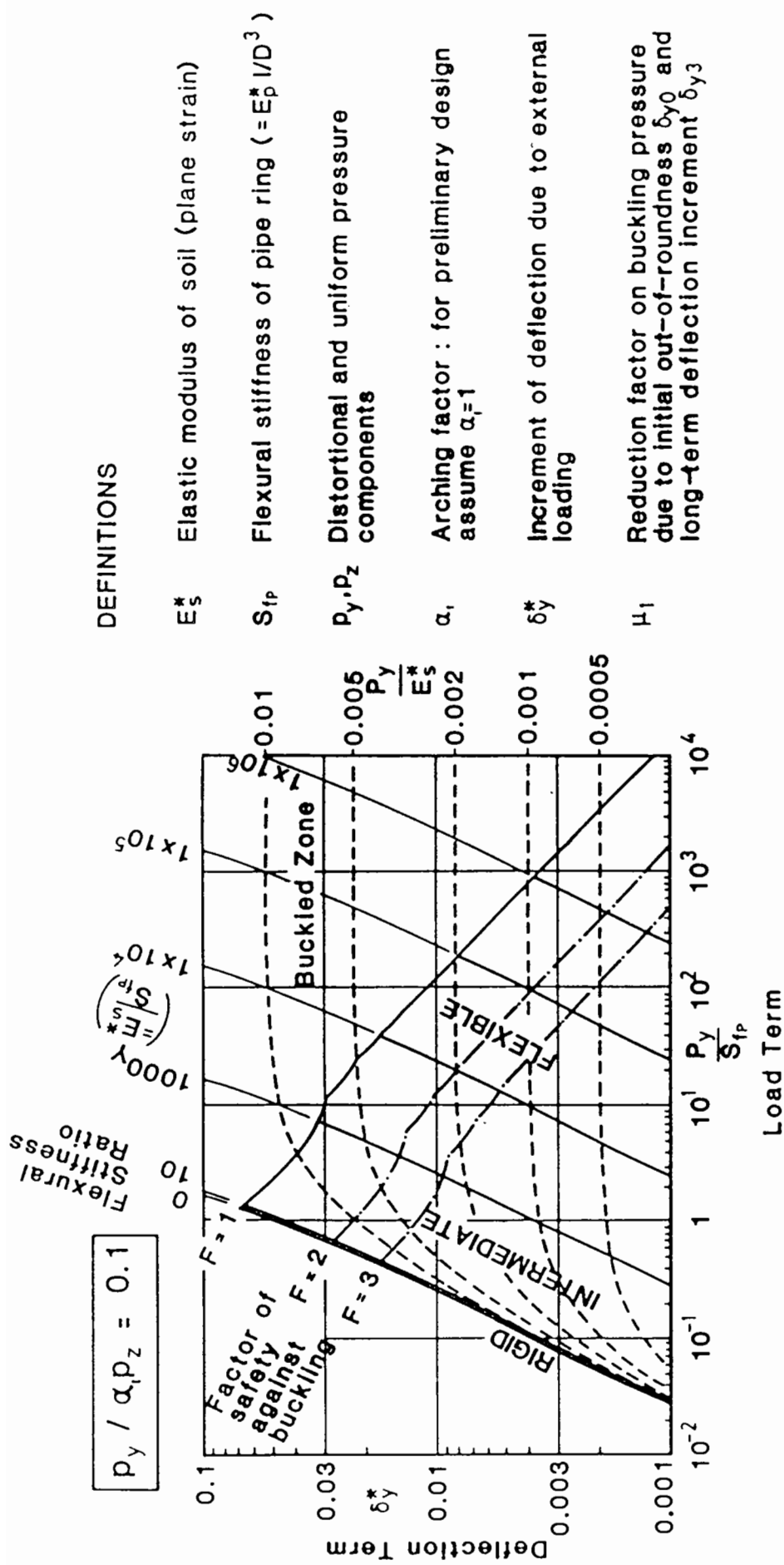
Short wavelength mode  
 (appears as local buckling  
 of pipe wall)

$Y < \sim 1000, n = 2$



Large deflection mode  
 (buckles by snap-through  
 of pipe crown)

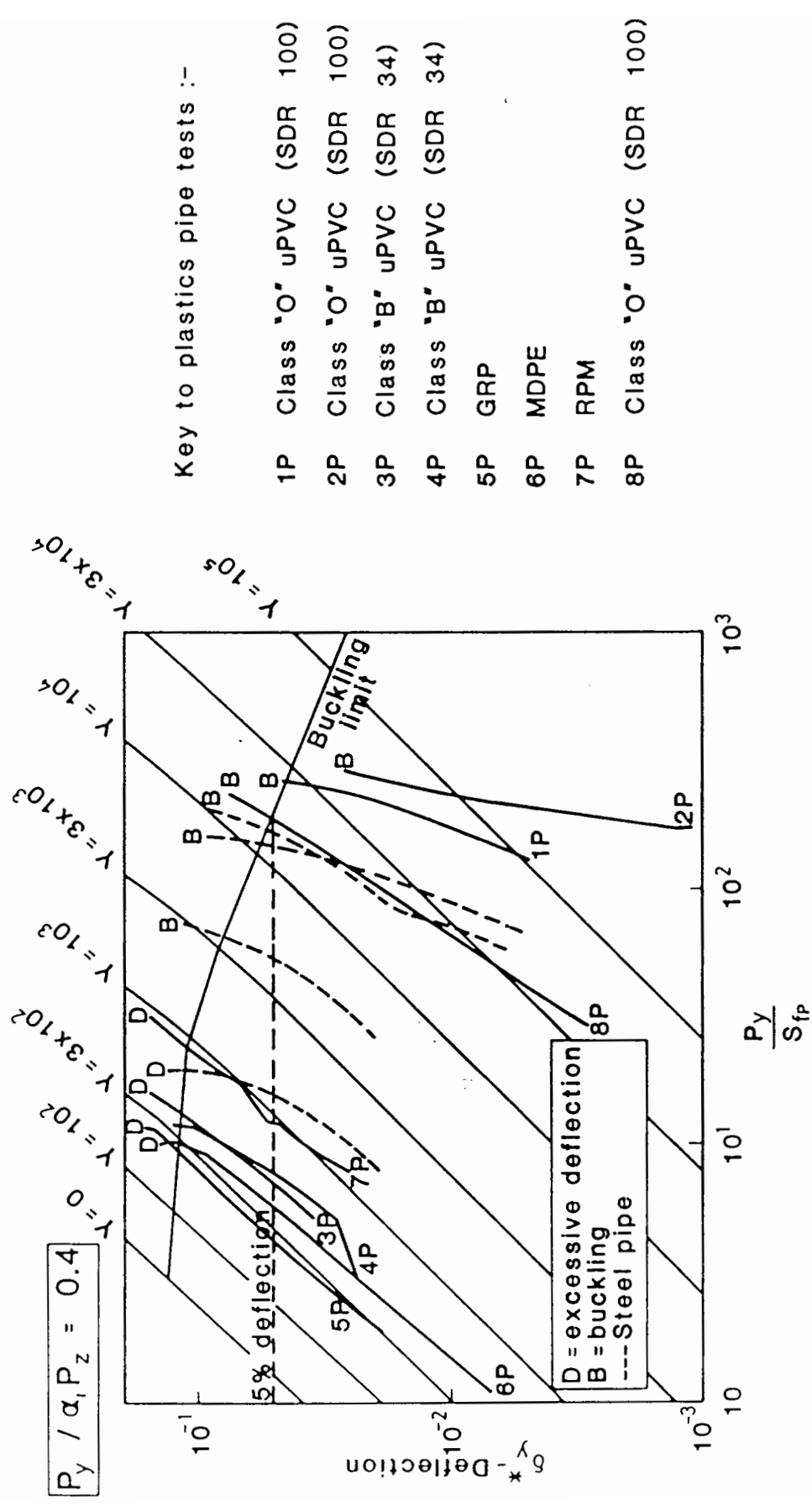
Fig. 2.13 Examples of Buckling Modes in Low and High Y Systems  
 (after Gumbel et al)



**DEFINITIONS**

- $E_s^*$  Elastic modulus of soil (plane strain)
- $S_{fp}$  Flexural stiffness of pipe ring ( $= E_p^* I / D^3$ )
- $P_y, P_z$  Distortional and uniform pressure components
- $\alpha_1$  Arching factor : for preliminary design assume  $\alpha_1 = 1$
- $\delta_y^*$  Increment of deflection due to external loading
- $\mu_1$  Reduction factor on buckling pressure due to initial out-of-roundness  $\delta_{y0}$  and long-term deflection increment  $\delta_{y3}$

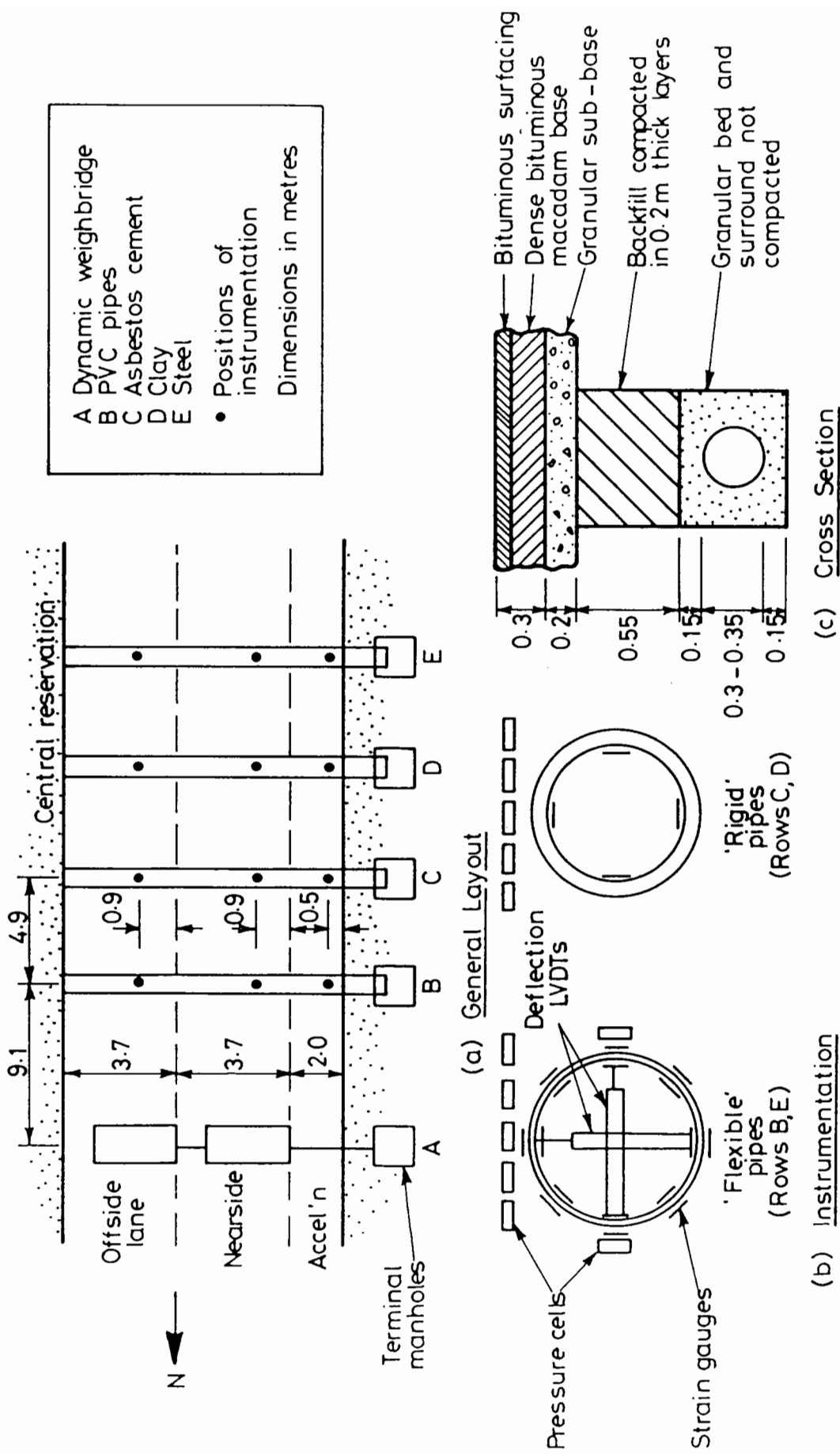
Fig. 2.14 Annotated Deflection - Buckling Chart (after Gumbel)



Key to plastics pipe tests :-

- 1P Class "O" uPVC (SDR 100)
- 2P Class "O" uPVC (SDR 100)
- 3P Class "B" uPVC (SDR 34)
- 4P Class "B" uPVC (SDR 34)
- 5P GRP
- 6P MDPE
- 7P RPM
- 8P Class "O" uPVC (SDR 100)

Fig. 2.15 Comparison of Test Data with Design Chart Predictions (after O'Reilly et al)



A Dynamic weighbridge  
 B PVC pipes  
 C Asbestos cement  
 D Clay  
 E Steel  
 • Positions of instrumentation  
 Dimensions in metres

Fig. 2.16 Experimental Pipes Beneath the Marlow - Bisham Bypass (after Trott and Gaunt)

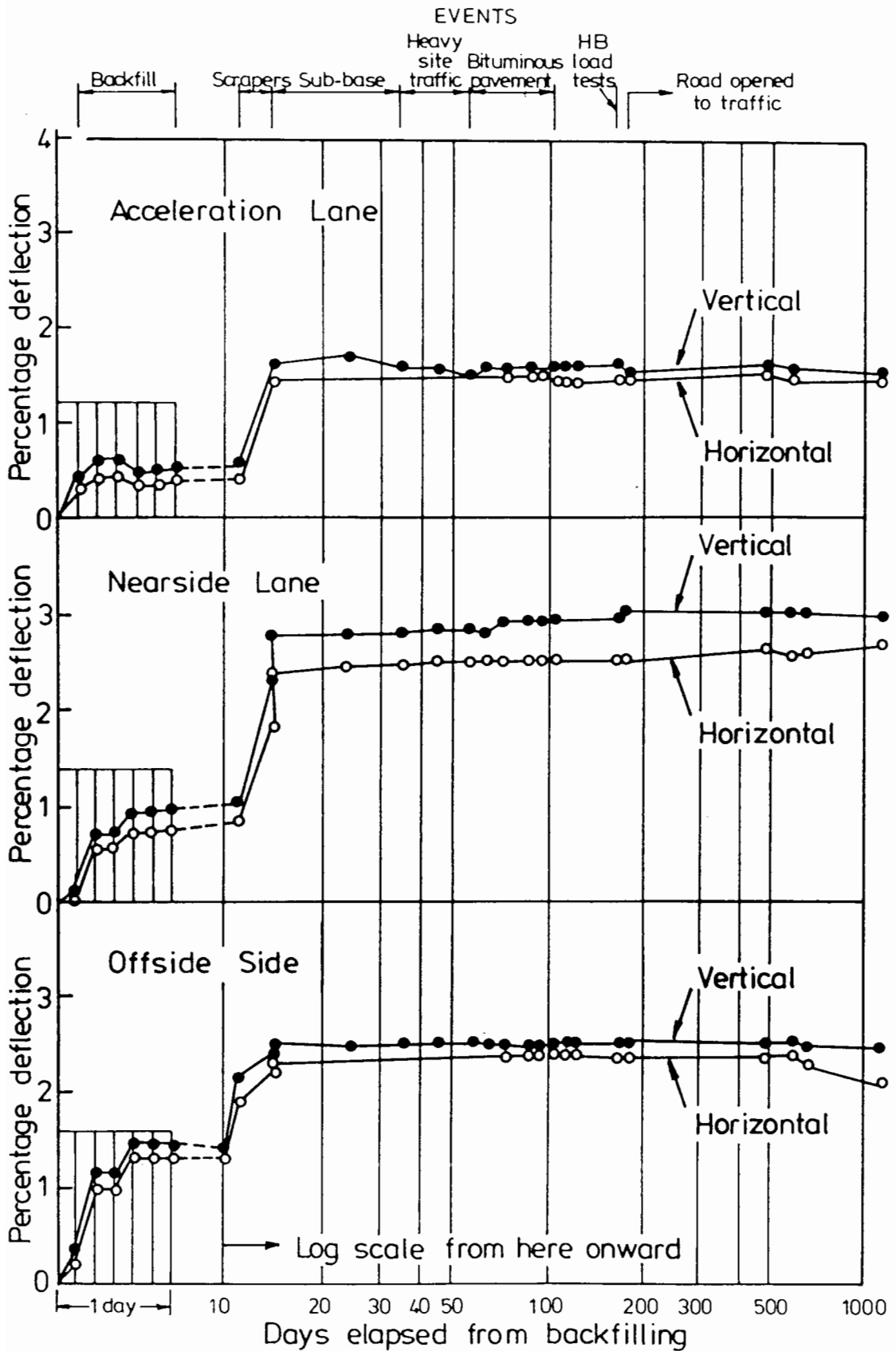


Fig. 2.17 Deformation of uPVC Pipe Laid Beneath the Marlow - Bisham Bypass (after Trott and Gaunt)

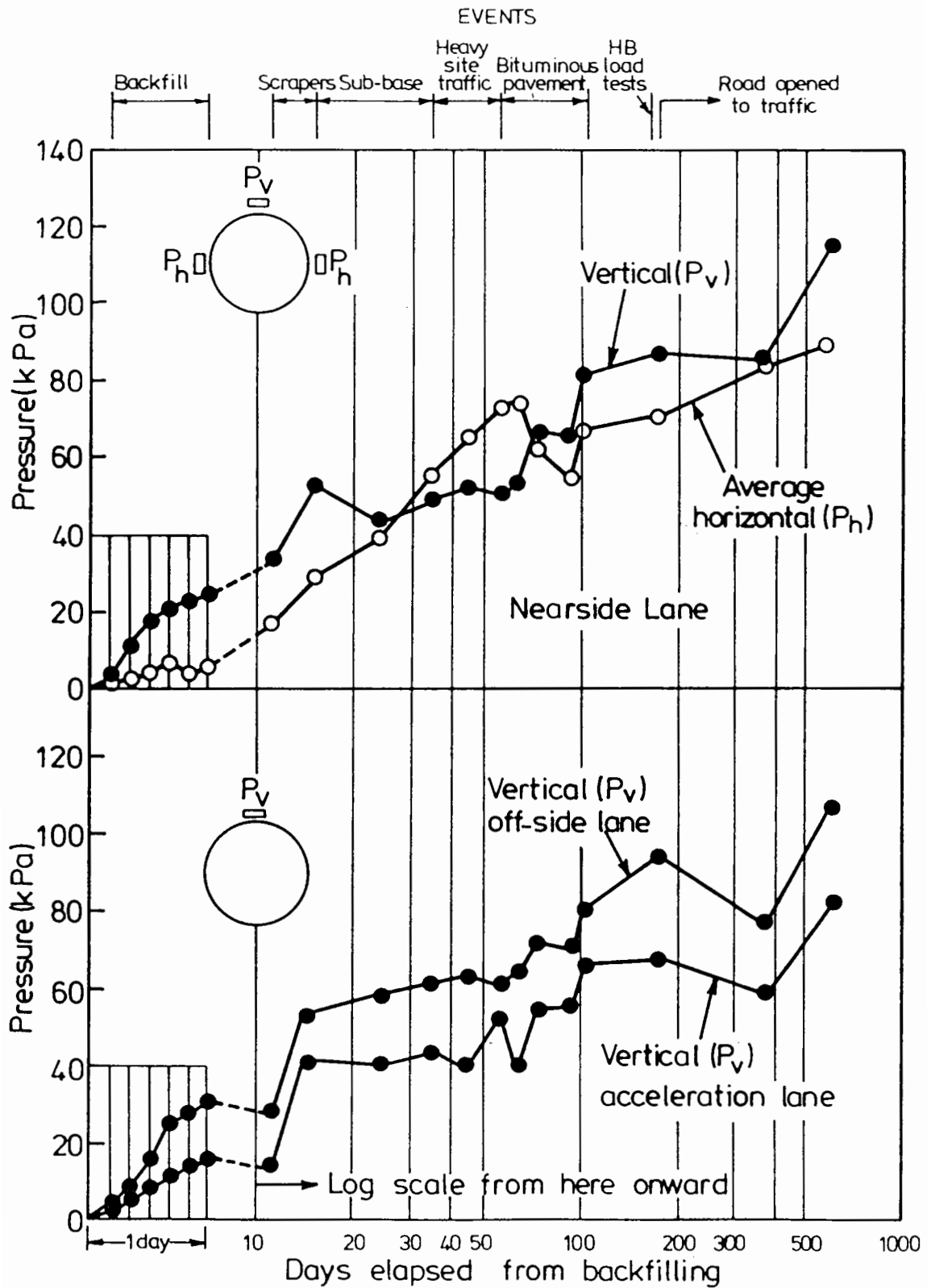


Fig. 2.18 Soil Pressures around uPVC Pipe, Marlow - Bisham Bypass (after Trott and Gaunt)

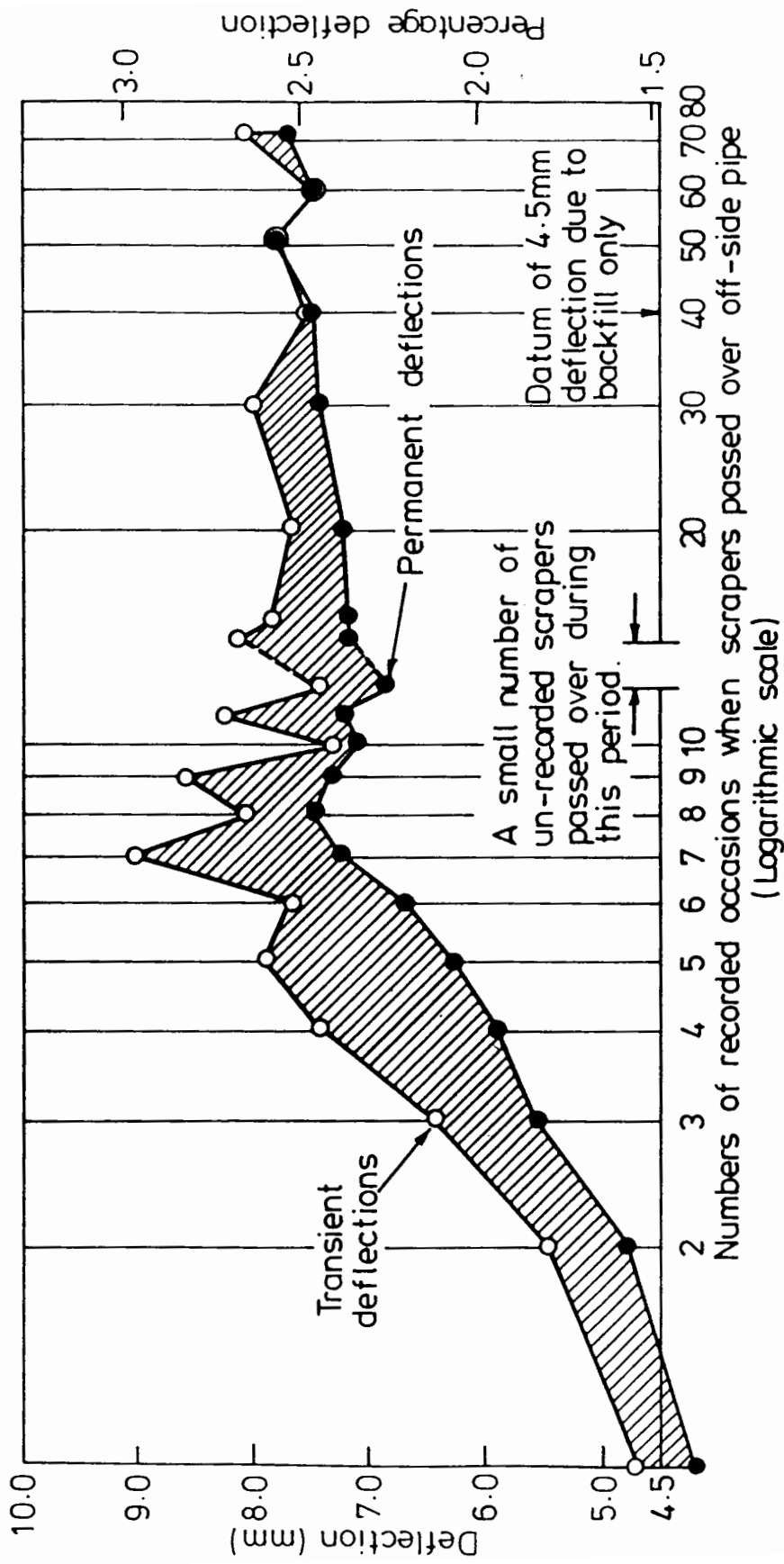


Fig. 2.19 Permanent and Transient Deformations of uPVC Pipe caused by Passage of Scrapers, Marlow - Bisham Bypass (after Trott and Gaunt)



--- Theoretical strain distribution produced by uniform pressures across the crown and invert

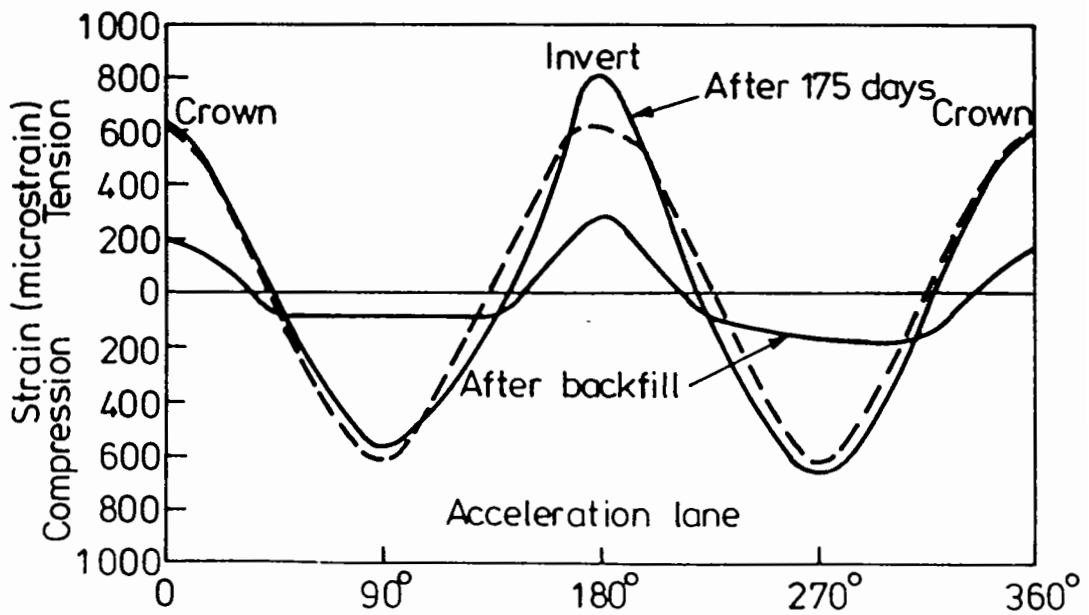
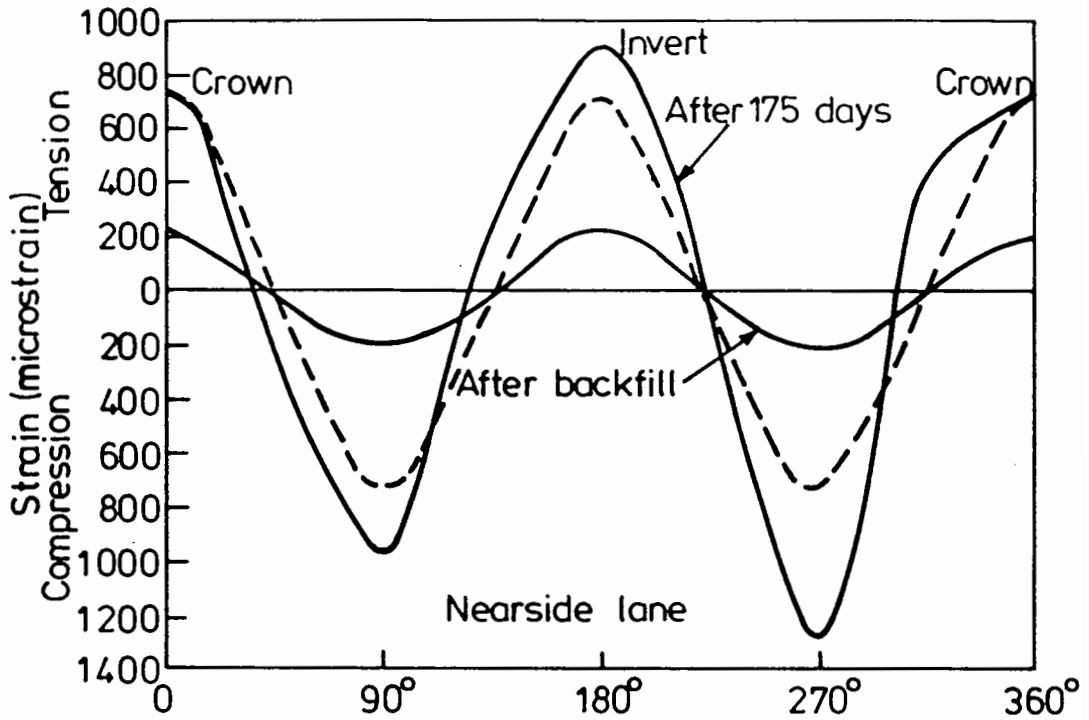


Fig. 2.20 Bending Strain Distribution around Stainless Steel Pipes, Marlow - Bisham Bypass (after Trott and Gaunt)

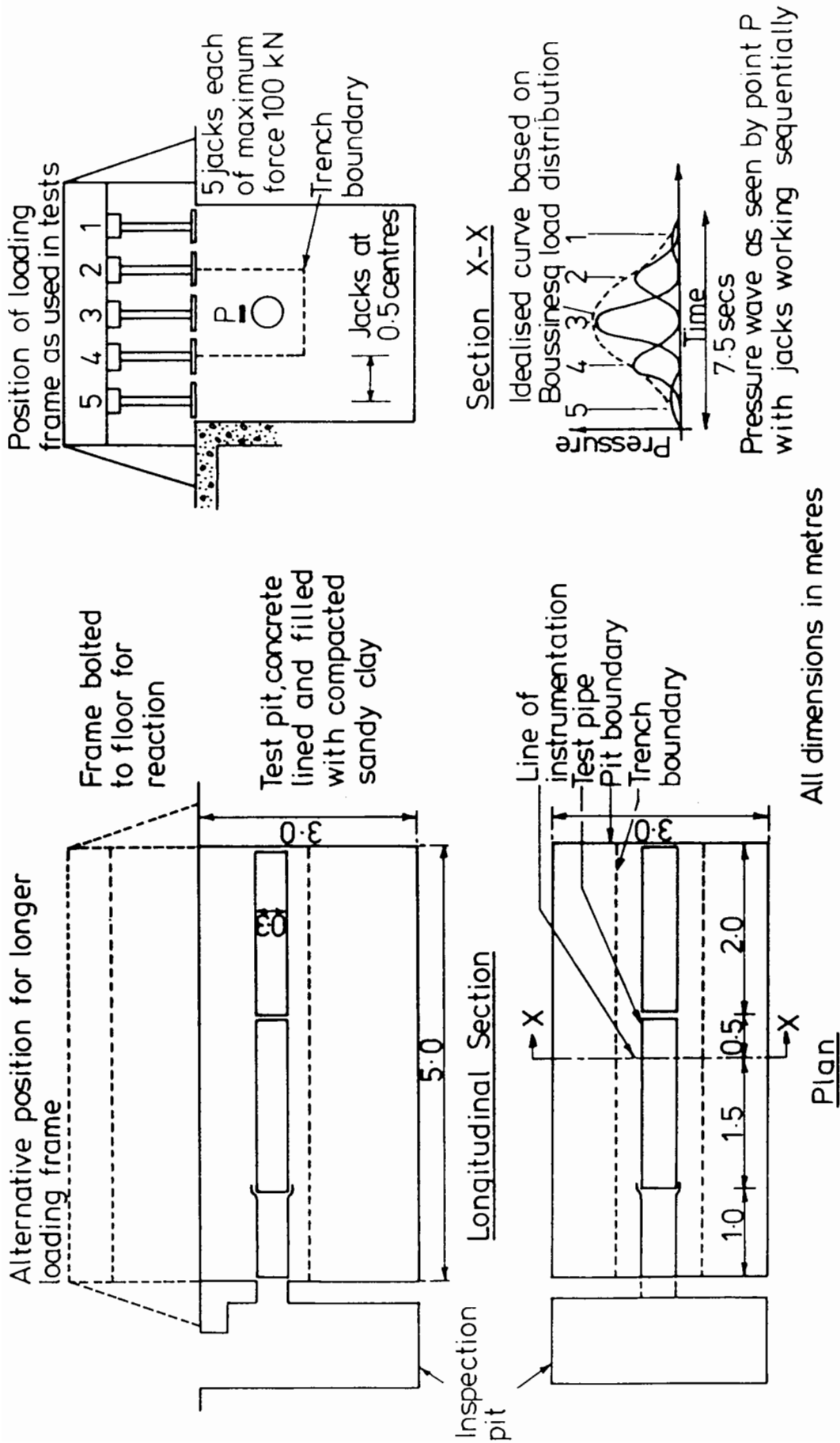
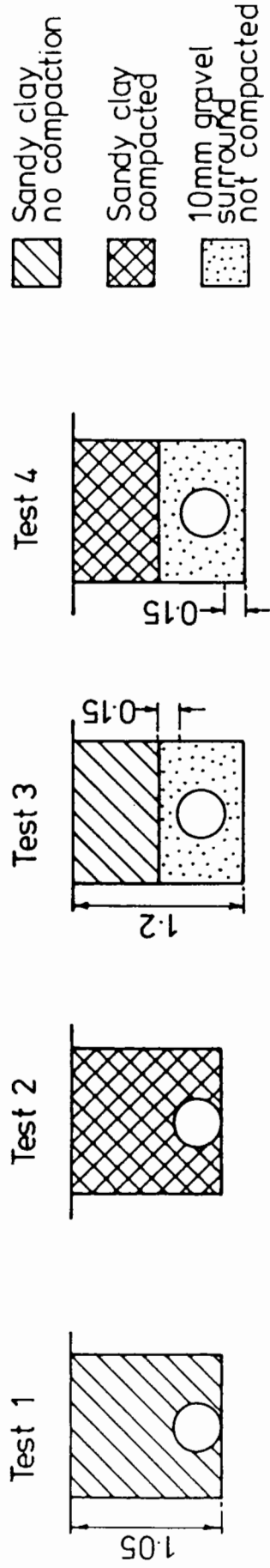


Fig. 2-21 Schematic Layout of Test Pit at the TRRL (after Gaunt et al)



Depth to pipe crown = 0.75 and trench width = 1.0 in all cases.  
 All pipes class B uPVC : 0.305 internal diameter and 0.321 external diameter.

(a) Test Programme

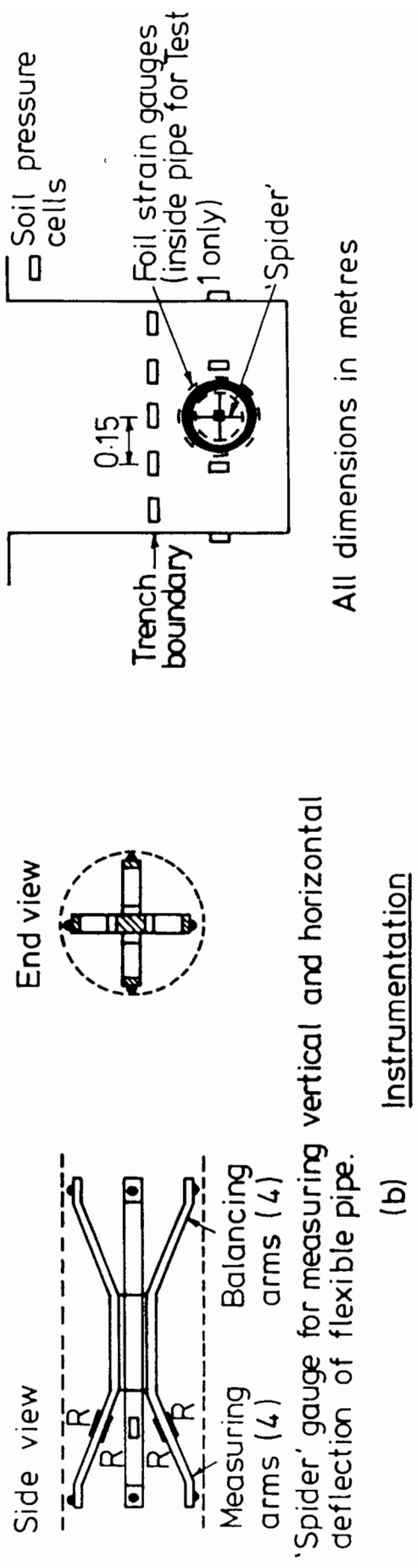


Fig. 2.22 Details of TRRL Laboratory Experiments (after Gaunt et al)

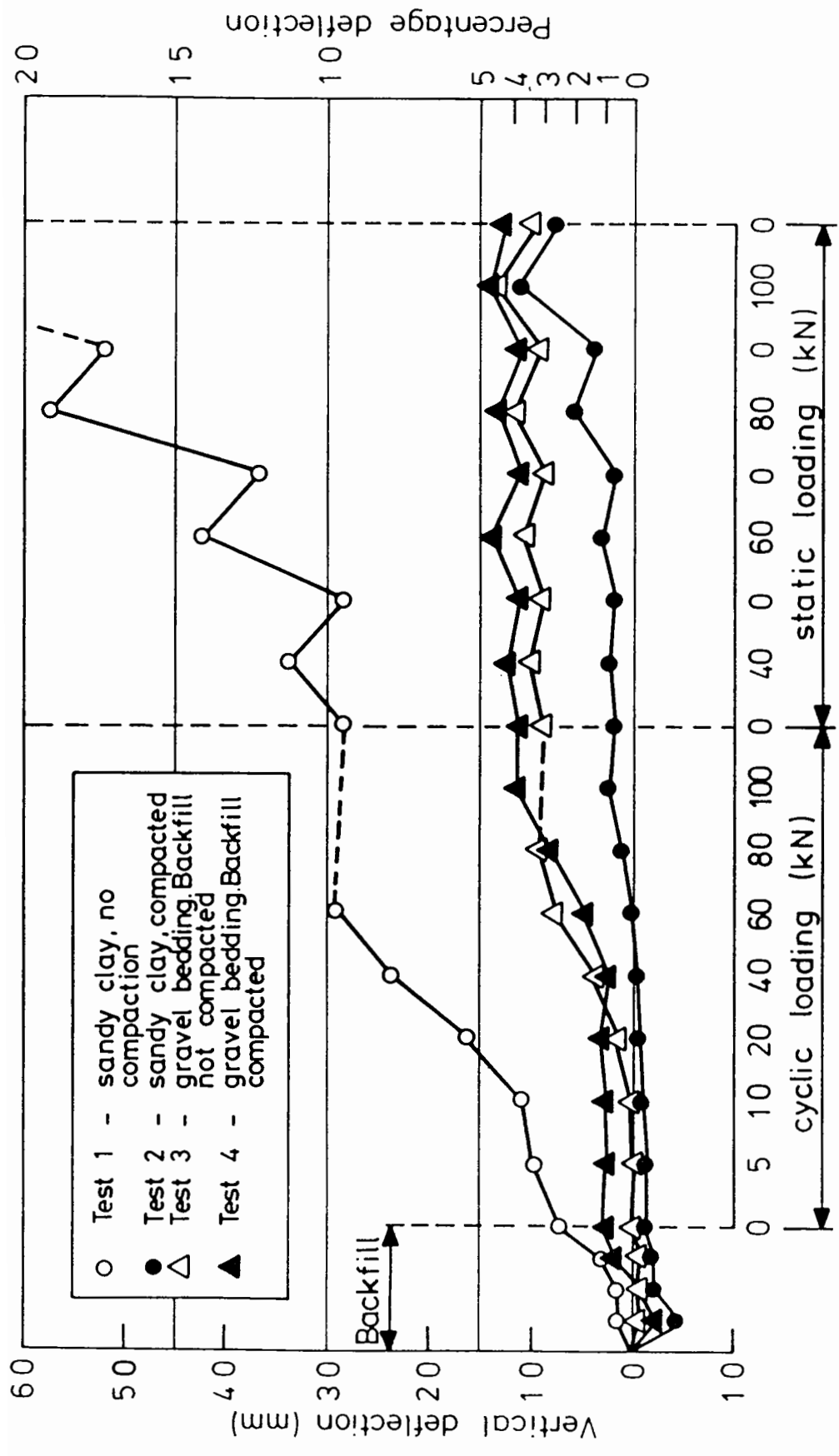


Fig.2.23 Effect of Installation Method on Pipe Deformation (after Gaunt et al)

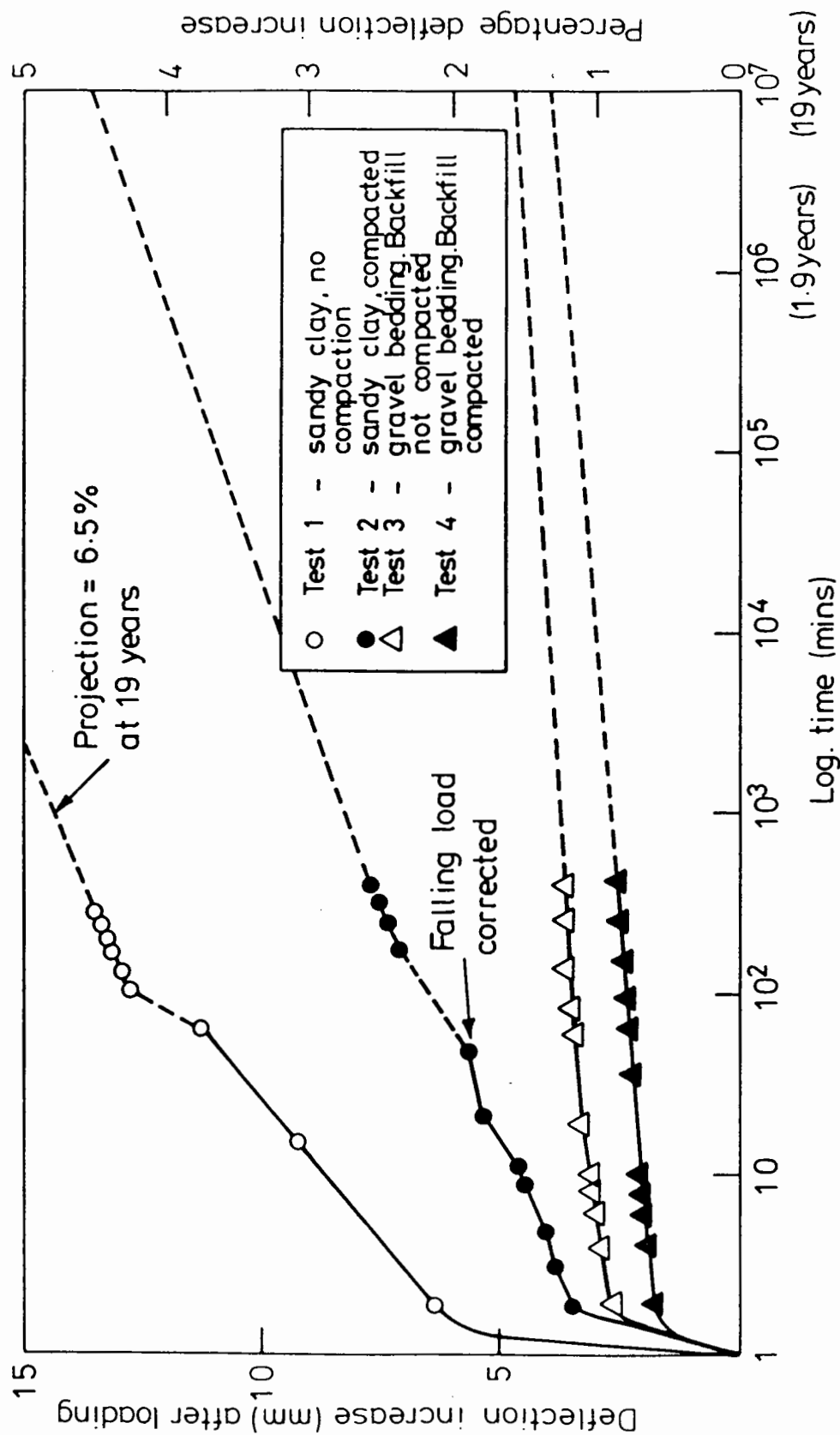
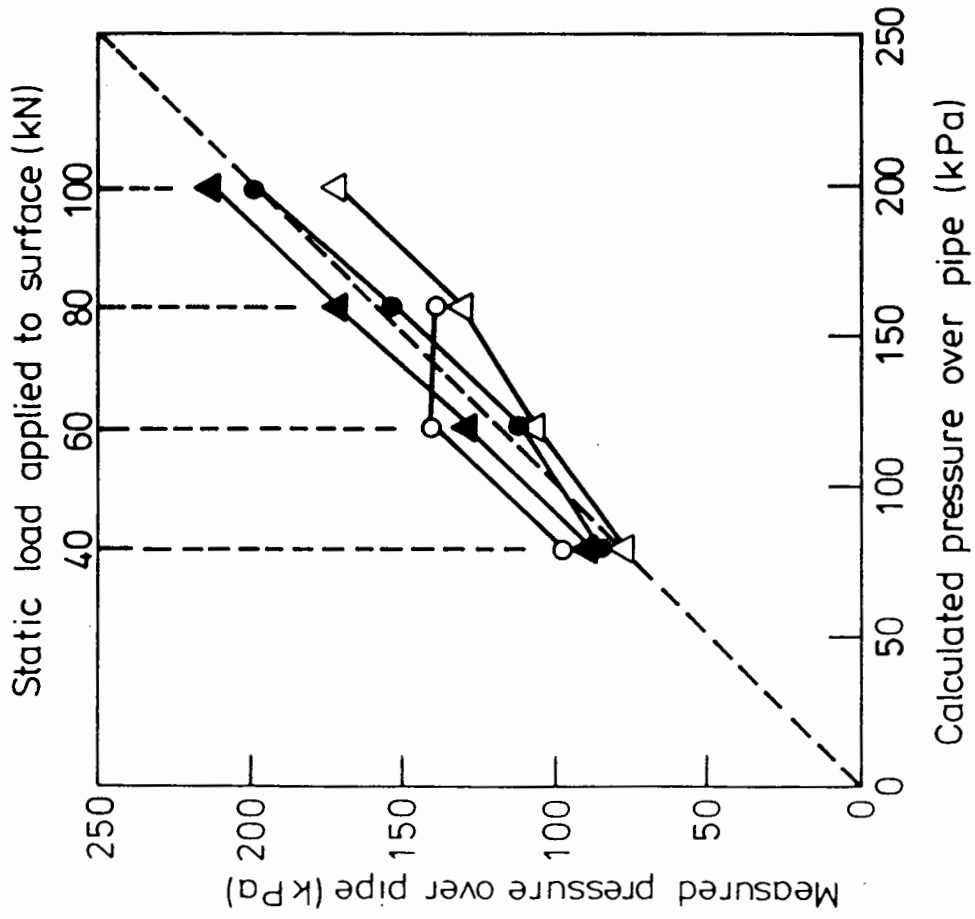
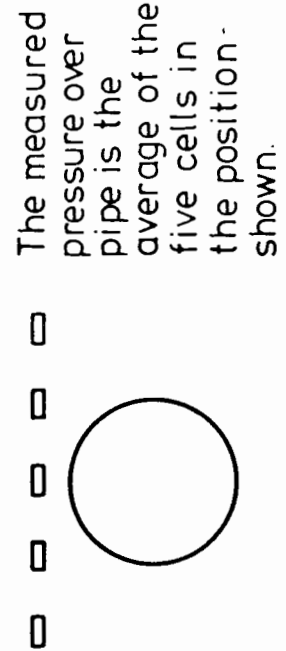


Fig. 2.24 Creep\* Effects of 300mm Diameter uPVC Pipes due to a Sustained Load of 100 kN (after Gaunt et al)

\* Gravel will not creep under these levels of load, the increase in deformation reflecting the increase in load reaching the pipe; the increase in deformation of the pipe in clay is primarily caused by consolidation.



- Test 1 - sandy clay, no compaction
- Test 2 - sandy clay, compacted
- △ Test 3 - gravel bedding, Backfill not compacted
- ▲ Test 4 - gravel bedding, Backfill compacted



The calculated pressure over pipe is obtained from the Boussinesq elastic theory and is based upon an average depth of 0.6m to the pressure cells.

Fig 2.25 Comparison of Theoretical and Measured Vertical Pressures (after Gaunt et al)

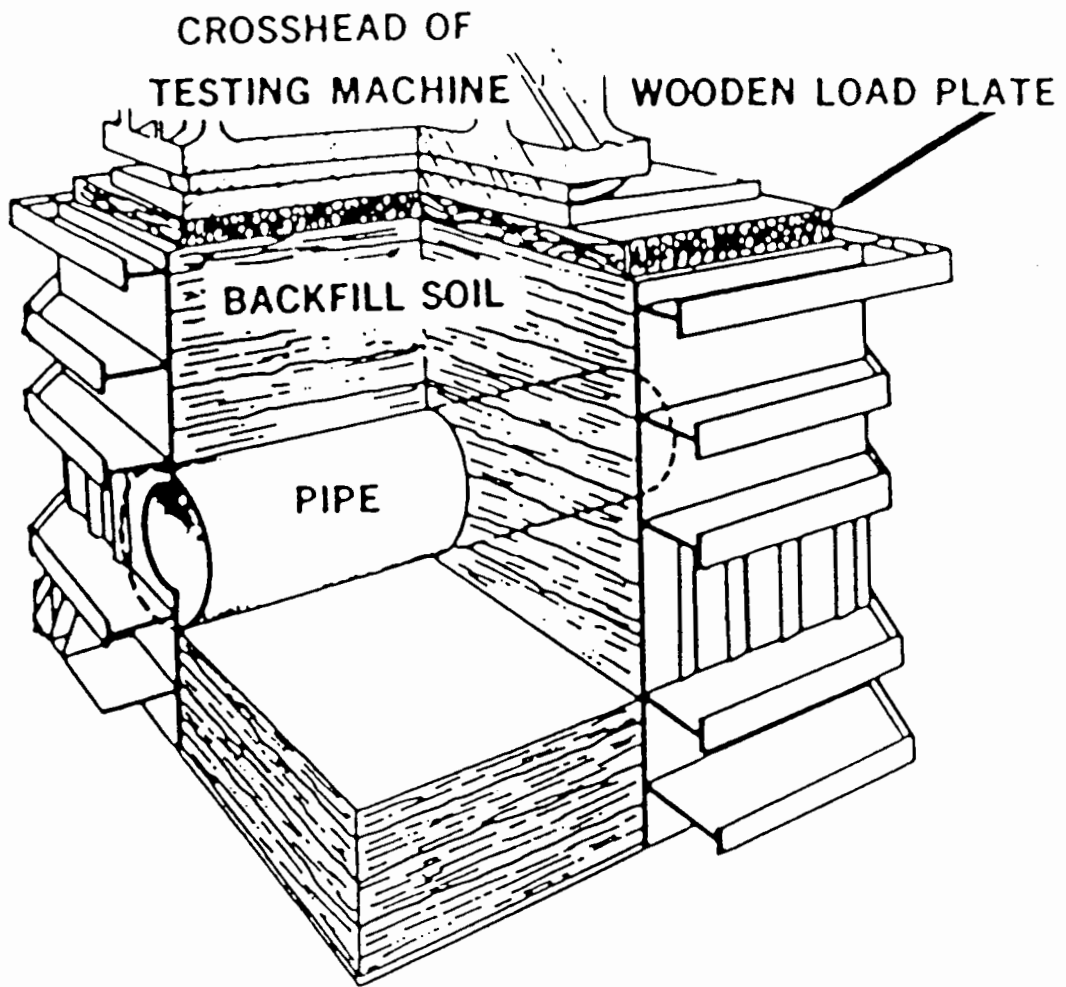
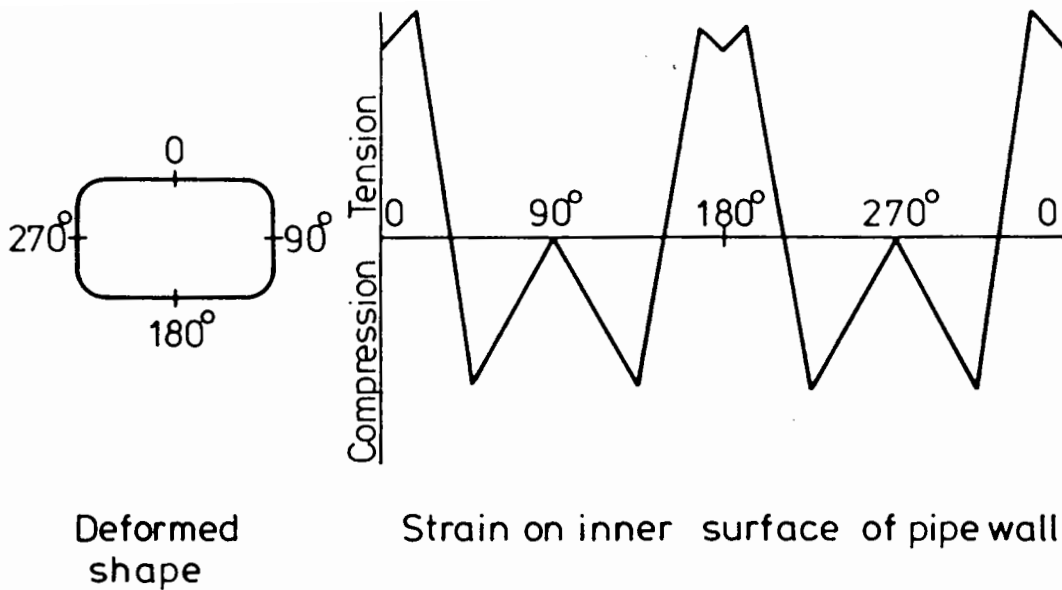
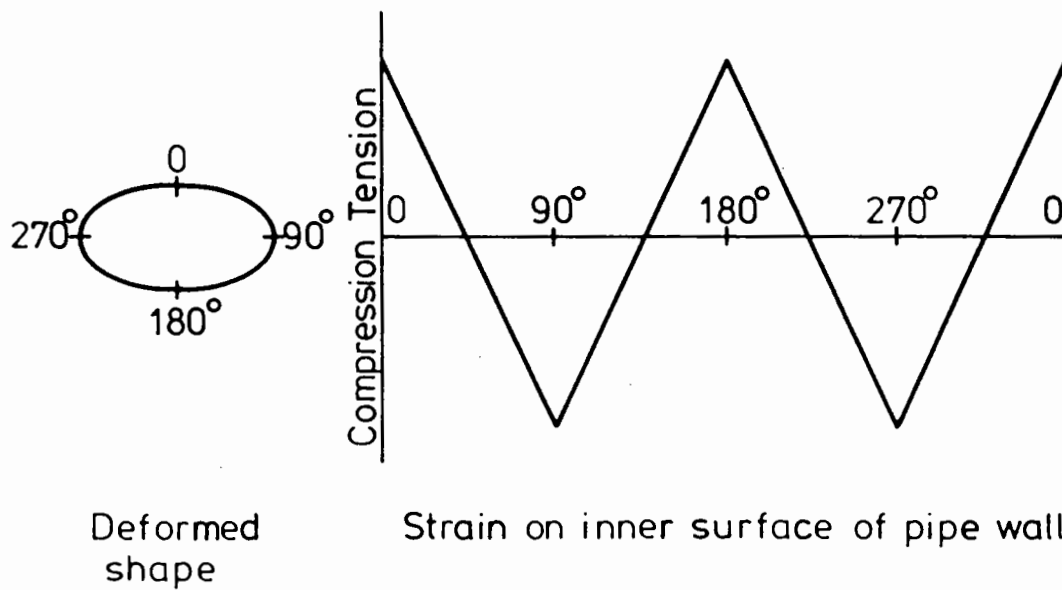


Fig. 2.26 Howard's Test Facility



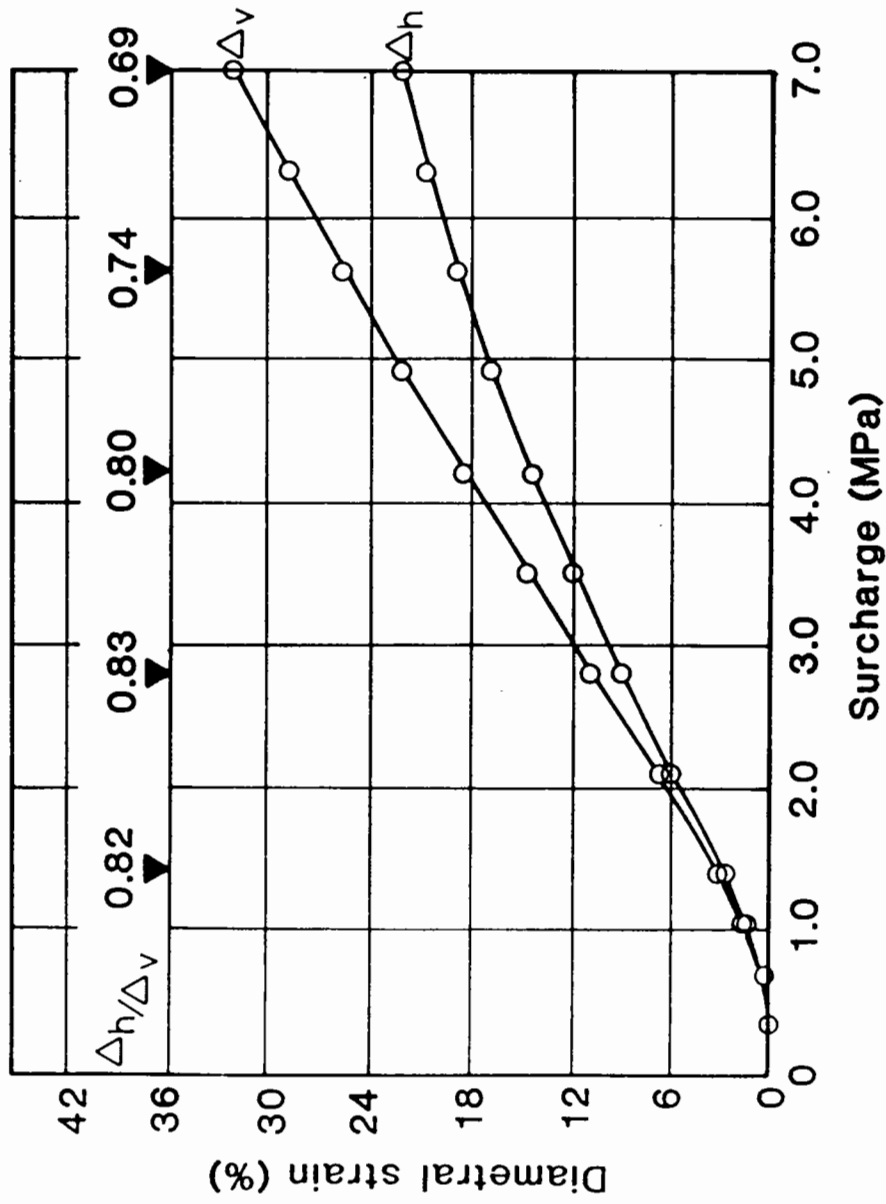
(a) Rectangular Pipe Deformation



(b) Elliptical Pipe Deformation

Fig. 2.27 A Comparison of Strain Profiles for Rectangular and Elliptical Pipe Deformations (after Howard 1972A)





$$E_p/r^3 = 490 \text{ kPa}$$

$\Delta_v$  = Decrease in vertical diametral measurement

$\Delta_h$  = Increase in horizontal diametral measurement

$\Delta_h/\Delta_v$  Deformed shape:

0.91 Ellipse

0.8-0.9 Roughly elliptical

0.6-0.8 Rectangular

Fig. 2.28 Load/Deformation Curves for 380mm Diameter uPVC Pipe (after Howard 1973)

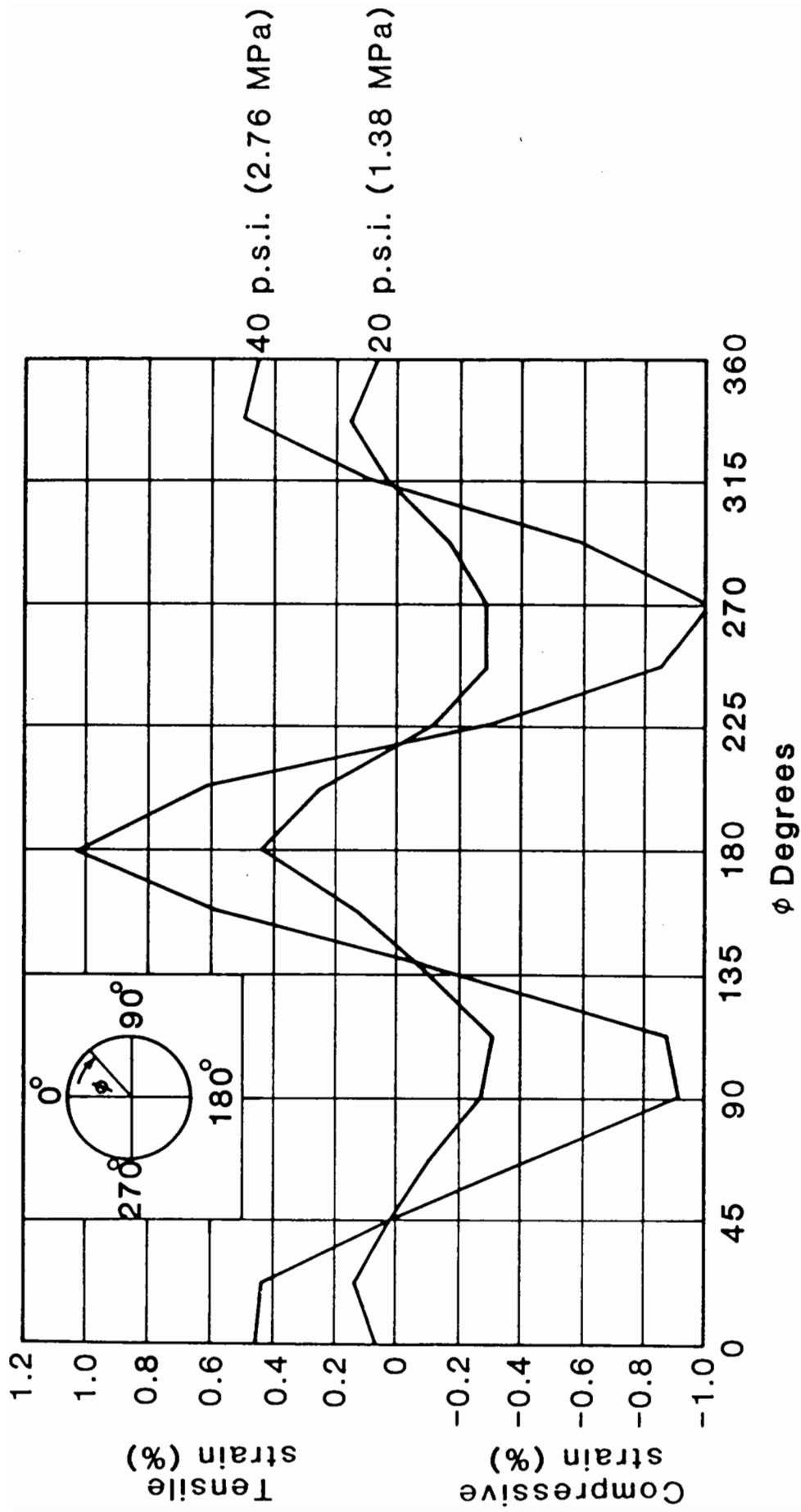


Fig. 2.29 Internal uPVC Pipe Wall Strain Profiles (after Howard 1973)

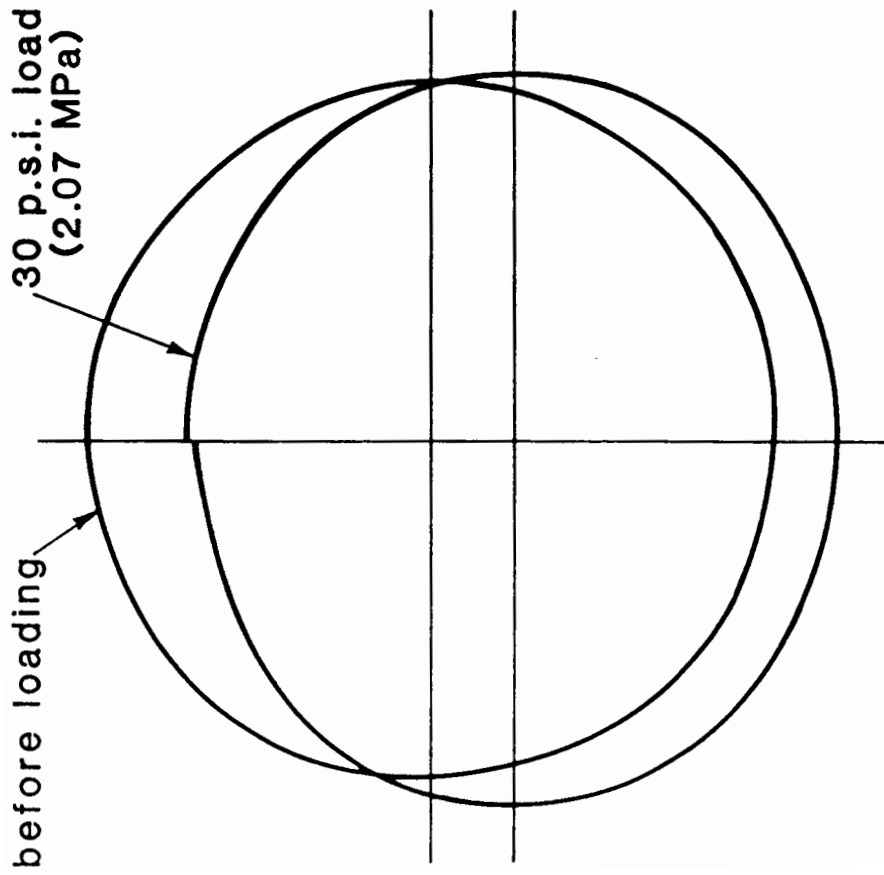


Fig. 2.30 Deformed Shape of uPVC Pipe (after Howard 1973)

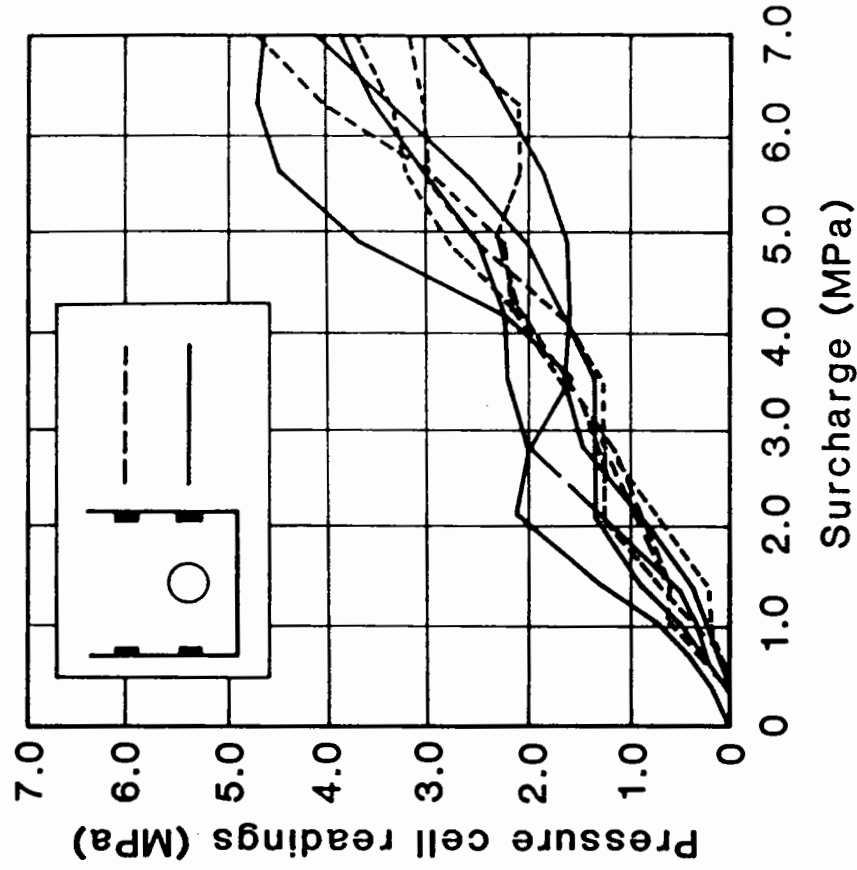


Fig. 2.31 Total Earth Pressures on Box Wall (after Howard 1973)

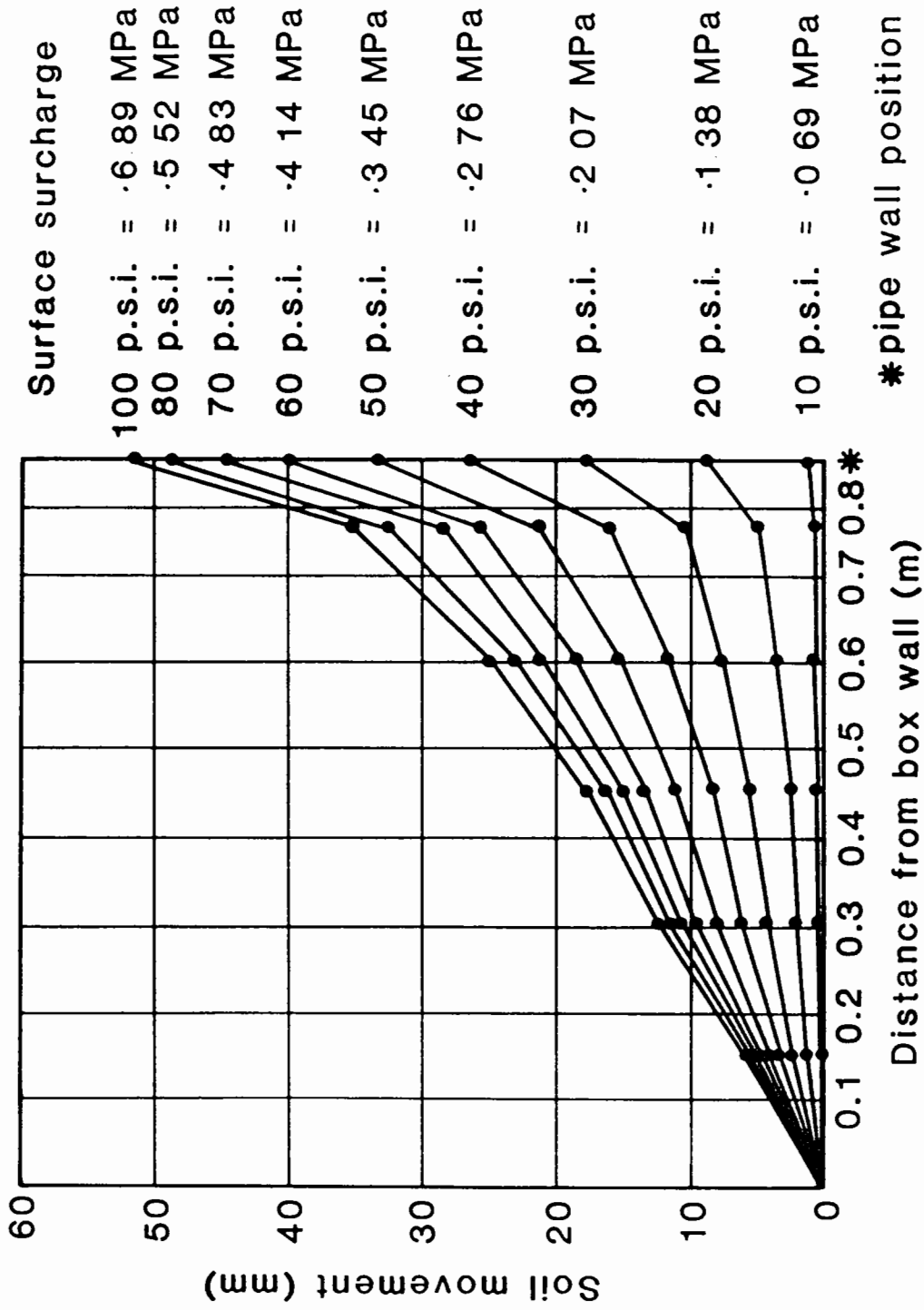
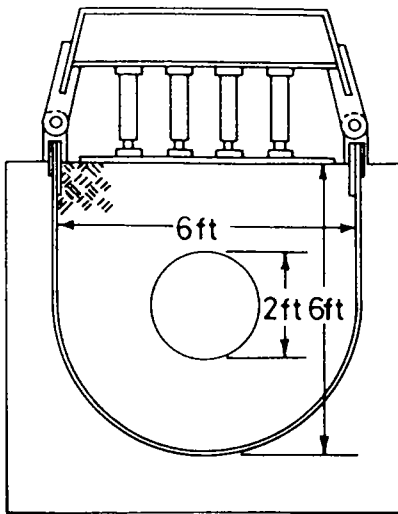
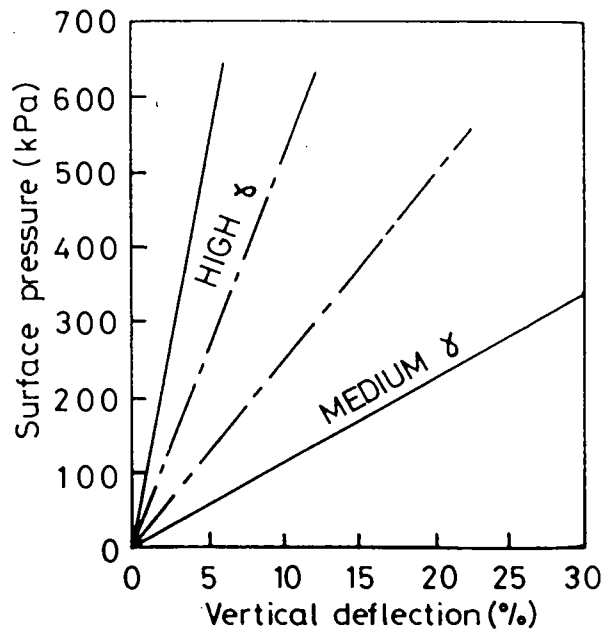


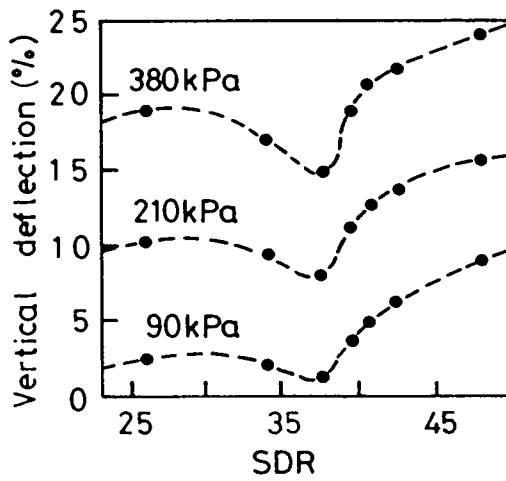
Fig. 2.32 Soil Movement beside a 450mm Diameter PE Pipe (after Howard 1973)



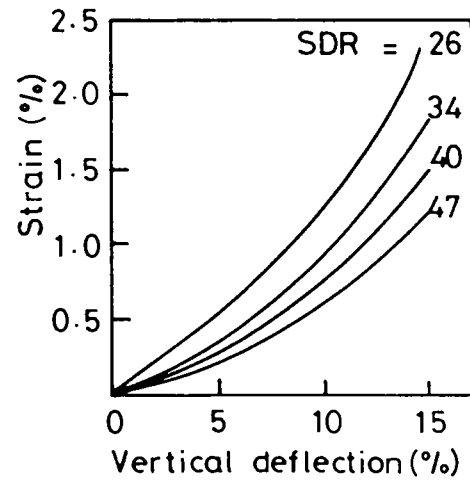
Diagrammatic sketch of the test cell.



Graph of surface pressure against deflection for pipes buried in sand of different densities.

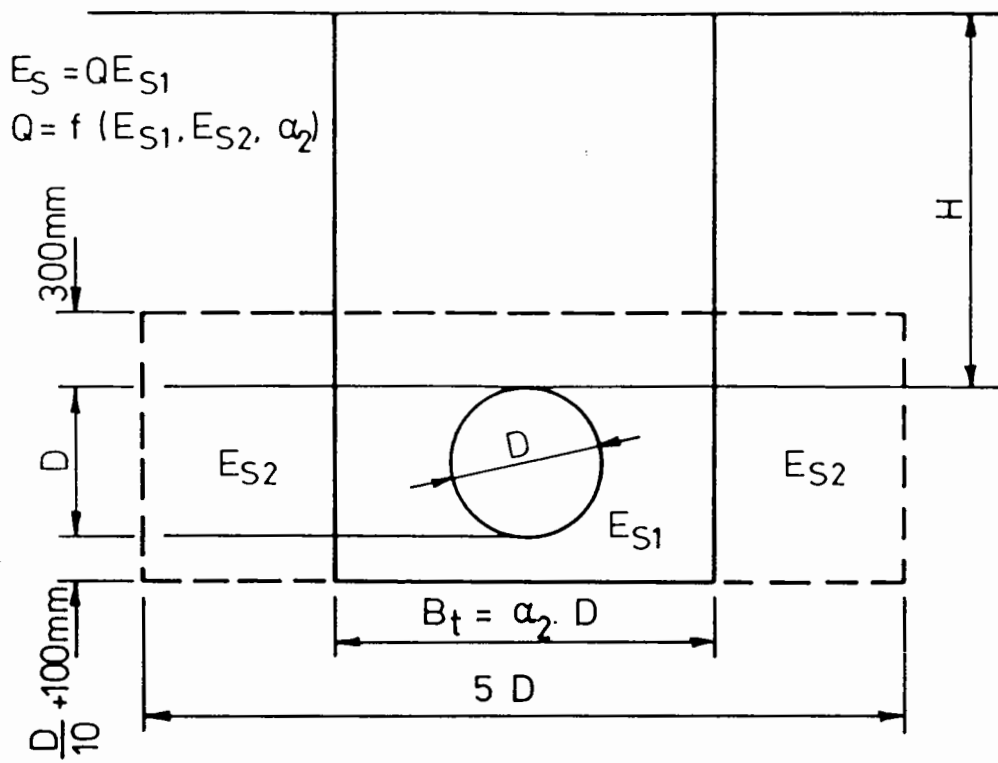


Graph of vertical deflection against pipe flexibility for constant surface pressure.

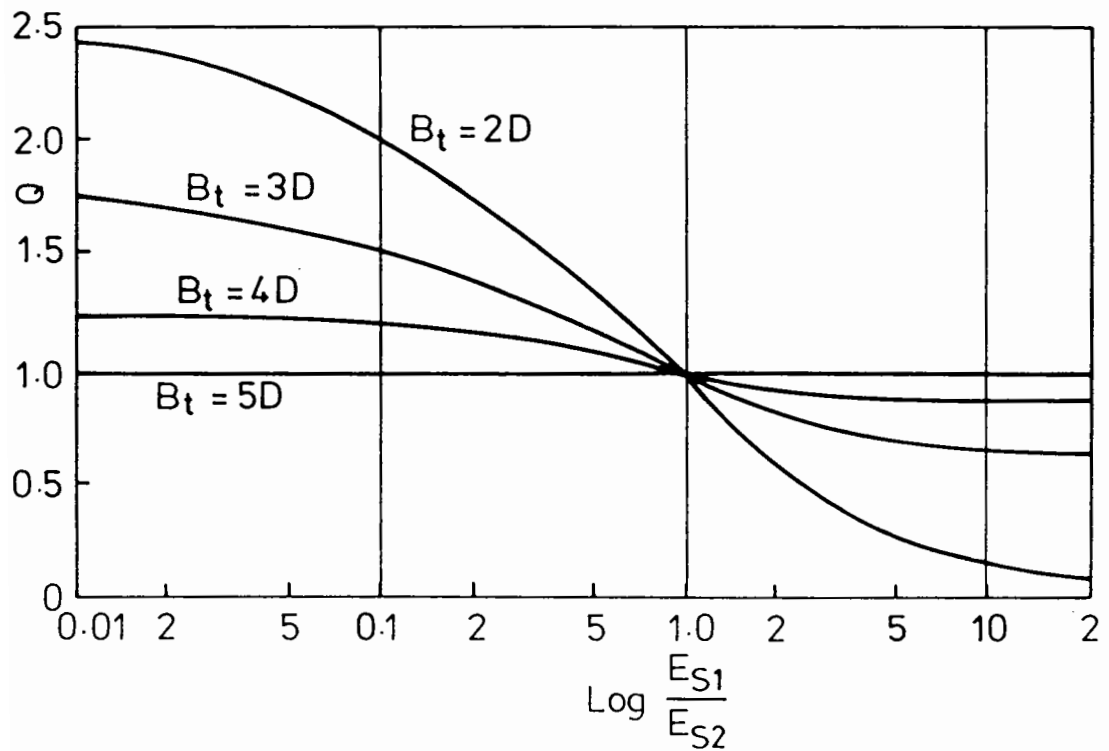


Graph of pipe wall strain at pipe crown against vertical deflection.

Fig. 2.33 Layout and Results of Laboratory Experiments on Buried uPVC Pipe (after Moser et al)

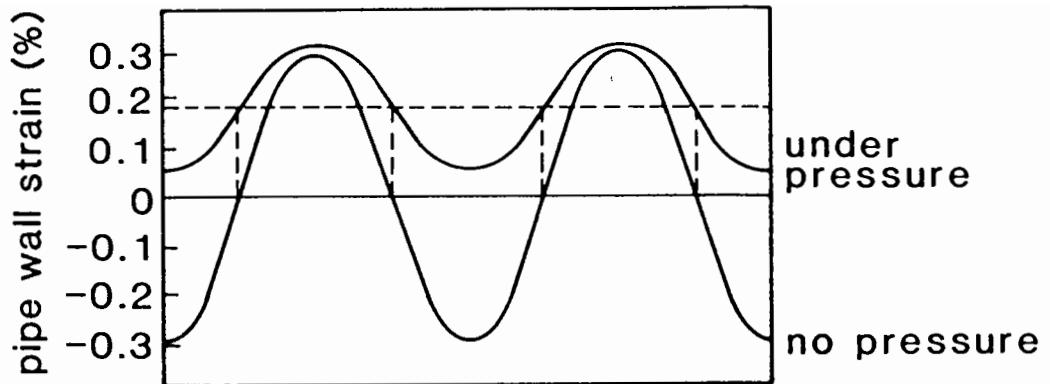


(a) Geometric Characteristics of Trench



(b) Graphical Determination of Soil Stiffness Correction Factor Q

Fig. 2.34 Definition of Soil Stiffness Correction Factor (after Dezsényi)



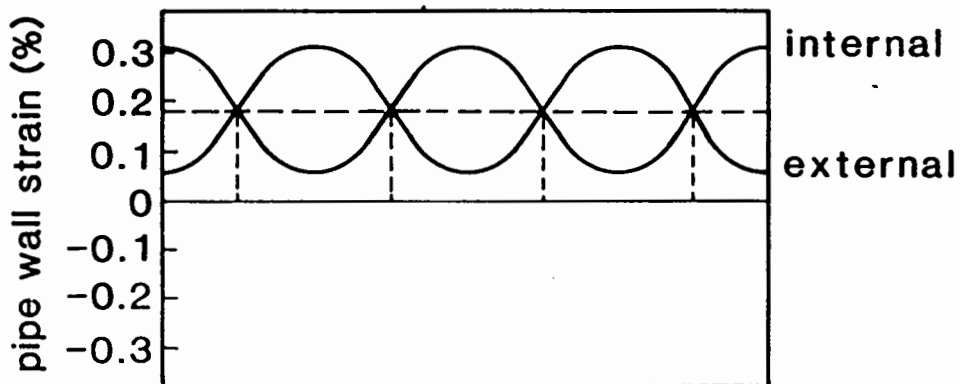
Pipe wall strain measured on external surface

Internal pressure = 0.35 MPa

V.D.S. before pressurisation = 3.5%

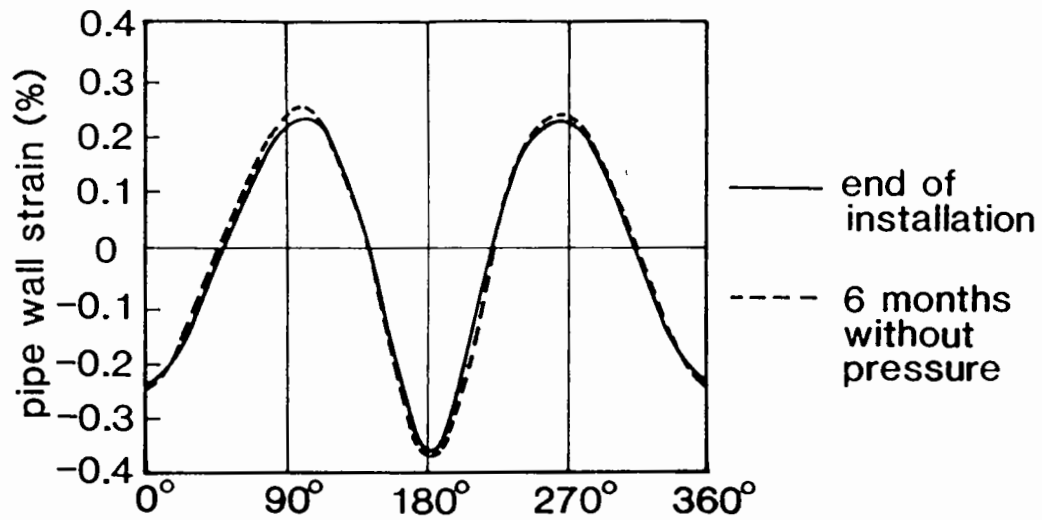
V.D.S. after pressurisation = 1.5%

(a) Influence of internal pressure on an elliptically deformed pipe

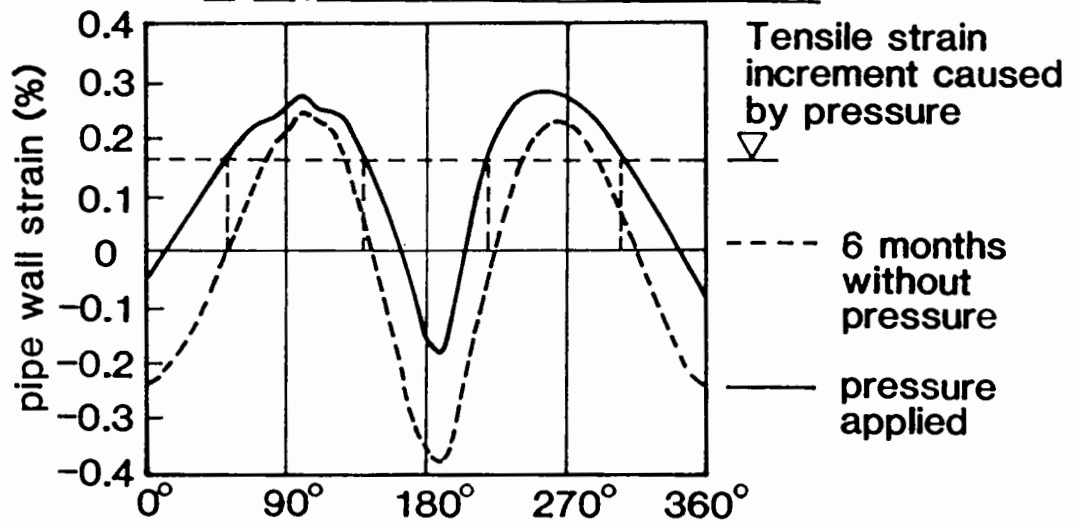


(b) Assumed pressure distributions on internal and external pipe surfaces

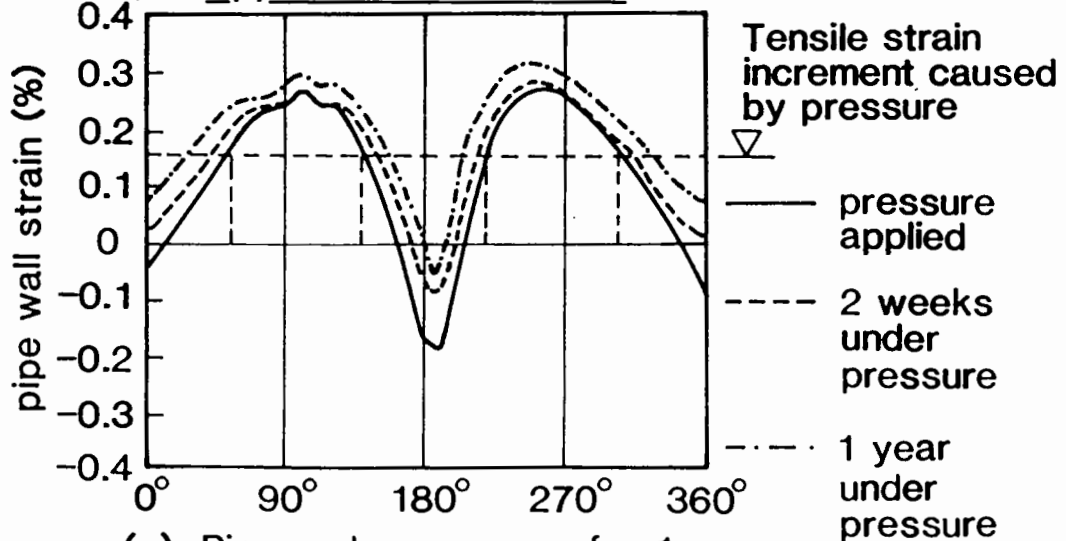
Fig. 2.35 Typical Strain Profiles (after Broere)



(a) Pipe pressureless for 6 months



(b) Application of Pressure



(c) Pipe under pressure for 1 year

Fig. 2.36 Pipe Wall Strain Profiles of 500 mm Diameter uPVC Pipe in Uncompacted Sand (after Broere)



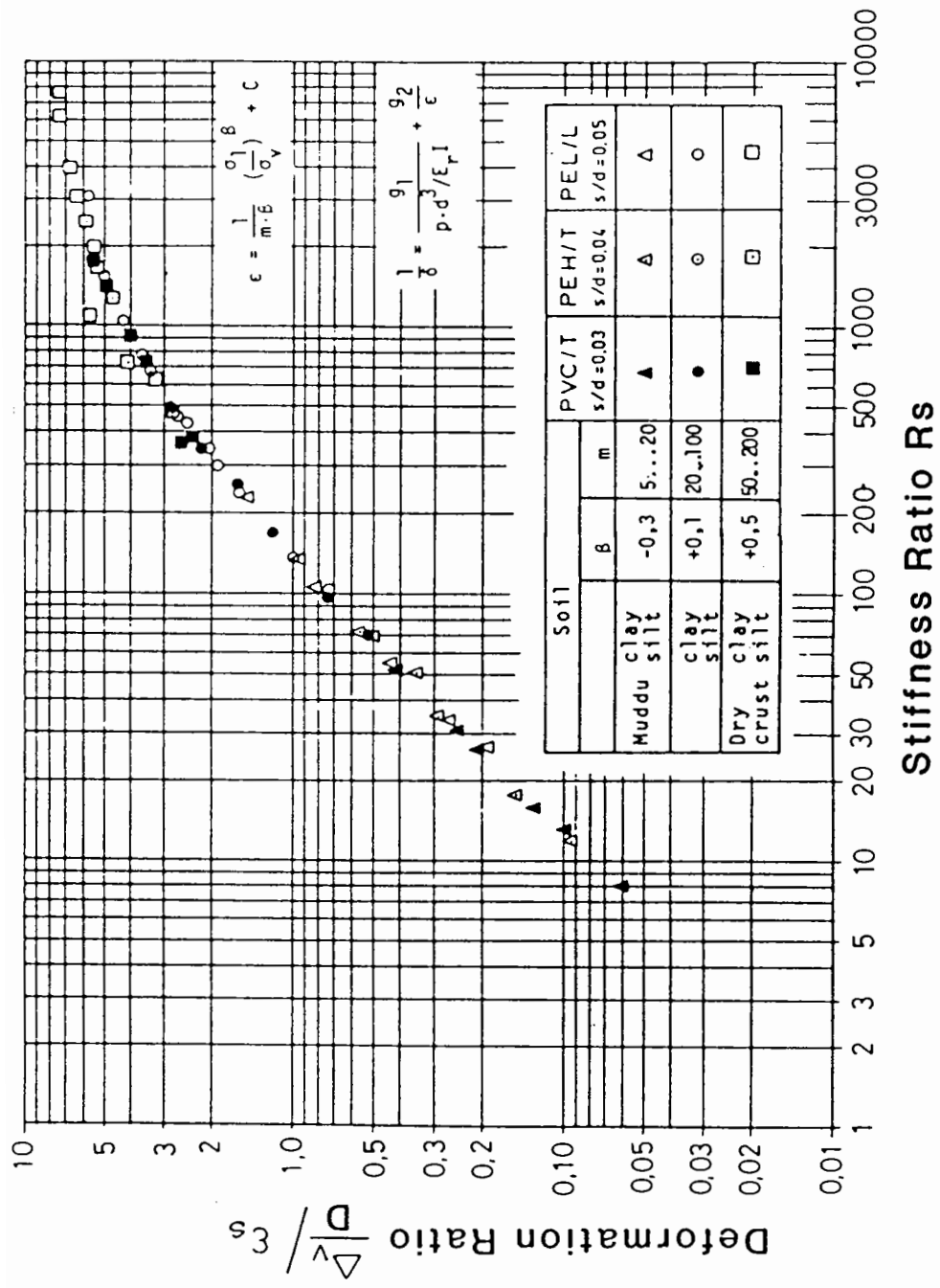
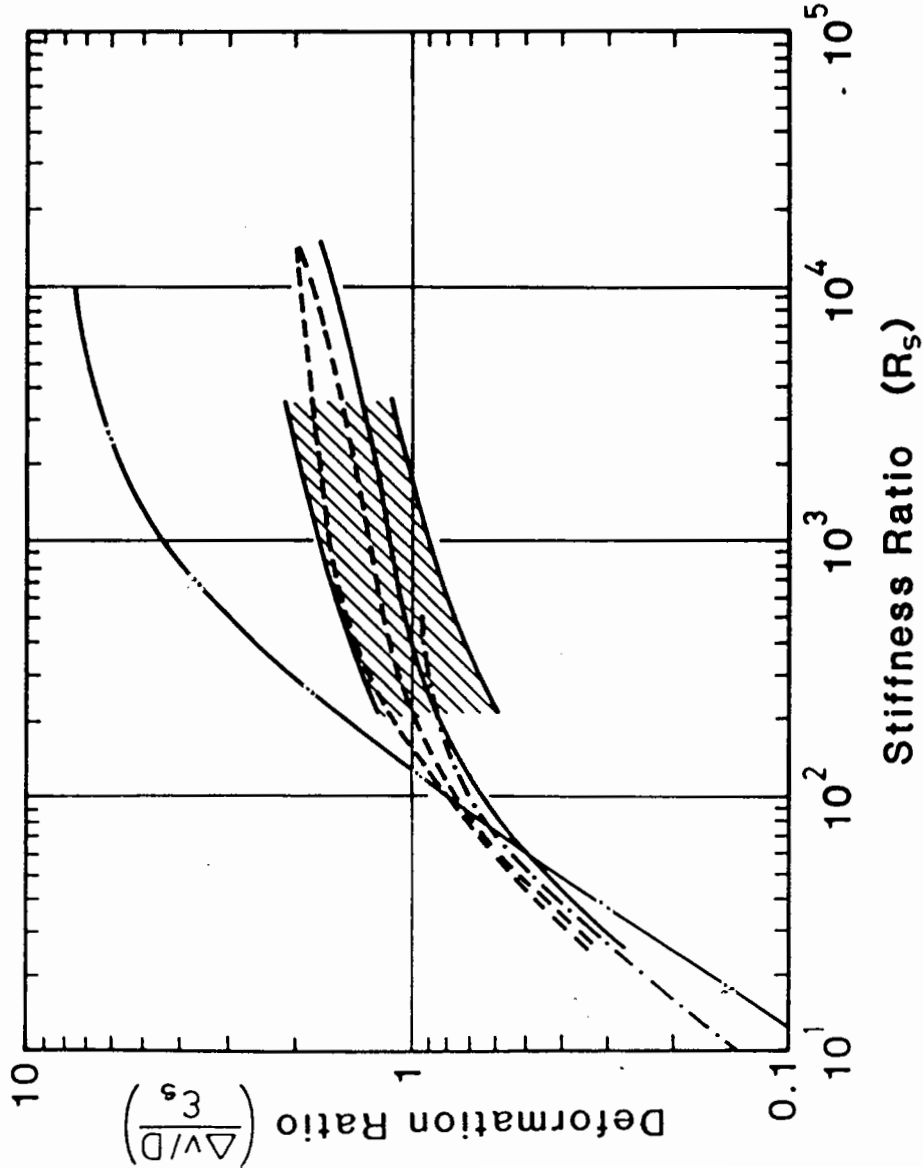


Fig. 2.37 Graph of Deformation Ratio against Stiffness Ratio (after Soini 1982A)



Empirical envelope for MDPE pipes in sand (Gaube, 1977)

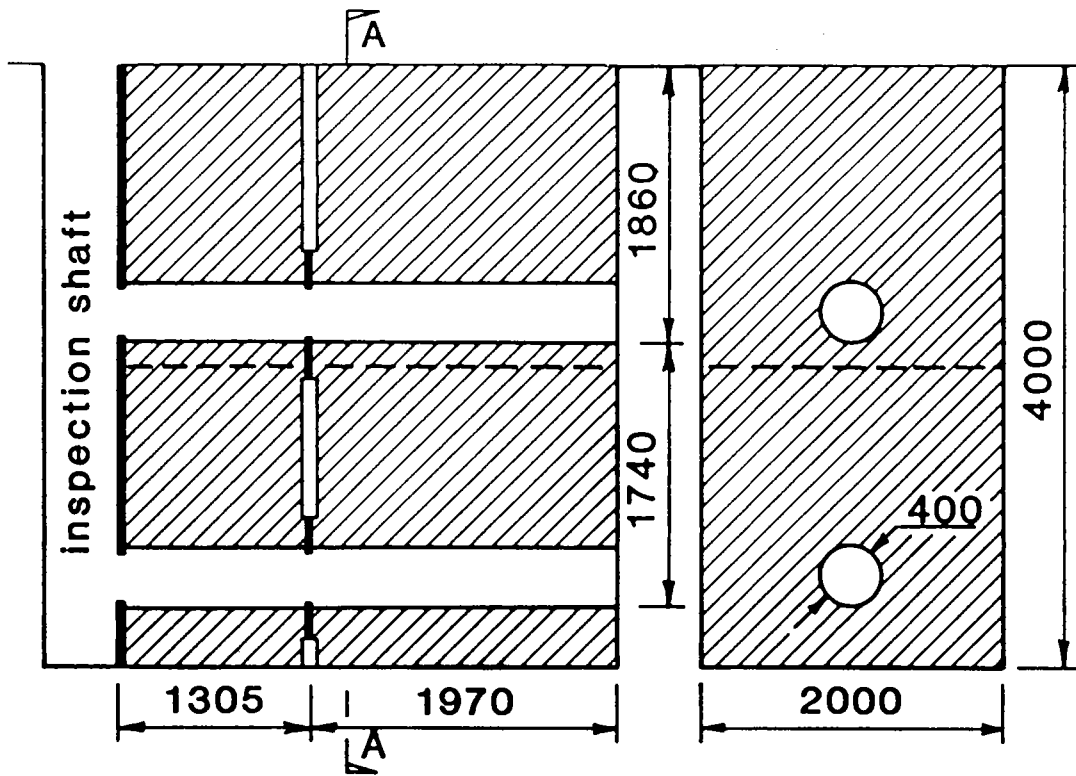
Corresponding theoretical envelope (Burns & Richards, 1964) assuming full slippage and  $0.3 \leq K \leq 0.5$

Alternative theoretical lower bound assuming no slippage

Watkins' empirical curve (see Fig. 2.10). Steel pipe in fine sand

Theoretical curve for thermoplastics pipe in soft soils (Soini, 1982)

Fig. 2.38 Combination of Deformation Ratio against Stiffness Ratio Data (after Gumbel)

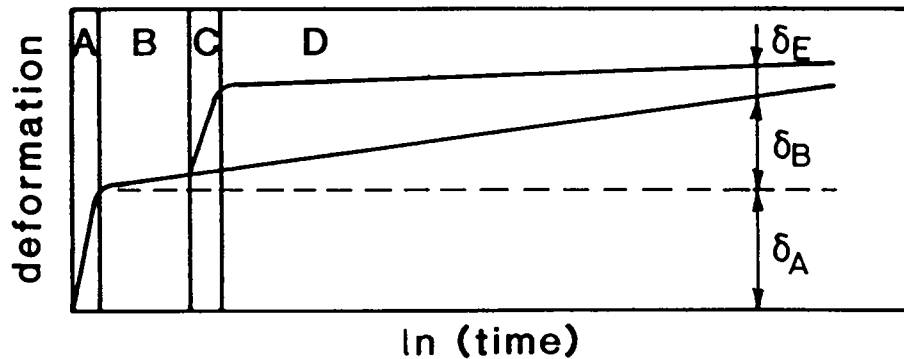


(a) Elevation

(b) Section AA

All dimensions are in millimetres

Fig. 2.39 Soini's Experimental Facility



A installation produces deformation  $\delta_A$

B soil consolidation produces  $\delta_B$

C traffic load applied

D further consolidation

} increase of  $\delta_E$

Fig. 2.40 S Shape Deformation Curve (Gehrels and Elzink 1979)

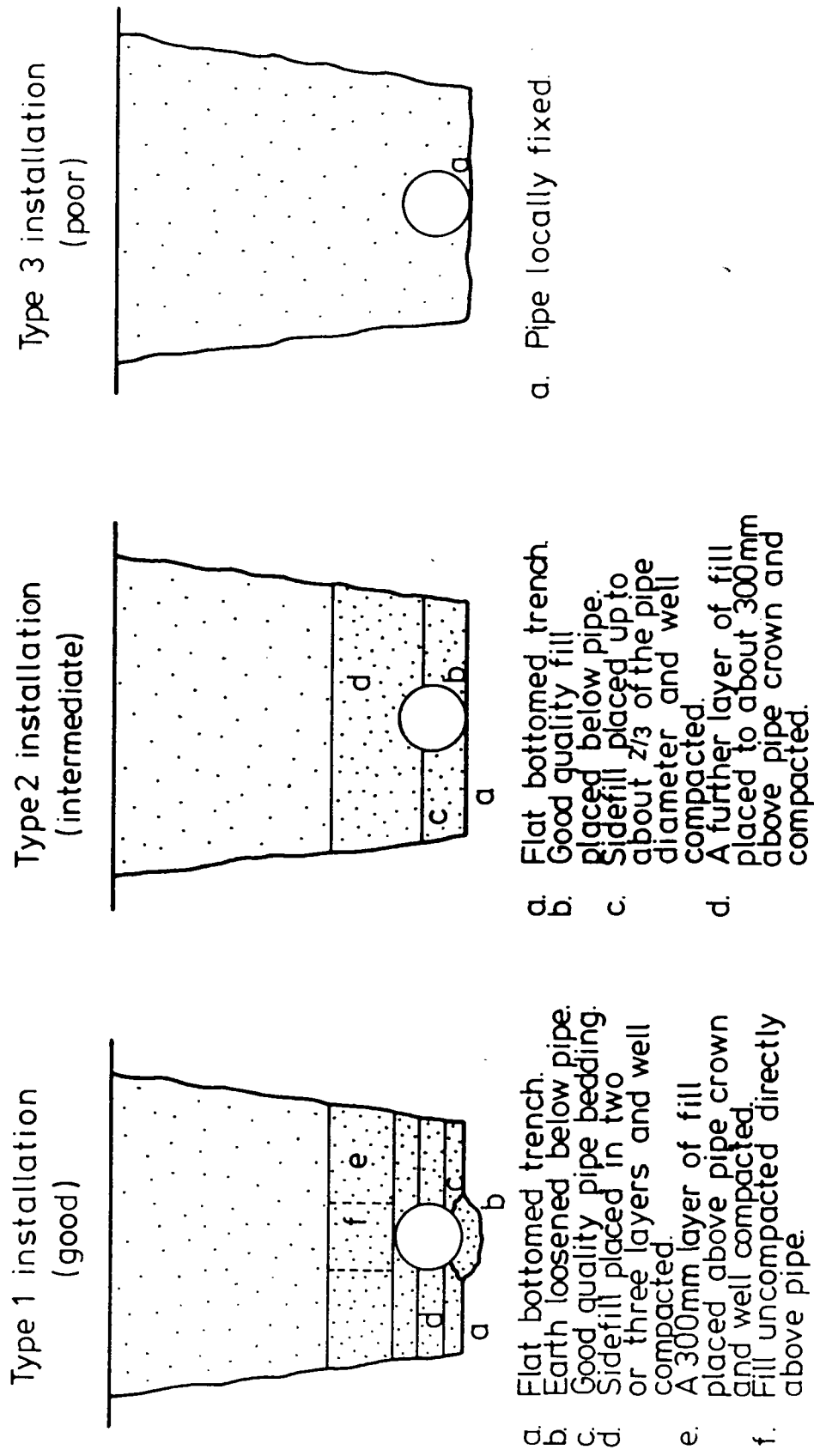


Fig. 2.41 Definition of Installation Types (after Gehrels and Elzink 1981)

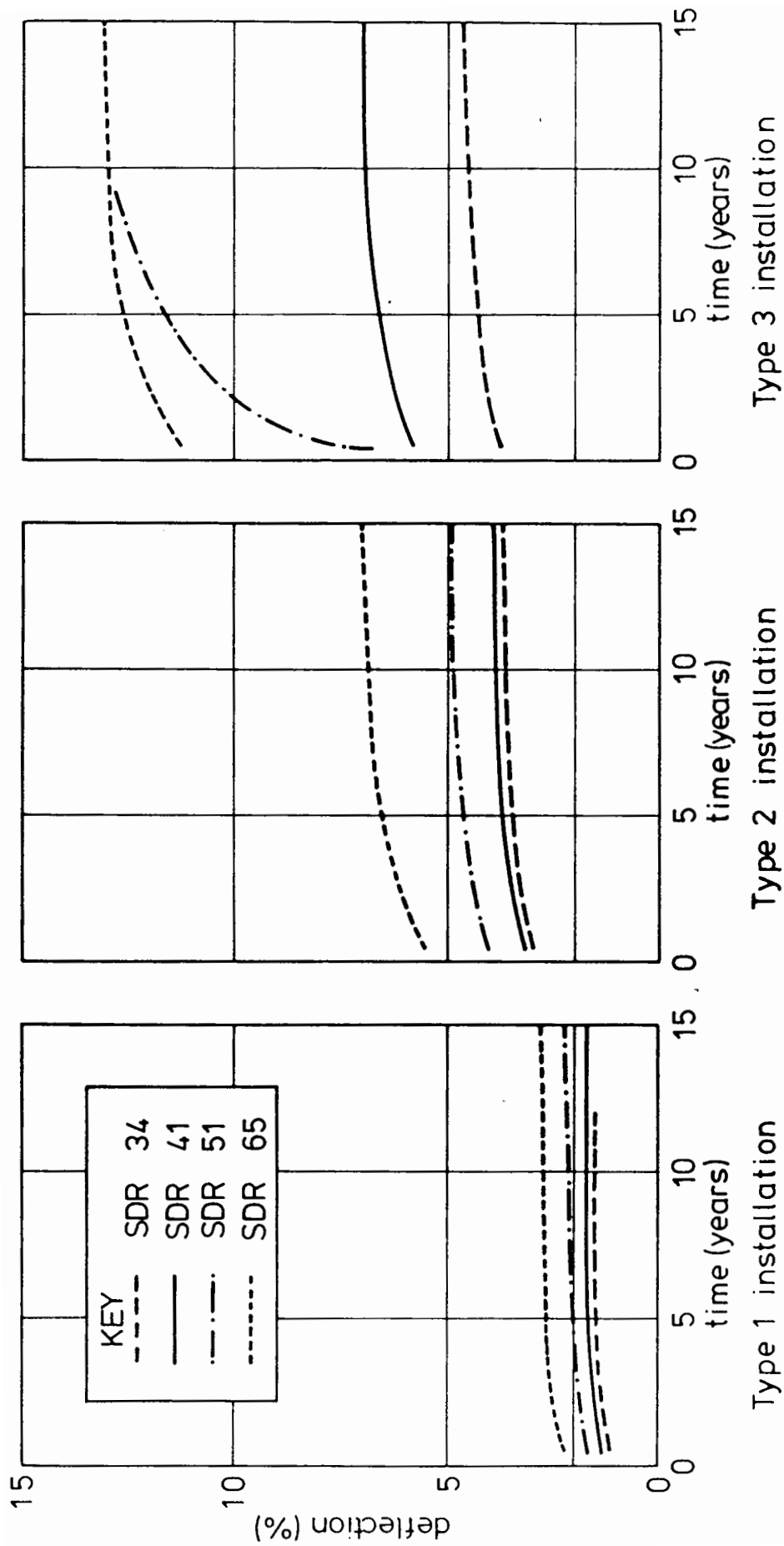


Fig. 2.42 The Influence of Installation Type and Pipe Class on the Deformation of uPVC Pipes in Sand Surrounds (after Gehrels and Elzink 1981)

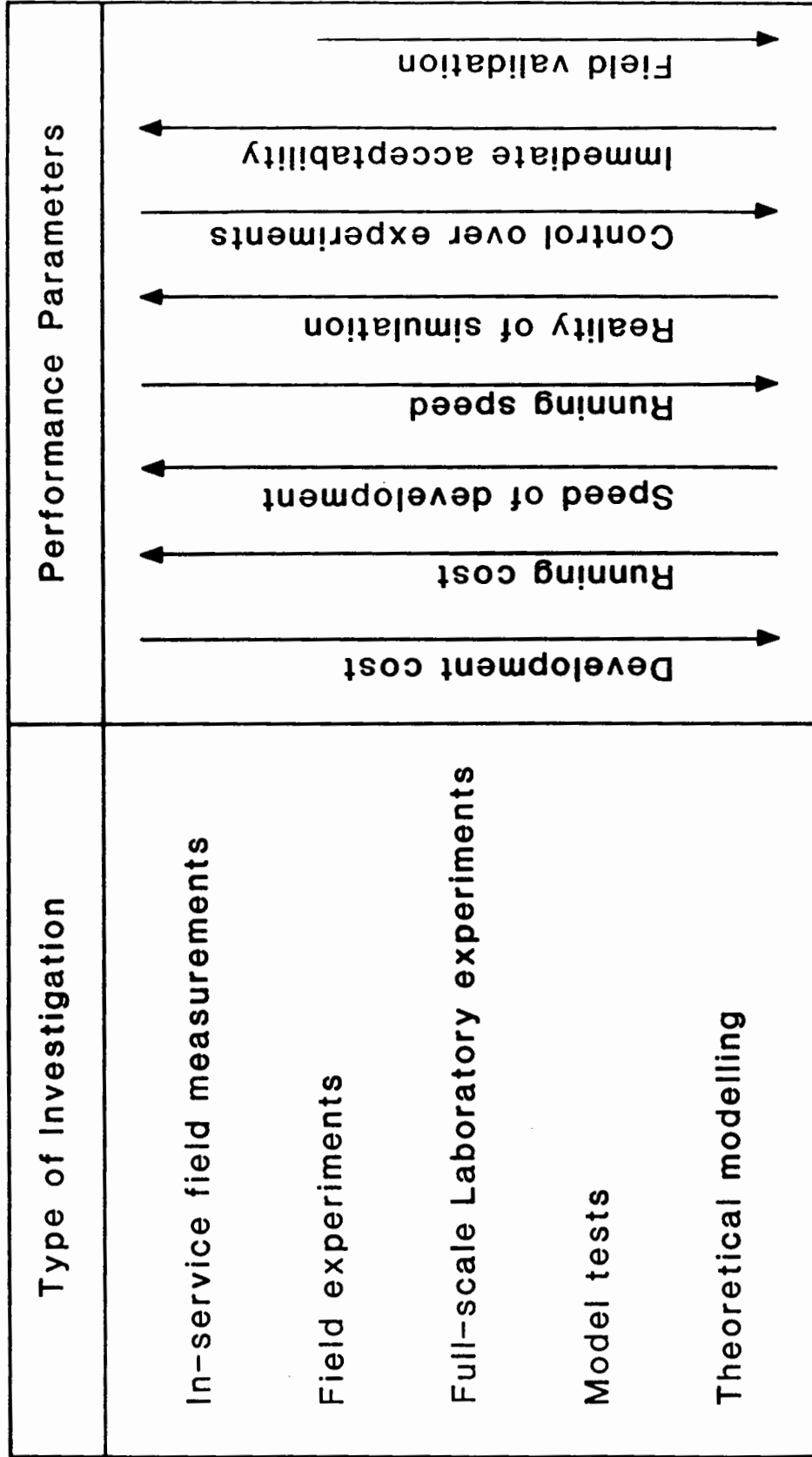
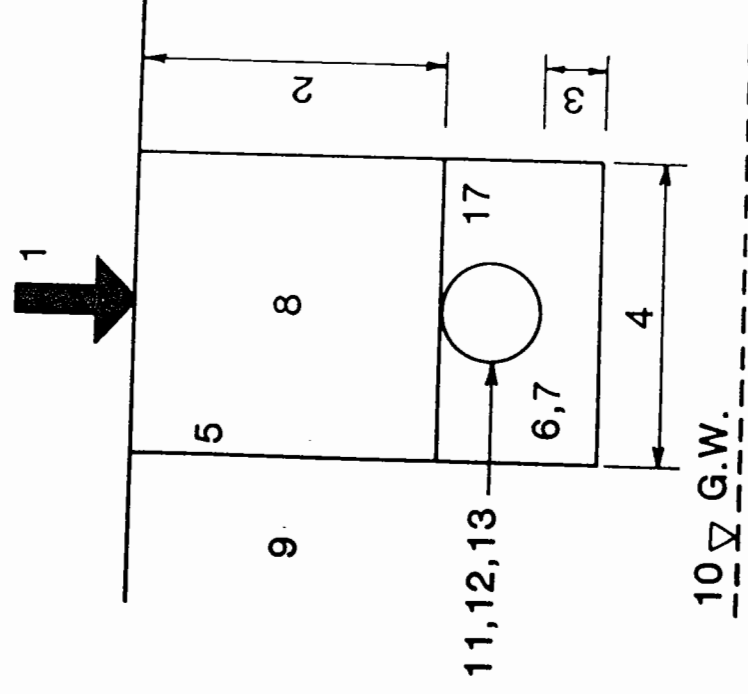
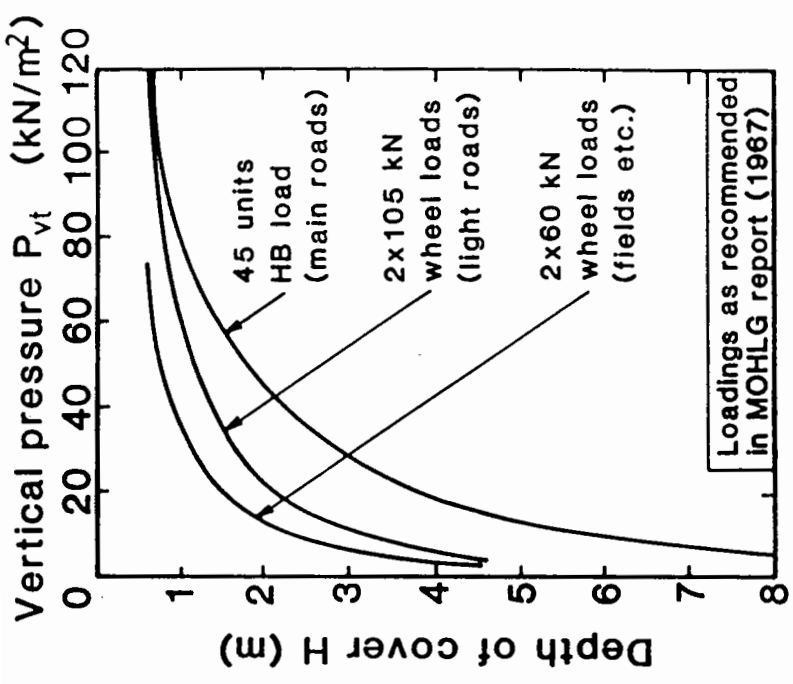


Fig. 3.1 Methods of Investigation

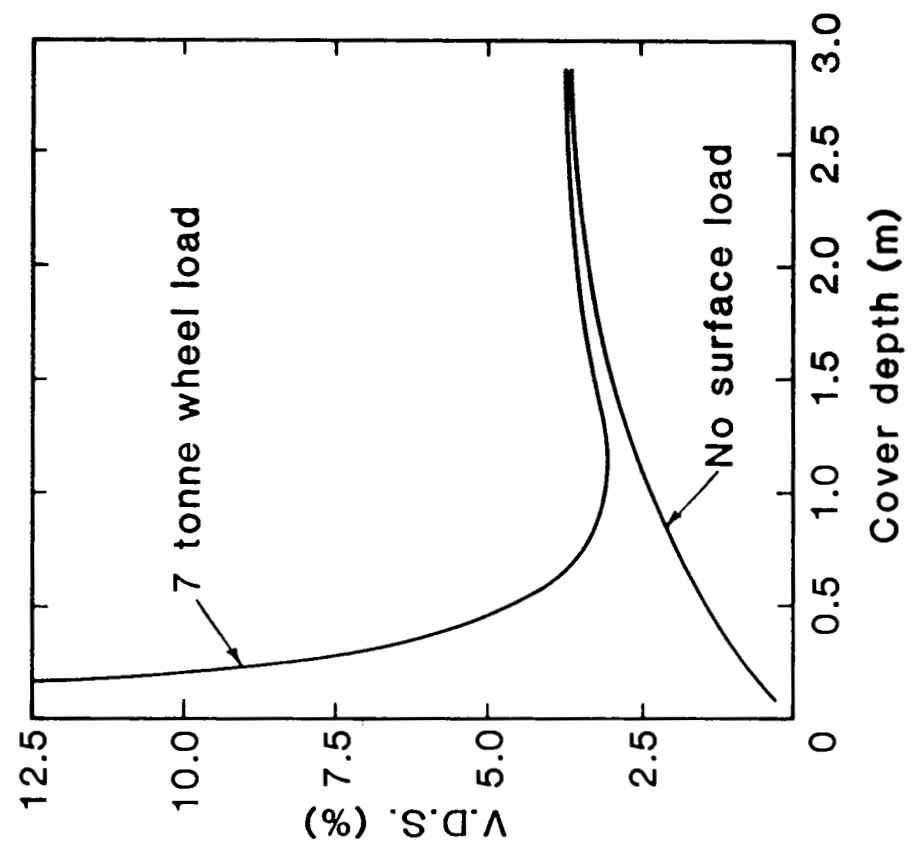
1. Surface load
2. Ratio of cover depth to pipe diameter
3. Ratio of bedding thickness to pipe diameter
4. Ratio of bench width to pipe diameter
5. Shape of trench
6. Type of bedding and sidefill
7. Method of laying bedding and sidefill
8. Type and method of laying backfill
9. Type and state of in situ soil
10. Groundwater level
11. Quality of pipe material
12. Pipe class (or S.D.R.)
13. Pipe abnormalities
14. Longitudinal bending effects
15. Temperature
16. Time
17. Settlement of pipe and fill



**Fig. 3.2 Factors Influencing Pipe Deformation**



$P_{vt}$  = maximum vertical pressure at depth caused by standard traffic loads in U.K



(a) Behaviour suggested by Gehrels (1982) (b) MOHLG's findings (after Gumbel)

Fig. 3.3 The Variation of Surface Load with Depth



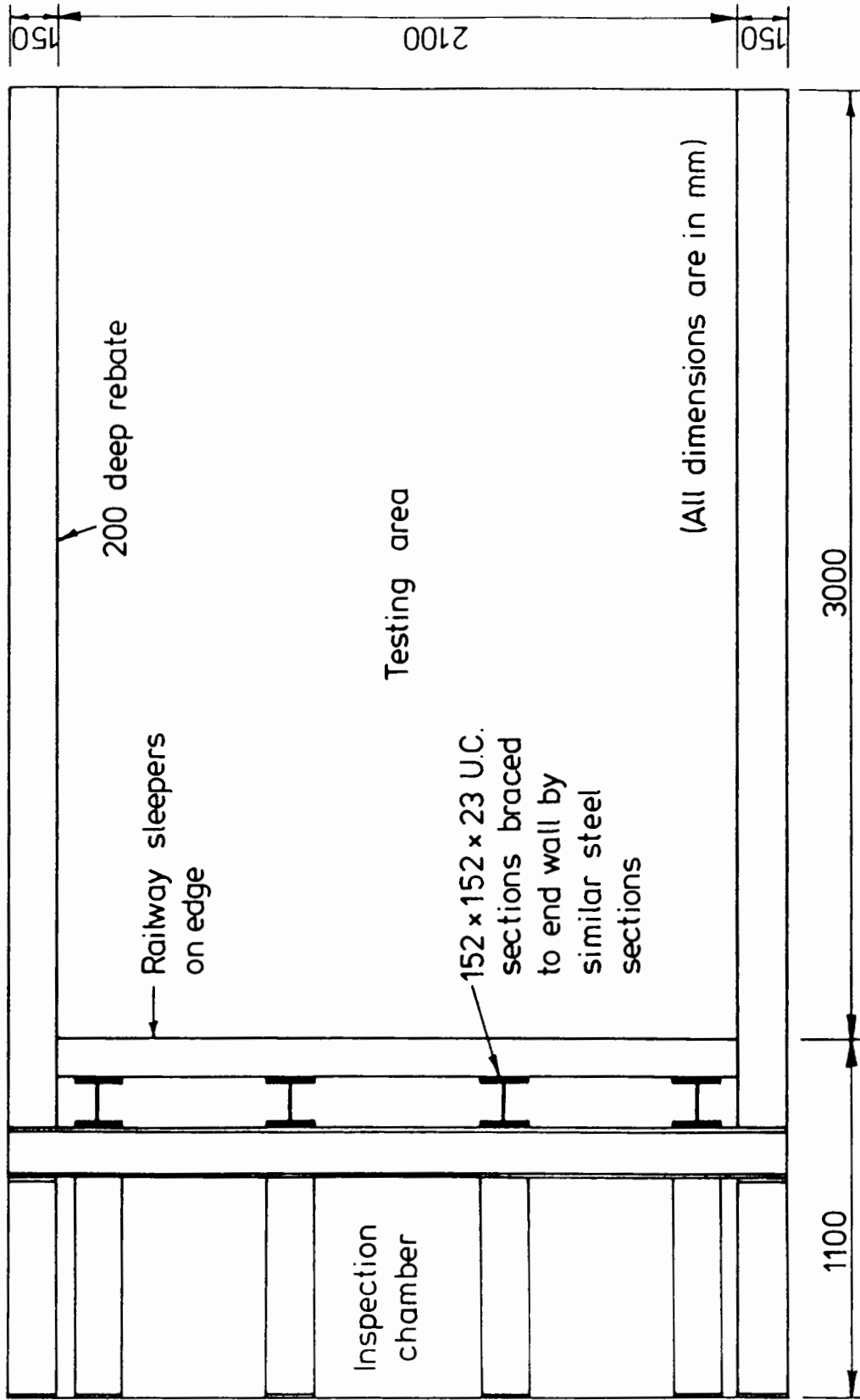
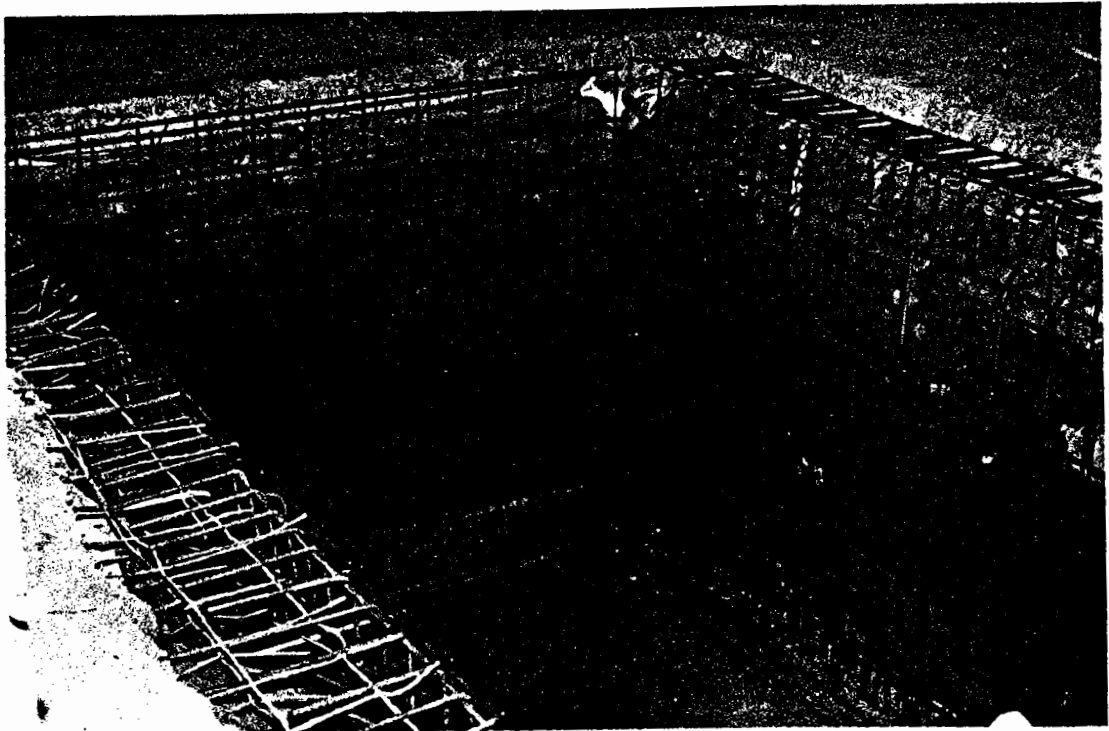
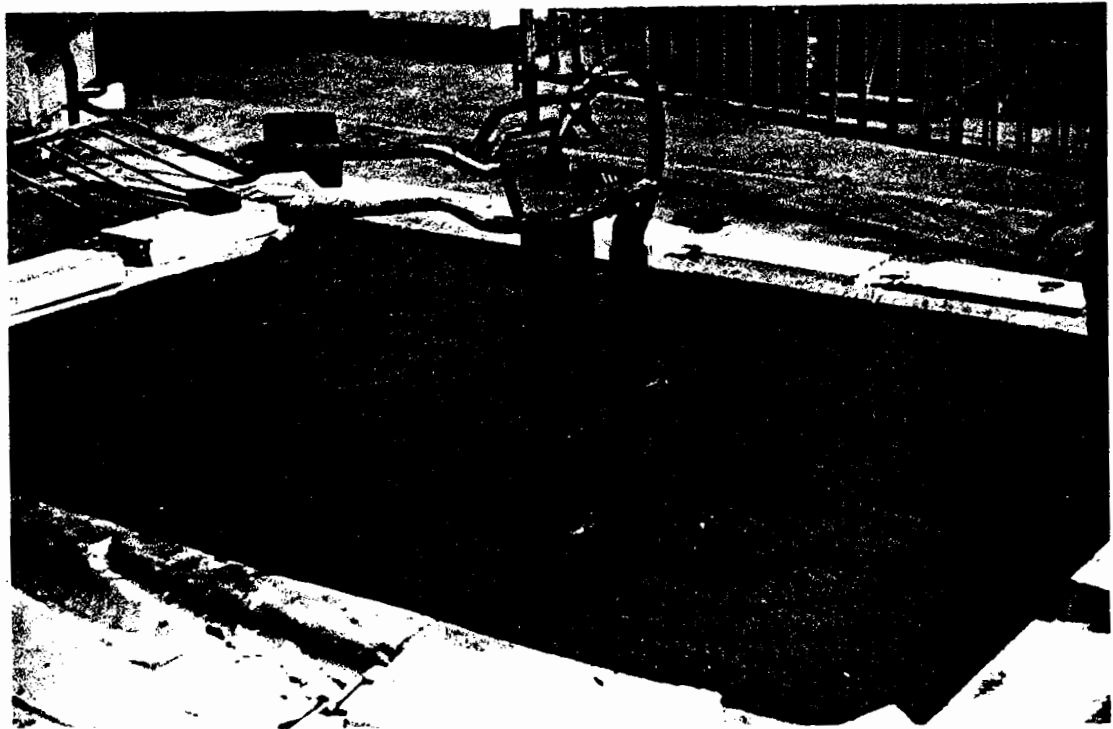


Fig. 4.1 Plan of Test Pit





**Fig. 4.3 The Test Pit Under Construction**

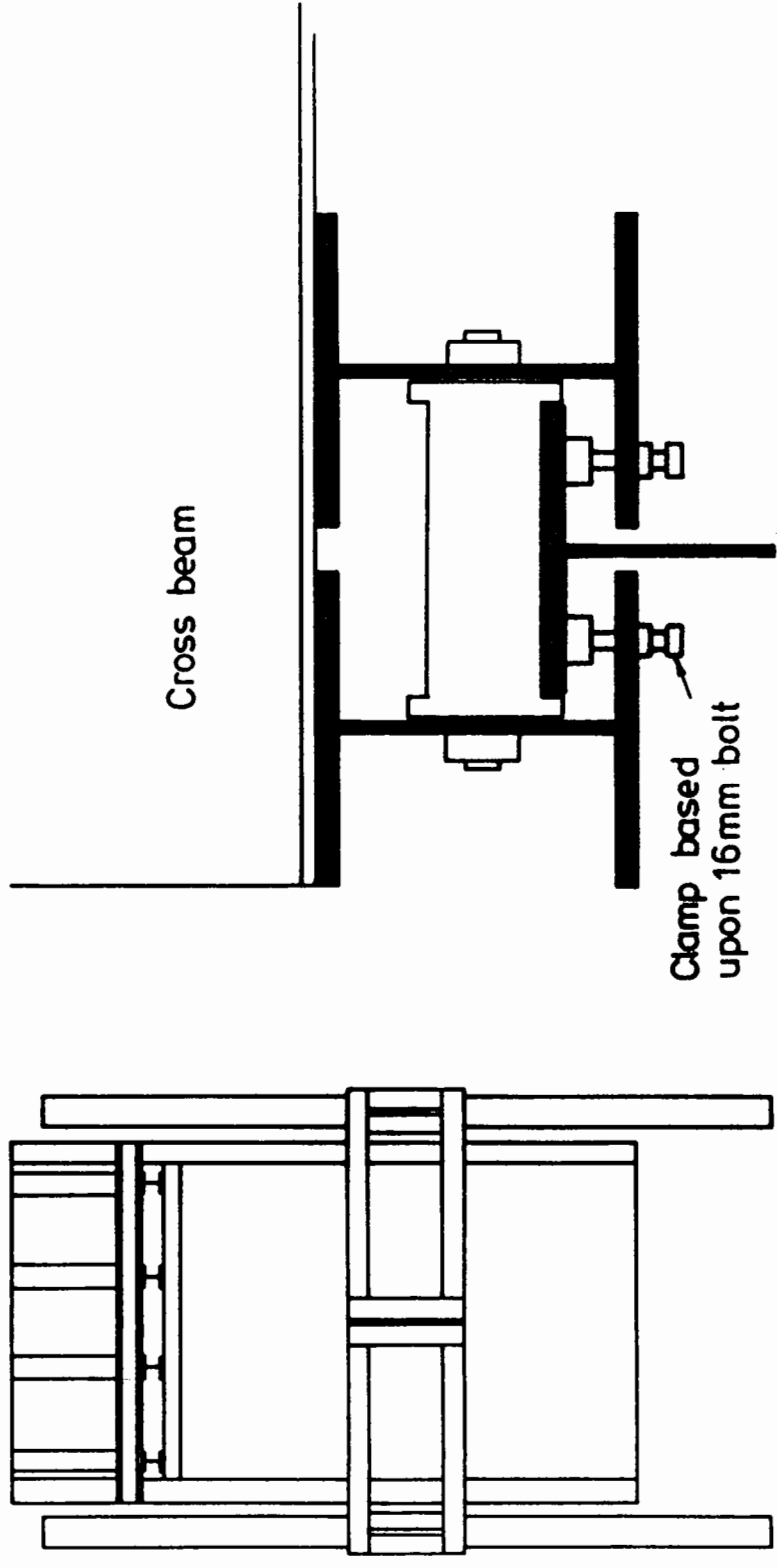


**4.4 The Triple Headed Pneumatic Tamper used to Compact the Keuper Marl in the Pit**





**Fig. 4.6 The Result of a Single Pass of the Triple Headed  
Tamper on the Keuper Marl Bricks**



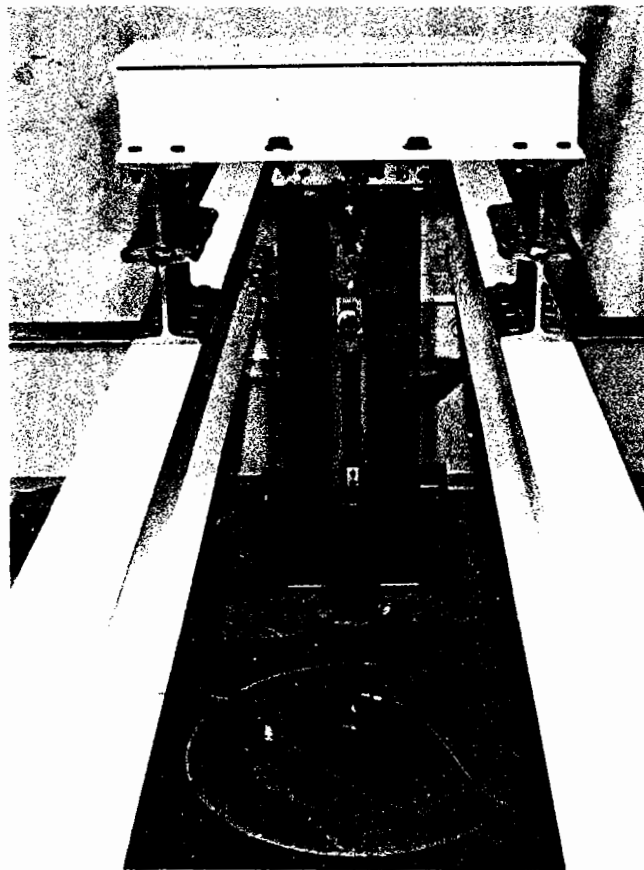
(a) Plan

(b) Roller arrangement

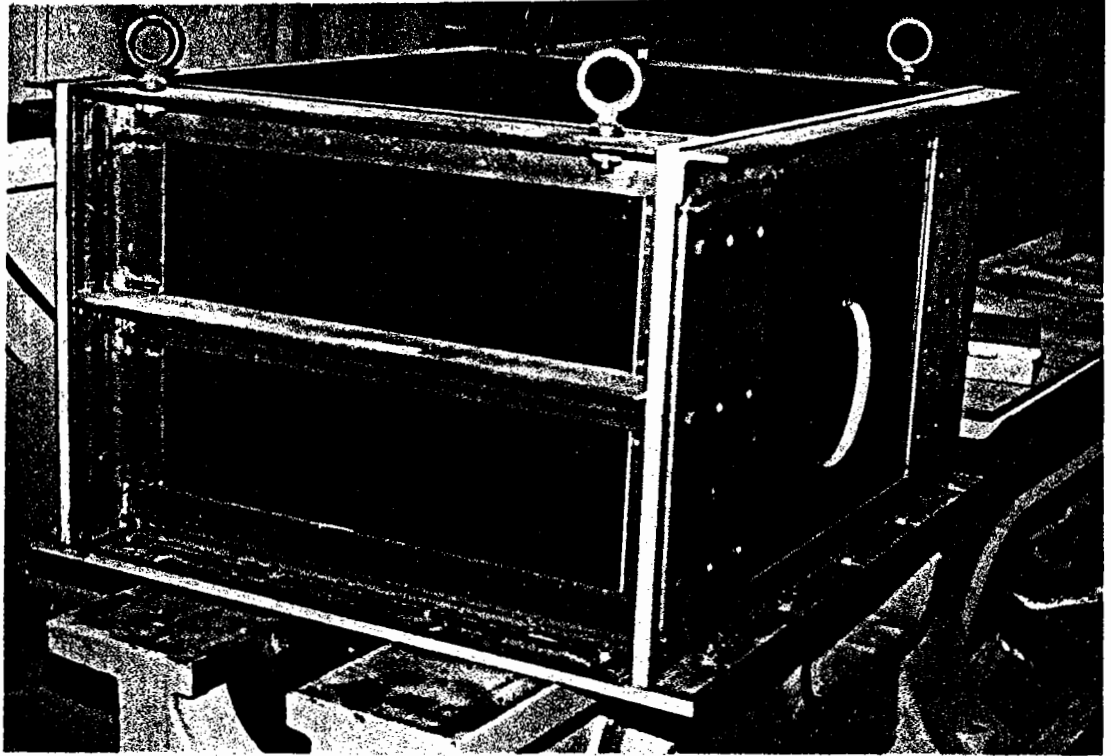
Fig. 4.7 Details of the Loading Rig



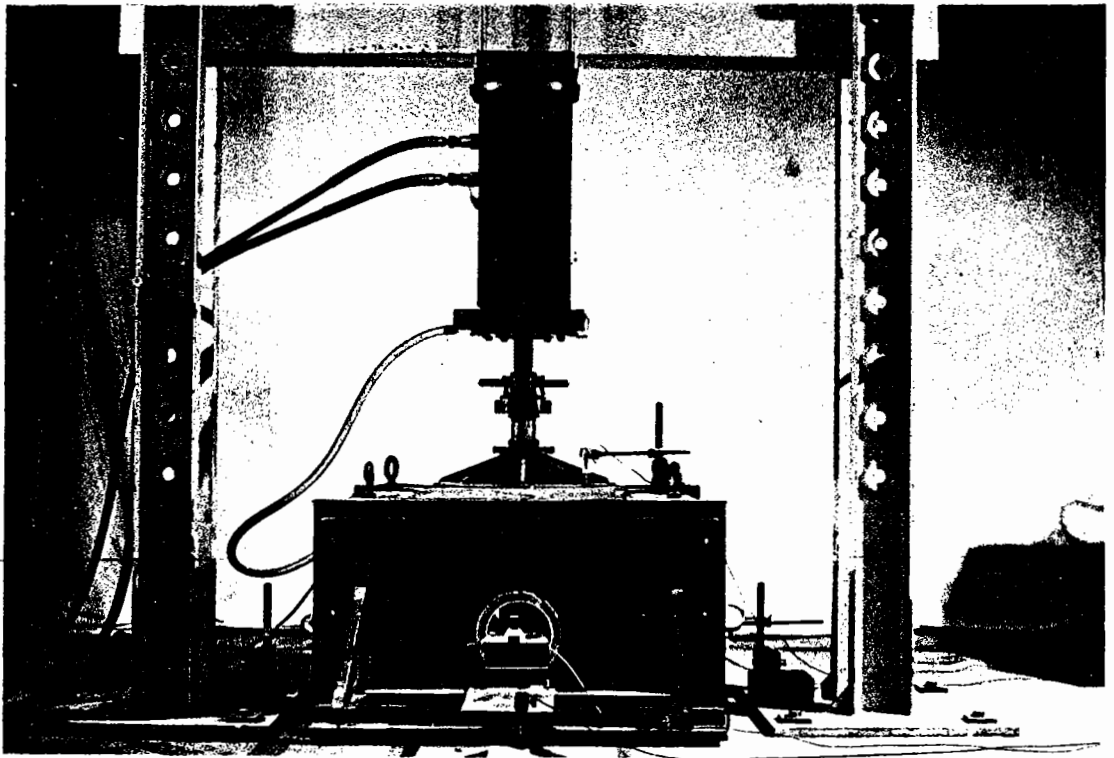
**Fig. 4.8 The Loading Rig**



**Fig. 4.9 The Loading Arrangement used in the Pit**



**Fig. 4.10 The Test Box**



**Fig. 4.11 An Experiment in Progress in the Box**



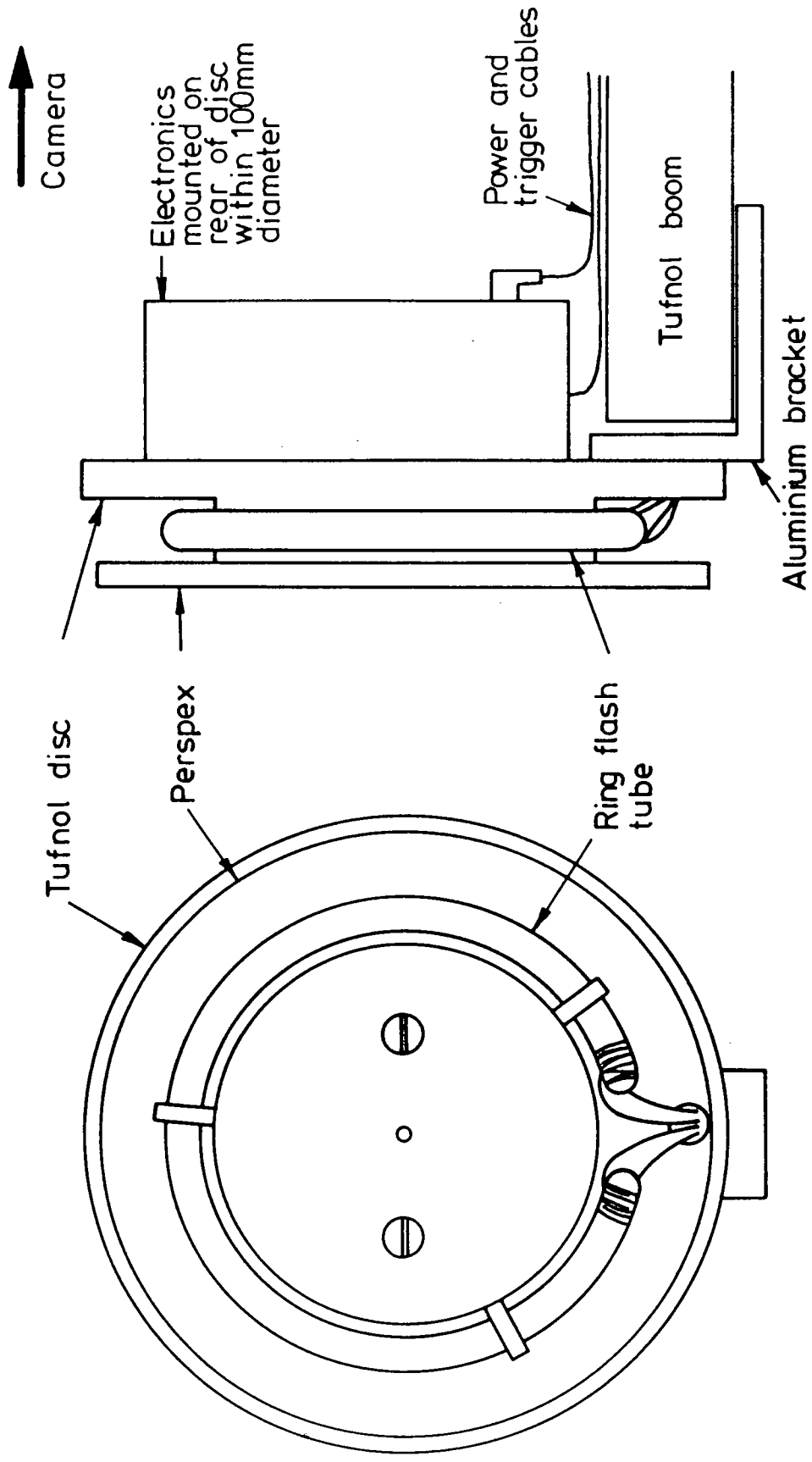
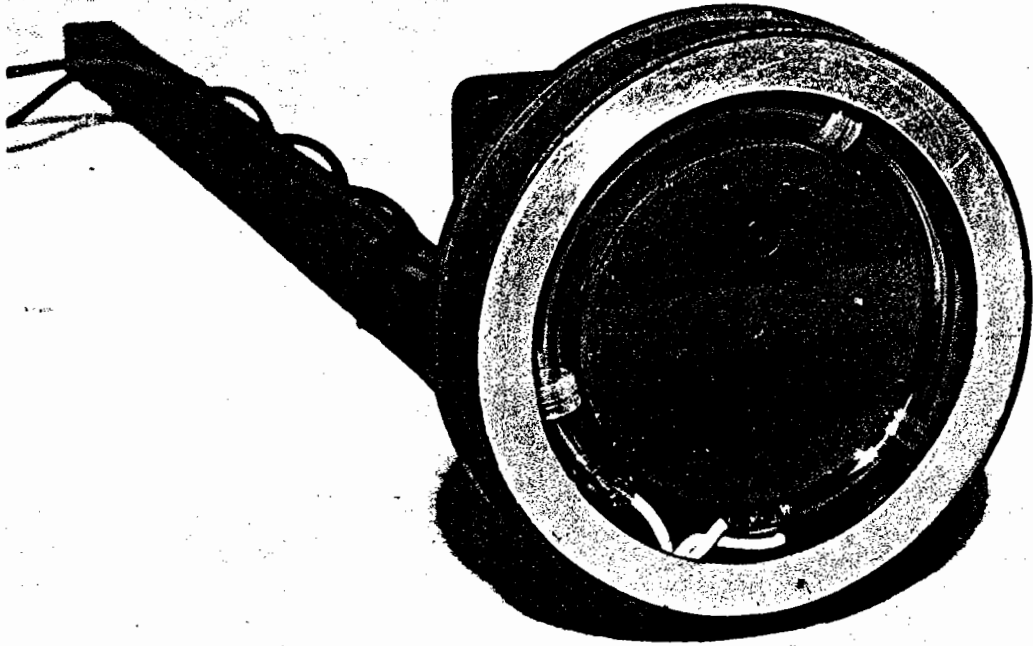
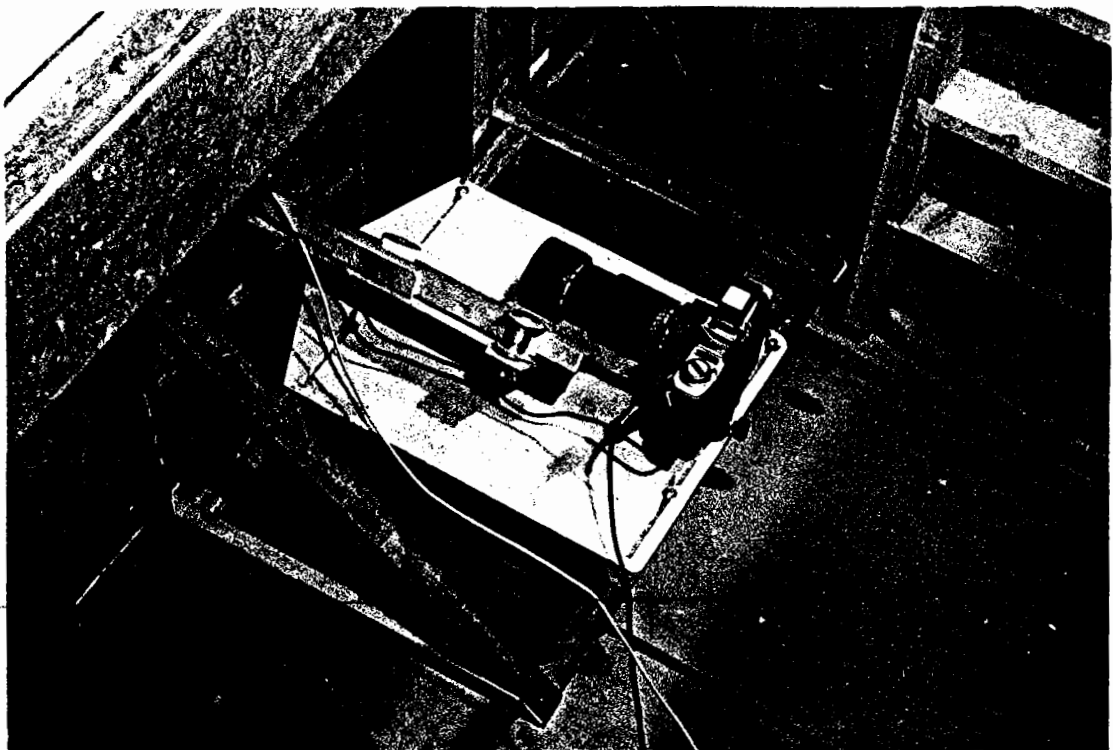


Fig. 4.12 Details of the Ring Flash (without shield)



**Fig. 4.13 The Ring Flash Head (with shield)**



**Fig. 4.14 Photographic Equipment Mounted in the Inspection Chamber**

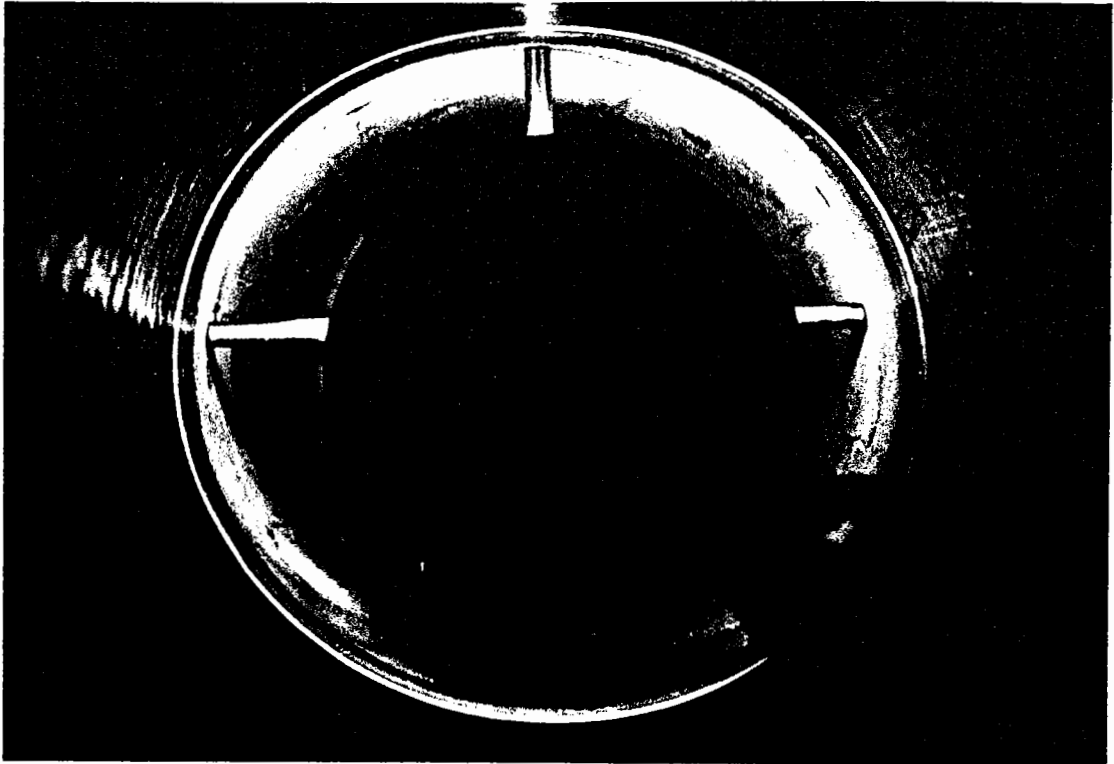


Fig. 4.15 Photograph Profile taken by the Ring Flash Camera

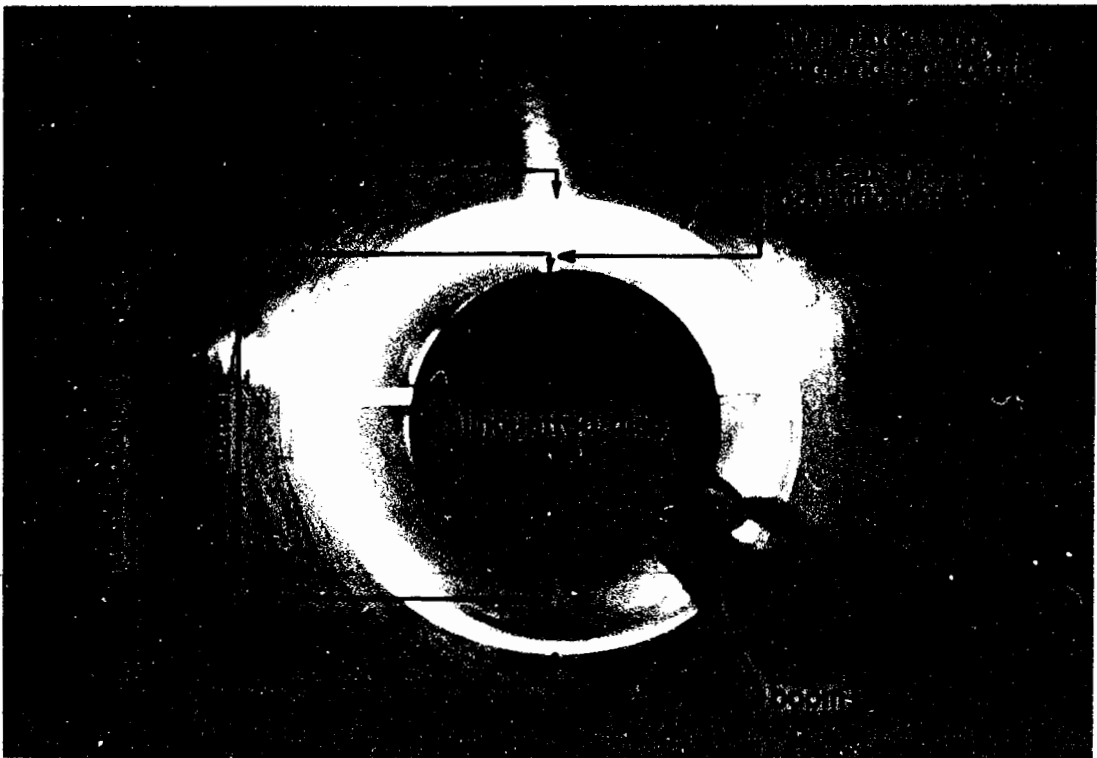


Fig. 4.16 Annotated Ring Flash Photograph

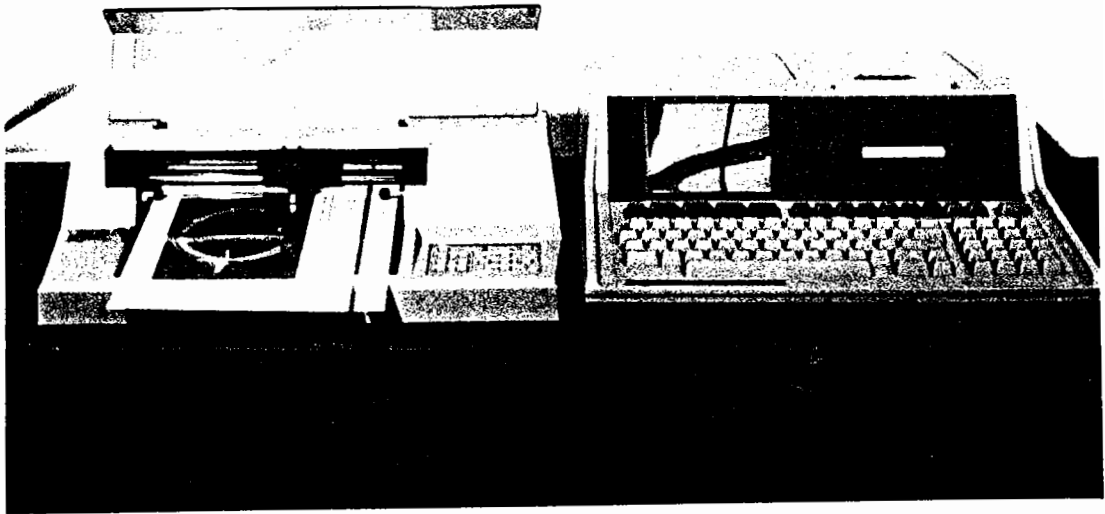


Fig. 4.17 Method of Digitizing Photographs

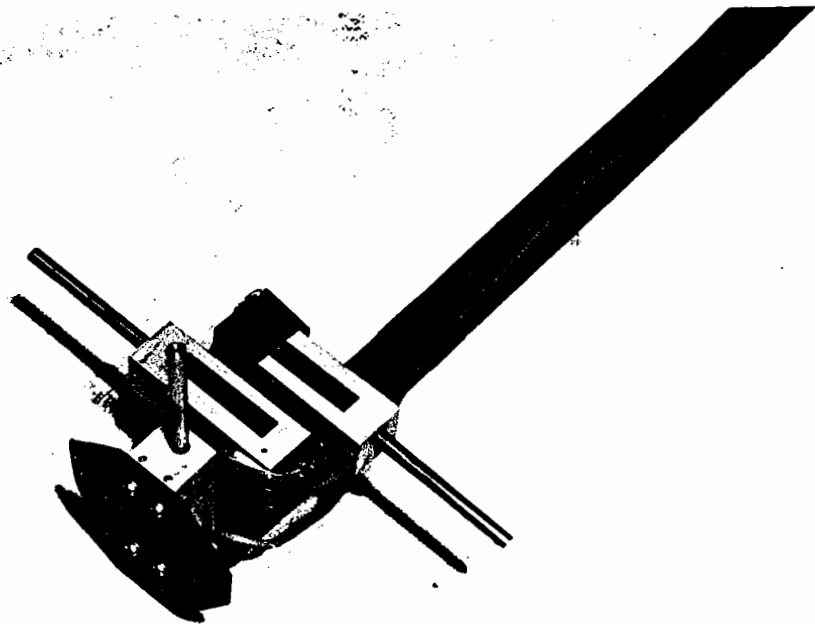
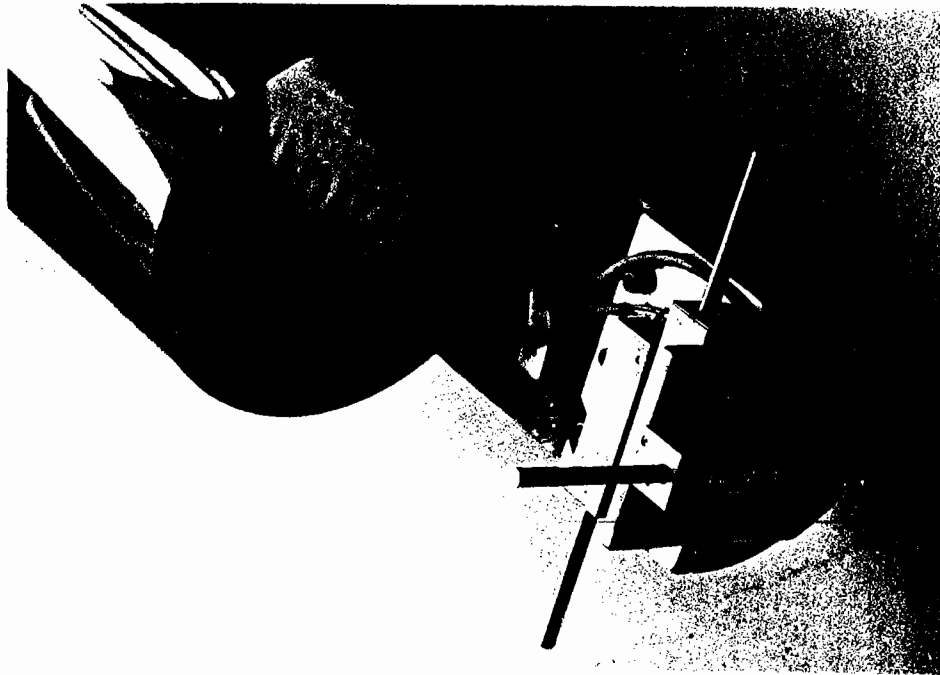
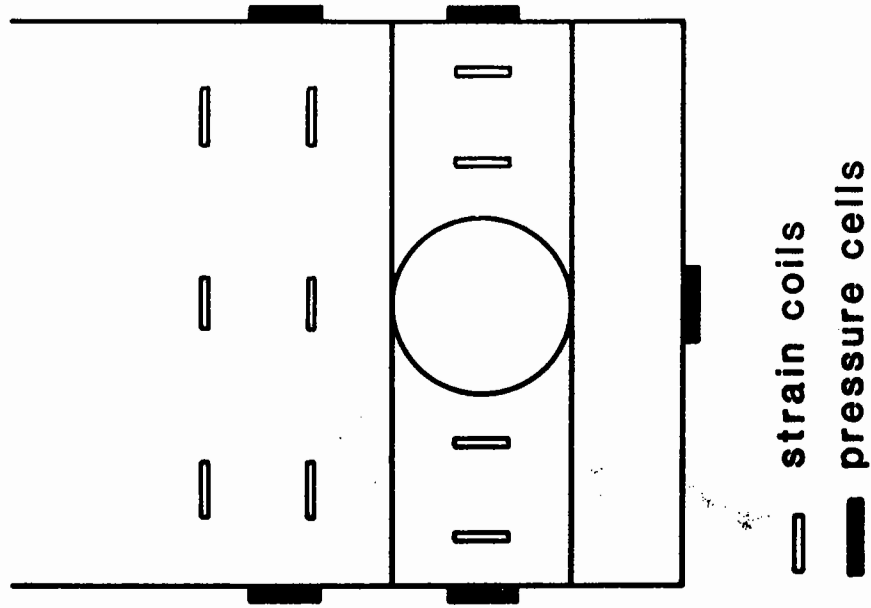


Fig. 4.18 Linear Potentiometer Arrangement used in the Box Experiments



**Fig. 4.19 Linear Potentiometers on Sledge  
used in the Pit Experiments**



**Fig. 4.20 Location of Soil  
Instrumentation**

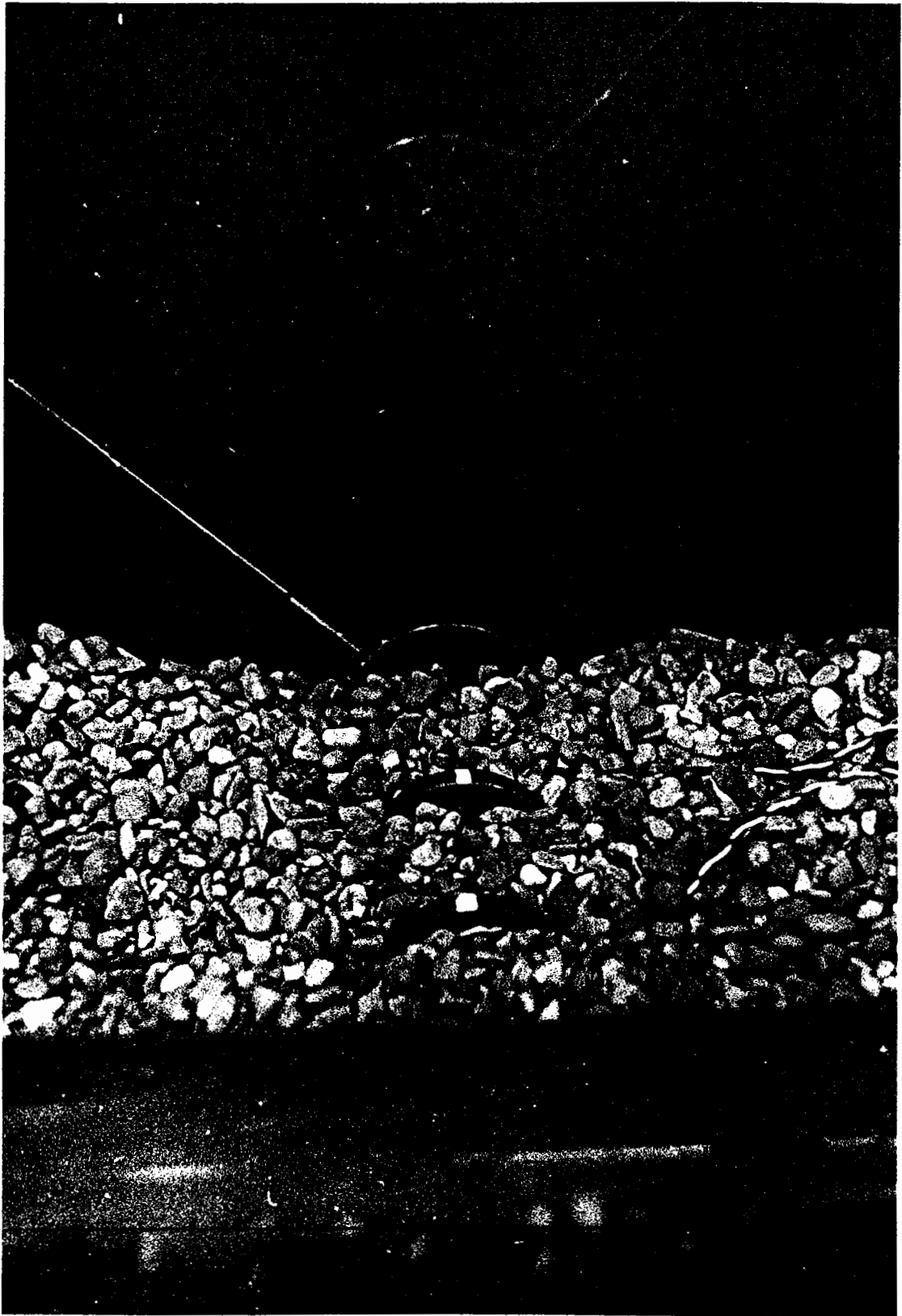
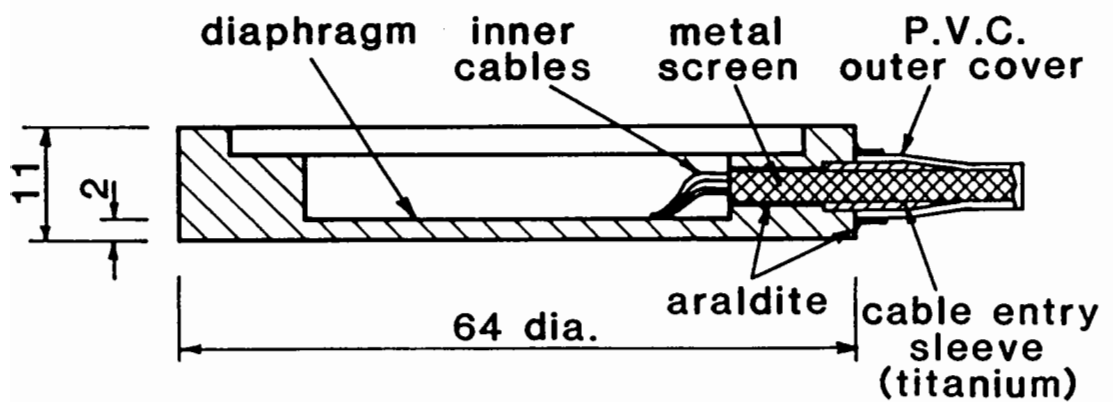
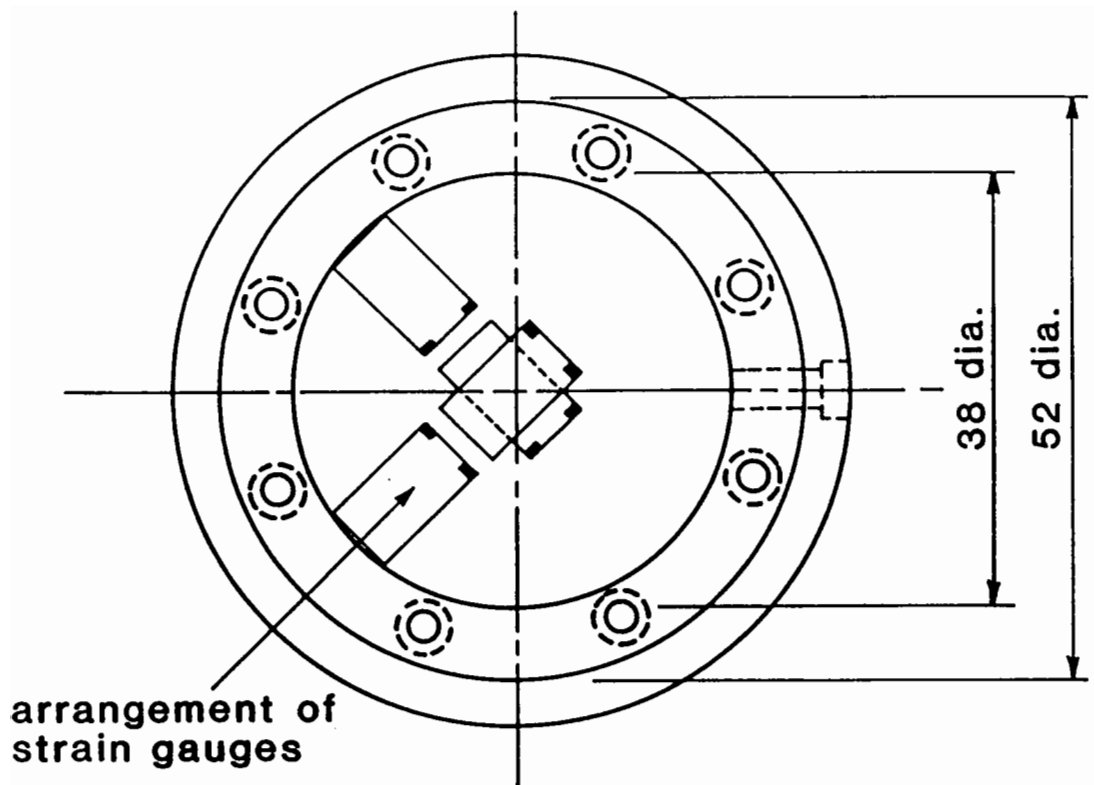
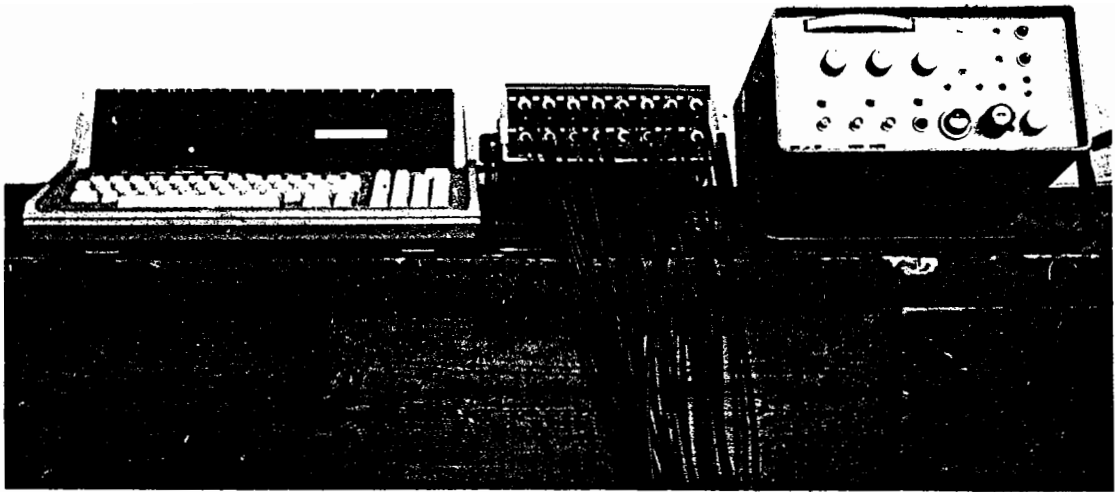


Fig. 4.21 Strain Coils and Pressure Cell in the Test Box

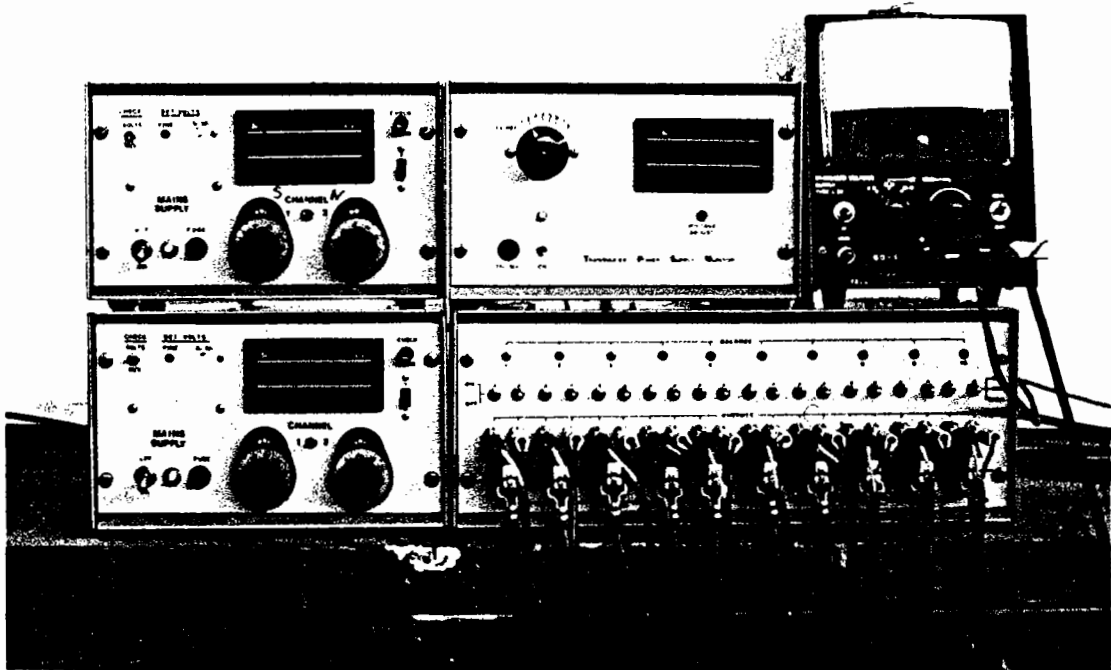


All dimensions are in millimetres

Fig. 4.22 The Nottingham Pressure Cell



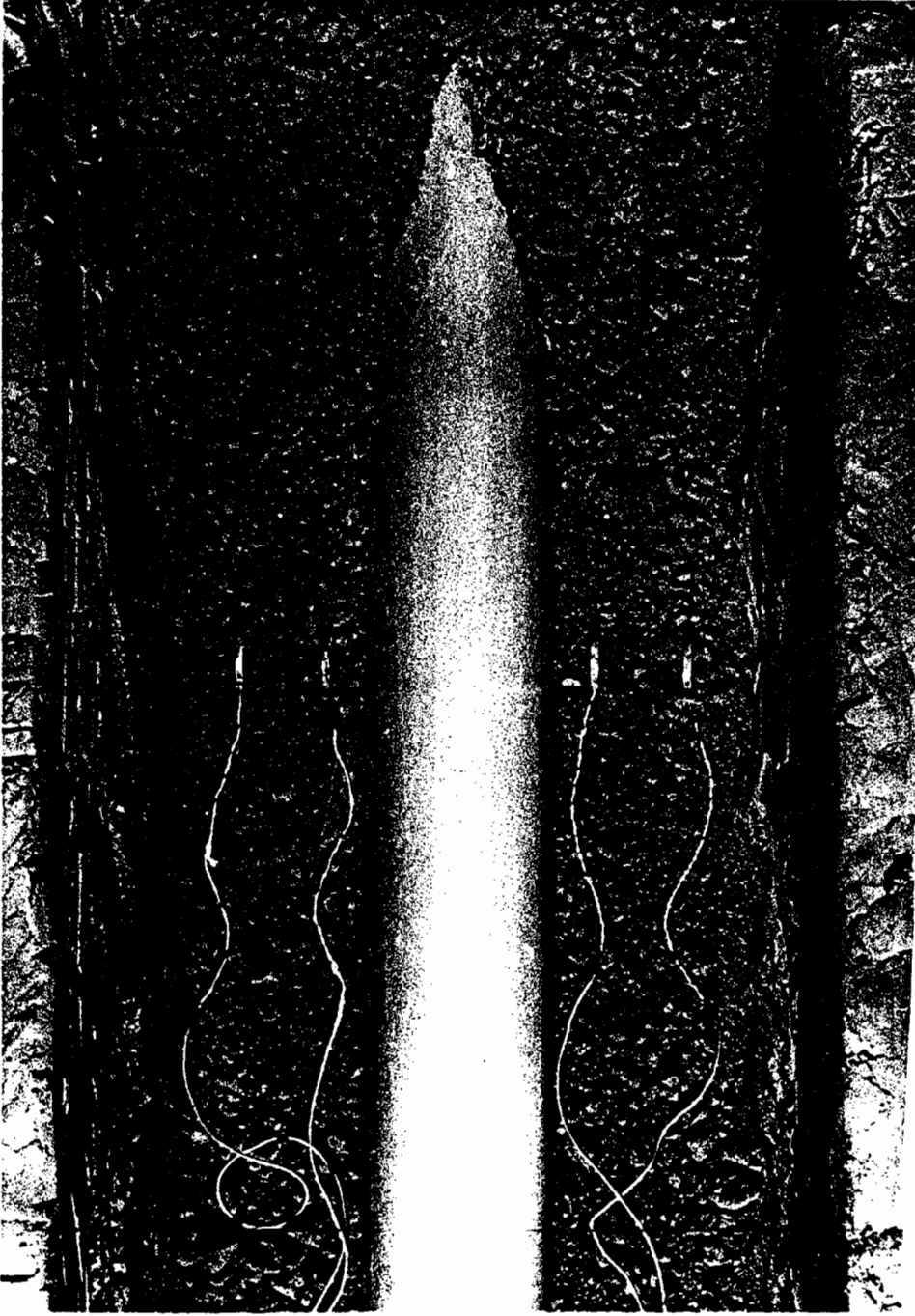
(a) Data logger and Soil Strain Gauge Unit



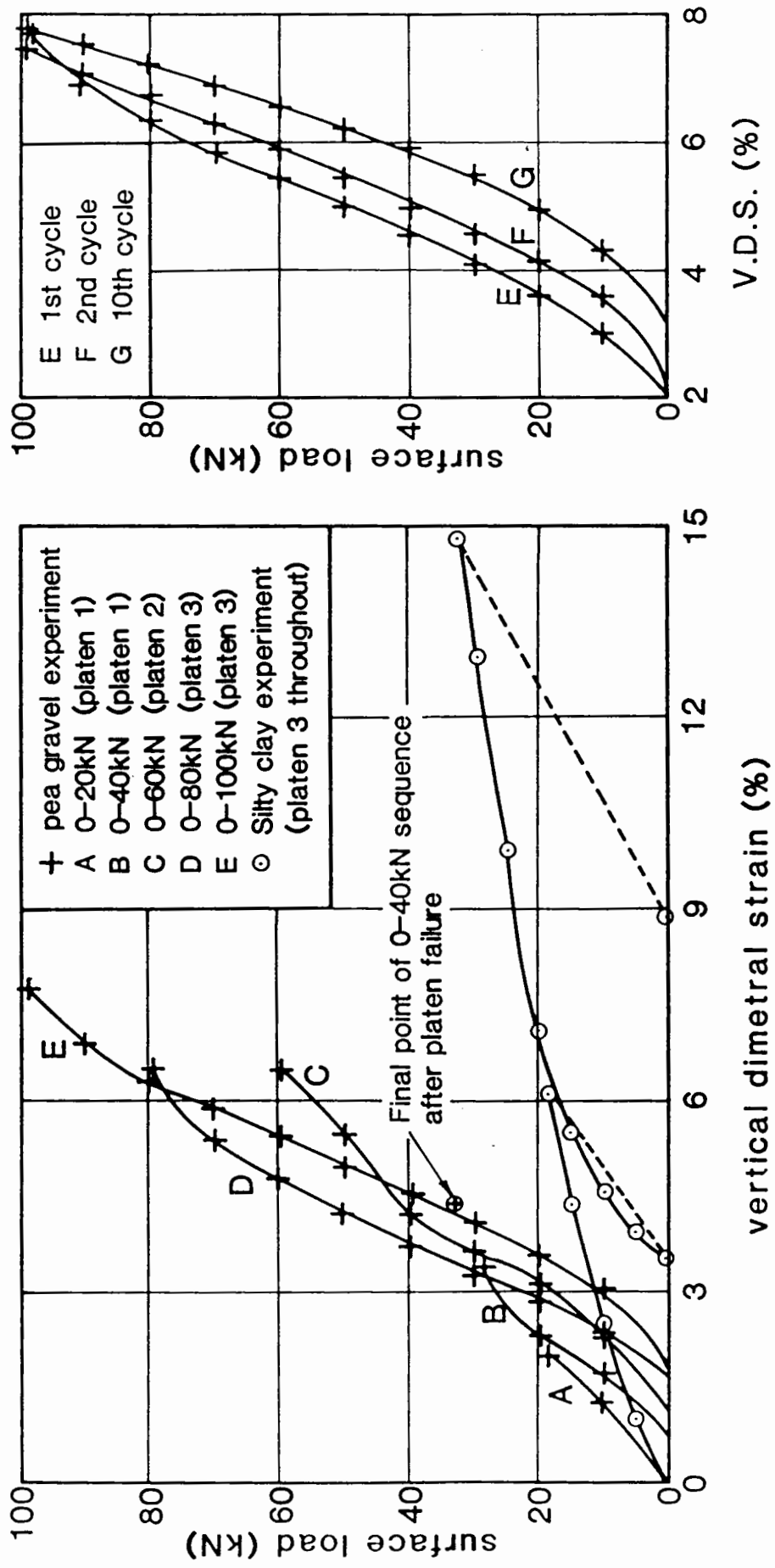
(b) Signal balancing and monitoring units

Fig. 4.23 Equipment used to Monitor Instrumentation and Log the Data





**Fig. 4.24 A Pipe Being Installed in the Test Pit**



(a) Incremental static load (pea gravel and silty clay) (b) Cycled load (pea gravel)

Fig. 5.1 Results of Preliminary Tests for Complete Surrounds of Gravel and Clay

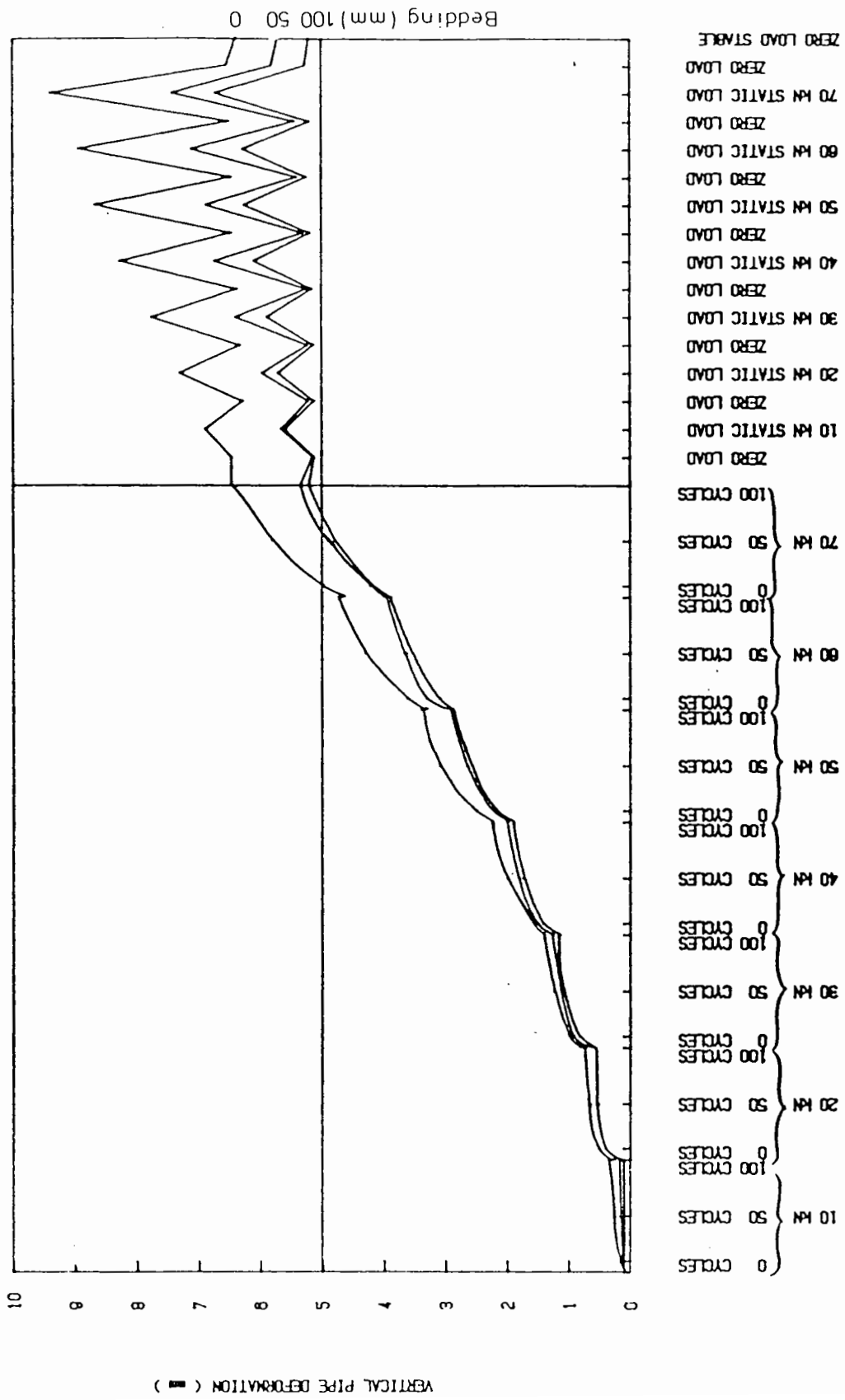


Fig. 5.2 Build-up of Vertical Deformation in Typical Pea Gravel Installations with Various Bedding Thicknesses (Preliminary Tests)

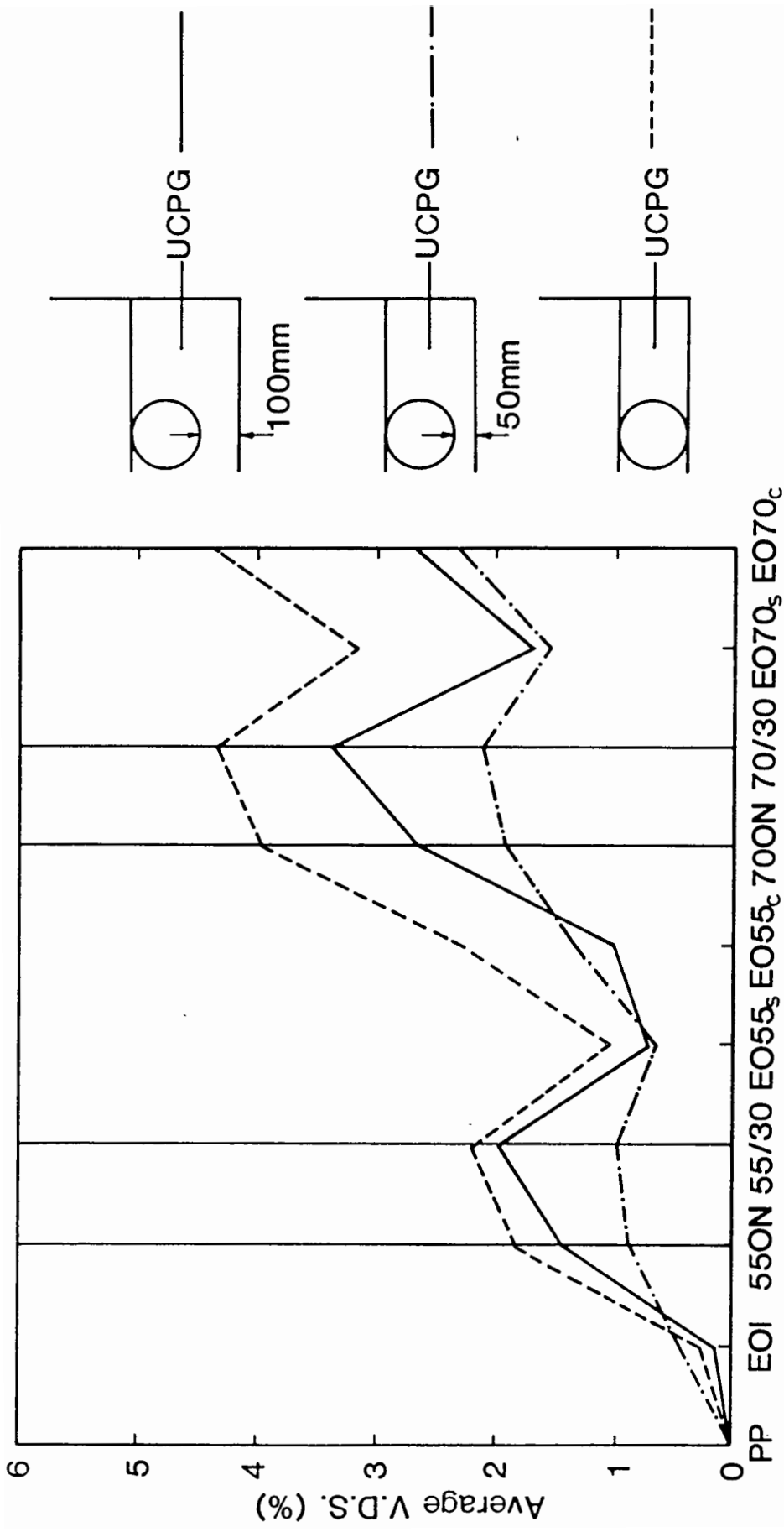


Fig. 5.3 Influence of Bedding on V.D.S. Measurements in the Pit

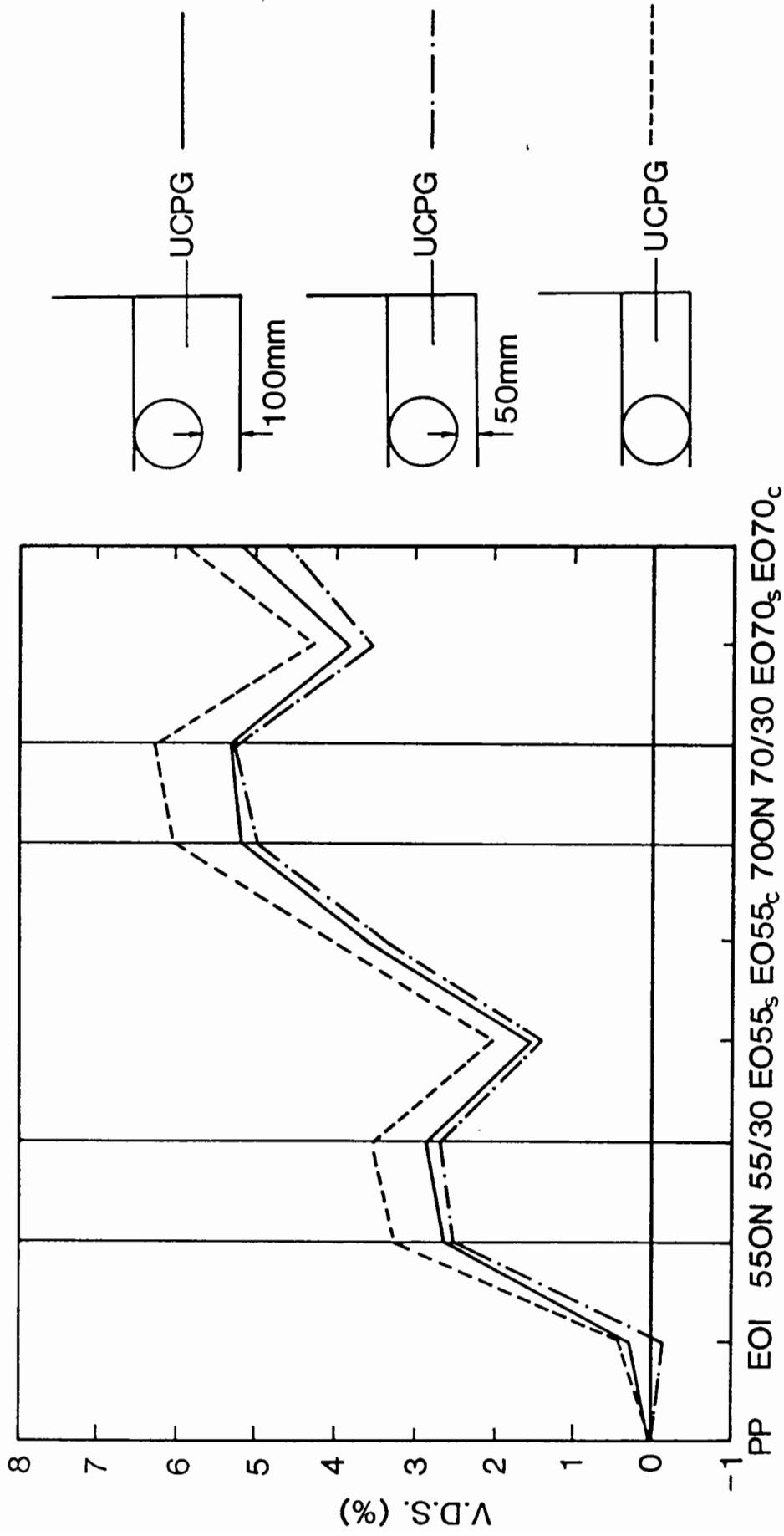


Fig. 5.4 Influence of Bedding on V.D.S. Measurements in the Box

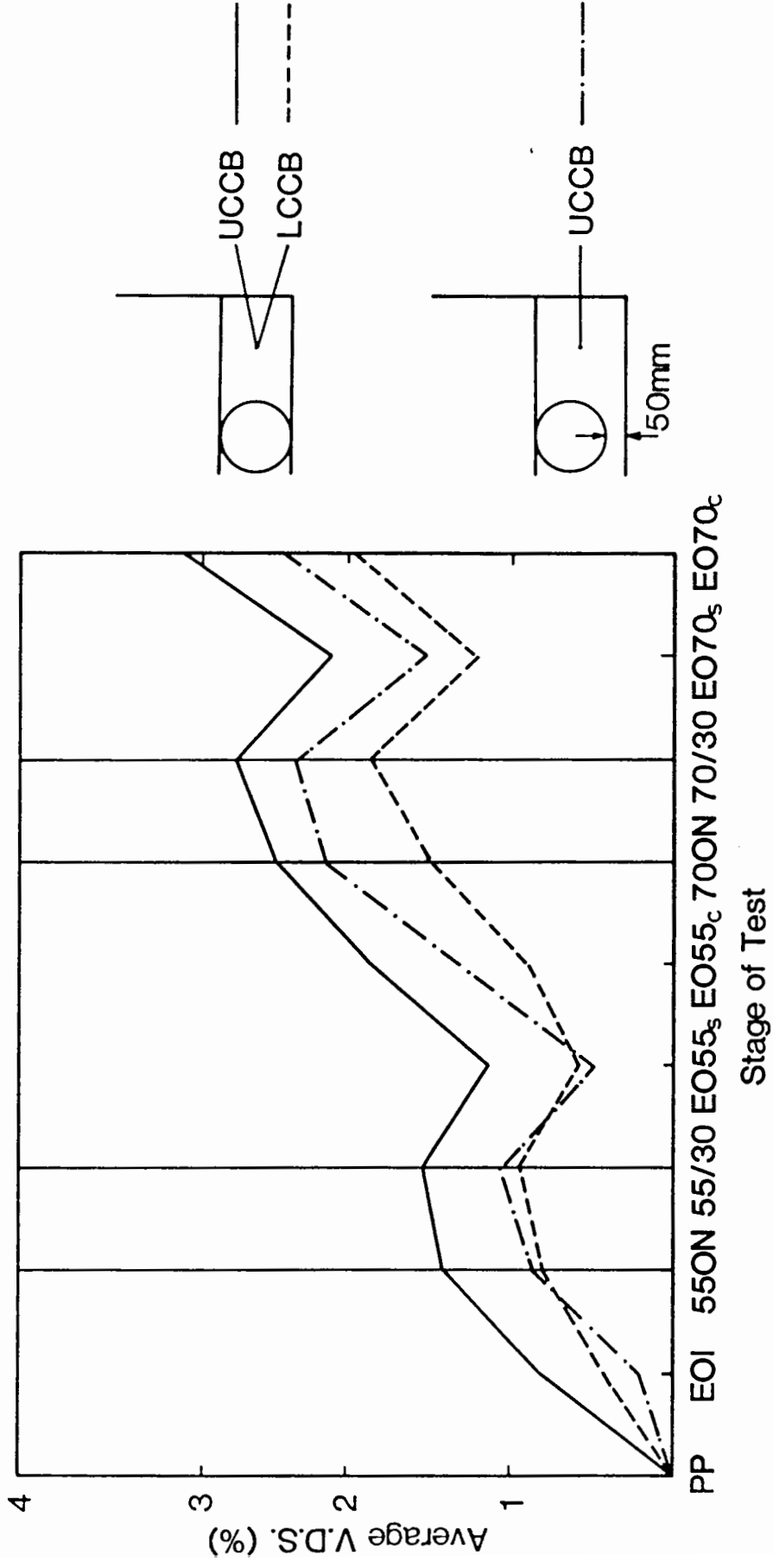


Fig. 5.5 Influence of Bedding and Compaction on the Performance of Concreting Ballast Sidefill

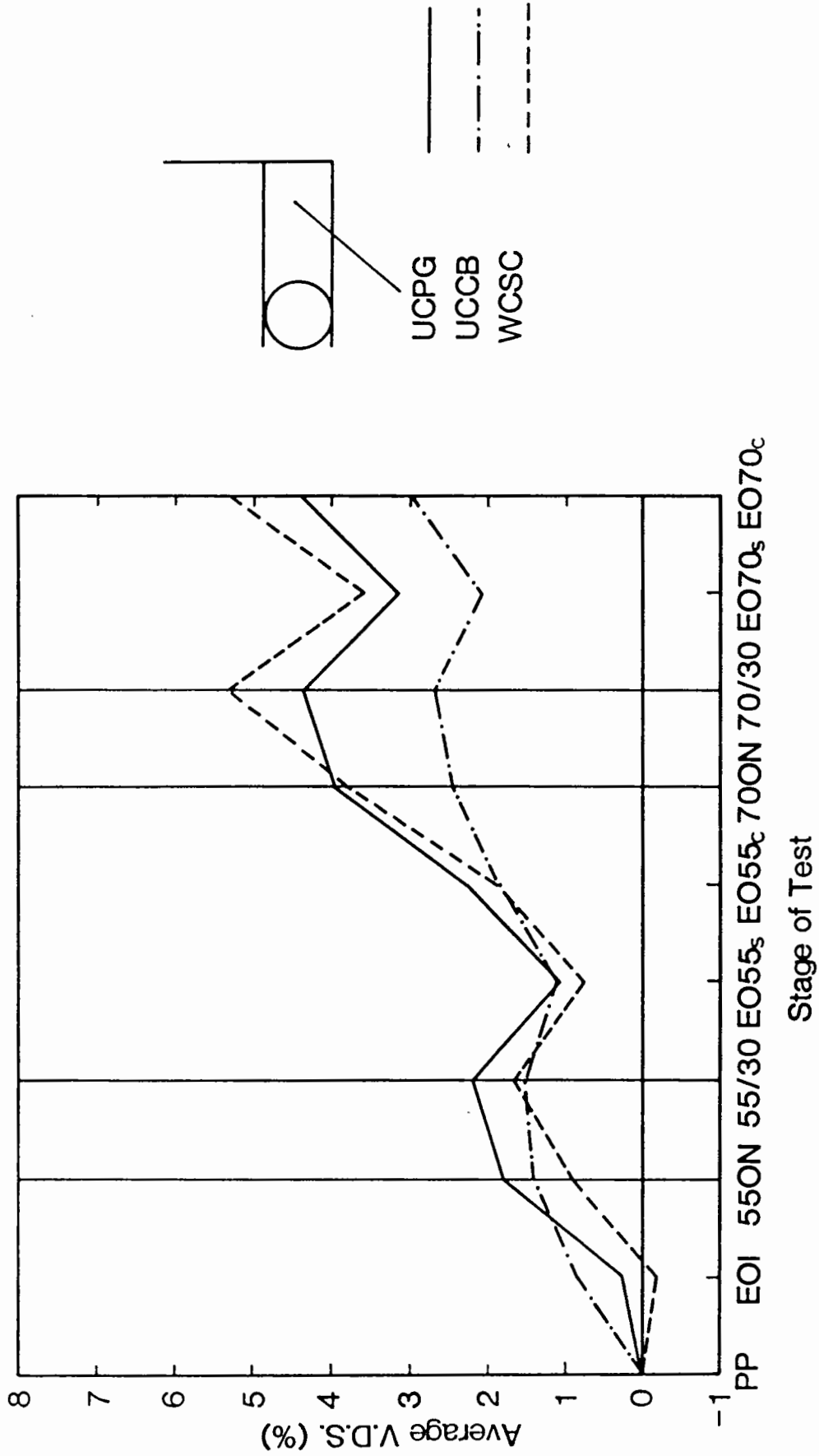


Fig. 5.6 Summary of V.D.S. Measurements for Three Sidefill Types in the Pit

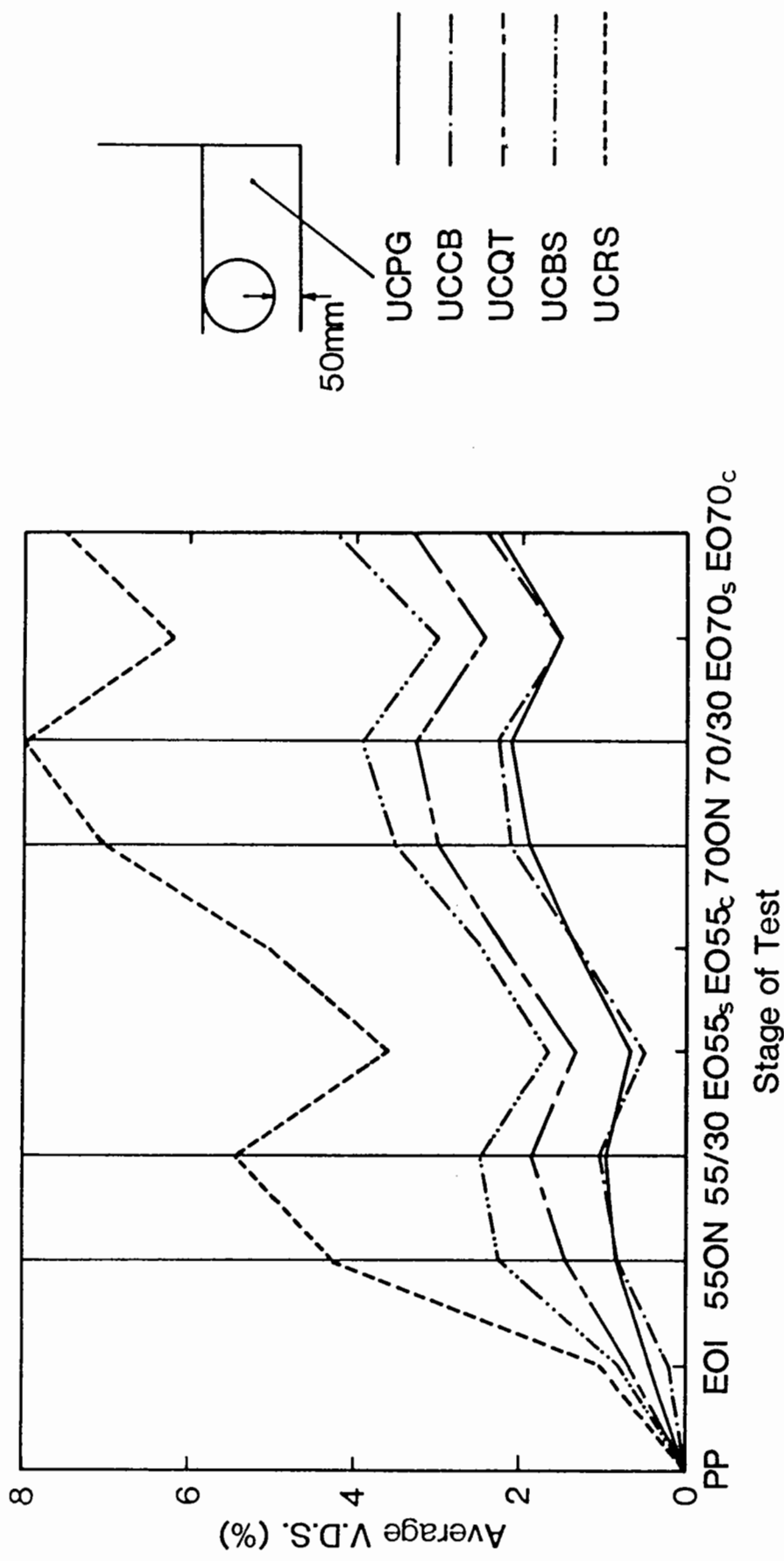
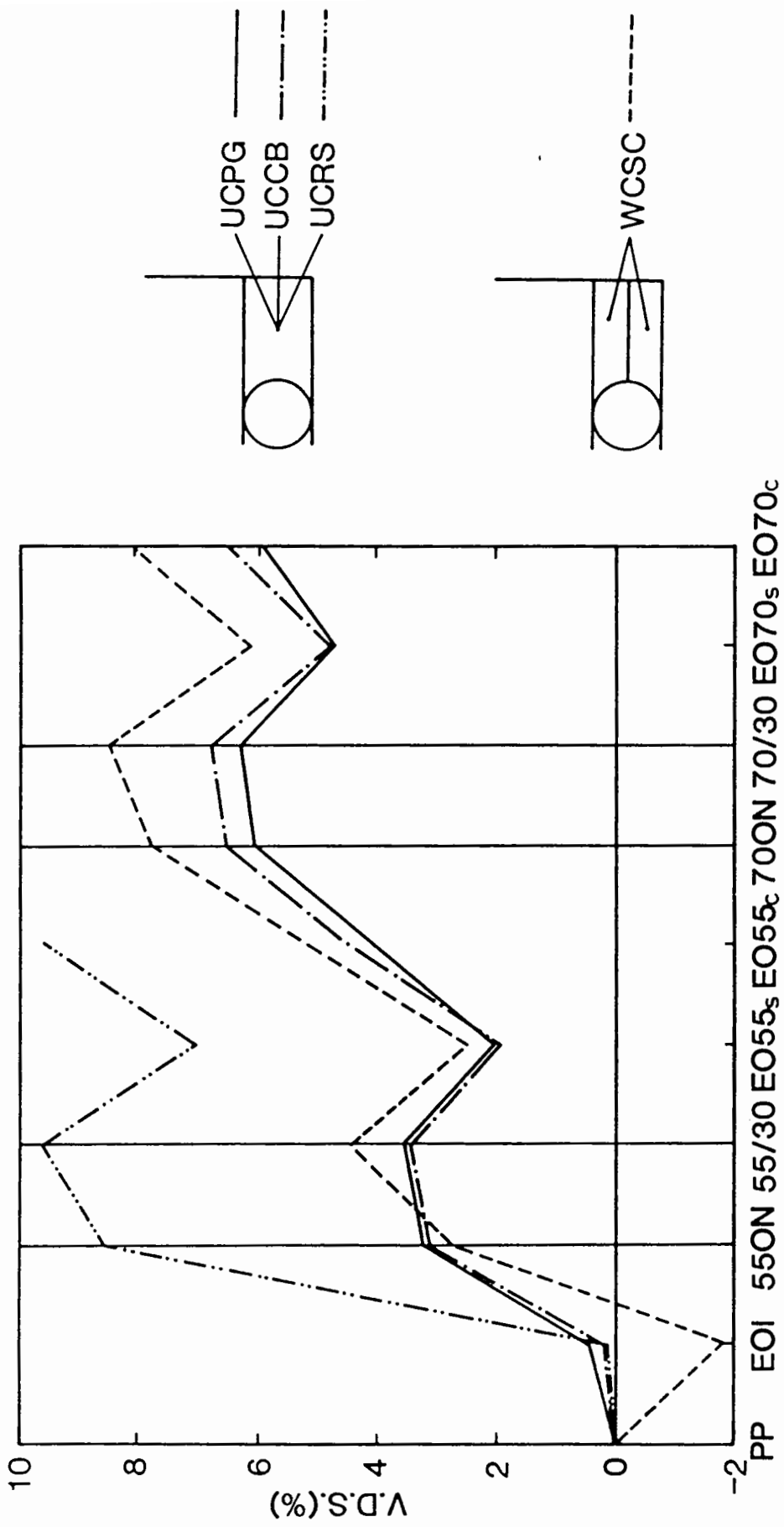


Fig. 5.7 Summary of V.D.S. Measurements for Five Sidefill Types in the Pit





Stage of Test

Fig. 5.8 Influence of Sidefill Type on Pattern of V.D.S. Measurements in the Box

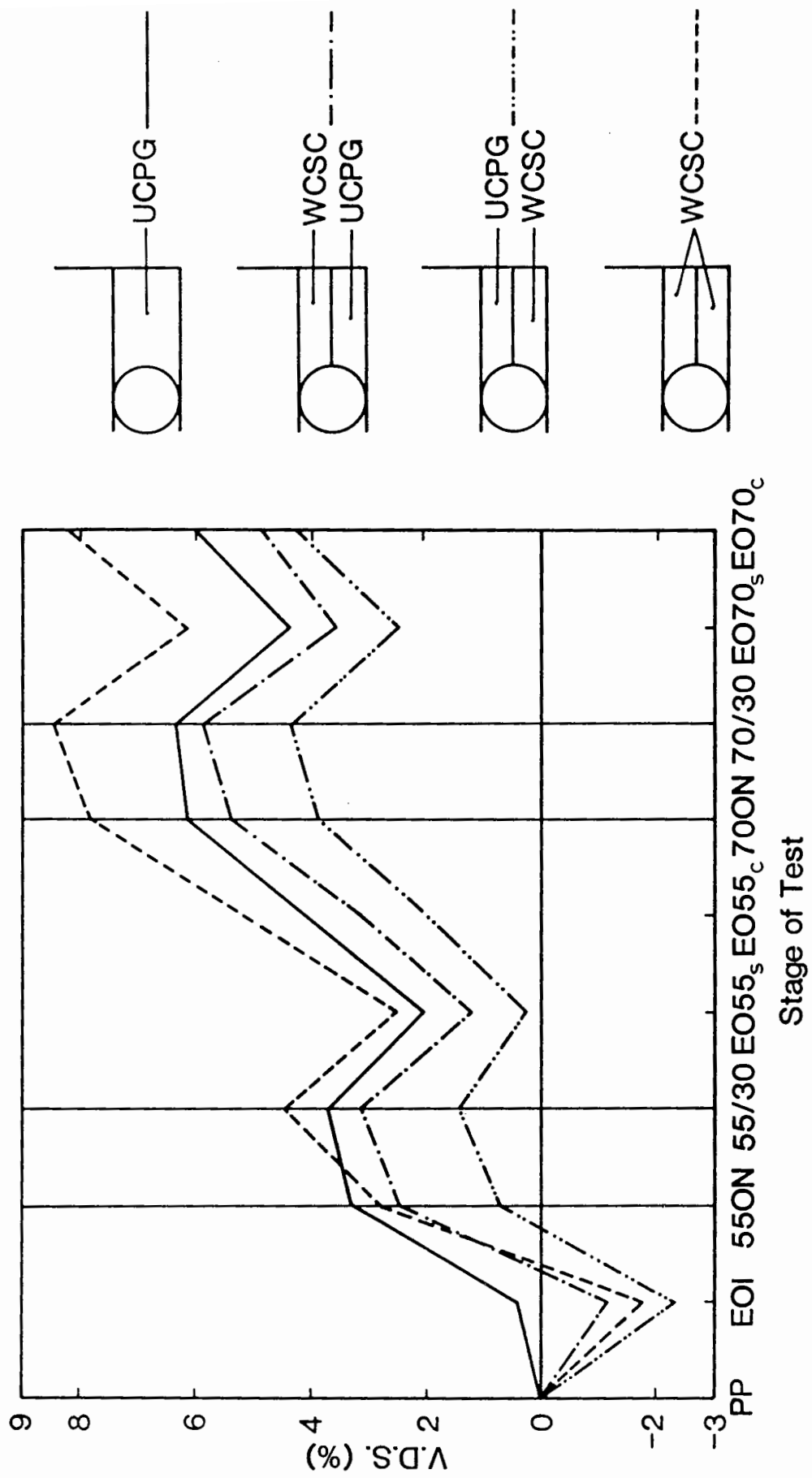


Fig. 5.9 V.D.S. Measurements for Four Combinations of Clay and Gravel in the Box

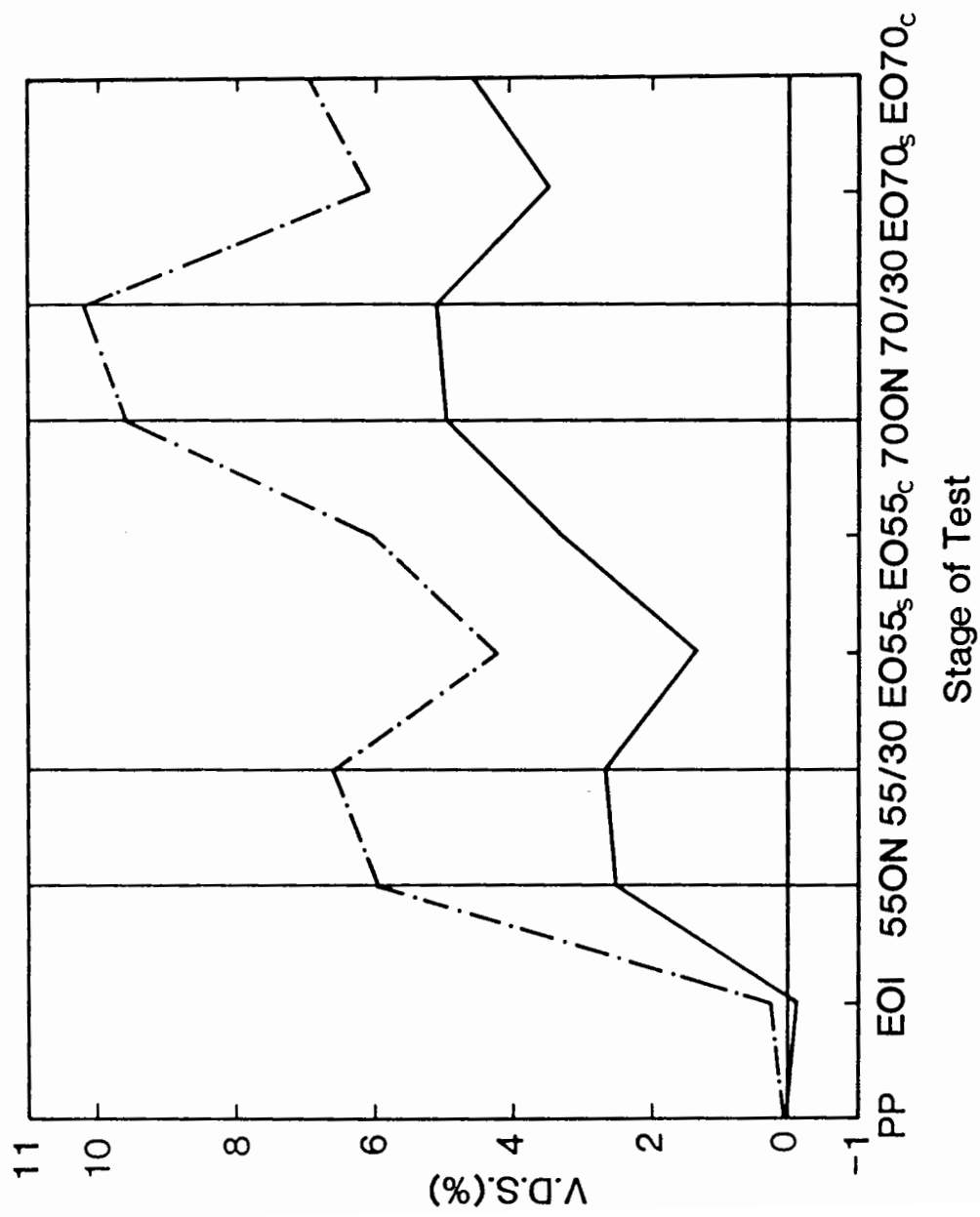


Fig. 5.10 V.D.S. Measurements for Two Pea Gravel Installations in the Box

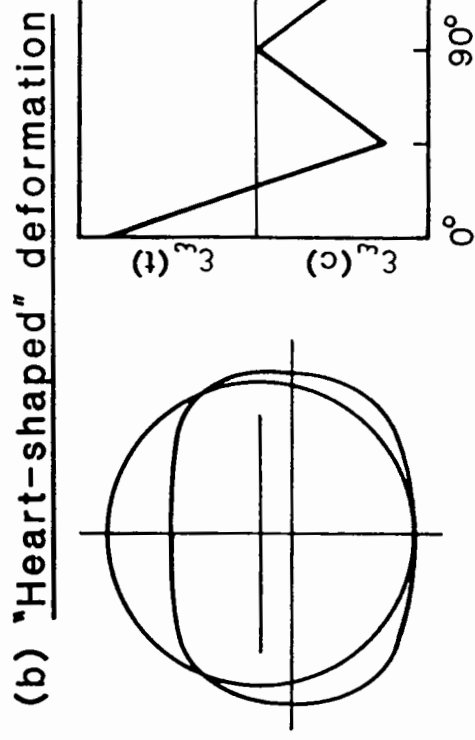
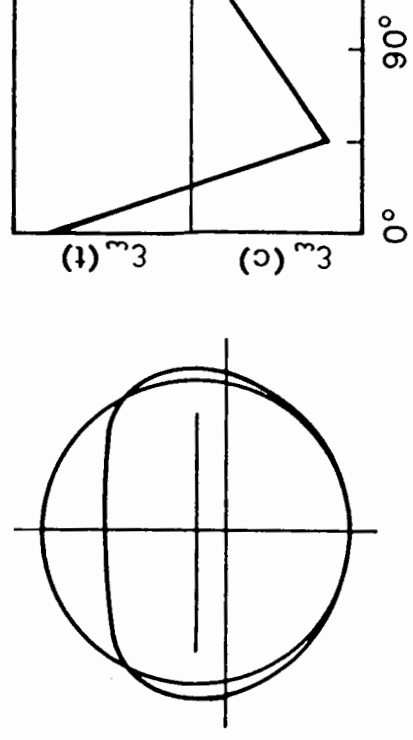
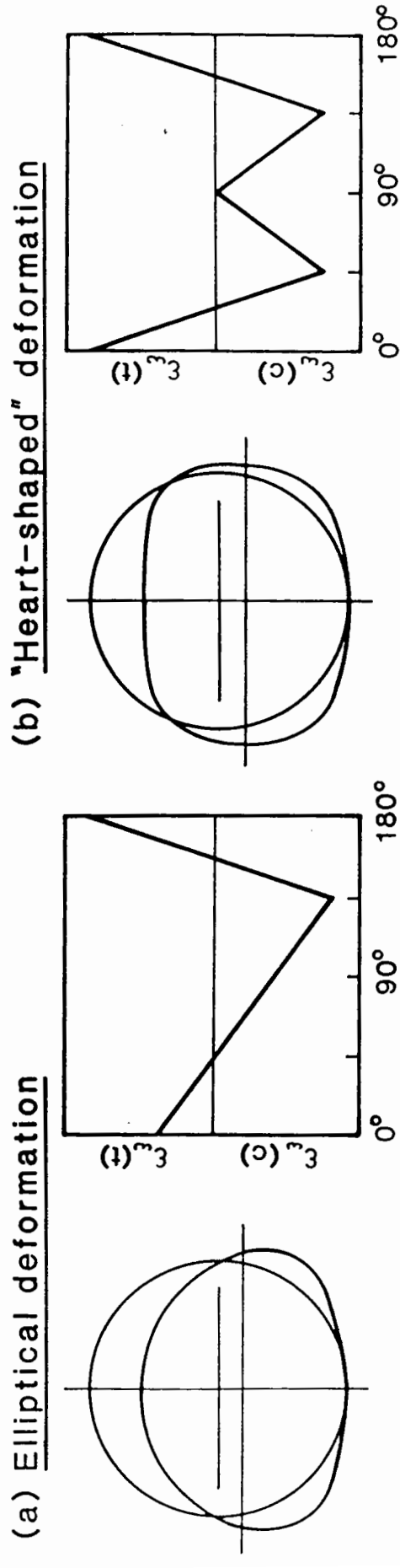
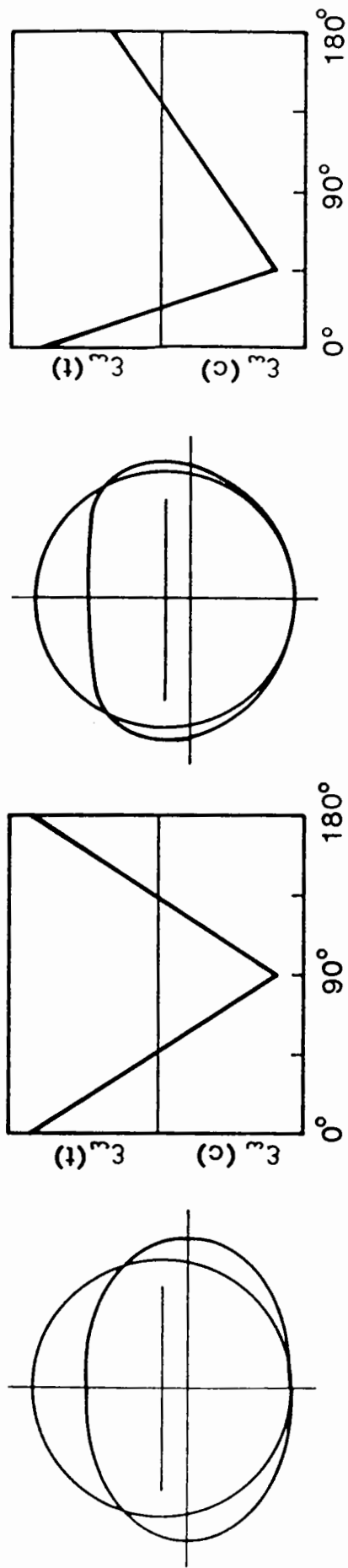


Fig. 5.11 Types of Deformation and Associated Strain Profiles

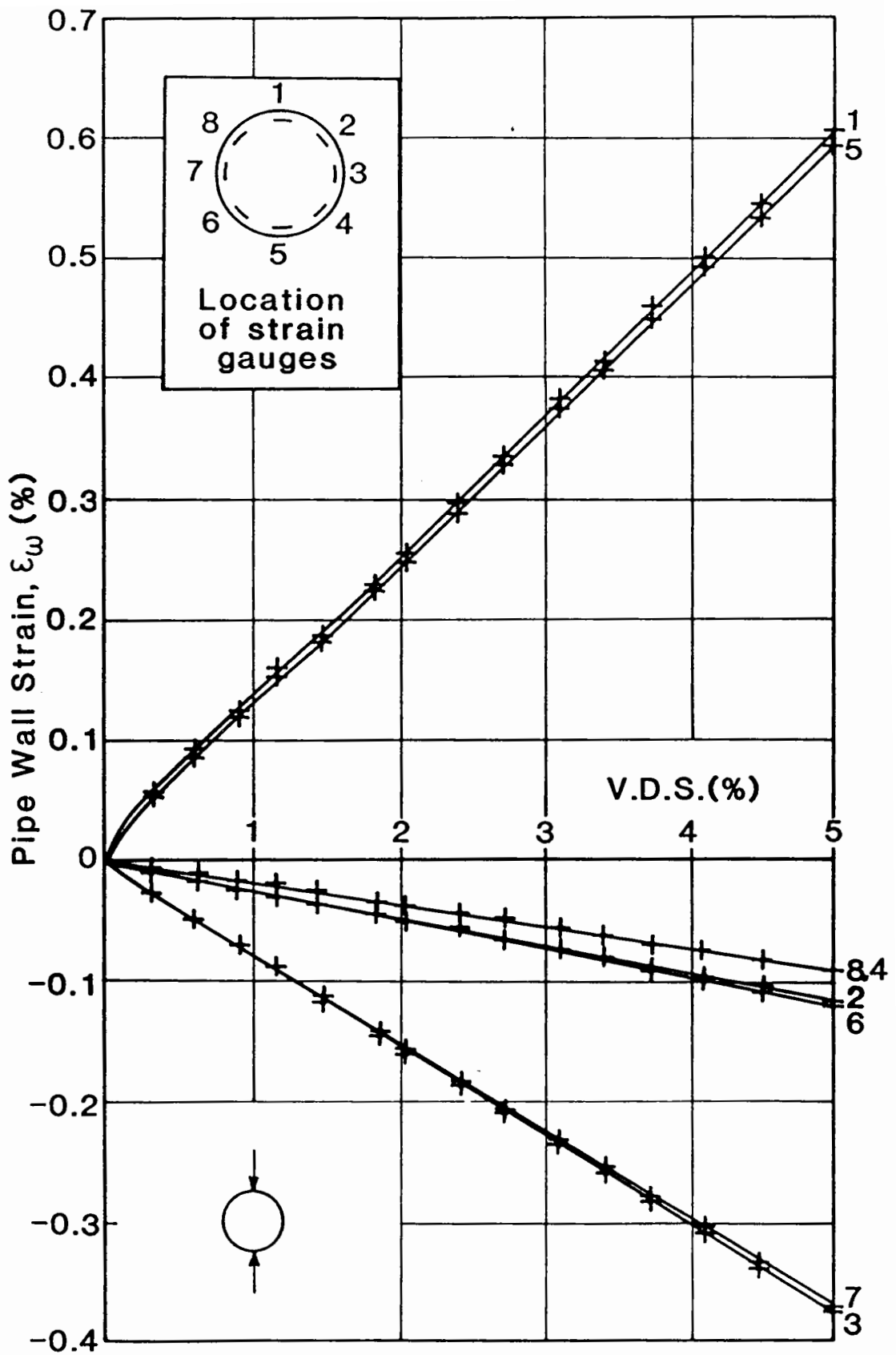


Fig. 5.12 Graph of Pipe Wall Strain against V.D.S. for Unconfined Line Load Tests

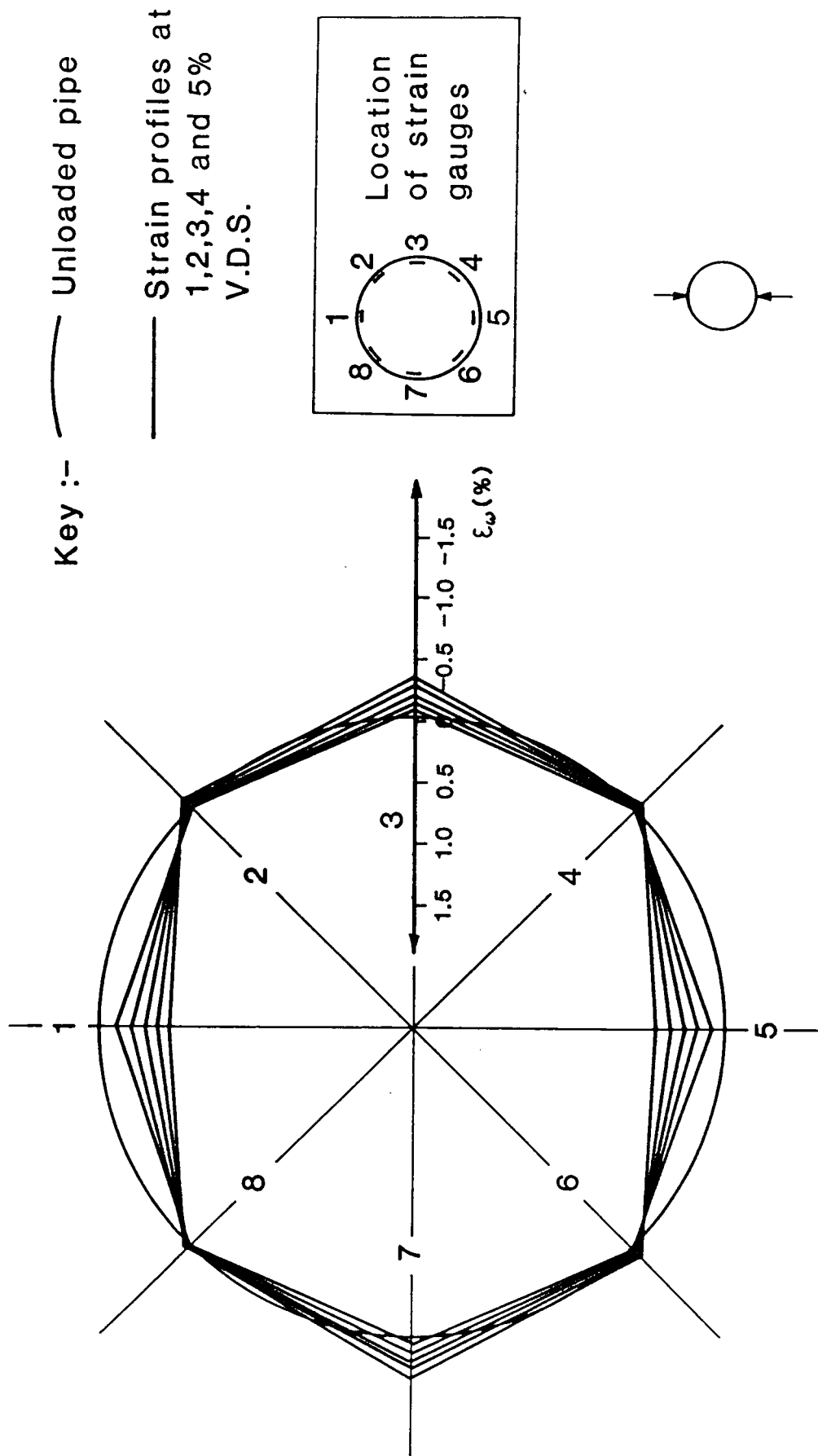


Fig. 5.13 Pipe Wall Strain Profiles for Unconfined Line Load Tests

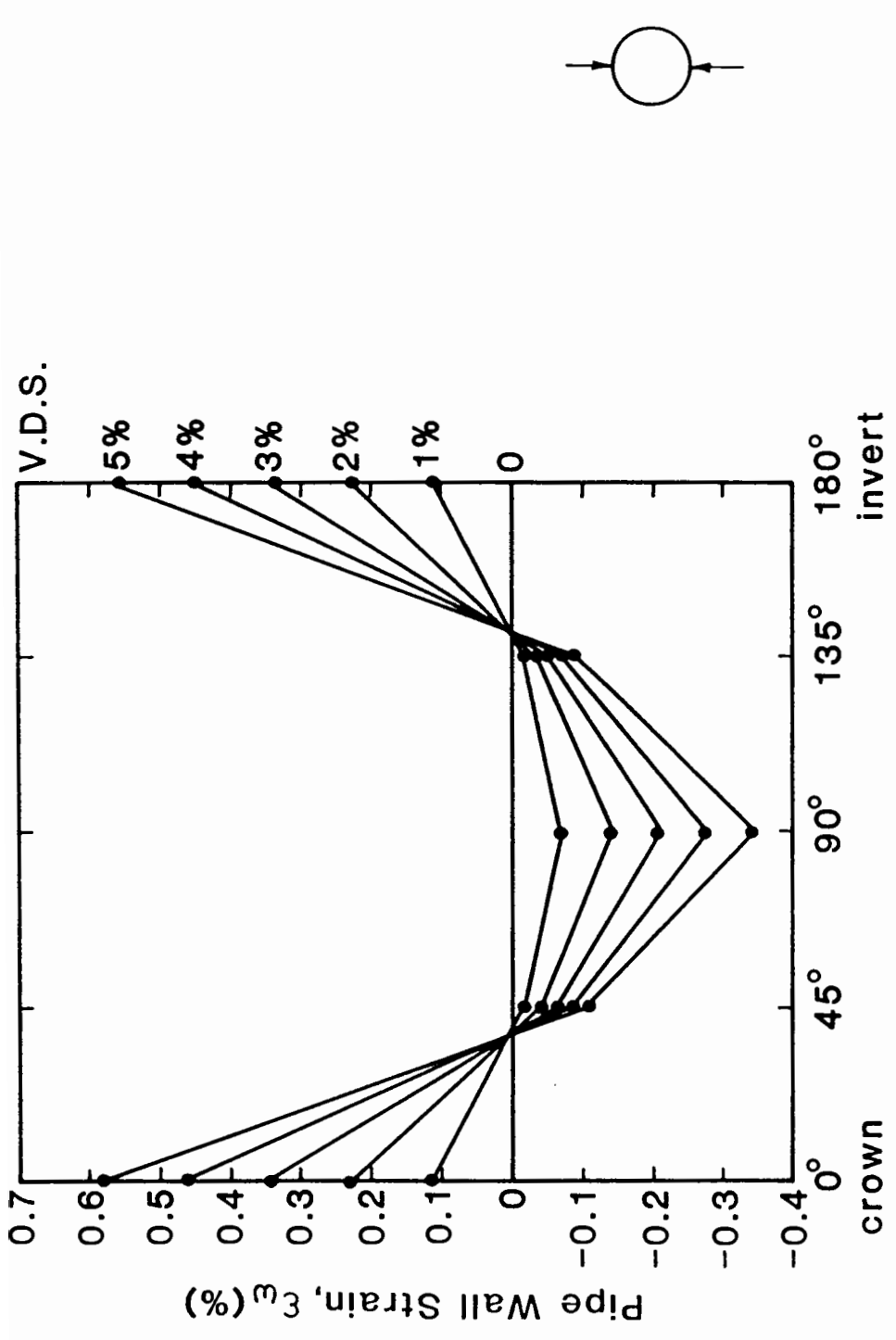
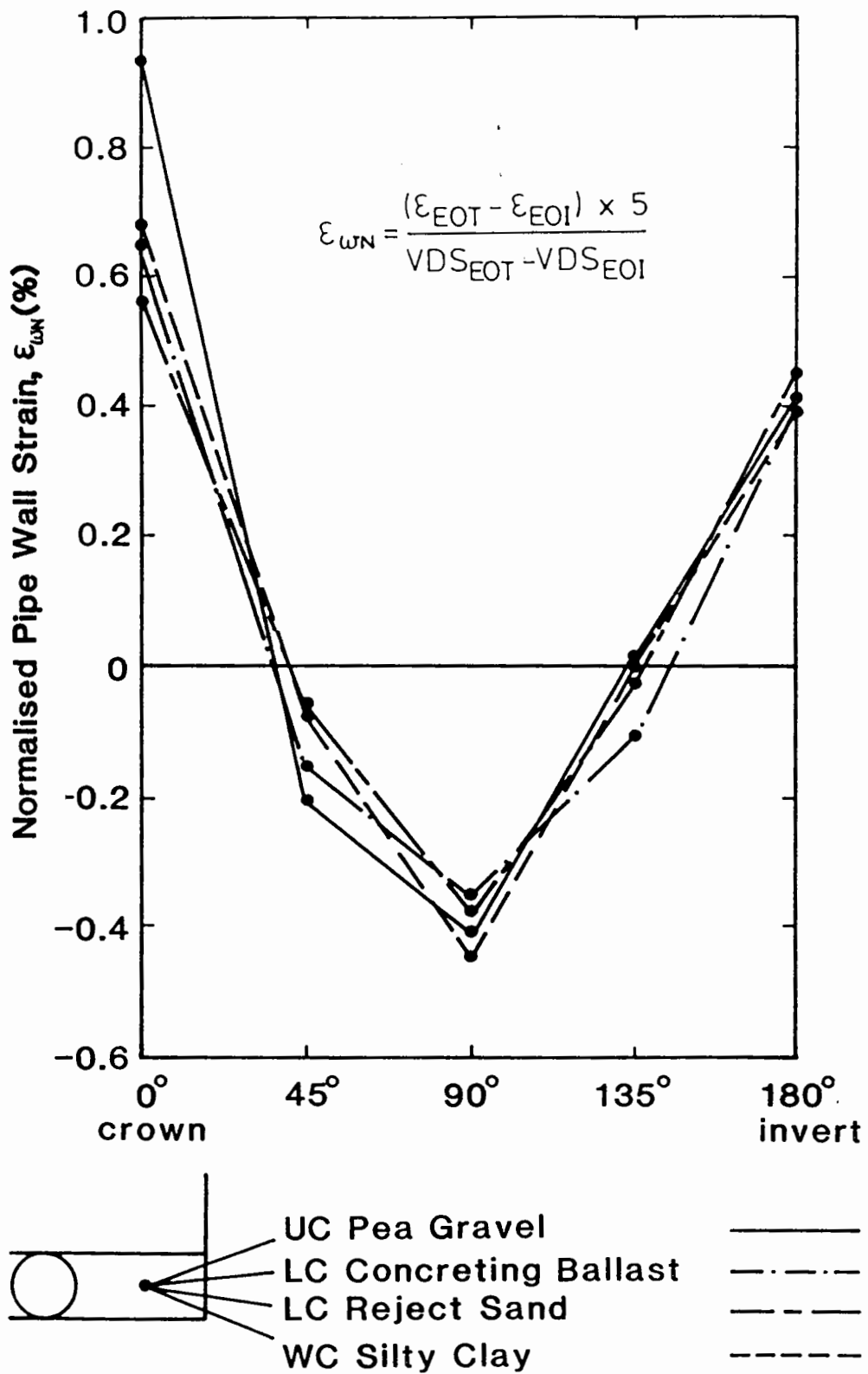
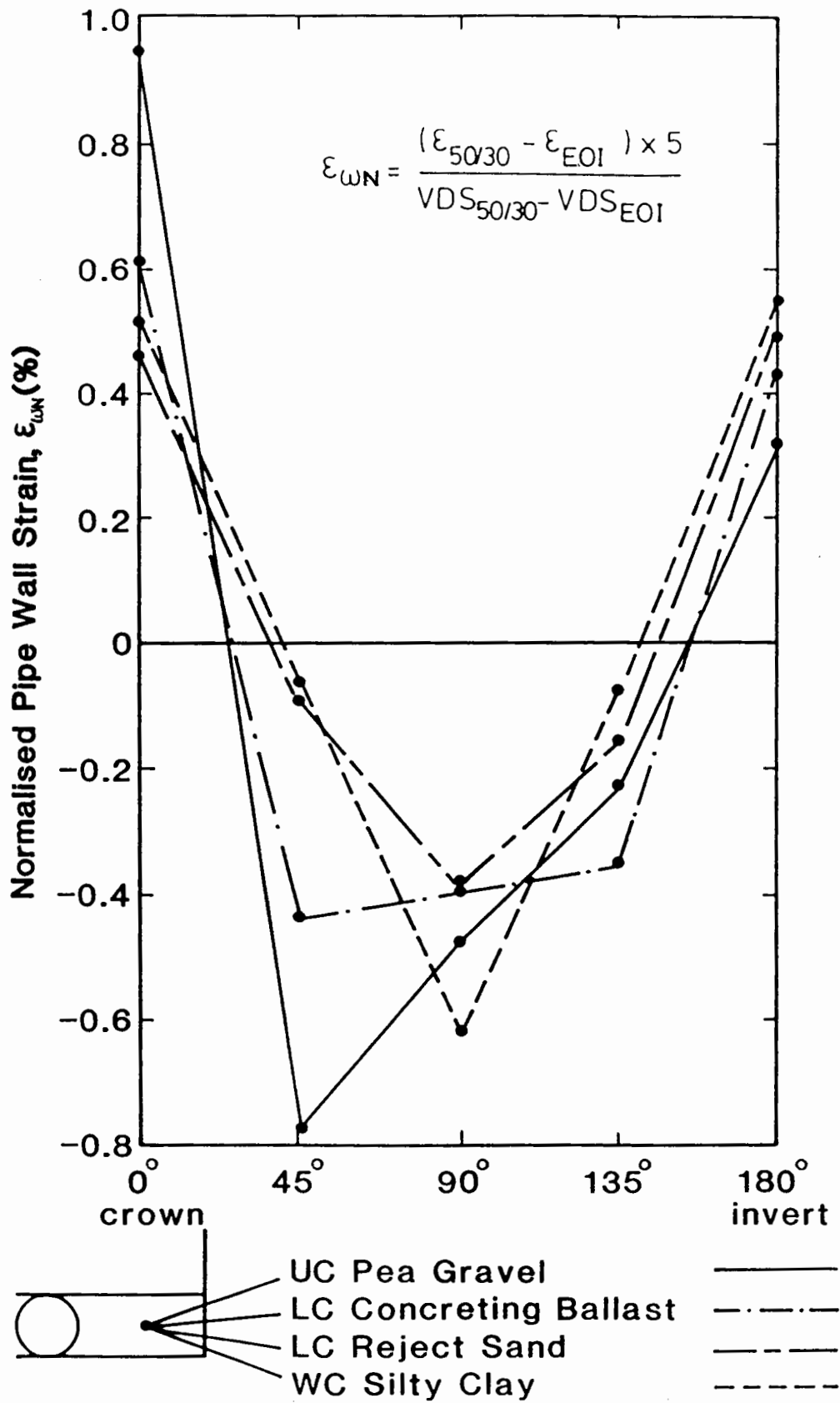


Fig. 5.14 Pipe Wall Strain Profiles for Unconfined Line Load Tests

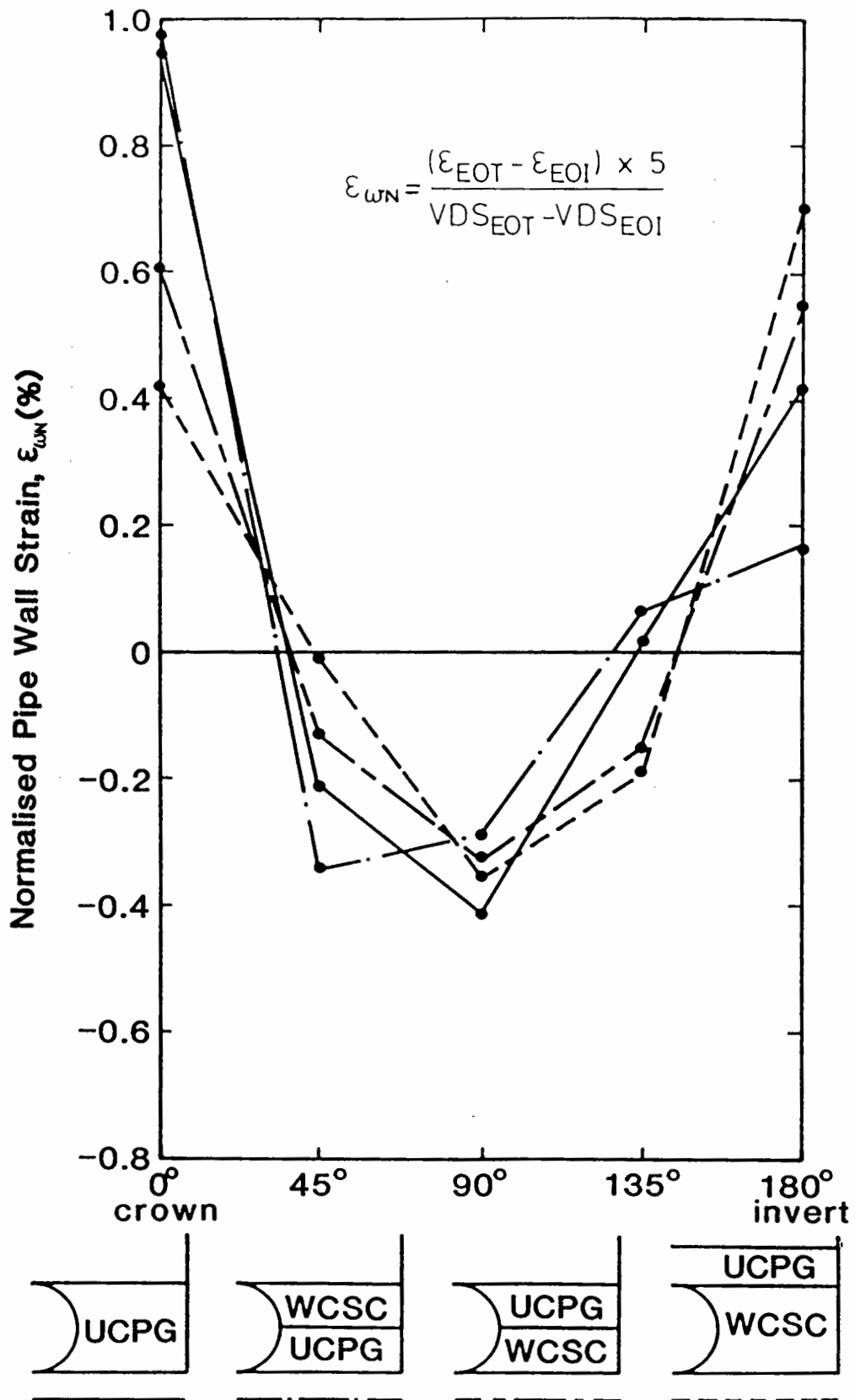


**Fig. 5.15 Normalised Strain Profiles at the End of Tests using Four Different Sidefills**

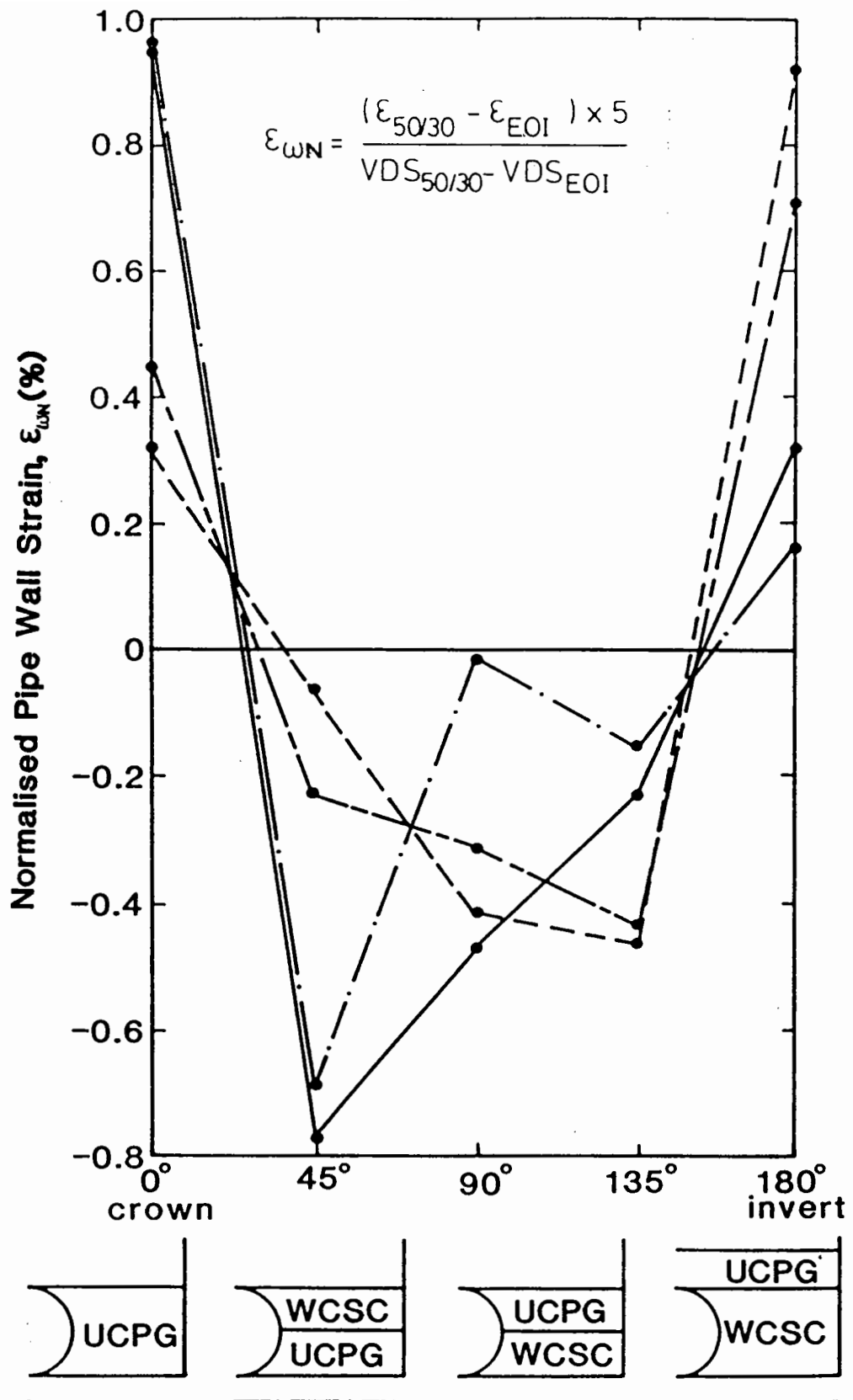




**Fig. 5.16 Normalised Strain Profiles Under 55kN Static Load using Four Different Sidefills**



**Fig. 5.17 Normalised Strain Profiles at the End of Tests Using Four Combinations of Gravel and Clay**



**Fig. 5.18 Normalised Strain Profiles Under 55kN Static Load Using Four Combinations of Gravel and Clay**

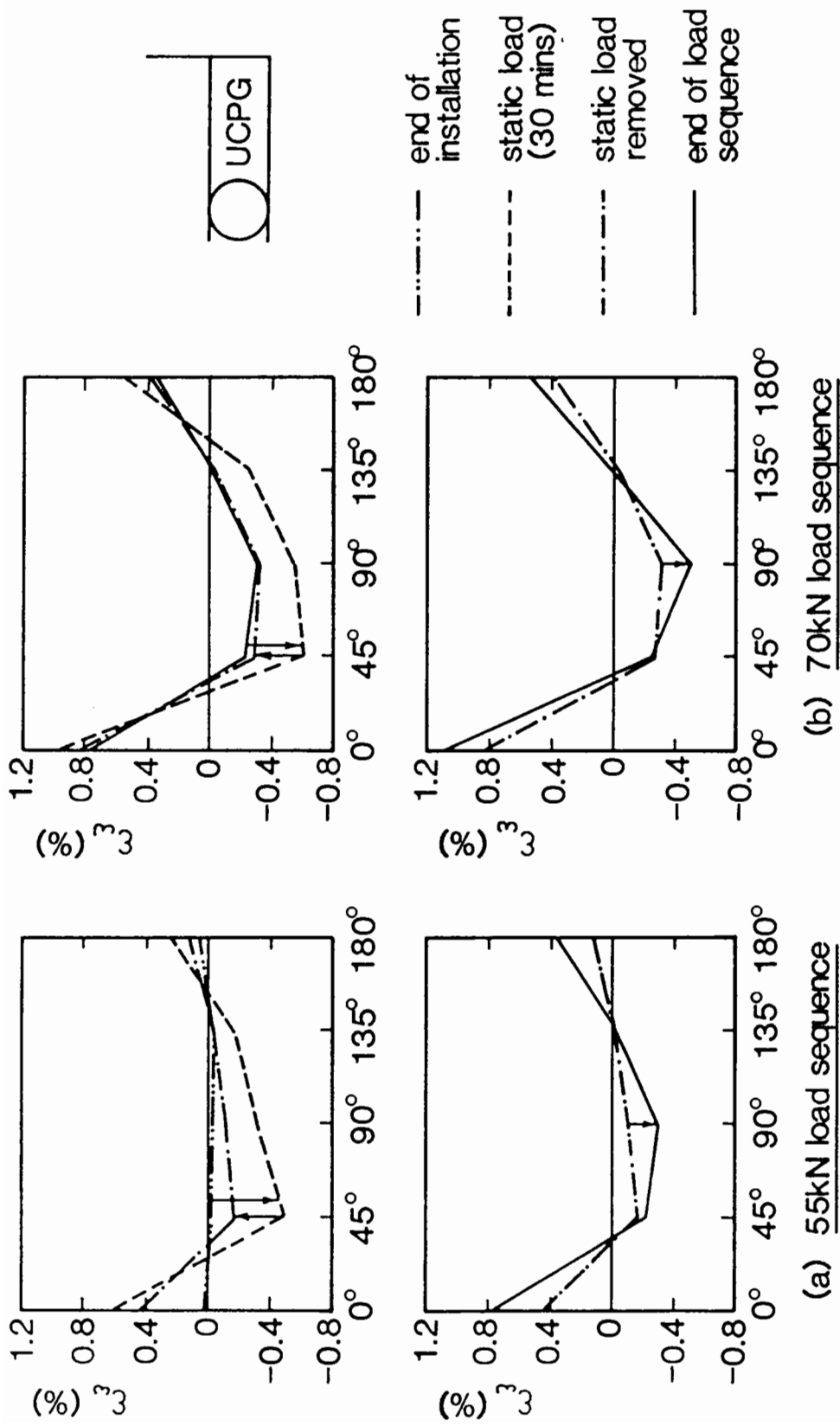
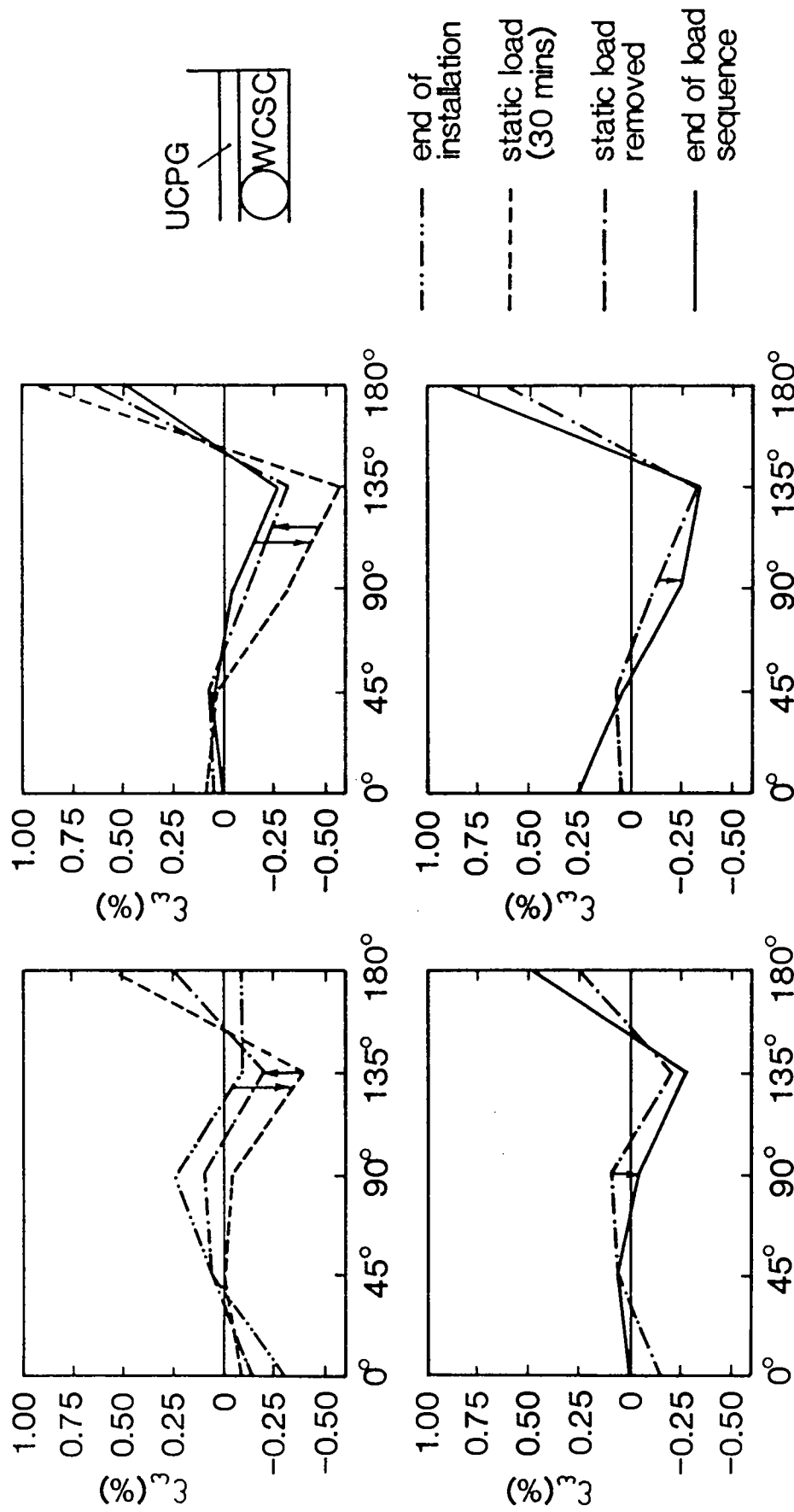


Fig. 5.19 Development of Pipe Wall Strains in Pea Gravel



(a) 55kN load sequence (b) 70kN load sequence

Fig. 5.20 Development of Pipe Wall Strains in Silty Clay

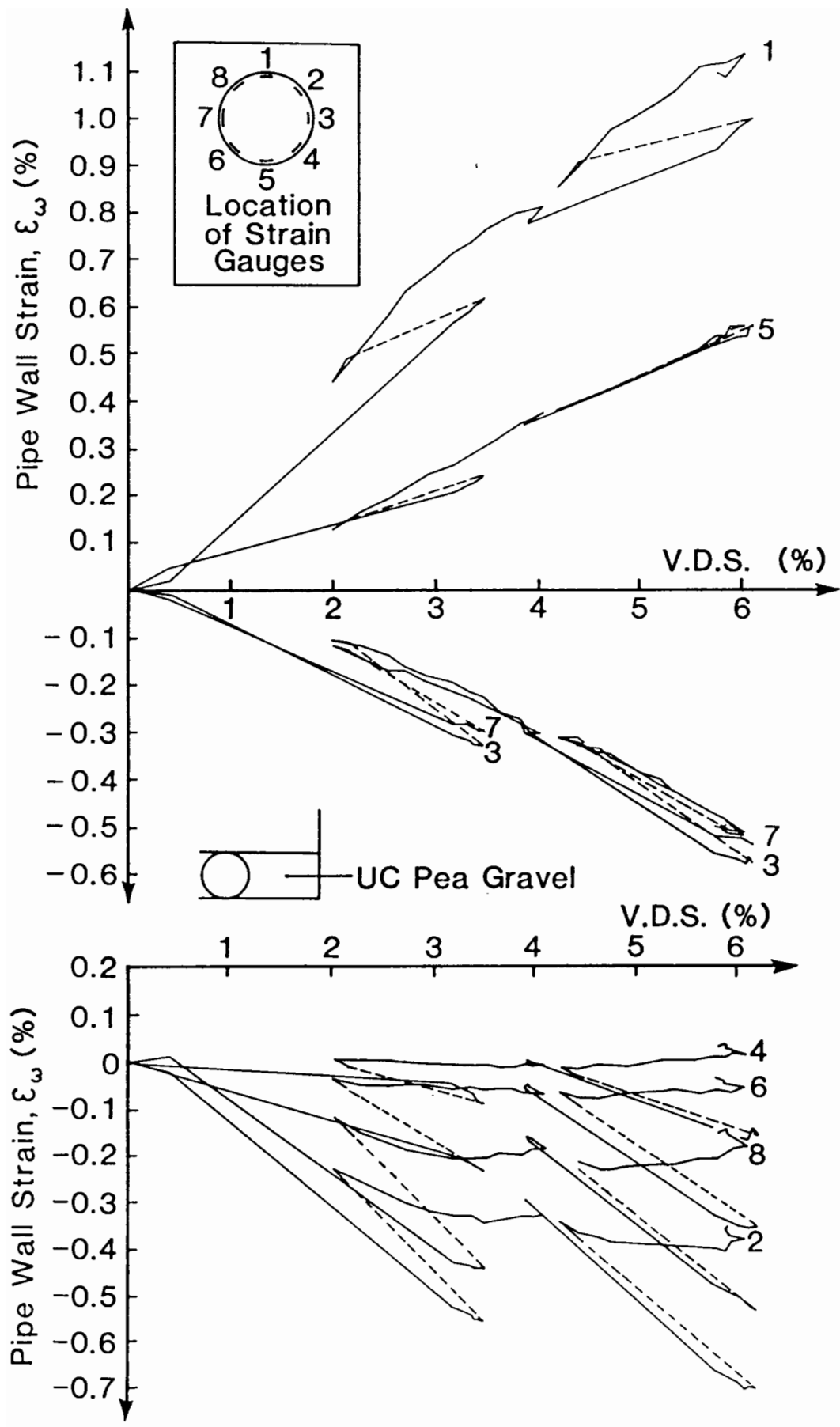


Fig. 5.21 Graph of  $\epsilon_\omega$  vs. V.D.S. for UCPCG Sidefill

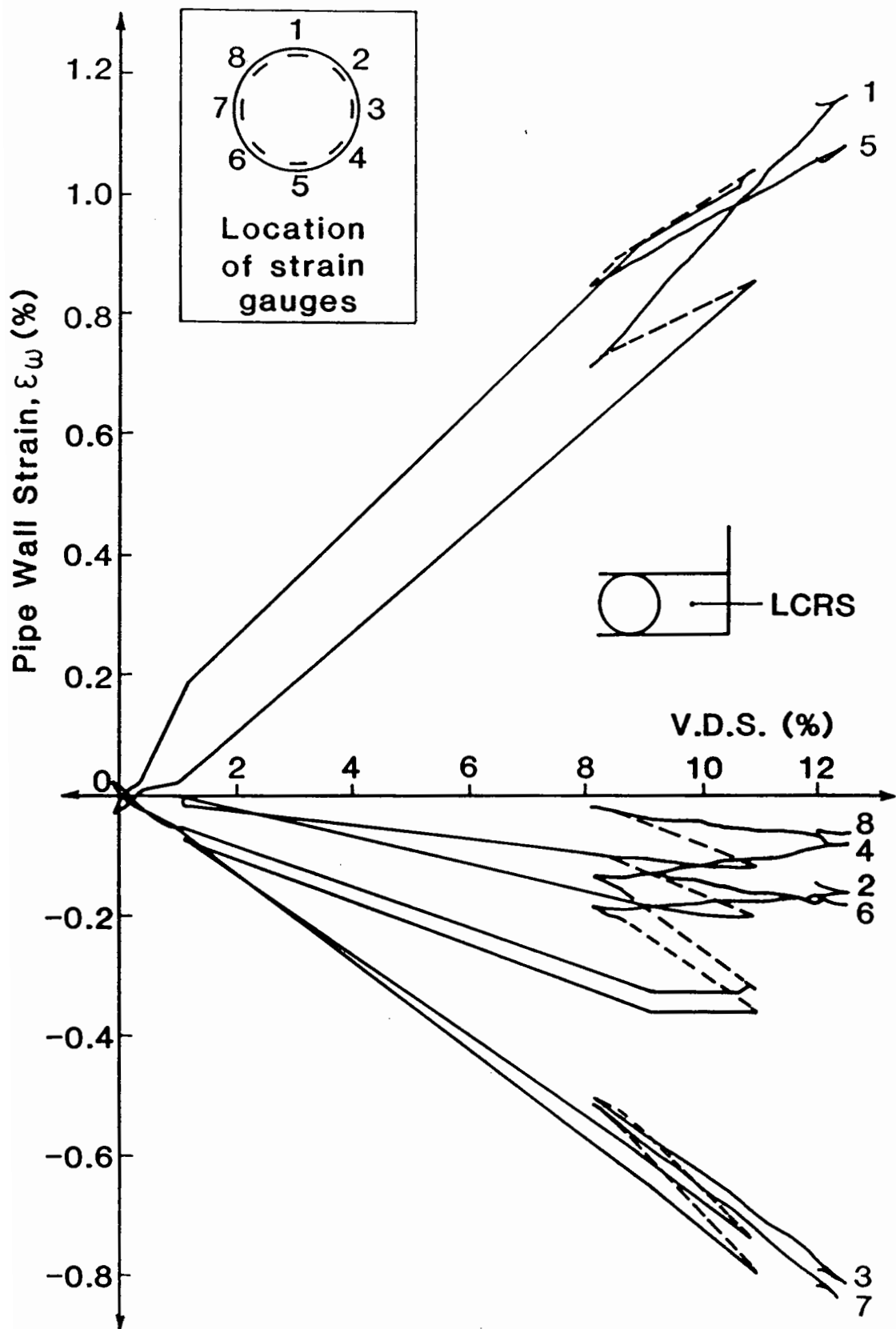
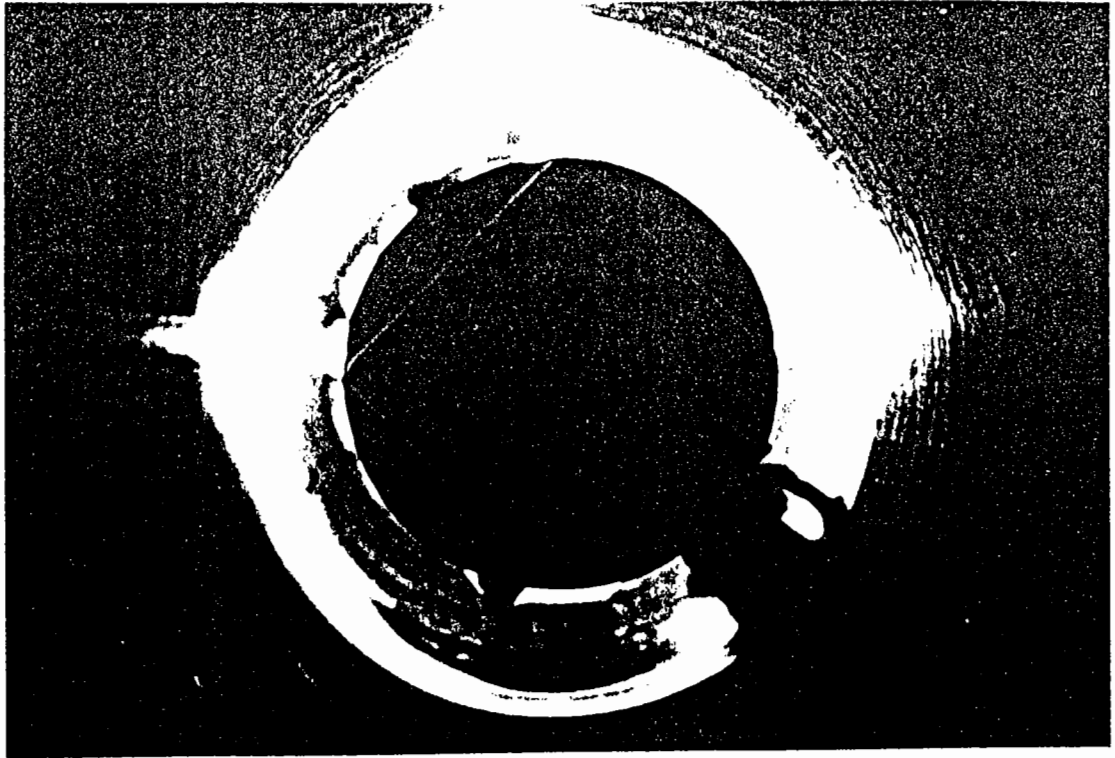


Fig. 5.22 Graph of  $\epsilon_{\omega}$  vs V.D.S. for LCRS Sidefill



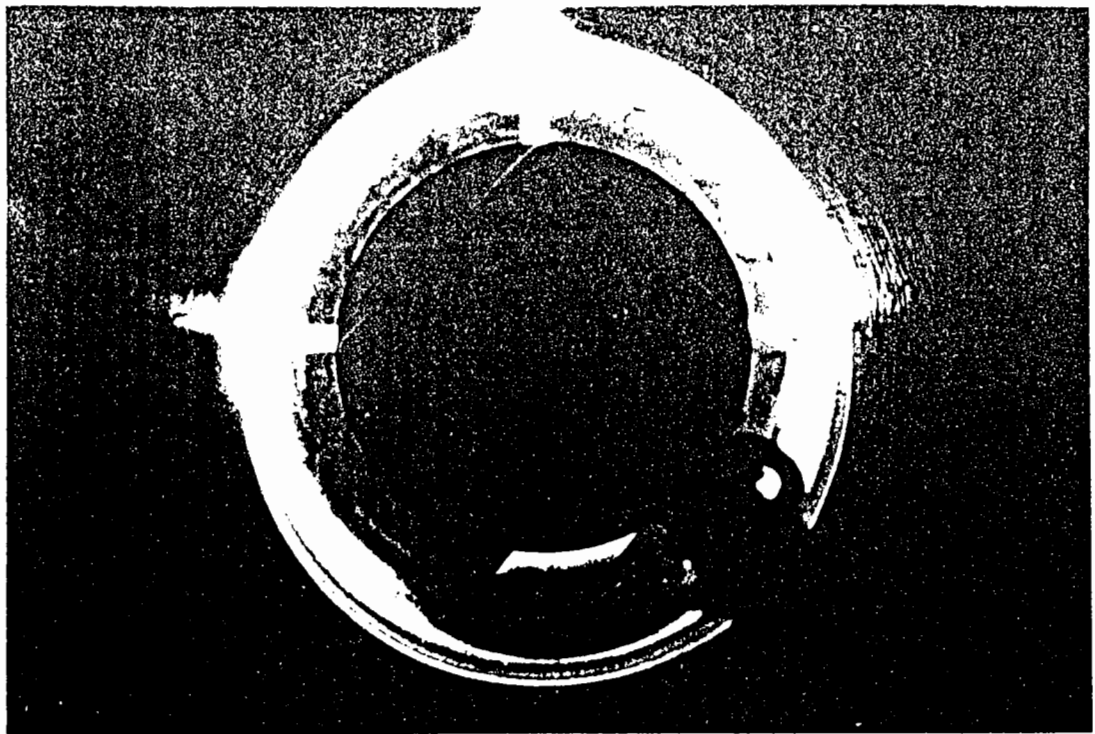
(a) End of installation of pipe



(b) Under 55kN static load

Fig 5.26 Photographs Showing Square Shaped Pipe Deformation in a Split Sidefill



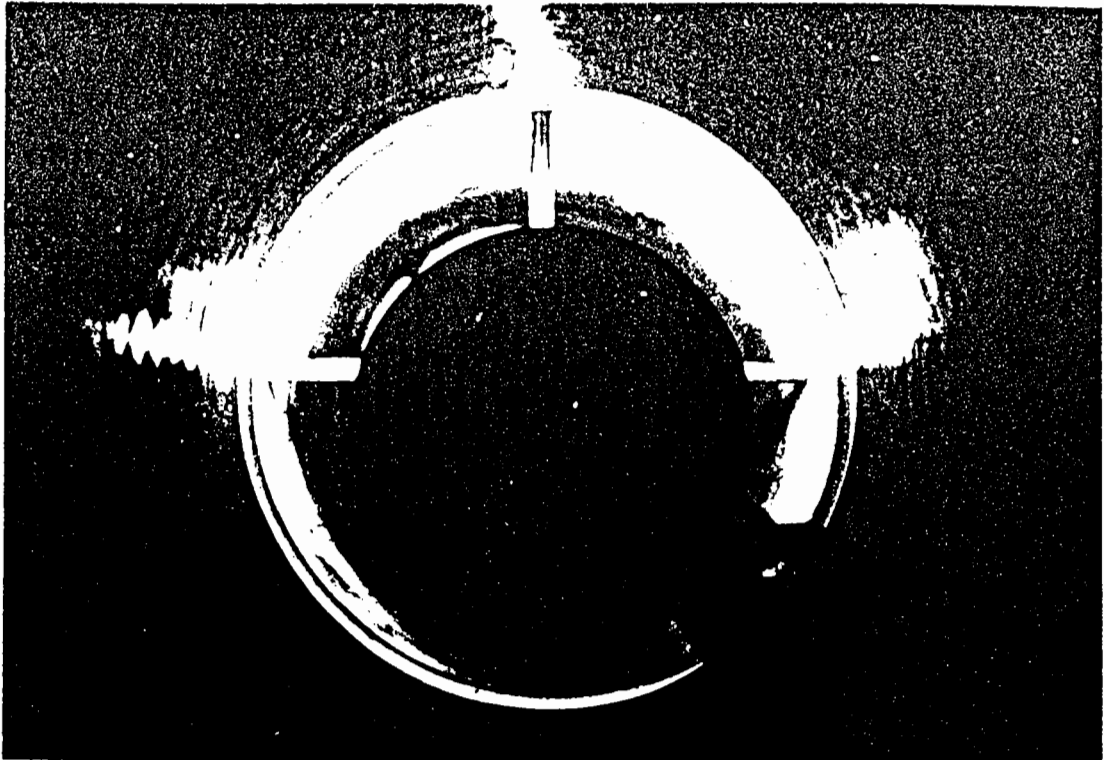


(a) End of installation of pipe

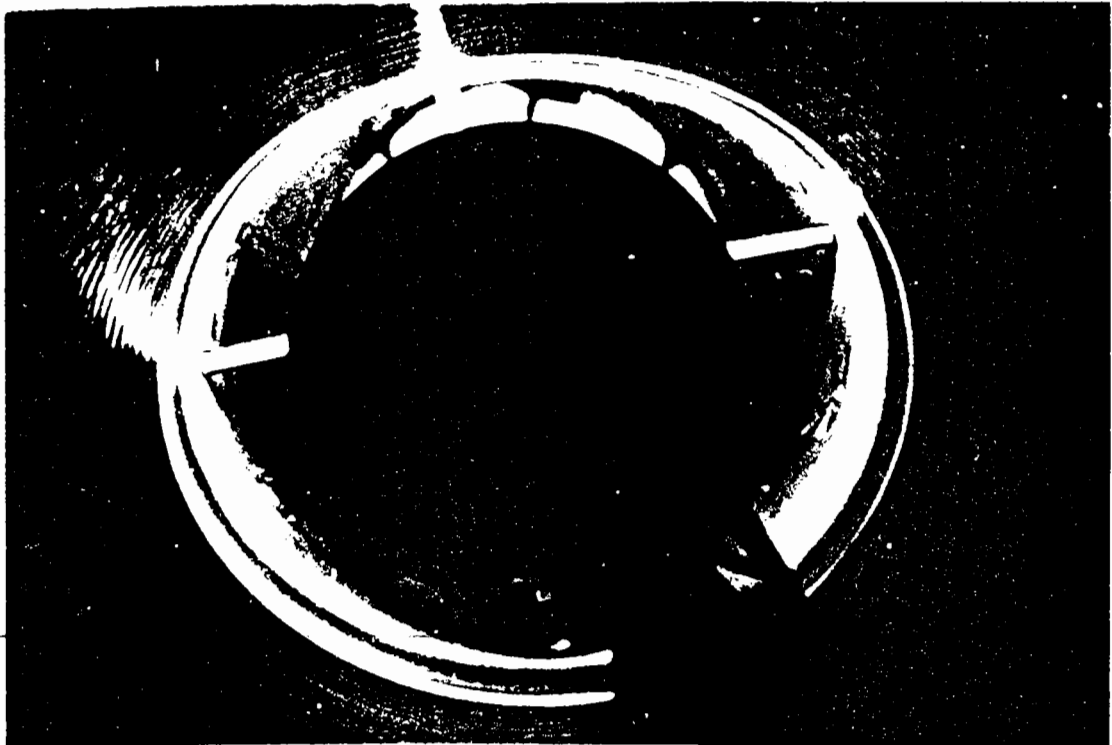


(b) Under 70kN static load

Fig. 5.25 Photographs Showing an Inverted Heart Shape Deformation of a Pipe under Static Load with a Pressure Inside the Pipe

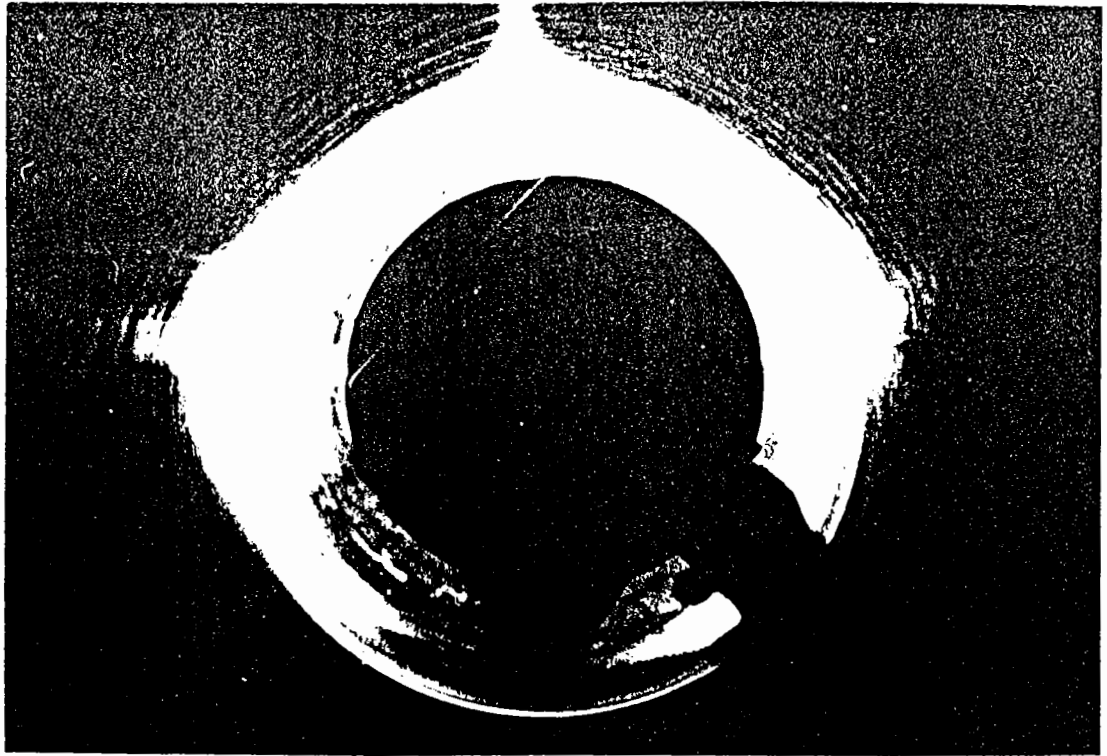


(a) Prior to installation of pipe

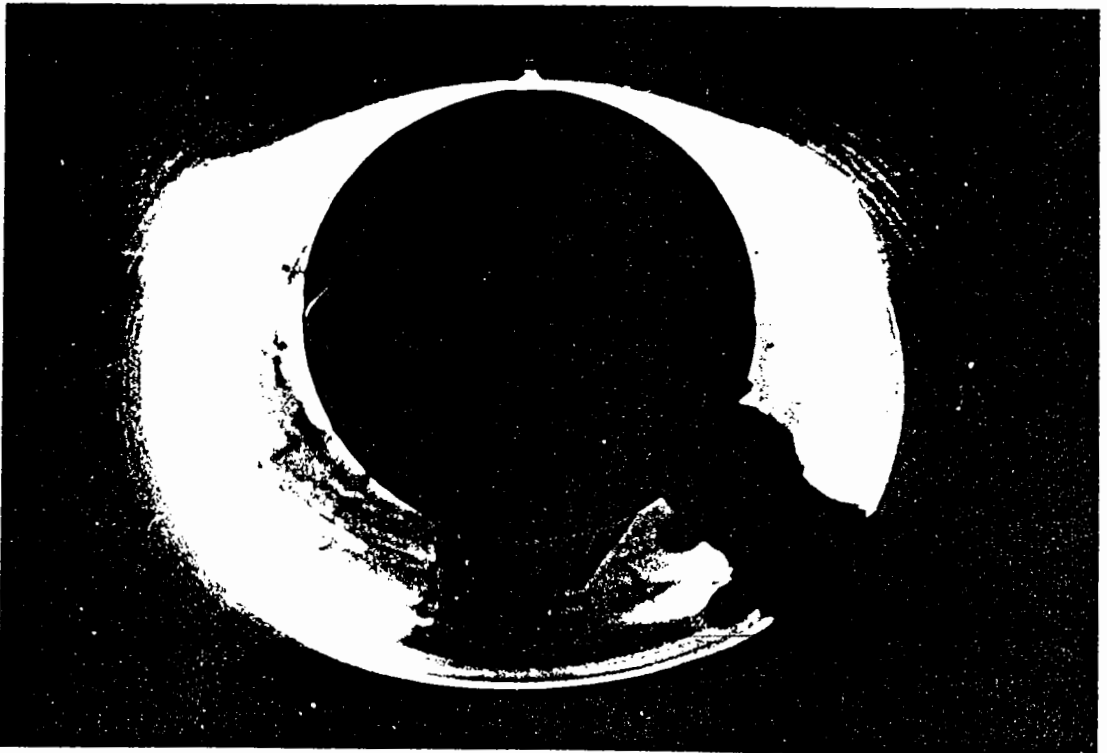


(b) Under 100kN static load

Fig. 5.24 Photographs Showing Heart Shaped Pipe Deformation in Pea Gravel



(a) Prior to installation of pipe



(b) End of Test

Fig. 5.23. Photographs Showing Roughly Elliptical Pipe Deformation in Rectangular

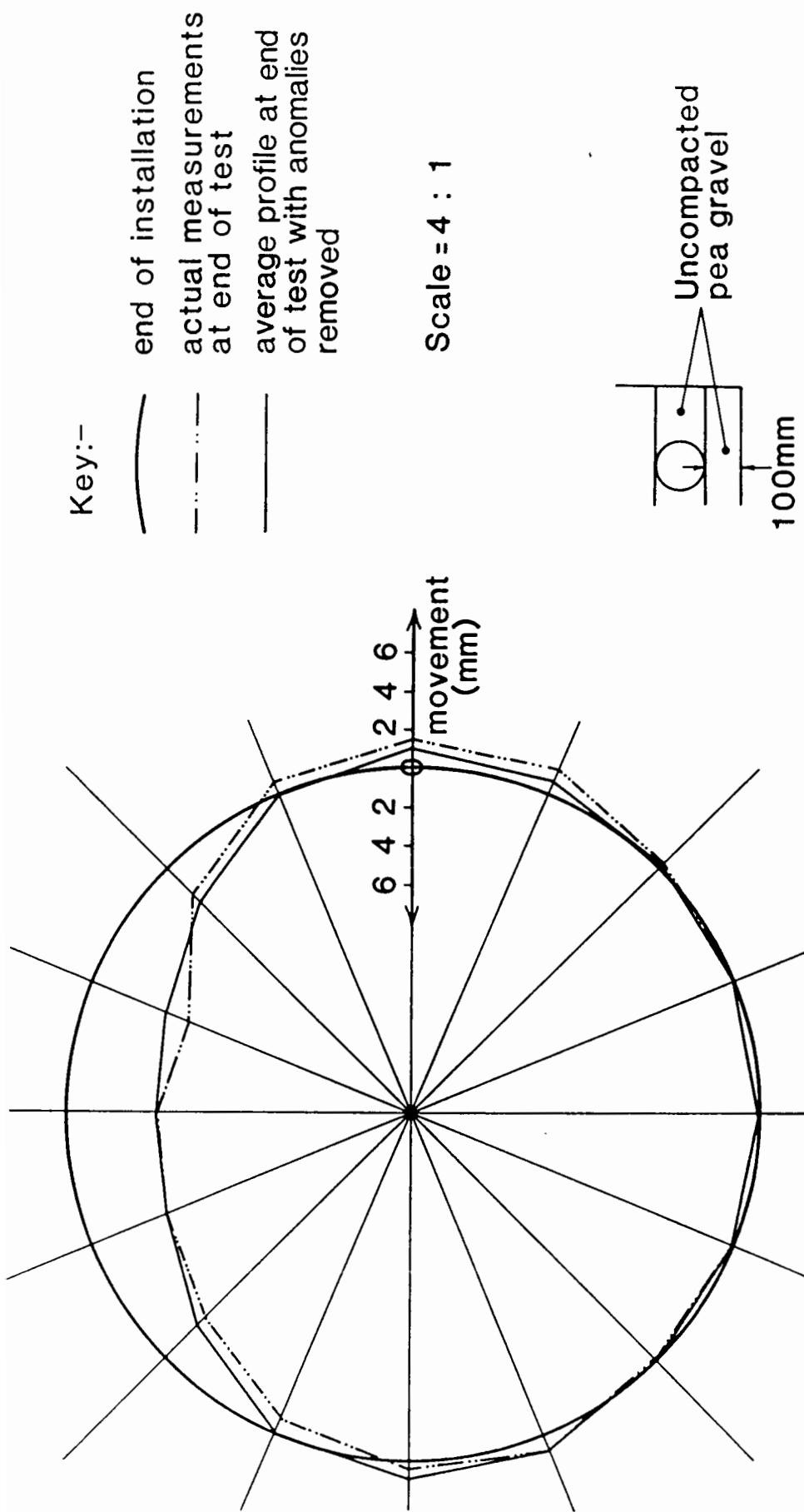


Fig. 5.27 Deformed Profile of Pipe Surrounded by Uncompact Pea Gravel

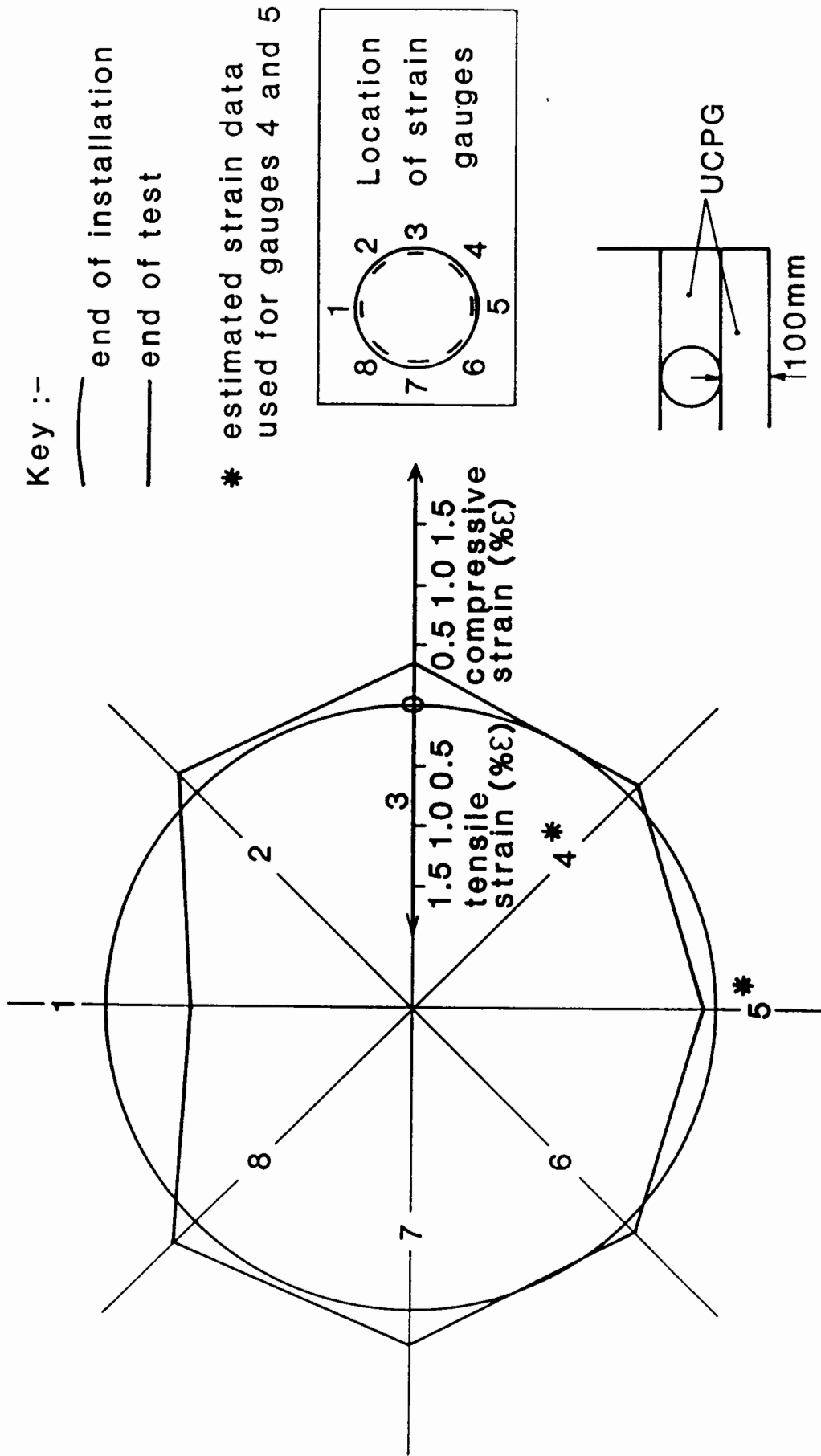


Fig. 5.28 Pipe Wall Strain Profiles for Pipe Surrounded by Pea Gravel

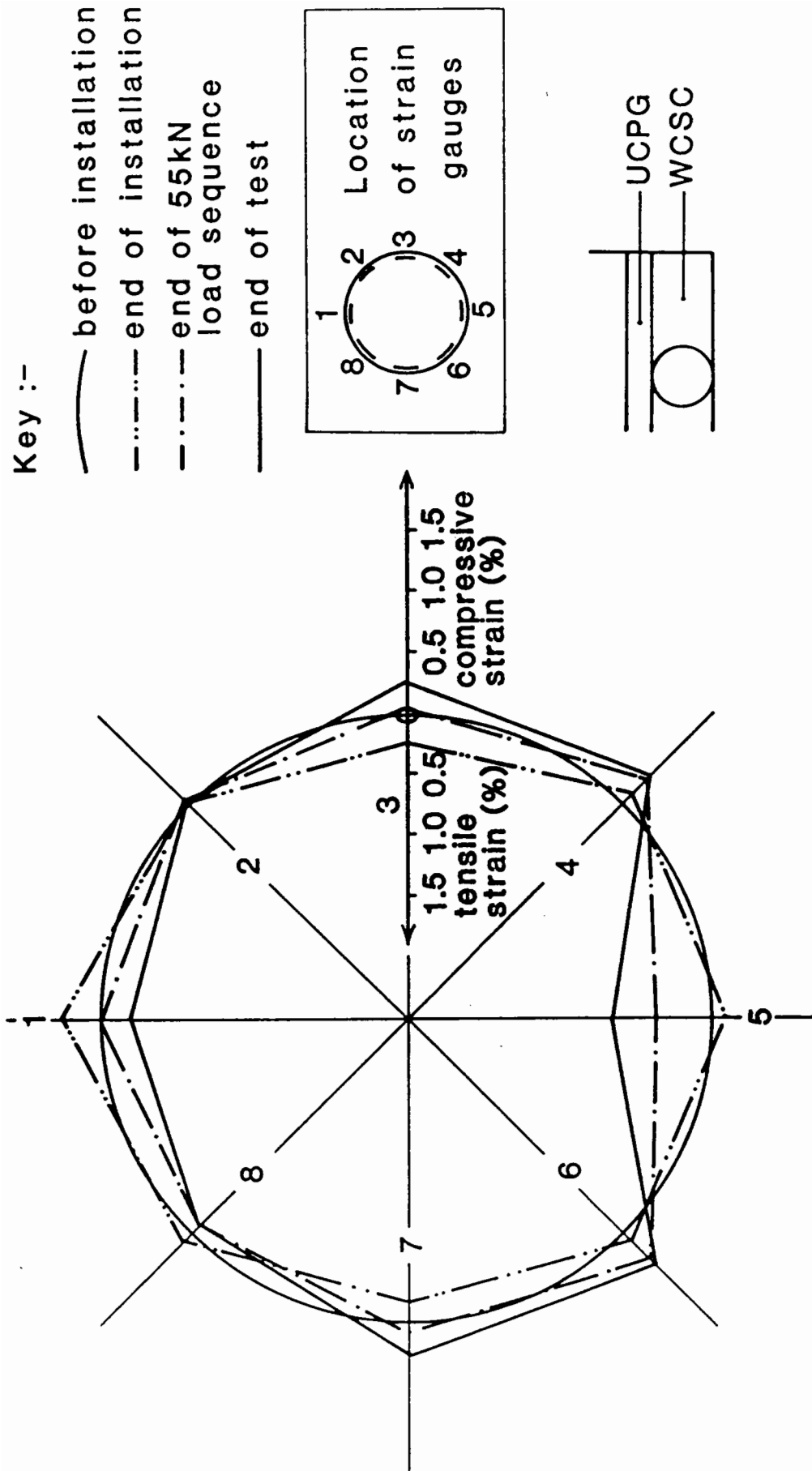


Fig. 5.29 Pipe Wall Strain Profiles for a Clay Sidefill with an Arching Layer

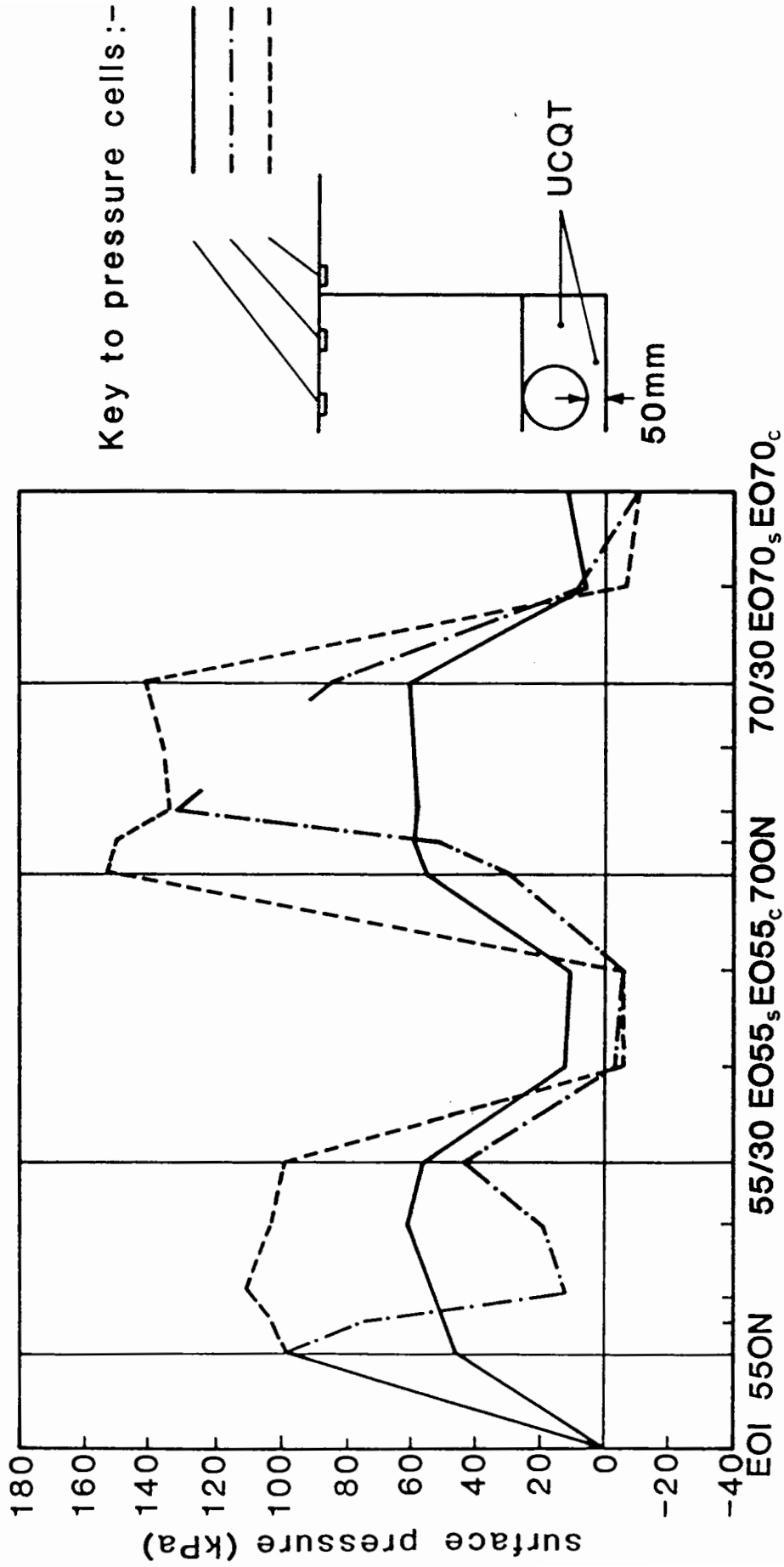


Fig. 5.30 Surface Pressure Measurements for UCQT Installation

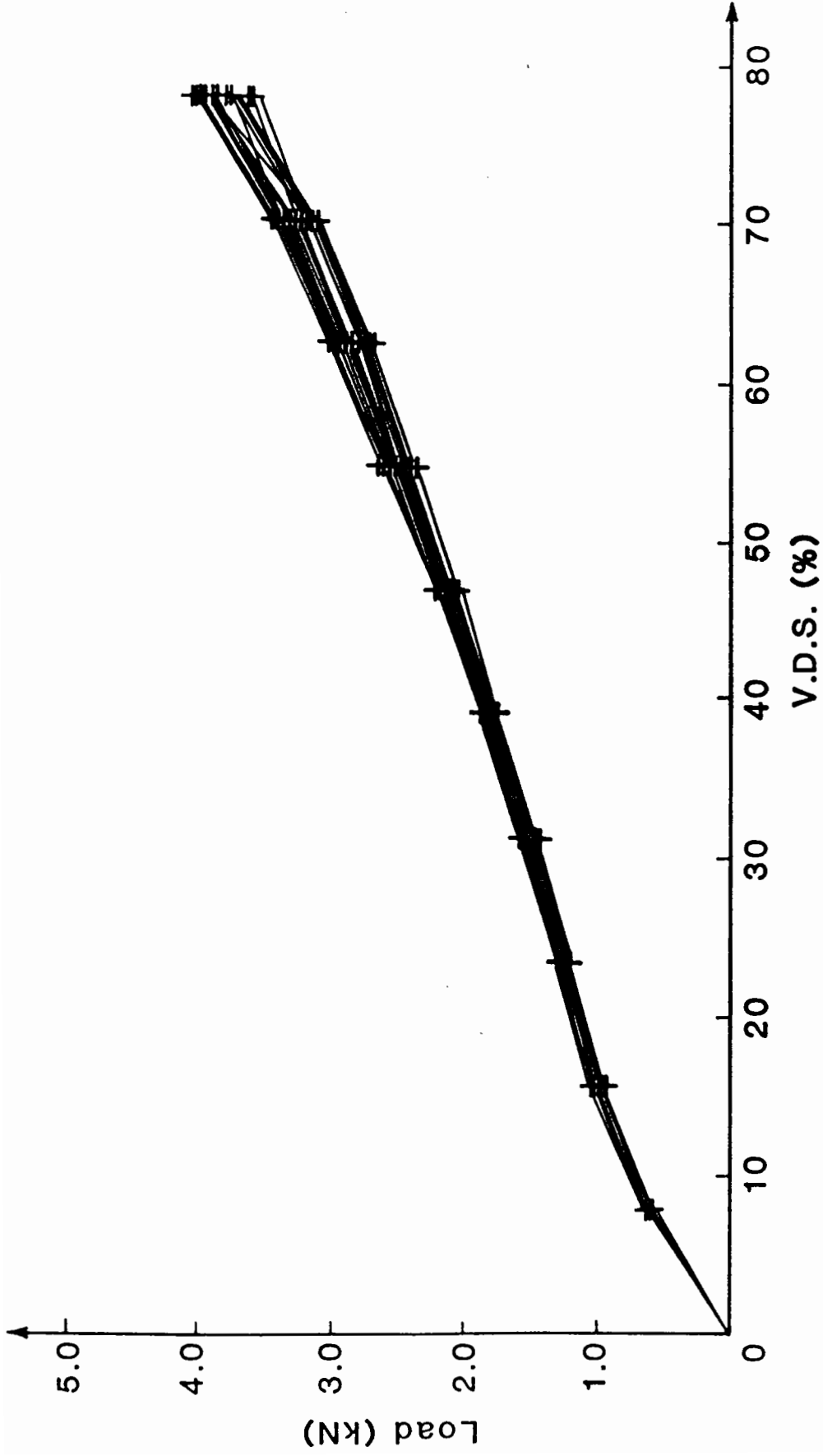
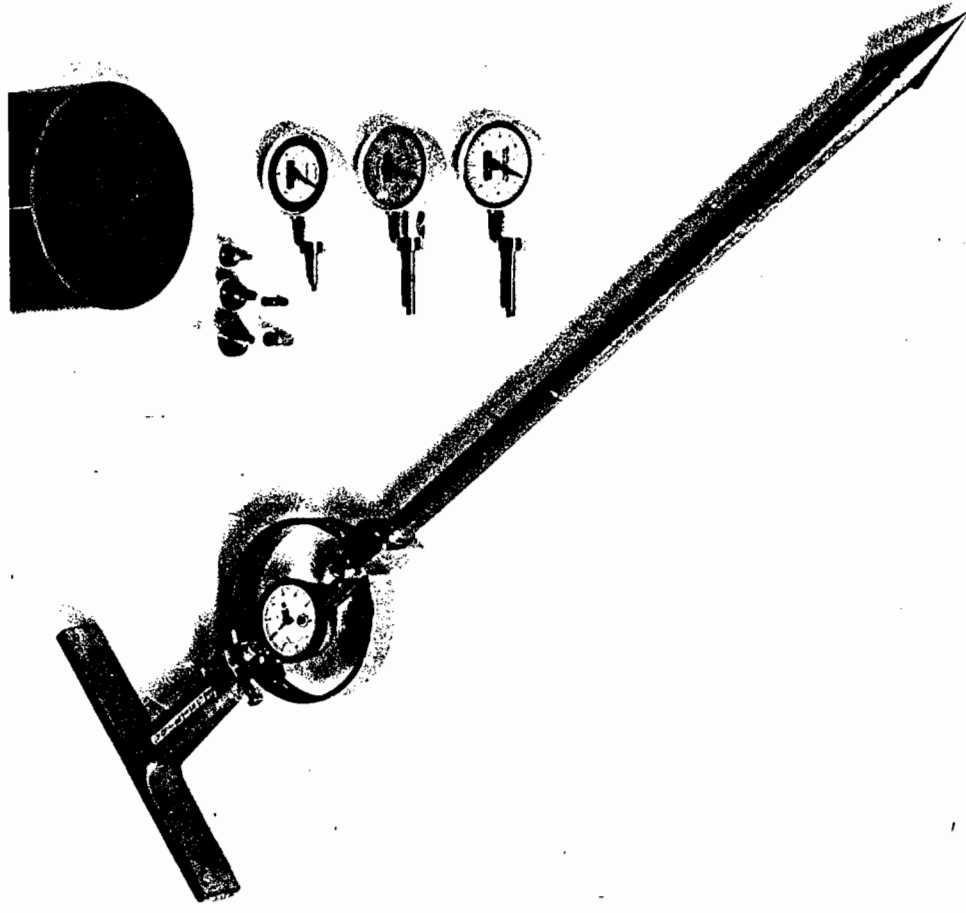


Fig. 5.31 Graph of Load Against V.D.S. for Pipe Characterisation Tests





**Fig. 6.1 The Insitu Soil Strength Testing Devices**

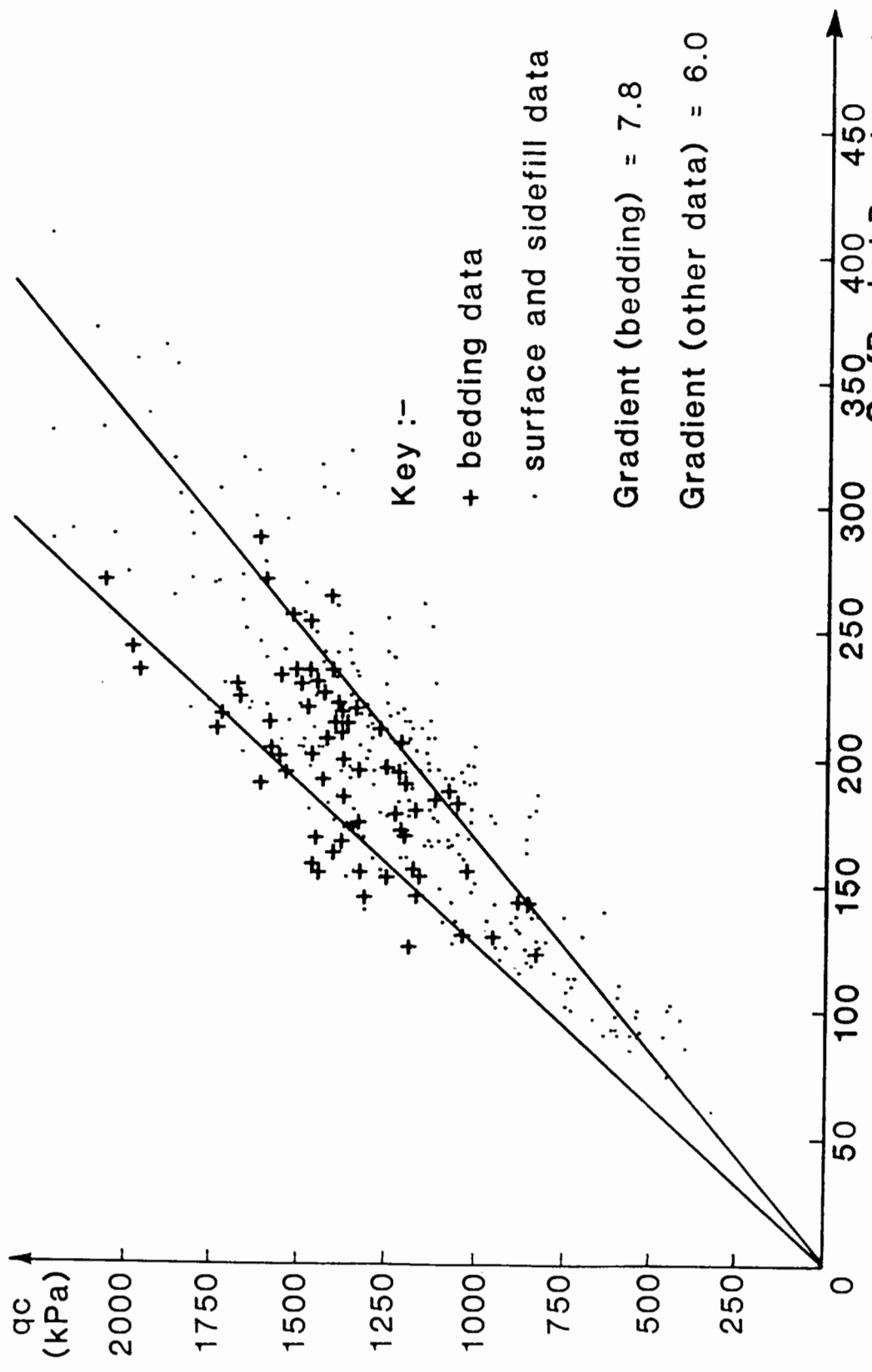


Fig. 6.2 Graph of  $q_c$  (Proving Ring Penetrometer) vs  $C_u$  (Pocket Penetrometers)  
for Keuper Marl

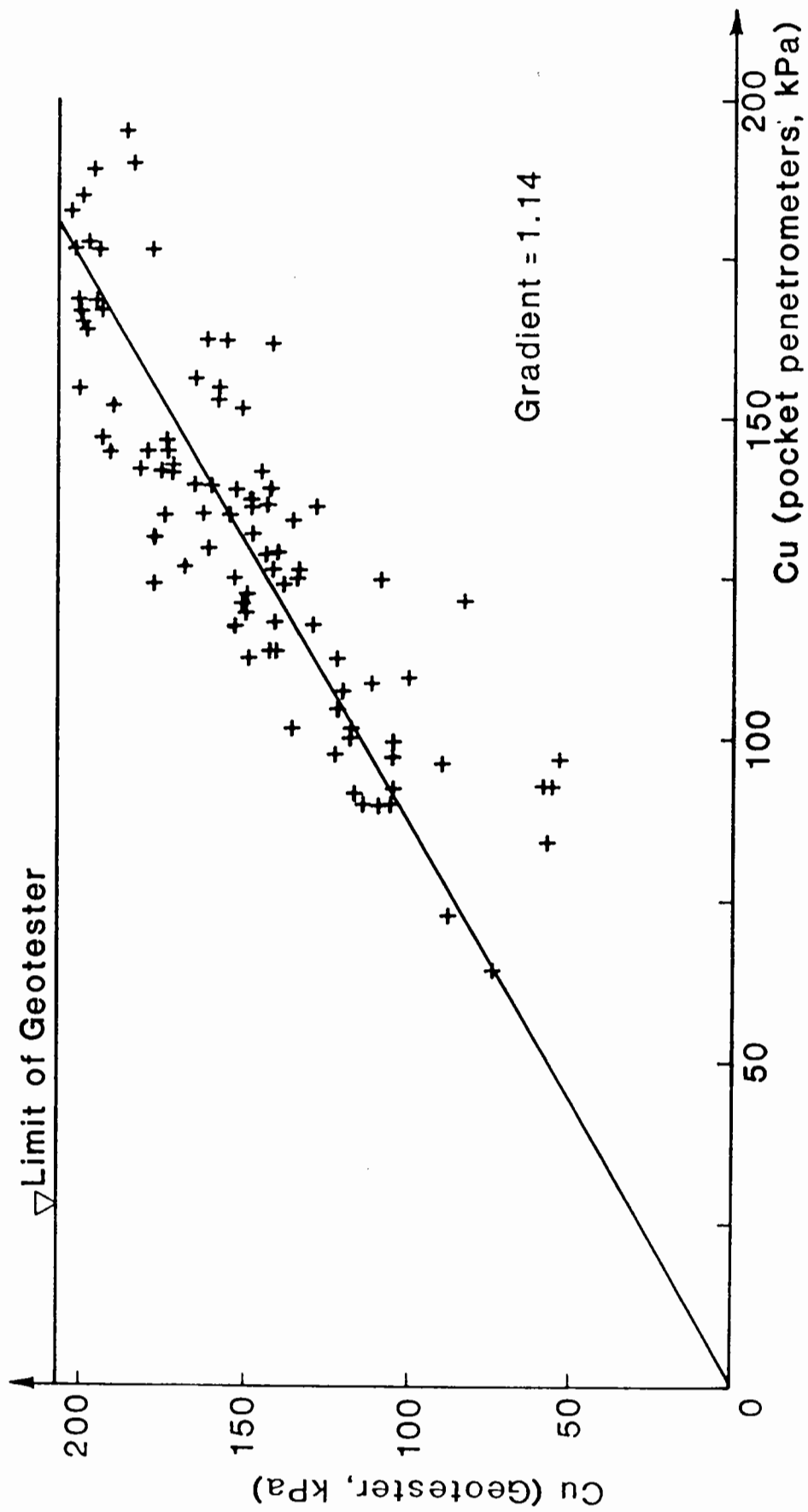


Fig. 6.3 Graph of Cu (Geotester) vs Cu (Pocket Penetrometers) for Keuper Marl

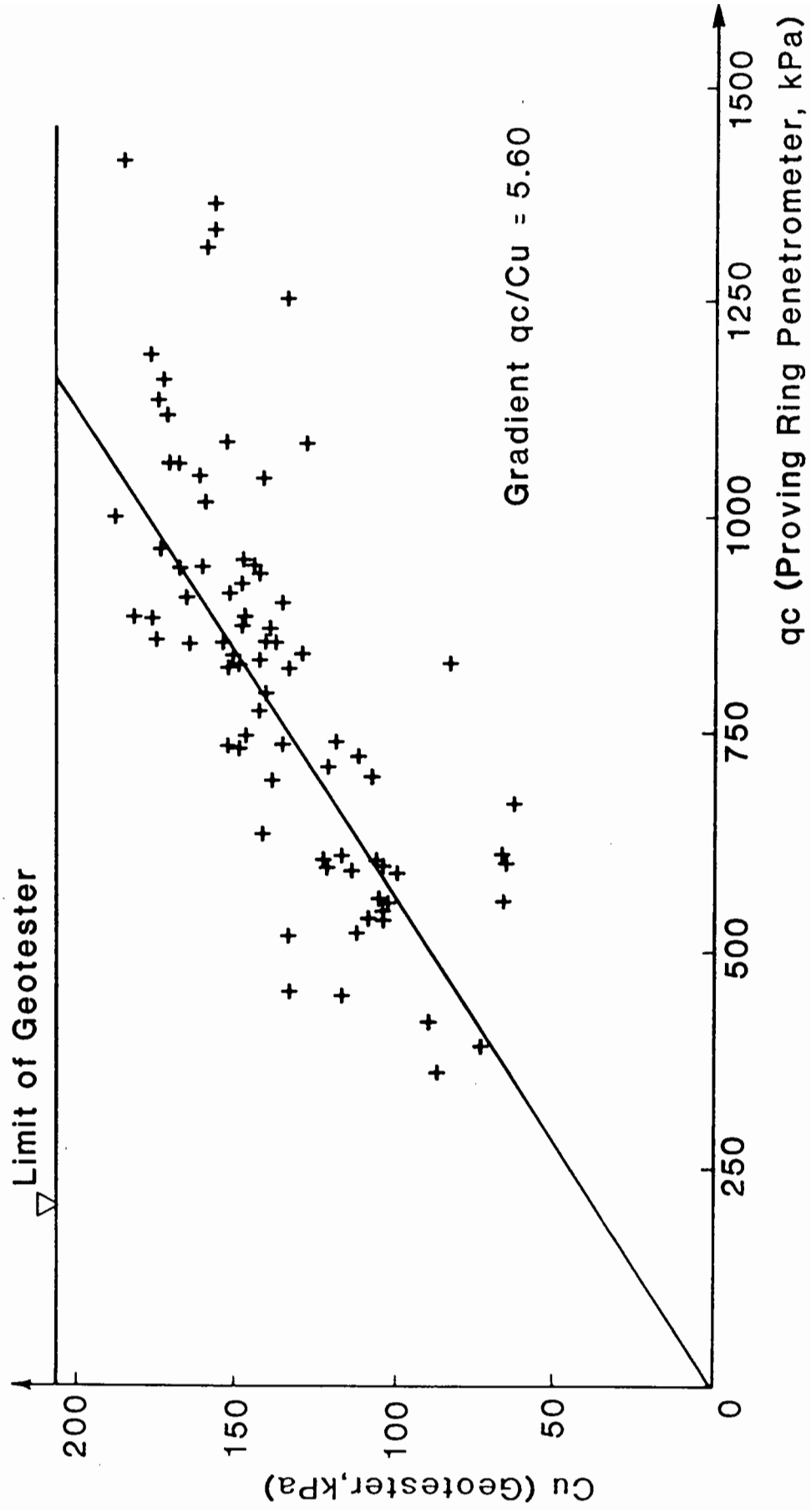


Fig. 6.4 Graph of  $C_u$  (Geotester) vs  $q_c$  (Proving Ring Penetrometer)

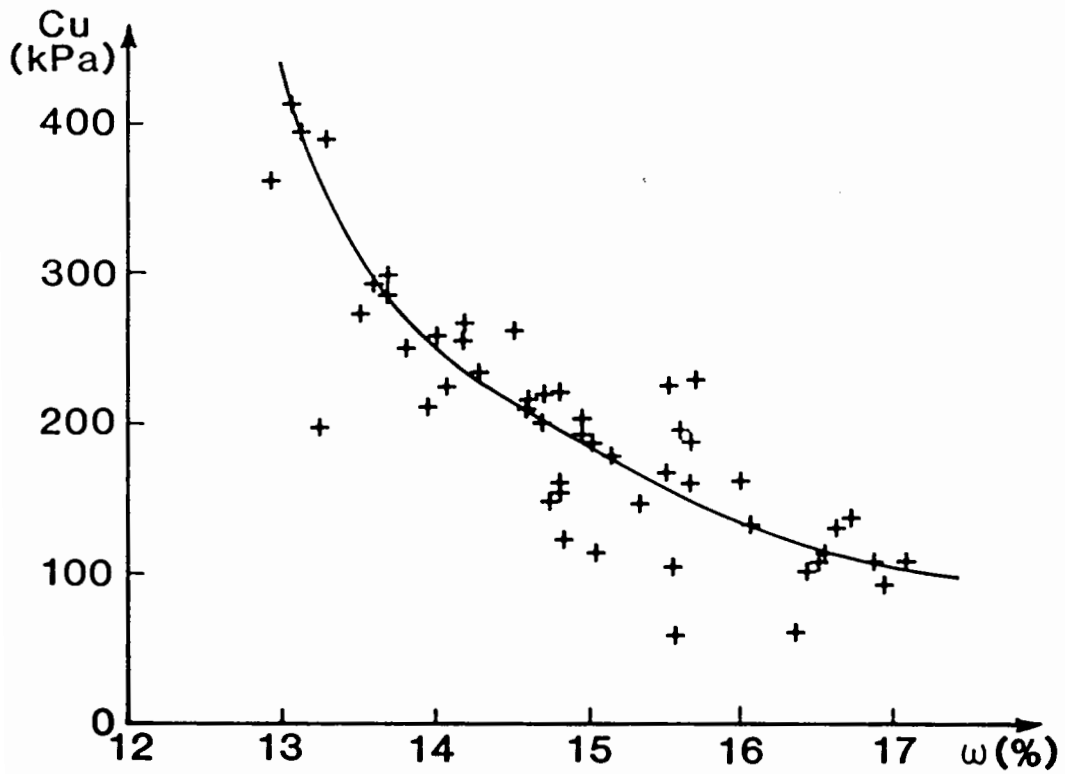


Fig. 6.5 Graph of  $C_u$  vs  $\omega$  for Keuper Marl using Triaxial Test Data

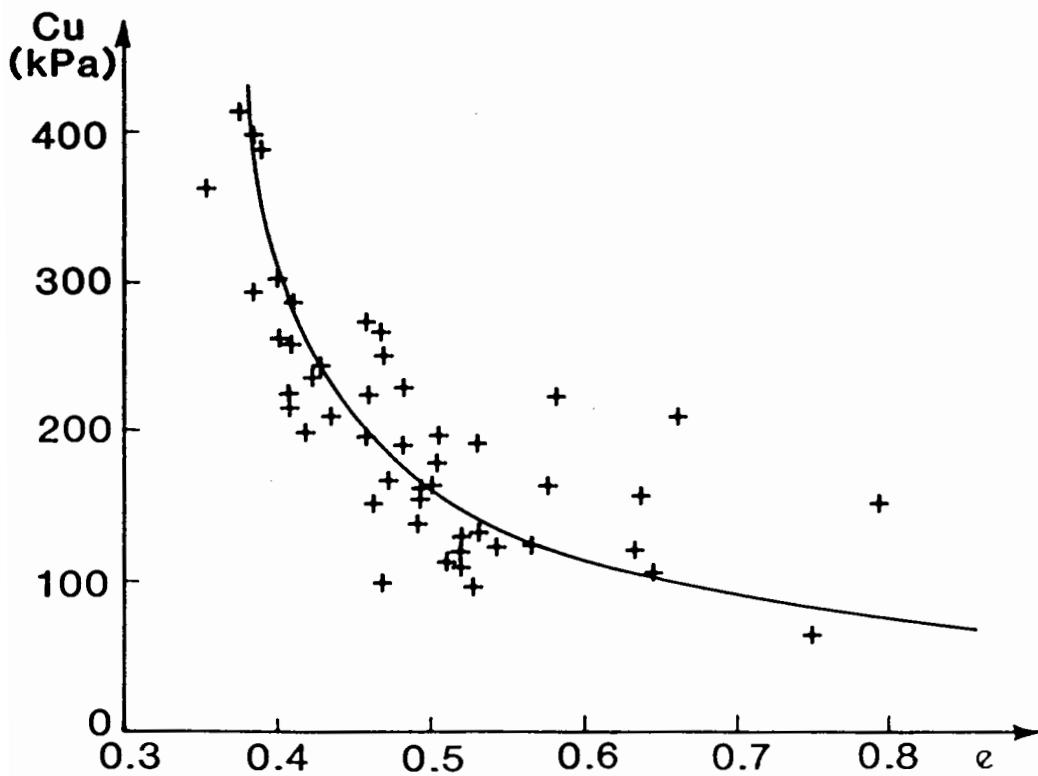


Fig. 6.6 Graph of  $C_u$  vs  $e$  for Keuper Marl using Triaxial Test Data

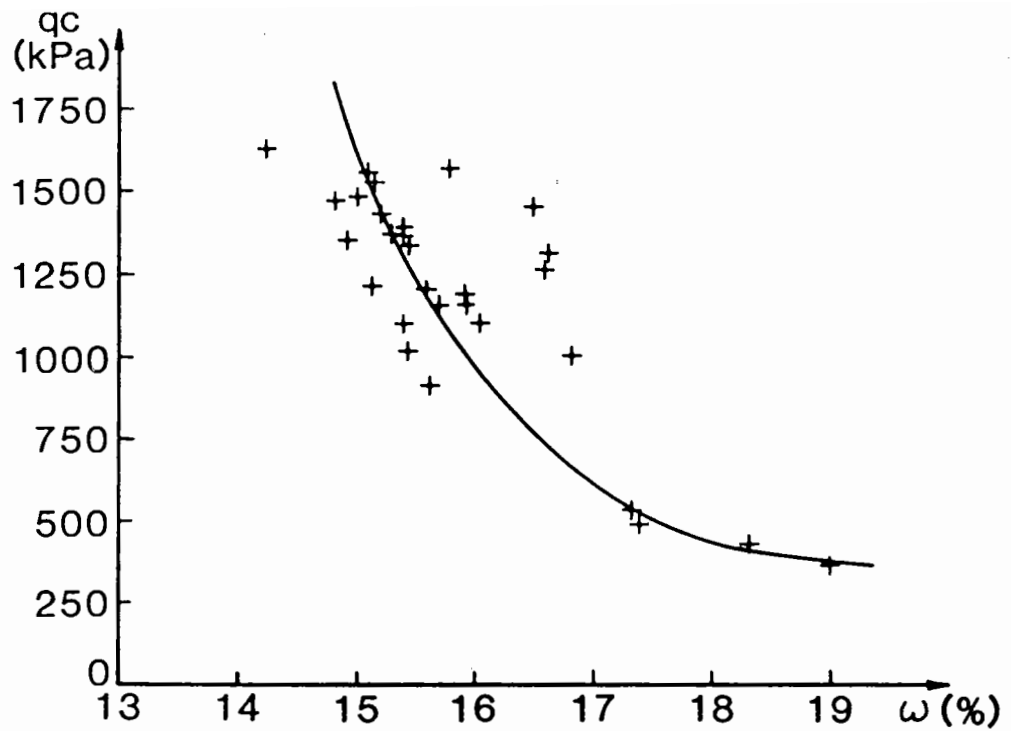


Fig. 6.7 Graph of  $q_c$  vs  $\omega$  for Keuper Marl using Proving Ring Penetrometer Data

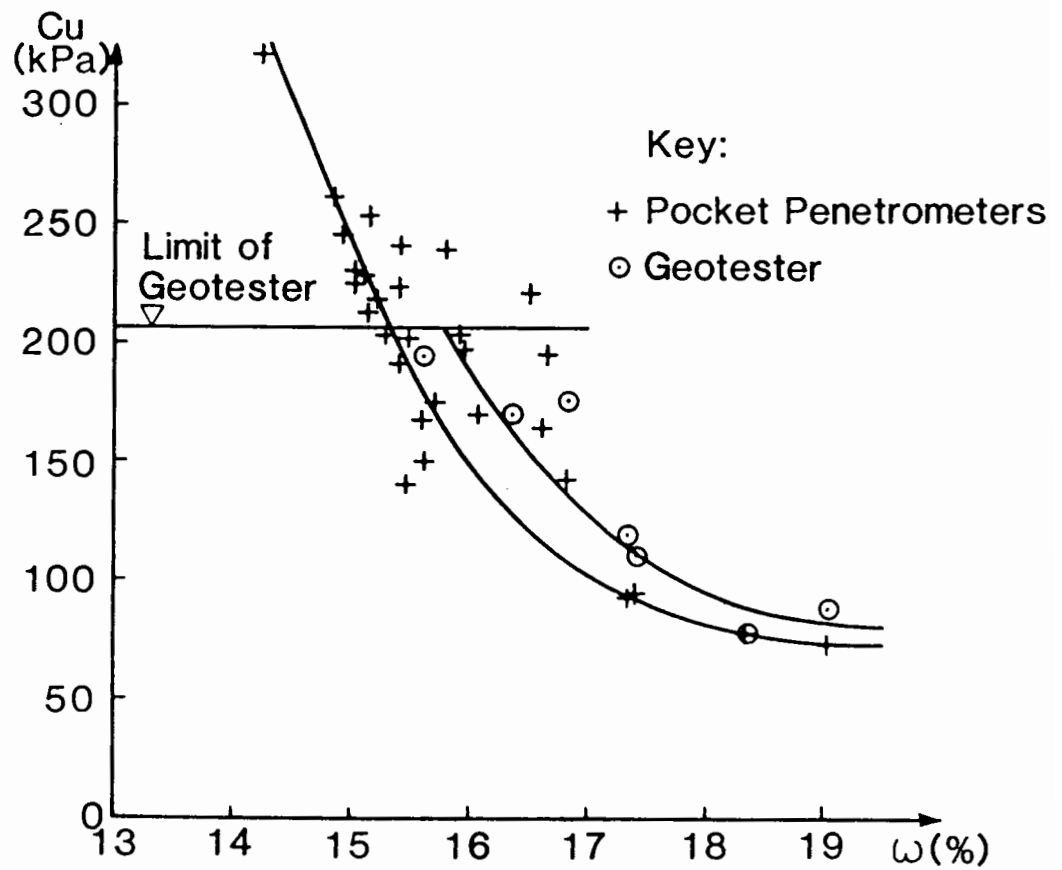


Fig. 6.8 Graph for  $C_u$  vs  $\omega$  for Keuper Marl using Pocket Penetrometers and Geotester Data

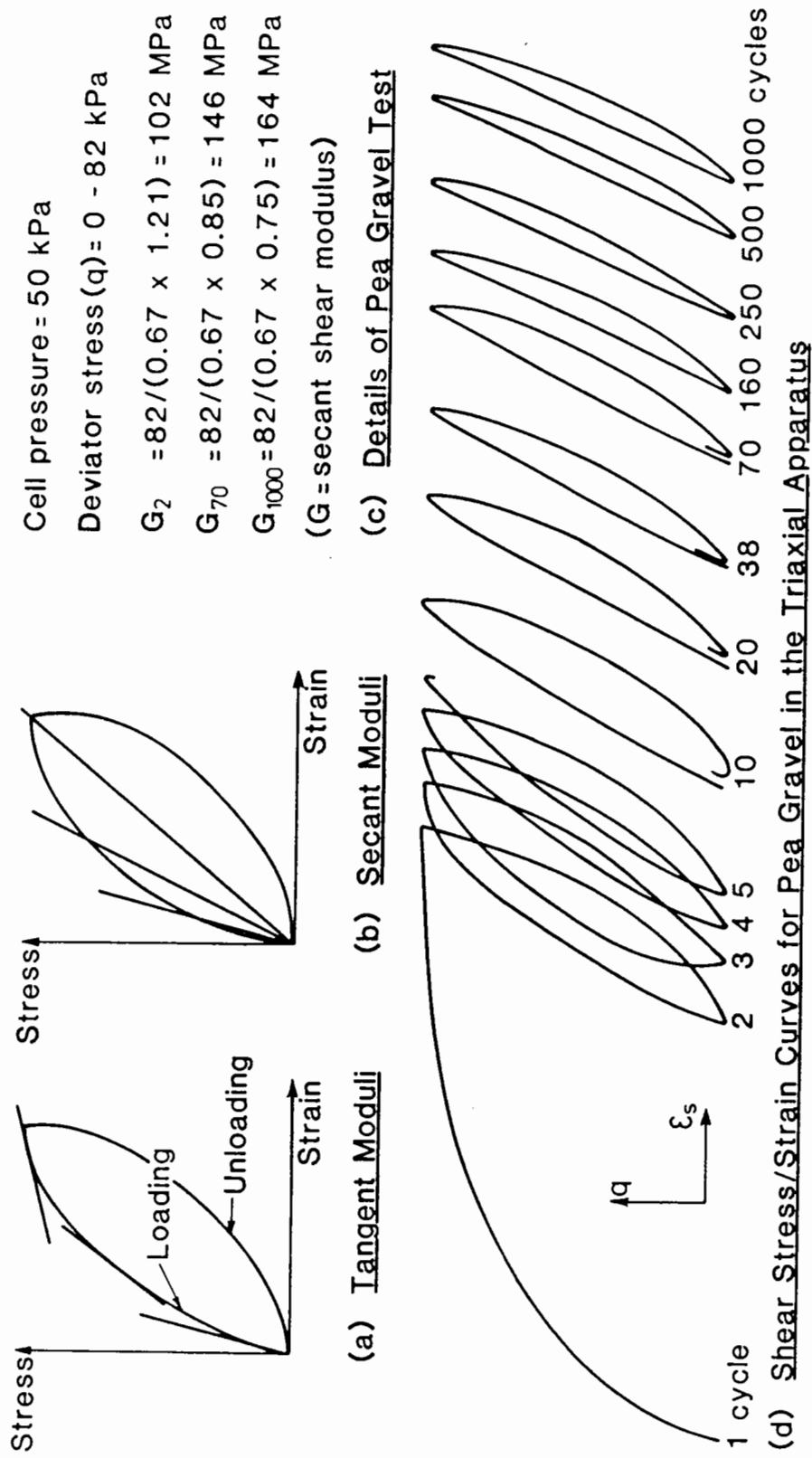


Fig. 6.9 Modulus Definition and Example Triaxial Test Results for Granular Materials

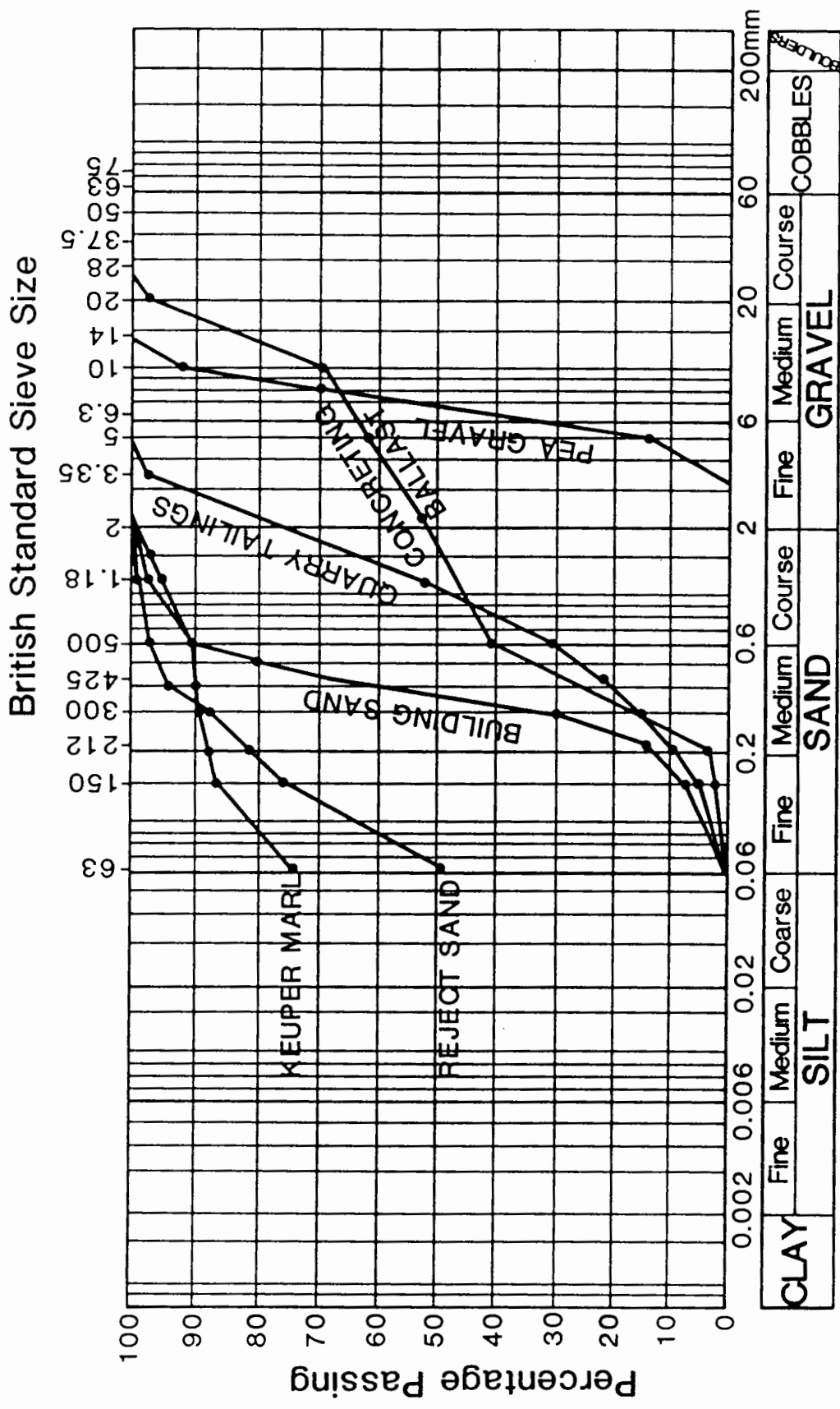


Fig. 6.10 Particle Size Distribution Curves



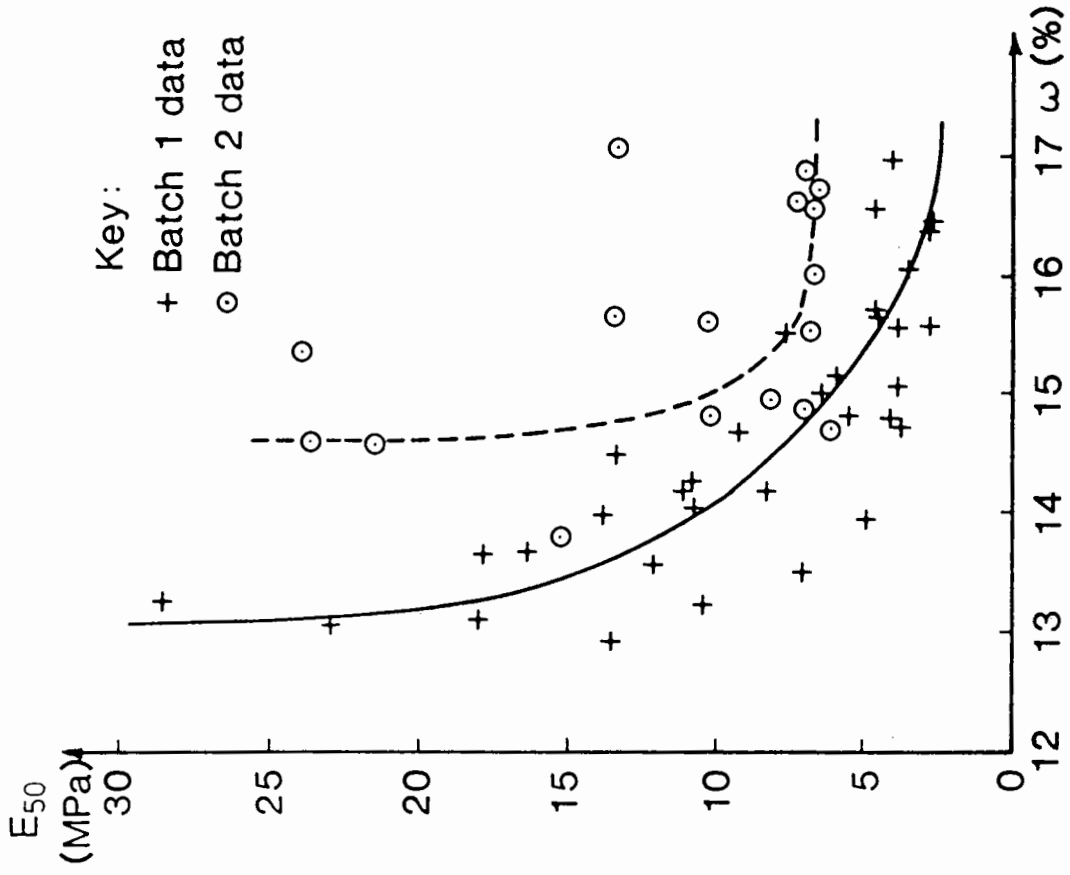


Fig. 6.11 Graph of  $E_{50}$  vs  $\omega$  for Keuper Marl

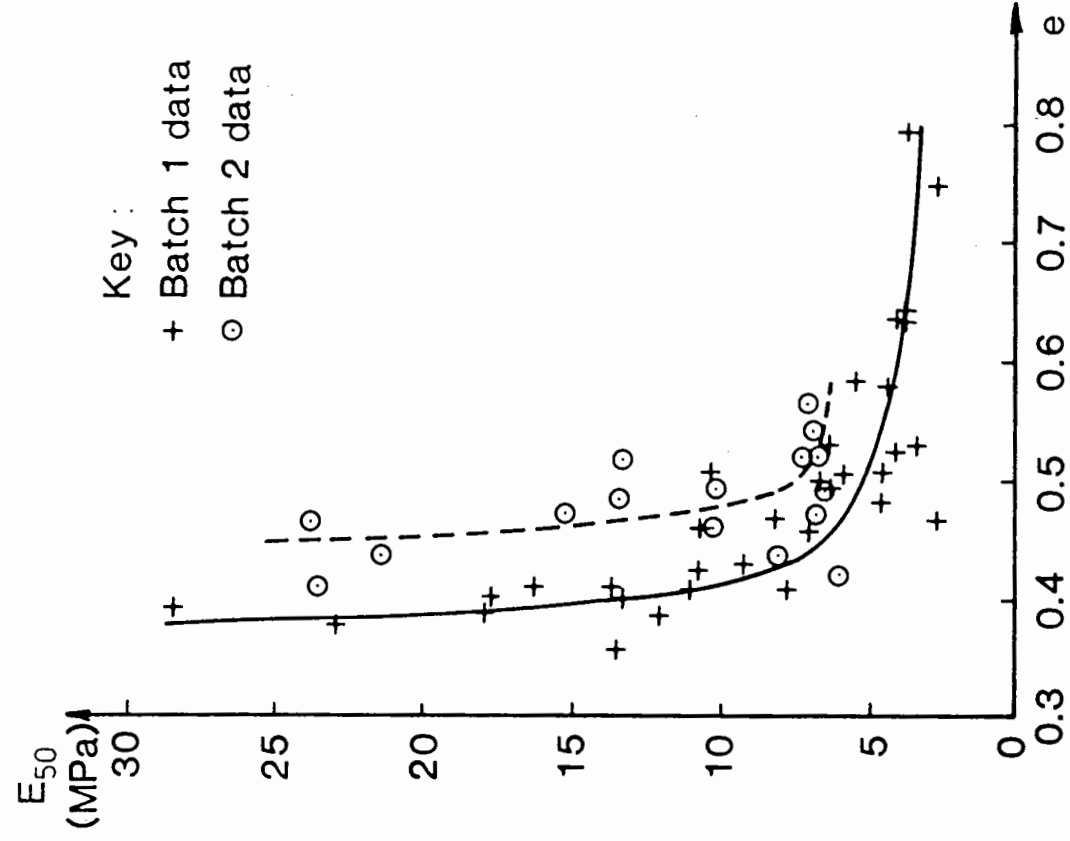


Fig. 6.12 Graph of  $E_{50}$  vs  $e$  for Keuper Marl

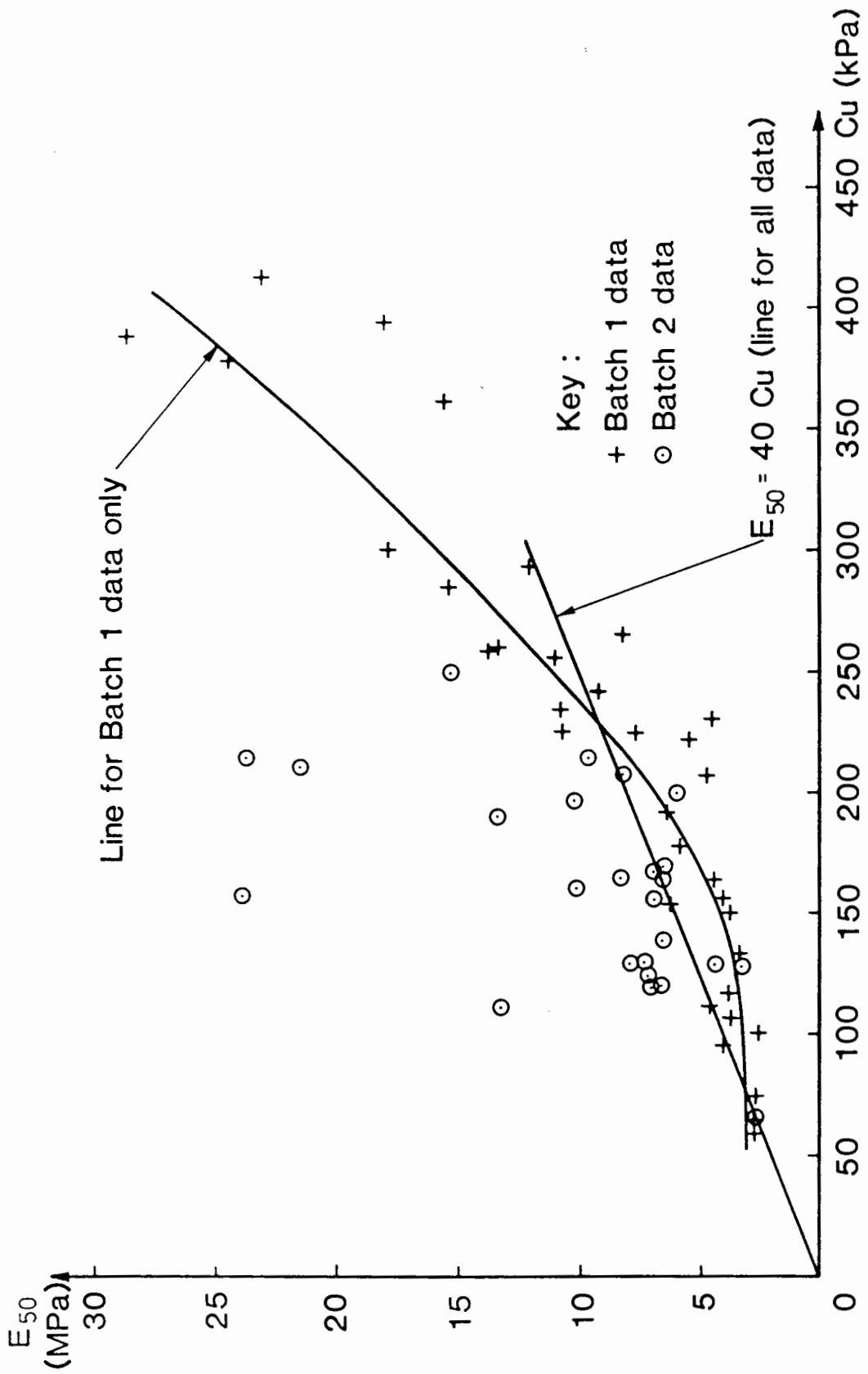


Fig. 6.13 Graph of  $E_{50}$  vs Cu for Keuper Marl using TT Data

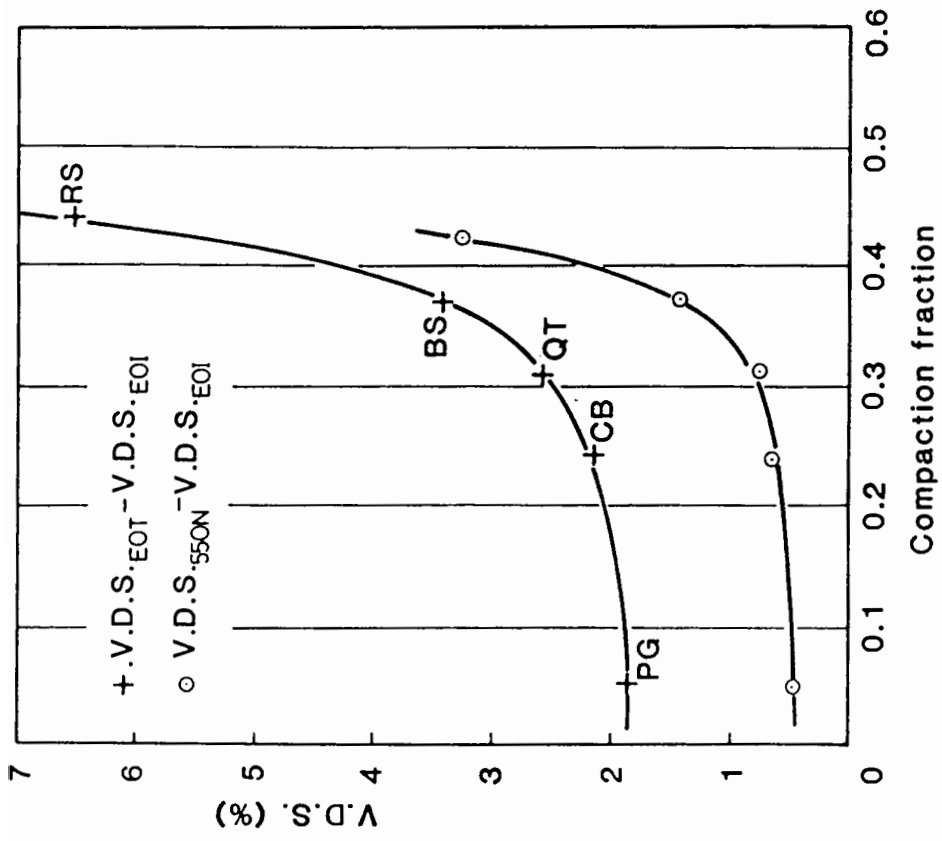


Fig. 6.14 Influence of Compaction Fraction Value of Sidefill on V.D.S. of Pipe

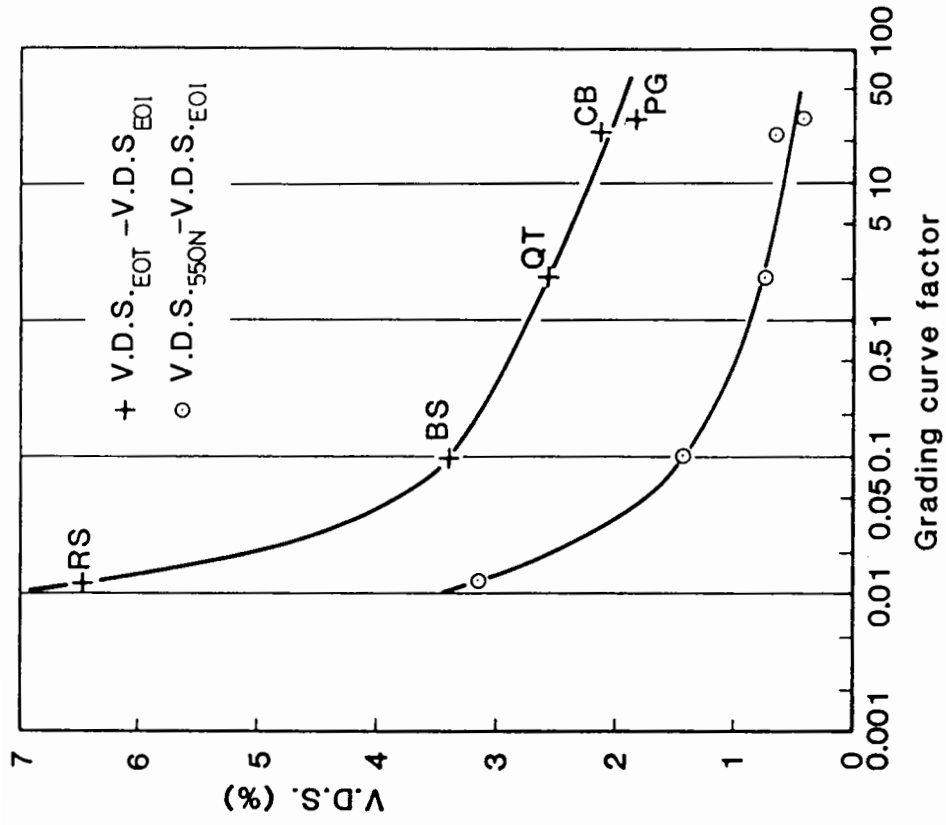


Fig. 6.15 Influence of Grading Curve Factor on V.D.S. of Pipe

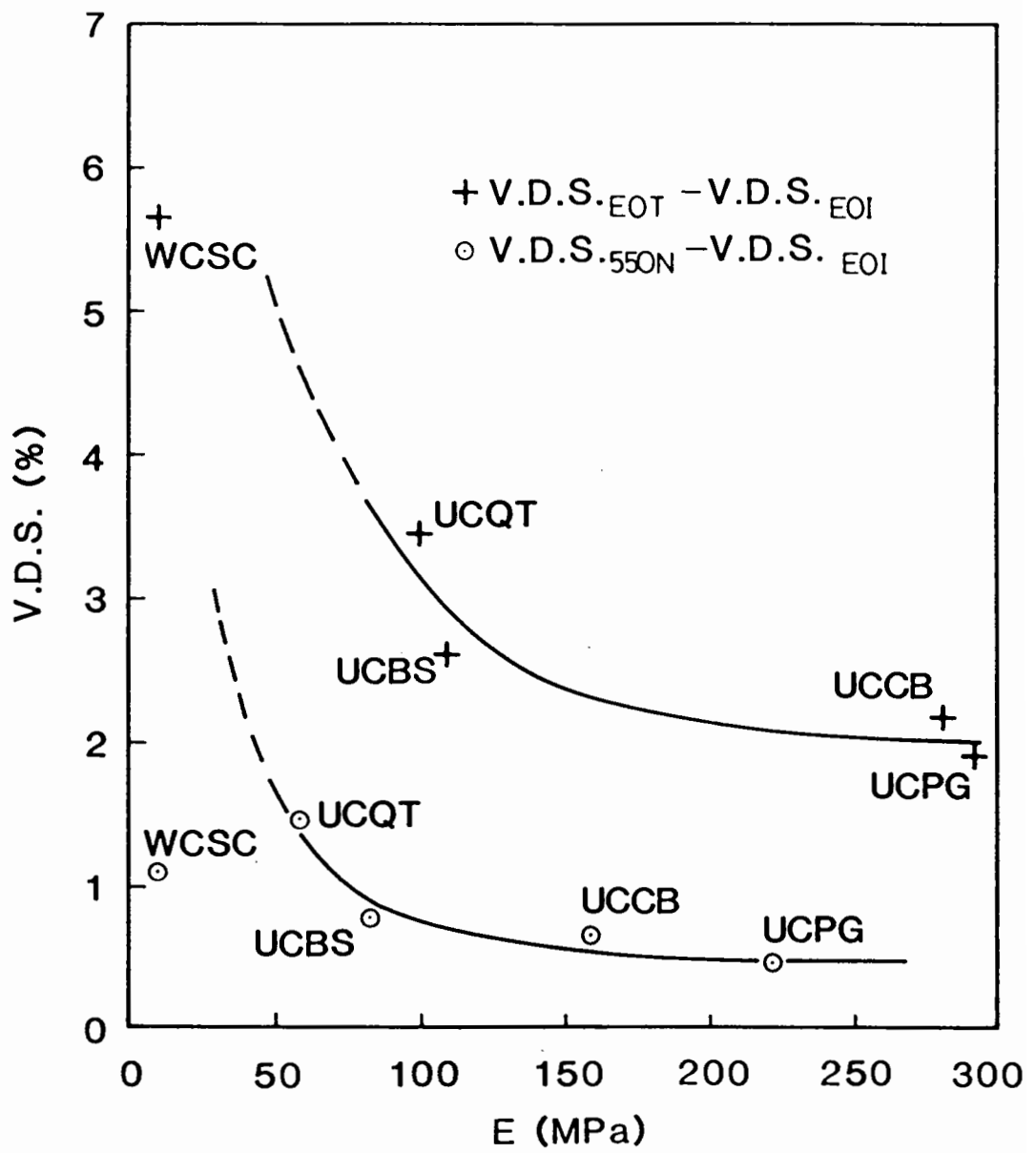
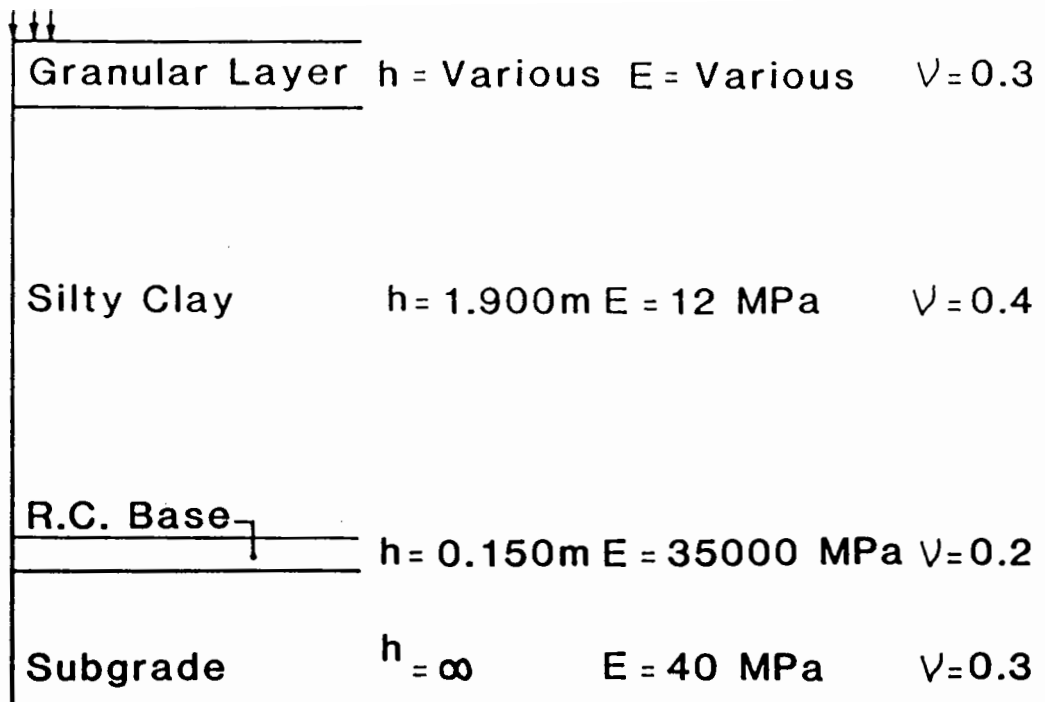
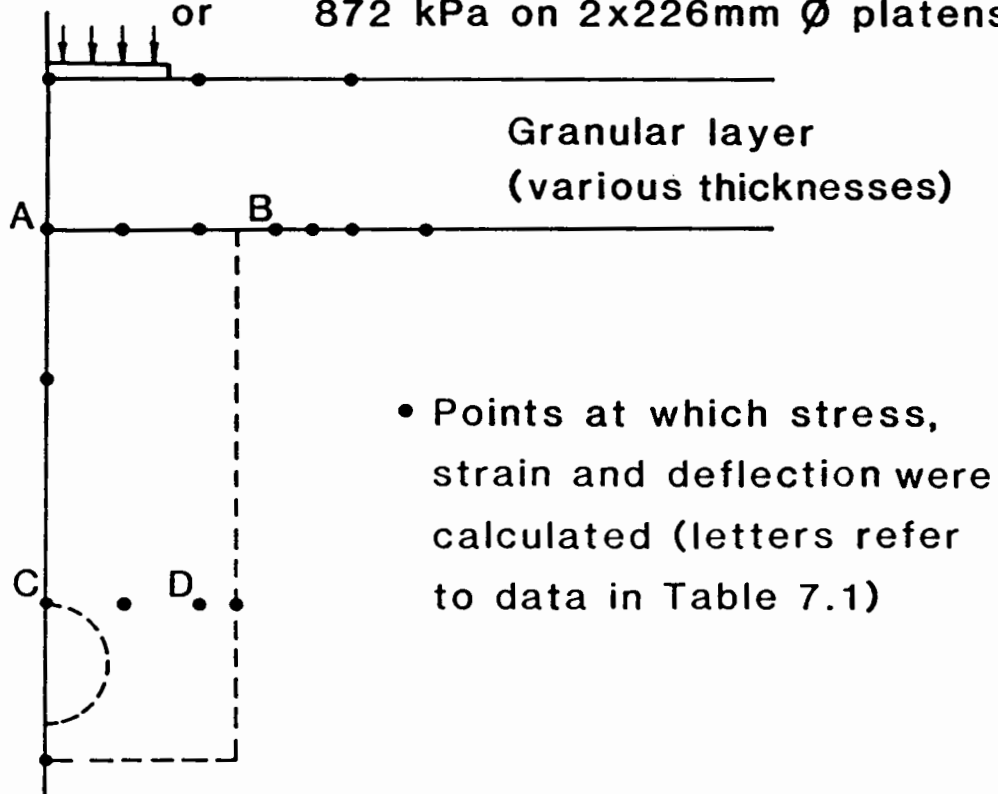


Fig. 6.16 Influence of Young's Modulus of Sidefill on V.D.S. of Pipe



**(a) The Structure**

Load either 870 kPa on 320mm  $\varnothing$  platen  
or 872 kPa on 2x226mm  $\varnothing$  platens



**(b) The Area of Detailed Analysis**

**Fig. 7.1 Linear Elastic Layer Analysis**  
**using BISTRO**

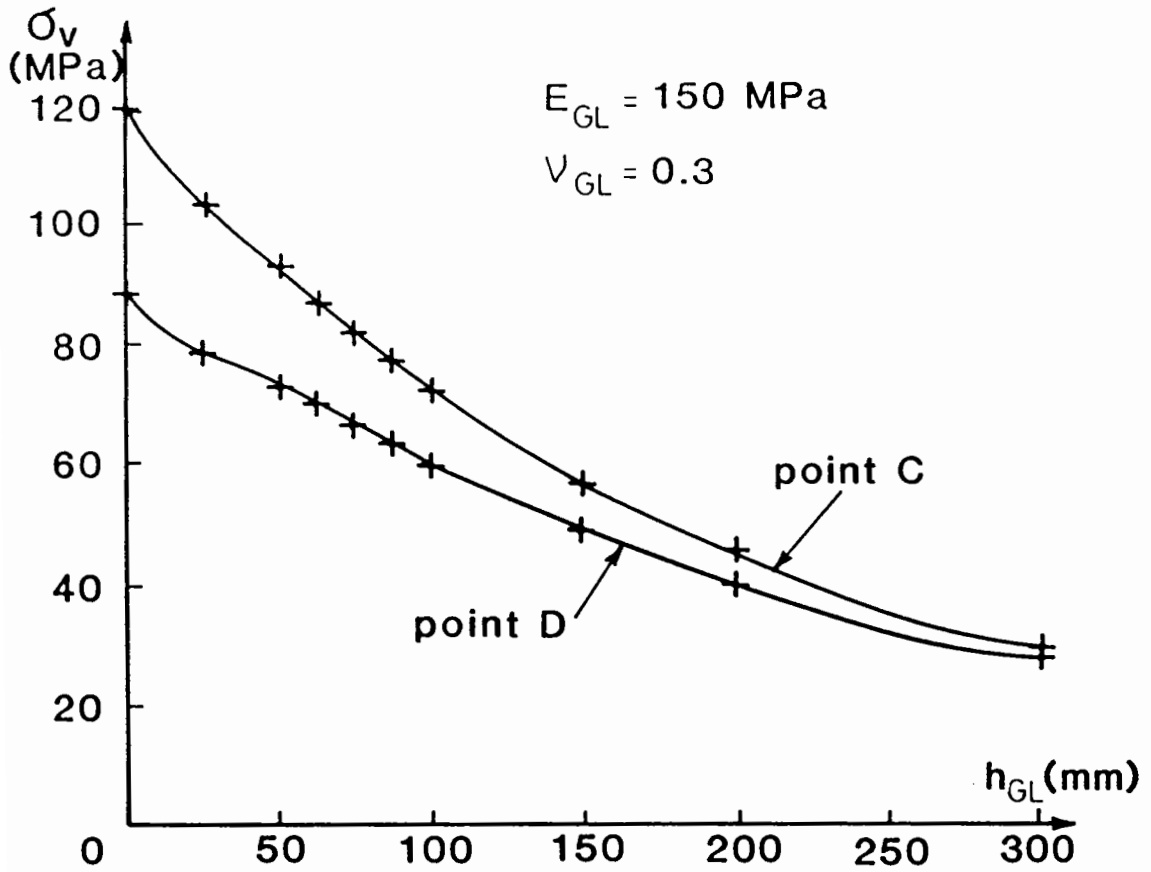


Fig. 7.2 Variation of Stress with Layer Thickness (BISTRO)

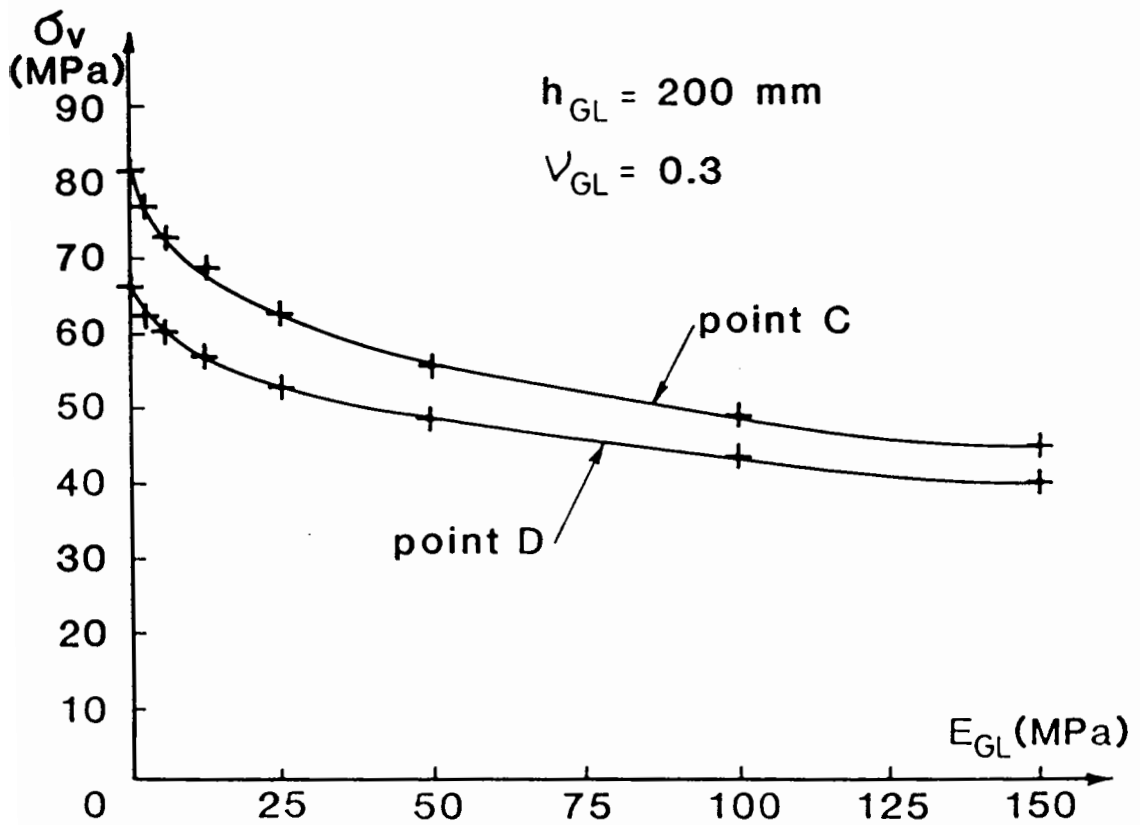


Fig. 7.3 Variation of Stress with Layer Stiffness (BISTRO)

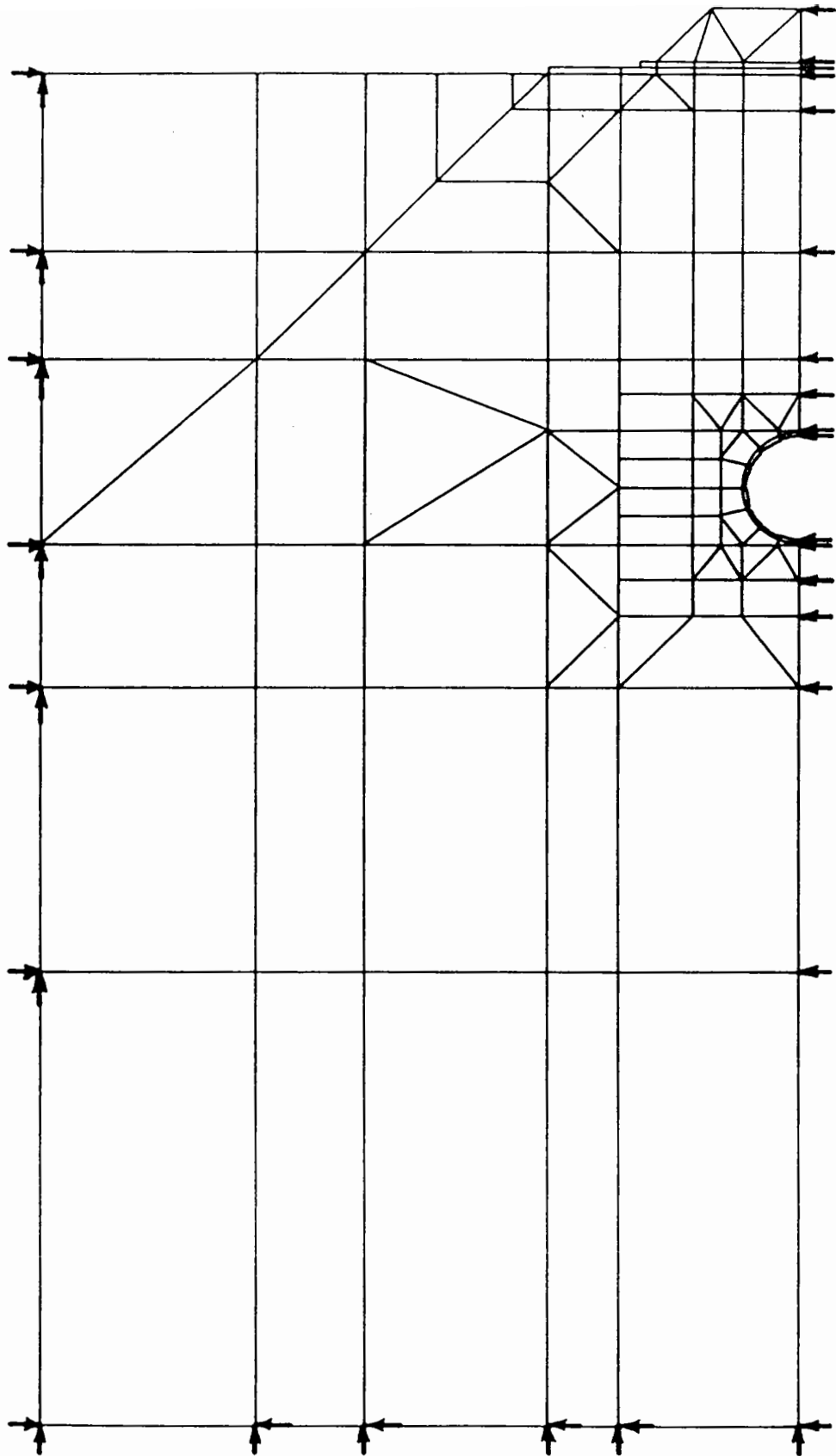
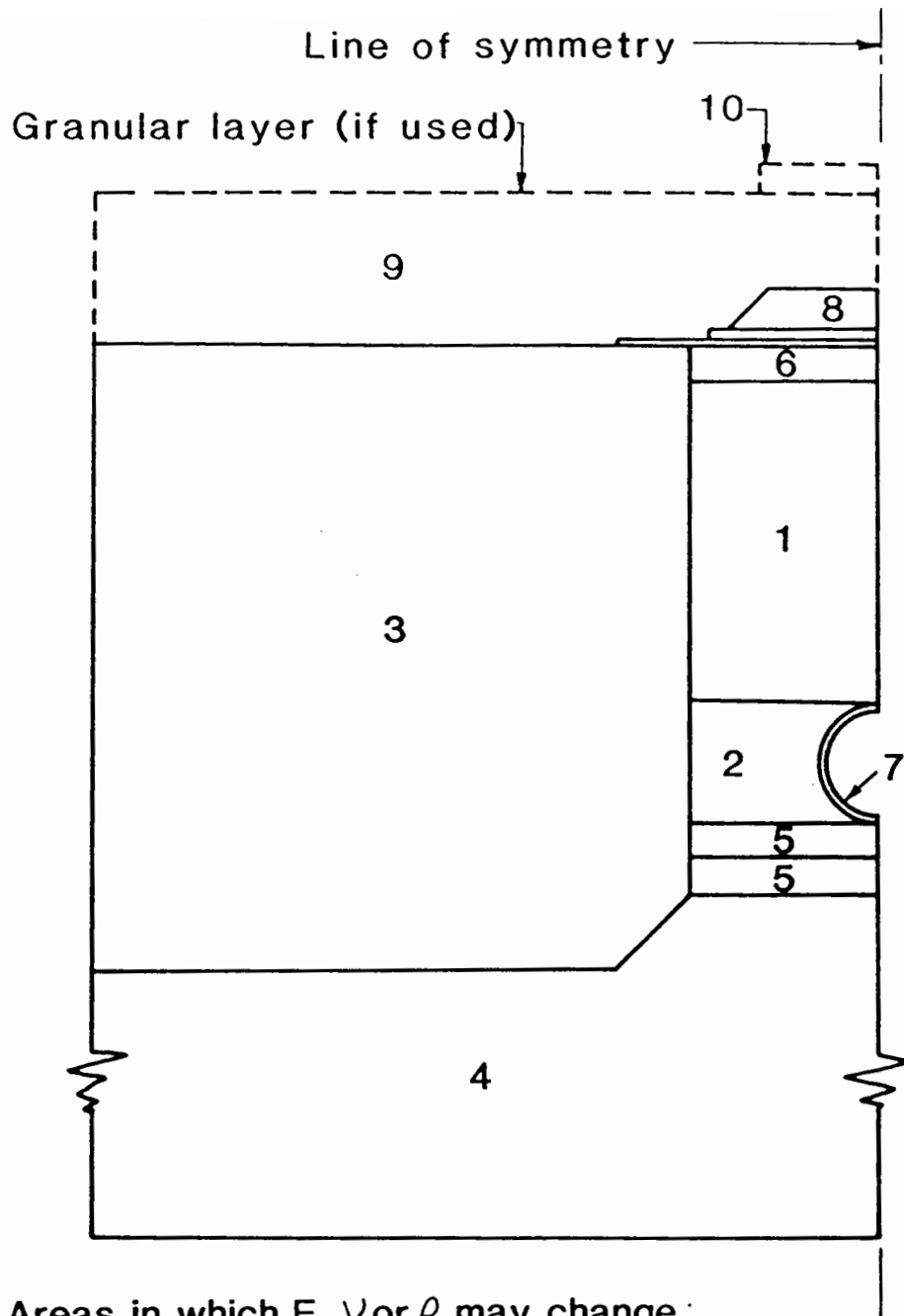


Fig. 7.4 PAFEC Mesh Showing Restraints



Areas in which  $E$ ,  $\nu$  or  $\rho$  may change :

- |                        |                         |
|------------------------|-------------------------|
| 1. Backfill            | 6. Backfill surface     |
| 2. Sidefill            | 7. uPVC pipe            |
| 3. Insitu soil to side | 8. Mild steel platen    |
| 4. Insitu soil below   | 9. Granular layer       |
| 5. Bedding layers      | 10. Stiff, light platen |

Fig. 7.5 Layout of Mesh used in PAFEC Analyses



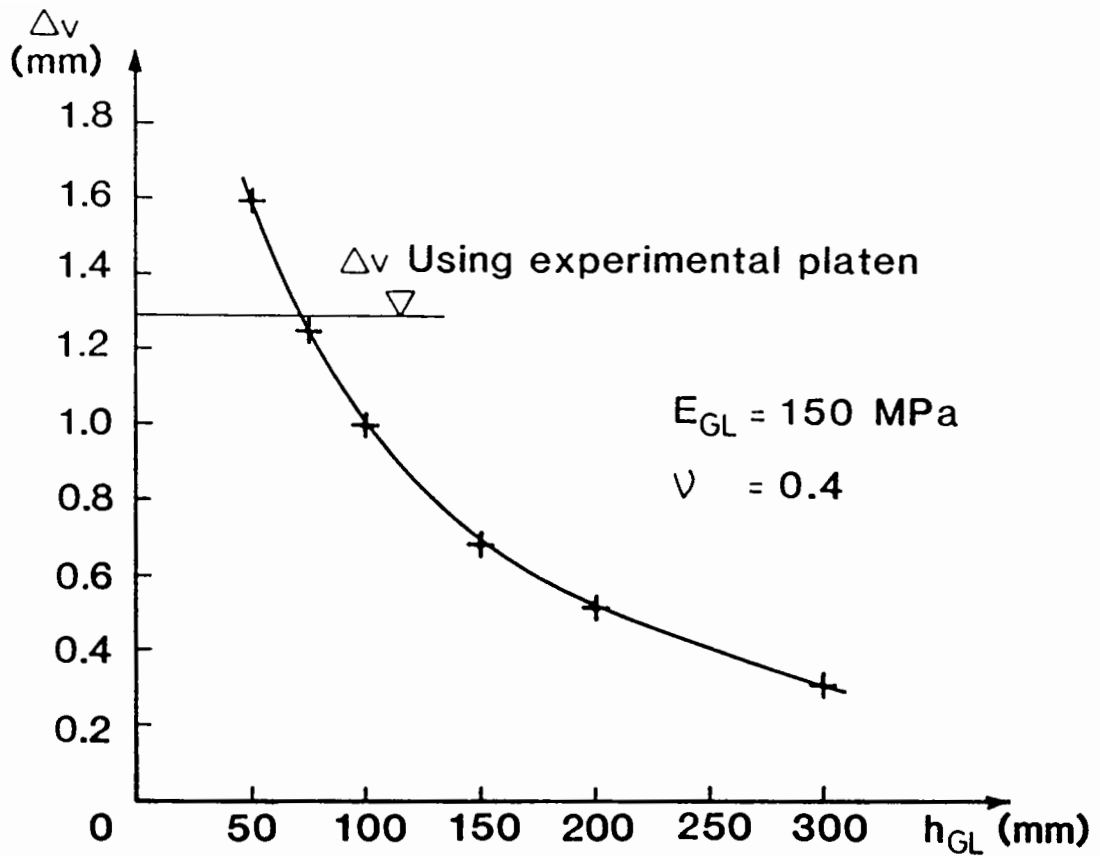


Fig 7.6 Influence of  $T_{GL}$  on Pipe Deformation

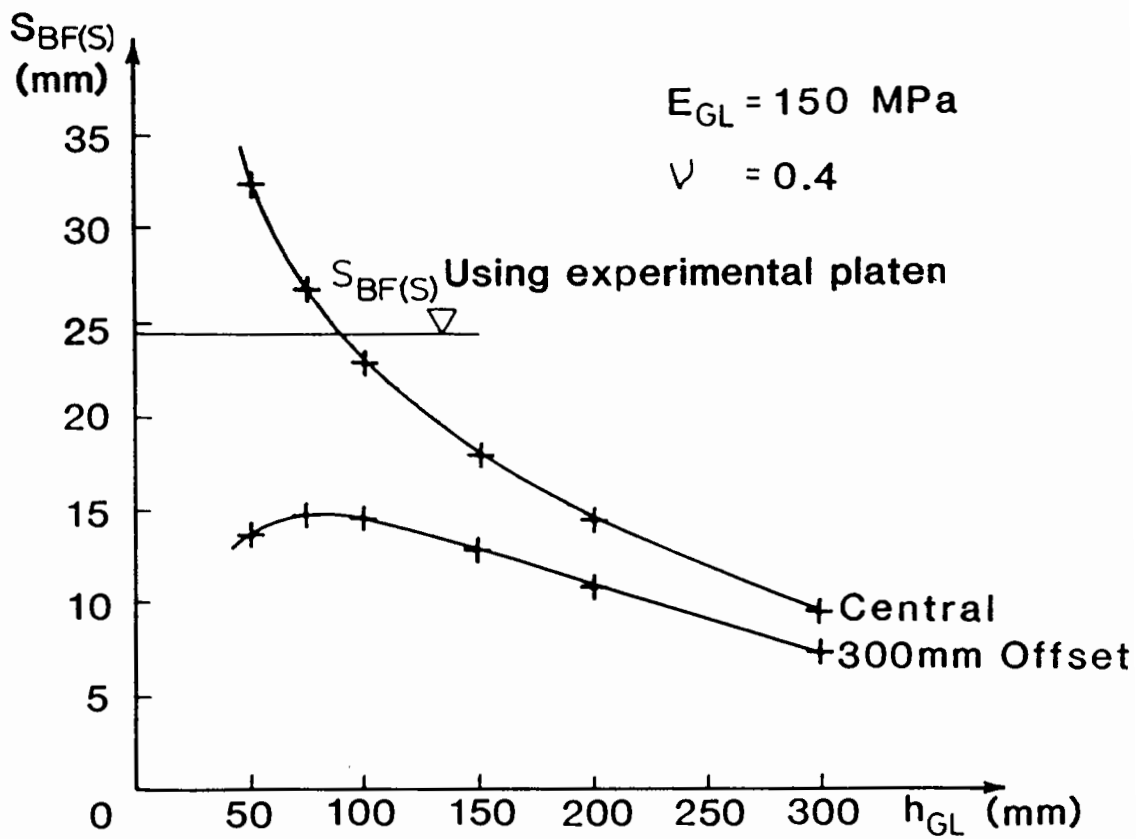


Fig. 7.7 Influence of  $T_{GL}$  on Surface Settlement

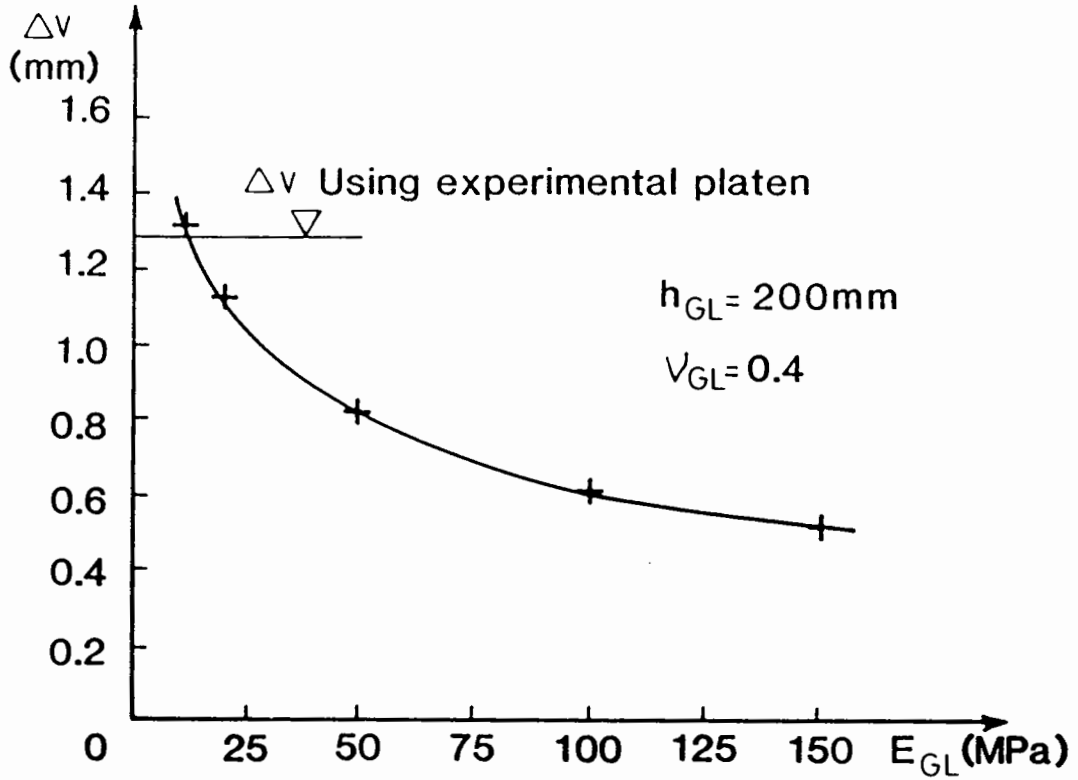


Fig. 7.8 Influence of  $E_{GL}$  on Pipe Deformation

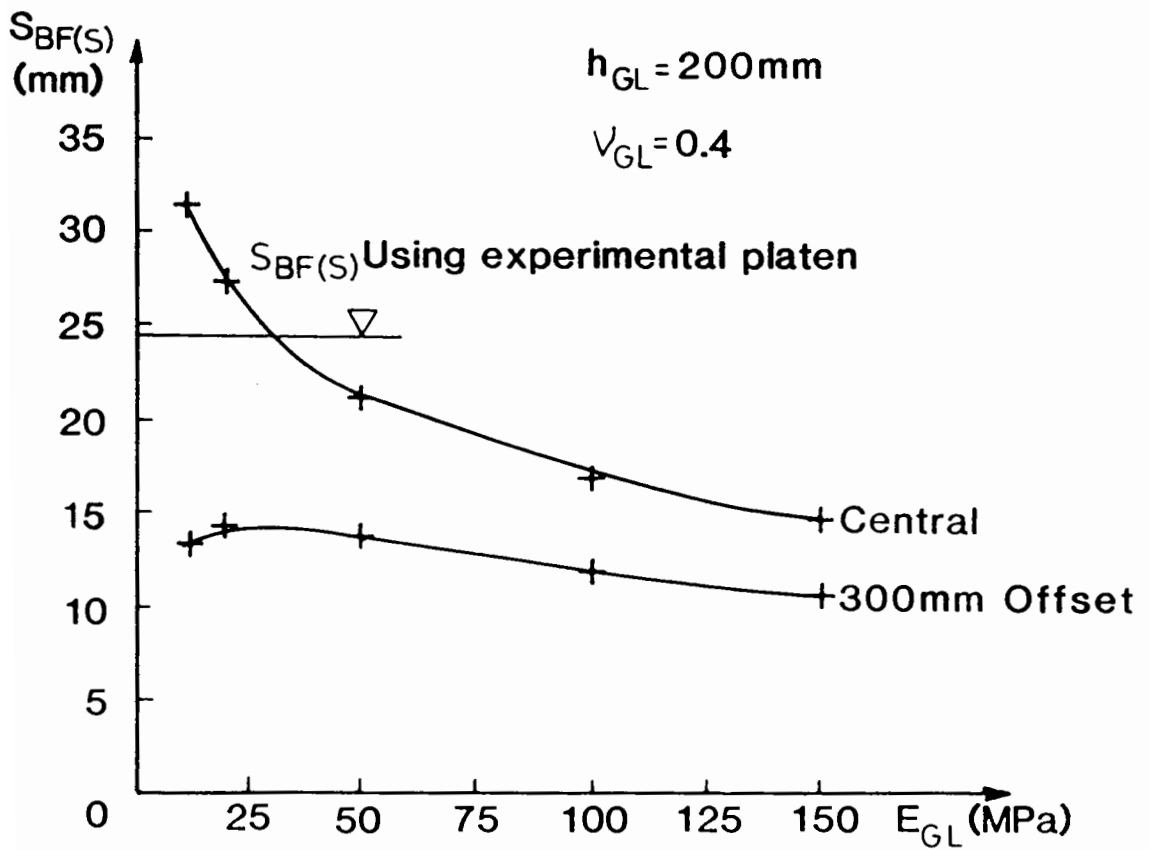


Fig. 7.9 Influence of  $E_{GL}$  on Surface Settlement

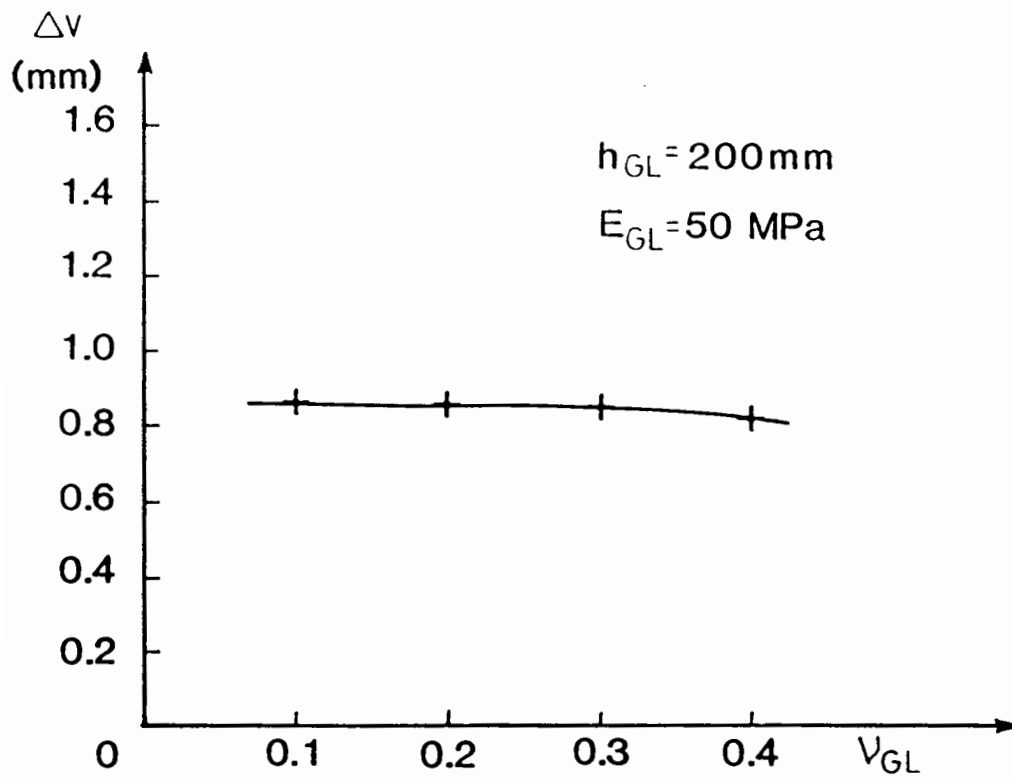


Fig. 7.10 Influence of  $V_{GL}$  on Pipe Deformation

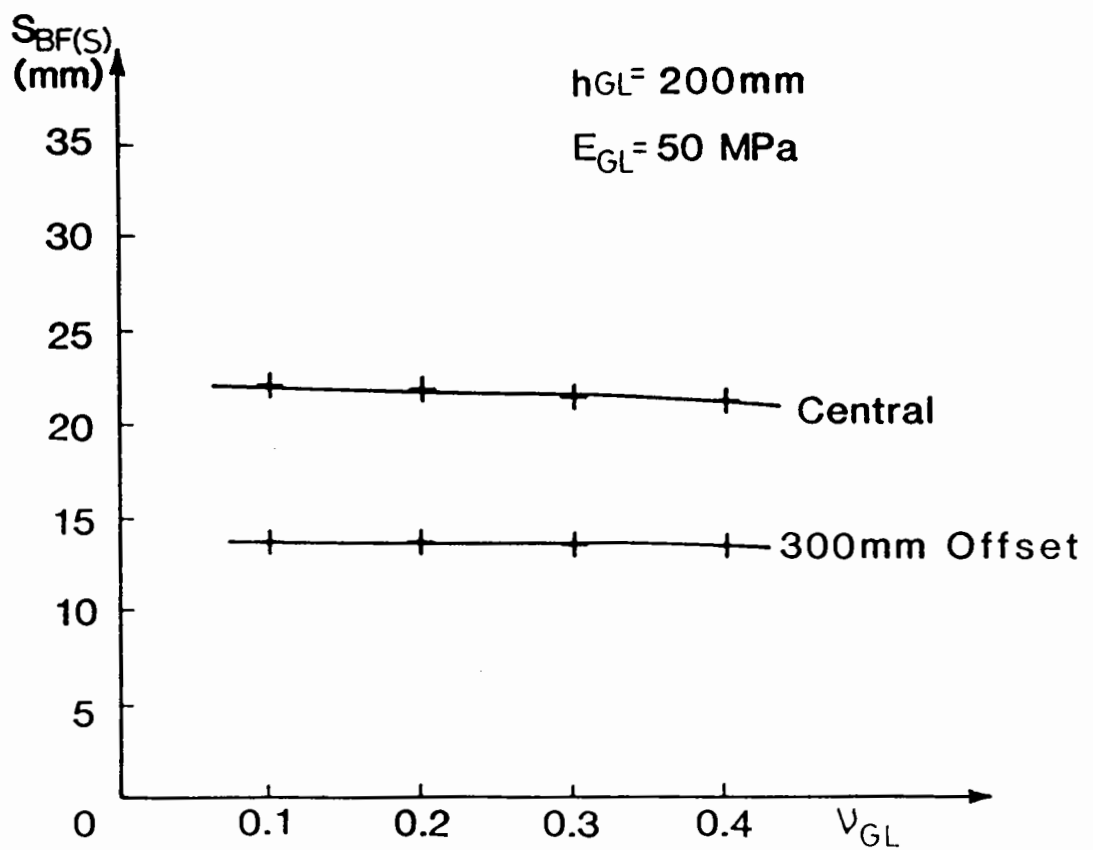
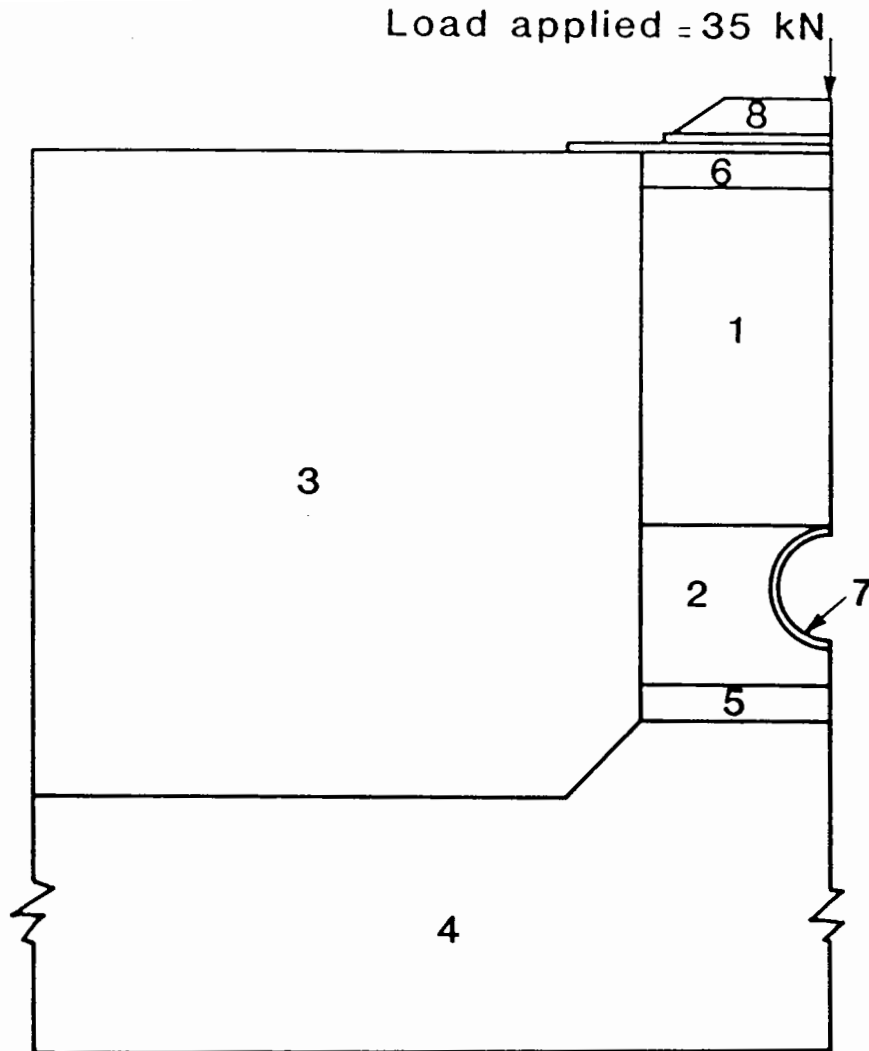


Fig. 7.11 Influence of  $V_{GL}$  on Surface Settlement



**Material properties taken as standard**

- |                               |                     |                              |
|-------------------------------|---------------------|------------------------------|
| 1. $E_{BF} = 3\text{MPa}$     | $\nu_{BF} = 0.4$    | 5. As 4 throughout           |
| 2. $E_{SF} = 50\text{MPa}$    | $\nu_{SF} = 0.4$    | 6. $E_{BF(S)} = 6\text{MPa}$ |
| 3. $E_{NS(S)} = 20\text{MPa}$ | $\nu_{NS(S)} = 0.4$ | 7. $E_P = 2.8\text{GPa}$     |
| 4. $E_{NS(B)} = 20\text{MPa}$ | $\nu_{NS(B)} = 0.4$ | 8. $E_{LP} = 209\text{GPa}$  |
|                               |                     | $\nu_{LP} = 0.38$            |
|                               |                     | $\nu_{LP} = 0.3$             |

**Values of Young's Modulus used in study**

1, 2, 3, 6, 12, 25, 50, and 100 MPa

**Fig. 7.12 Details of Parameter Study**

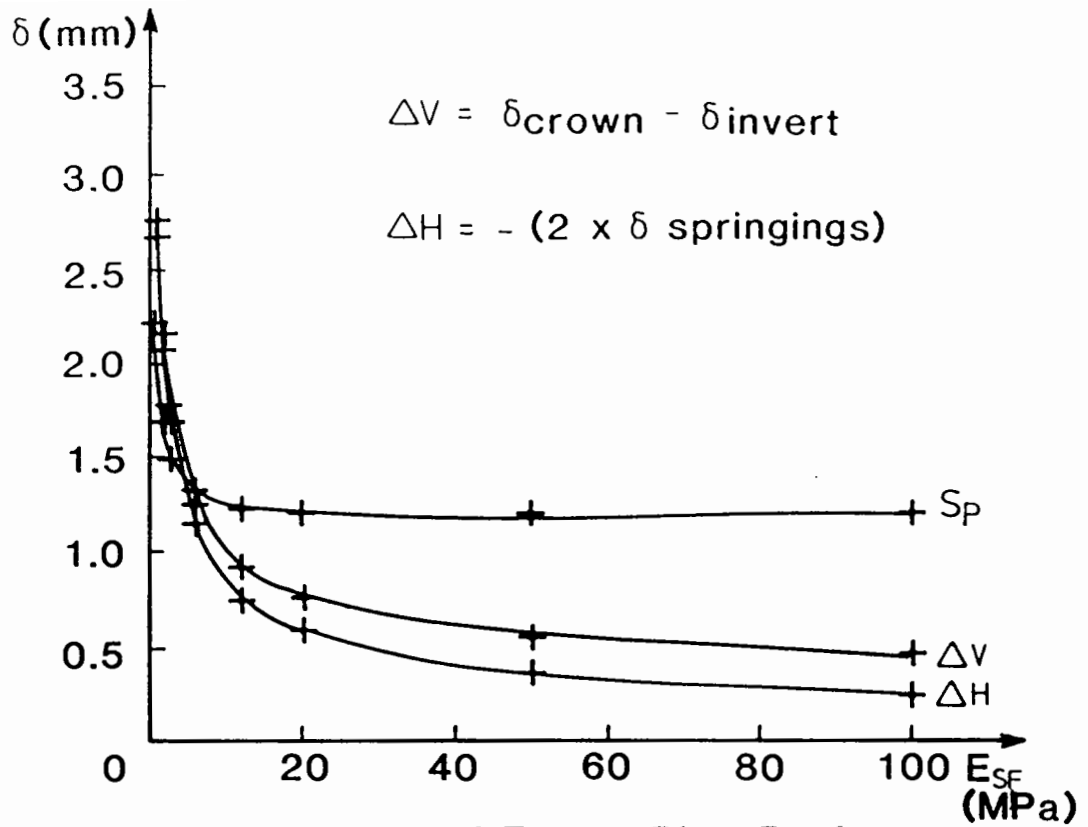


Fig. 7.13 Influence of  $E_{SF}$  on Pipe Performance

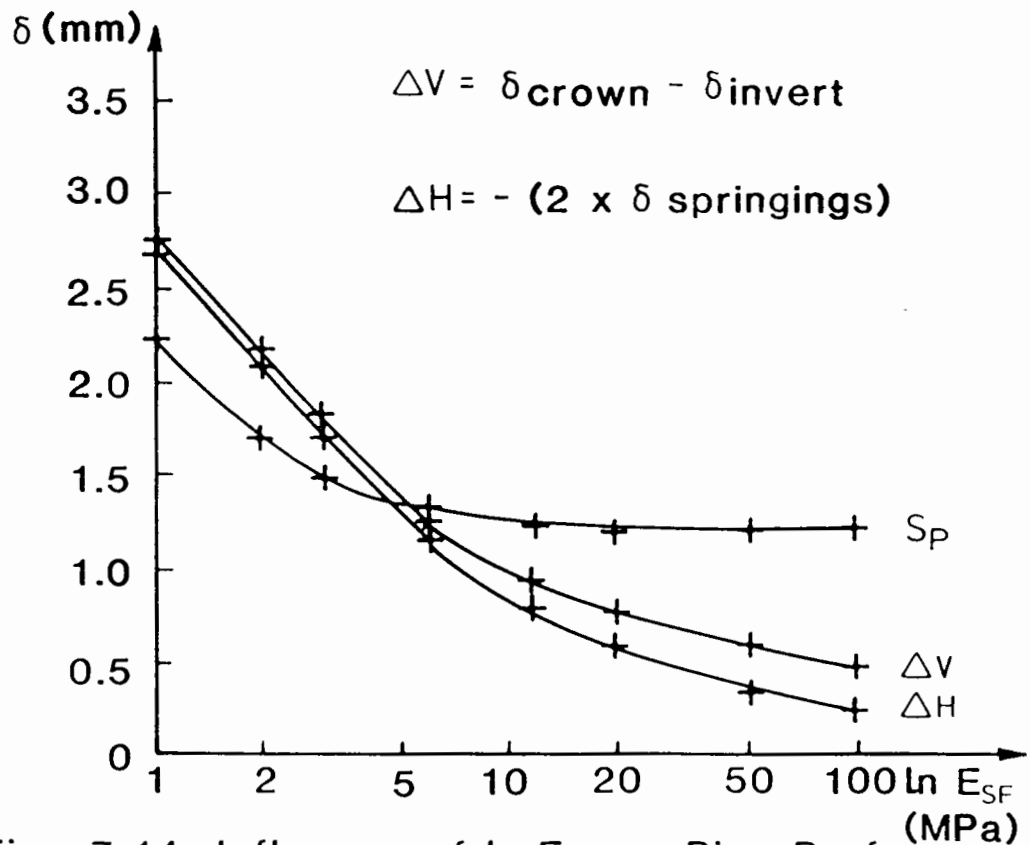


Fig. 7.14 Influence of  $\ln E_{SF}$  on Pipe Performance

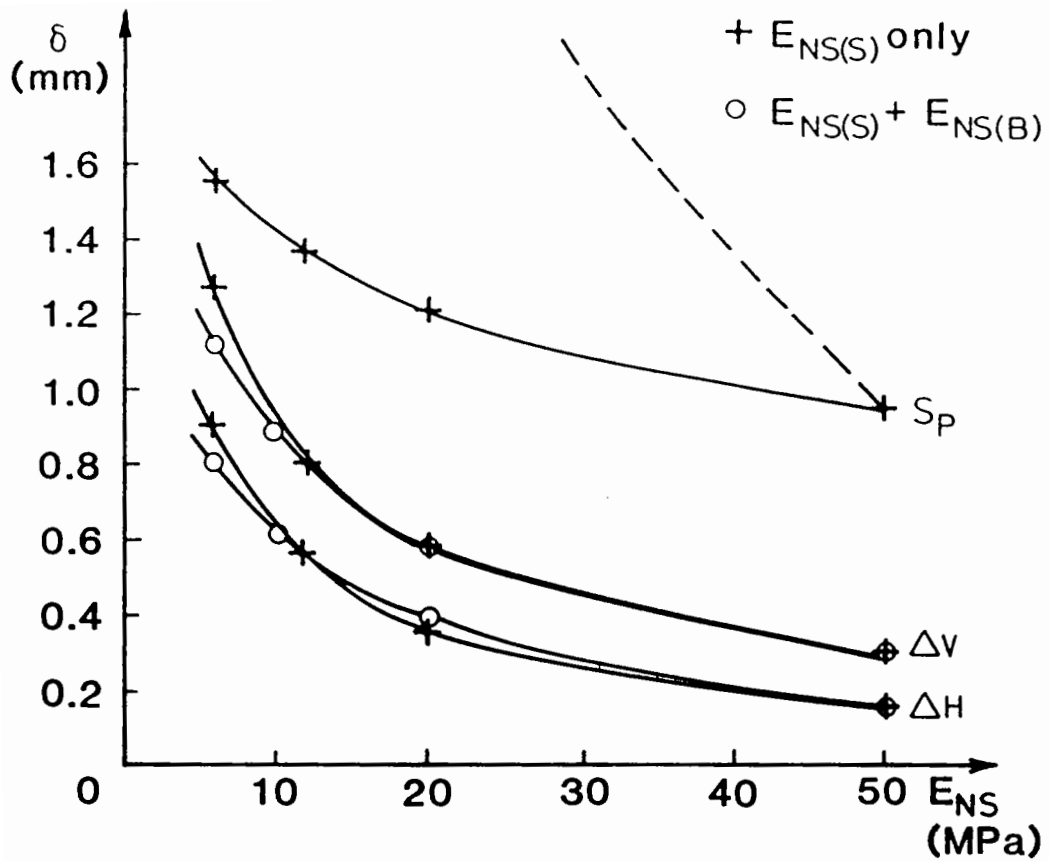


Fig. 7.15 Influence of  $E_{NS}$  on Pipe Performance

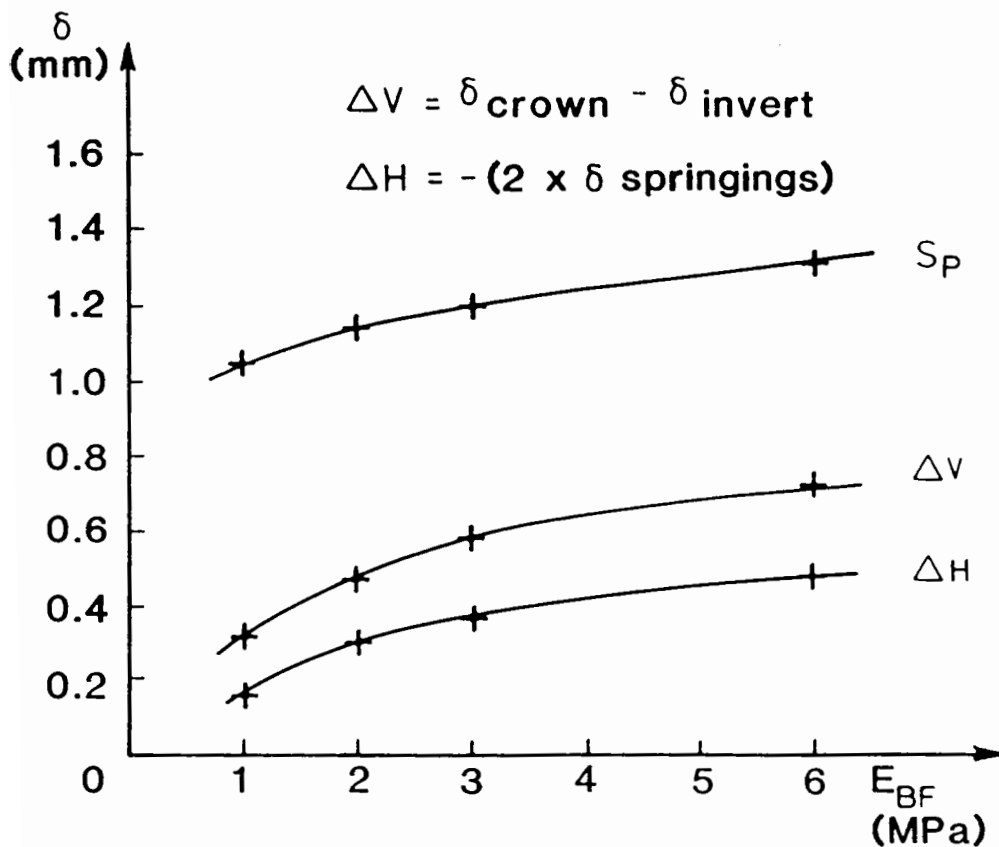


Fig. 7.16 Influence of  $E_{BF}$  on Pipe Performance

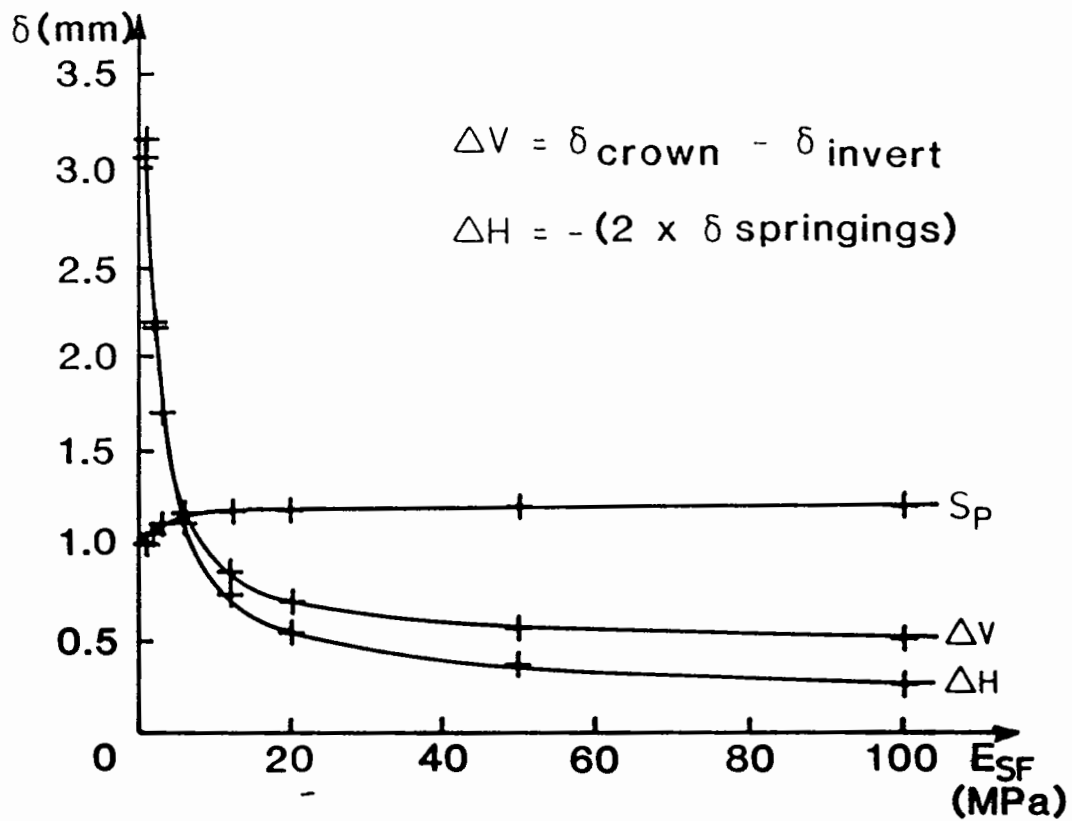


Fig. 7.17 Influence of  $E_{SF}$  on Pipe with no Bedding

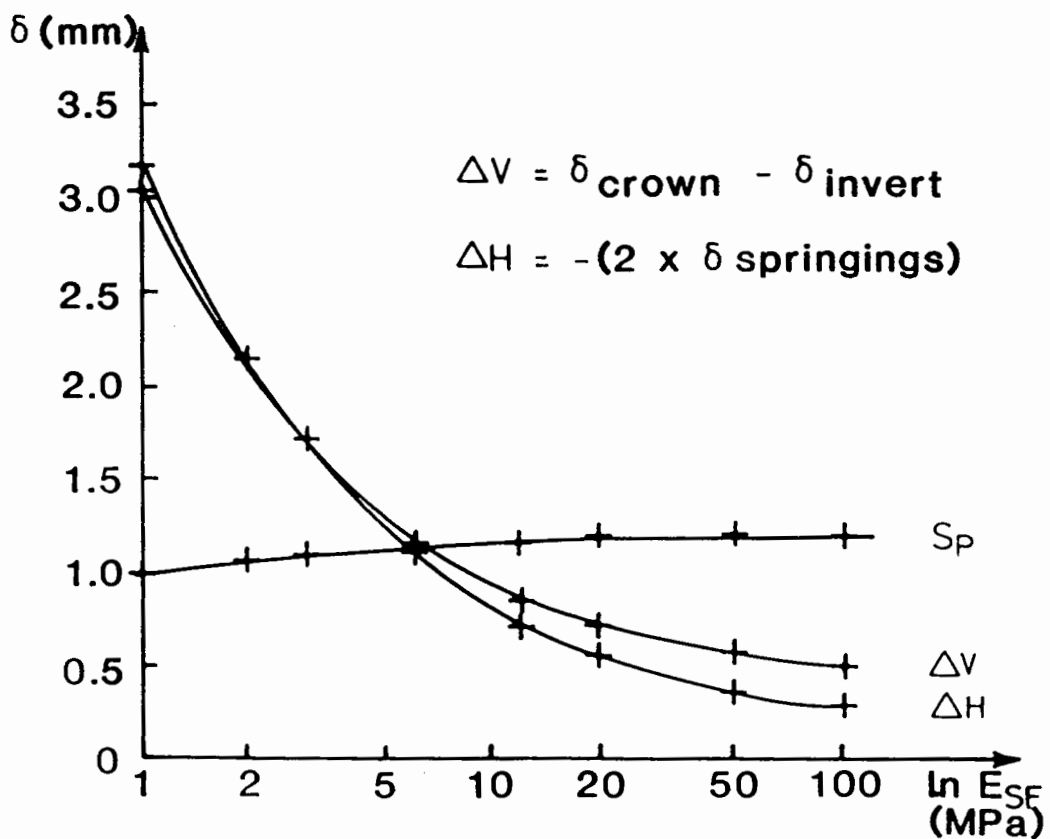
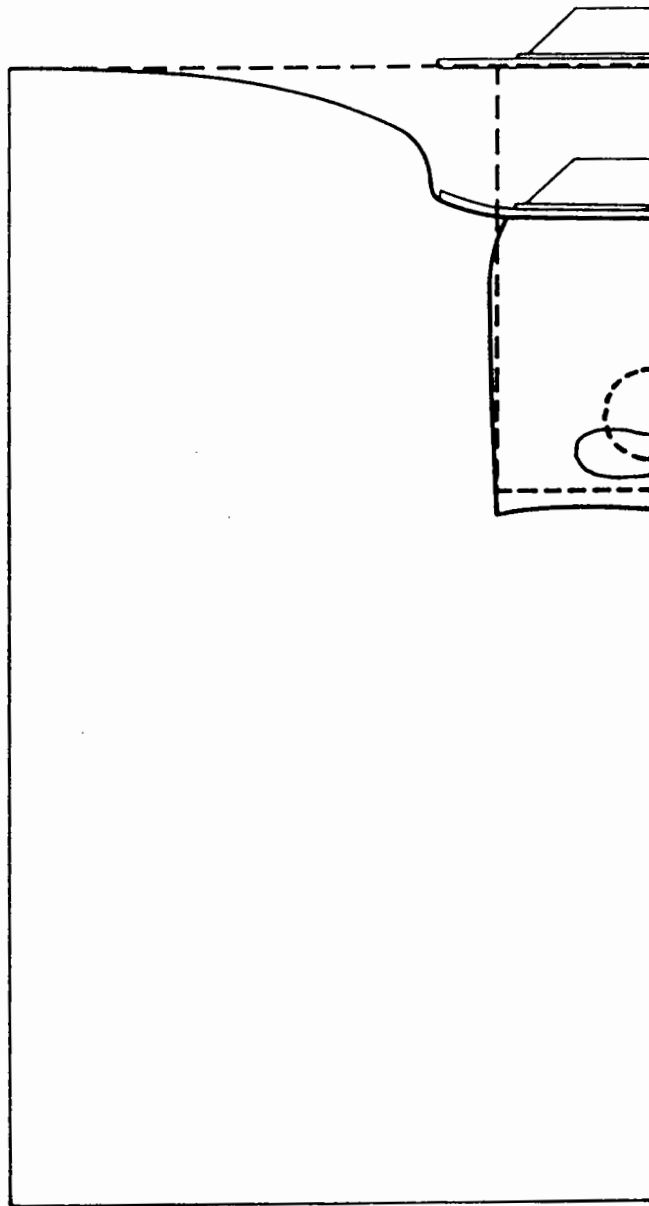


Fig. 7.18 Influence of  $\ln E_{SF}$  on Pipe with no Bedding



Key : ----- Structure before loading  
 ————— Deformed profile

Scale 0 1 2 3 4 5 6 mm deformation  
 0 250 500 750 mm structure

Fig. 7.19 Deformation Profile for Installation with very low  $E_{SF}$  and no Bedding Layer